ASPIRIN AFFECTS EARLY PHASES OF METASTASIS THROUGH THE INHIBITION OF COX-1-THROMBOXANE A_2 AXIS

Serena Lucotti

Green Templeton College

Thesis submitted to the Medical Sciences Division of the University of Oxford in partial fulfilment of the requirements for the degree of Doctor of Philosophy

CRUK/MRC Oxford Institute for Radiation Oncology

Department of Oncology

University of Oxford

Trinity 2016

ABSTRACT

Metastasis is the major cause of cancer related mortality, due to a poor understanding of the metastatic process and a subsequent lack of effective anti-metastatic therapies. Evidence from experimental studies and clinical trials has shown that aspirin reduces the incidence of distant metastases. It is well established that aspirin inhibits cyclooxygenase (COX)-1 and COX-2, triggering anti-thrombotic and anti-inflammatory effects, respectively. However, the mechanisms underlying the anti-metastatic effect of aspirin are still largely unknown.

By using an experimental model of pulmonary metastasis, we have found that the anti-metastatic effect of aspirin is associated with the inhibition of COX-1. In support of this, metastasis establishment was impaired in COX-1 deficient mice, suggesting a pivotal role of this isoform in the metastatic process. Looking in more detail into the metastatic cascade, we found that COX-1 contributes to the intravascular phase of metastasis and promotes the early persistence of tumour cells in the lung vasculature. In particular, COX-1 inhibition decreased the interaction of platelets with tumour cells and was associated with the reduction of endothelial activation, of tumour cell adhesion to the endothelium, of recruitment of metastasis-promoting monocytes/macrophages and of transendothelial migration. We have identified platelet-derived thromboxane A_2 (TXA_2) as the main product of COX-1 responsible for its permissive effect on metastasis. Indeed, TXA_2 delivered to mice in combination with aspirin was able to abrogate the anti-metastatic effect of aspirin.

Taken together, our data suggest that the inhibition of COX-1:TXA_2 axis by aspirin is sufficient to exert an anti-metastatic effect. In particular, the inhibition of platelet-derived TXA_2 seems to affect multiple early steps of the haematogenous transit of tumour cells. In this perspective, TXA_2 might represent a more selective therapeutic target for the prevention of metastasis.

In loving memory of Pino Rainaldi

ACKNOWLEDGEMENTS

This DPhil thesis stands as a work of an individual, but it would not exist without the support of a number of people.

First, I would like to express my sincere gratitude to Prof Ruth Muschel for her continuous support and for believing in me during the whole DPhil and beyond. Without her guidance and knowledge I would not have made it until this point.

I also thank Dr Ana Gil-Bernabé for her guidance throughout this DPhil, she has been an invaluable source of learning and a drive to improve.

I am extremely grateful to my fellow labmates for their encouragement and for being not only terrific scientist, but also invaluable friends. I also thank all the colleagues at the RRI, past and present, for creating such pleasant and stimulating place to work in.

My sincere thanks goes to my collaborators Dr Paul Armstrong, Dr Camilla Cerutti and Dr Magali Soyer for their valuable advice and for making my time in London both constructive and enjoyable.

My journey here in Oxford would have been much harder if my path did not cross with people that I can now call friends. In particular, I would like to thank Kleopatra Andreou for being an irreplaceable friend and companion along the same path towards the DPhil. I am also extremely grateful to Nikola Vlahov for being the most supportive (and patient) listener and Zuzana Kalivodova for always being there for me. My journey would have not been the same without Duccio Conti, Margherita Murgiano and Edoardo Andreoni for the memorable moments together. I would also like to acknowledge my friends back home, in particular Serena Innocenti, Francesca Bianconi and Irene Petrizzo, who have been a constant presence in my life.

Immense thanks need to go to all members of my family, because no distance can refrain them to support me. To Francesco Meghini, for being the centre of my world. To my

parents, because through their caring support and teachings they made me get to where I am now. To my little sister, for being each other's biggest fans. To my grandmothers, for believing that my research is relevant even if they do not know what a cell is. To my aunts and uncle, for being the proudest supporters of my successes and the comforter of my failures.

Finally, the hugest acknowledgement goes to all the mice that have given their lives to perform this research and the research to come. Their sacrifice is a gift to the whole mankind for the advancement of cancer therapies and for such I was, am and will always be grateful.

CONTRIBUTIONS TO THE WORK PRESENTED

Figure 3.5B: *In vivo* experiment was performed by Dr Ana M. Gil-Bernabé, *ex vivo* quantification was performed by Dr Ana M. Gil-Bernabé and Serena Lucotti.

Figure 3.5D: HPLC analysis of urinary SUA was performed by Dr Michael Stratford.

Figure 3.6C-D and **3.8E**: *In vivo* experiment was performed by Serena Lucotti, MRI scan of lungs was performed by Dr Ana Da Silva Gomes, by employing scans developed by Dr Sean Smart and Dr Paul Kinchesh and a robot carriage system developed by Dr Stuart Gilchrist and Dr John Beech.

Figure 5.1 and **5.3**: The measurement of clot and cluster volumes was performed by Serena Lucotti by employing a MATLAB script designed by Dr Philip D. Allen.

Figures 5.6-5.9: Experiments were performed by Dr Camilla Cerutti, Serena Lucotti and Dr Magali Soyer, all authors contributed equally. Data analysis was performed by Serena Lucotti with the expert advice of Dr Bostjan Markelc.

TABLE OF CONTENTS

LIST OF ABBREVIATIONS

ADP	Adenosine diphosphate
AJ	Adherens junction
ASA	Acetylsalicylic acid
ATCC	American Type Culture Collection
BMDC	Bone marrow derived cell
COX	Cyclooxygenase
CSF-1	Colony stimulating factor-1
CTC	Circulating tumour cell
CTM	Circulating tumour microemboli
DC	Dendritic cell
DMEM	Dulbecco's Modified Eagle Medium
ECM	Extracellular Matrix
ELAM	Endothelial cell leukocyte adhesion molecule
ERK	Extracellular-signalling-regulated kinase
FOV	Field of view
FBS	Fetal Bovine Serum
GP	Glycoprotein
HETE	Hydroxyeicosatetraenoic acid
HR	Hazard ratio
IL	Interleukin

ICAM-1	Intercellular adhesion molecule
IQR	Interquartile range
LTA	Light transmission aggregometry
MAM	Metastasis associated macrophage
MBD	Membrane Binding Domain
MIP	Maximum intensity projection
MCP-1	Monocyte chemotactic protein-1
MHC	Major histocompatibility complex
MMP	Matrix metalloproteinase
MP	Microparticle
MUC1	Mucin 1
NSAIDs	Non-steroidal anti-inflammatory drugs
OR	Odds ratio
PAR	Protease activated receptor
PI3K	Phosphoinositide 3 kinase
PG	Prostaglandin
PGES	Prostaglandin E_2 synthase
PGHS	Prostaglandin H_2 synthase
PGIS	Prostaglandin I_2 synthase
PPP	Platelet poor plasma
PRP	Platelet rich plasma
PSGL-1	P-selectin glycoprotein ligand-1

ROCK	RHO-associated kinase
SA	Salicylic acid
SUA	Salicyluric acid
TAM	Tumour associated macrophage
TCIPA	Tumour cell-induced platelet aggregation
TEM	Transendothelial migration
TGF-ß1	Transforming growth factor-ß1
TF	Tissue factor
TJ	Tight junction
TNF	Tumour necrosis factor
TP	Thromboxane A_2 receptor
TSP-1	Thrombospondin-1
TXA_2	Thromboxane A_2
TXAS	Thromboxane A_2 synthase
VCAM-1	Vascular cell adhesion molecule
VEGF	Vascular endothelial growth factor
VAP-1	Vascular adhesion protein-1
vWF	von Willebrand Factor
ZEB	Zinc-finger E-box binding

LIST OF FIGURES

LIST OF TABLES

SUPPLEMENTARY FIGURES

Supplementary figure S1 – Daily intake of drinking water per mouse.

Supplementary figure S2 – Levels of plasmatic SA and SUA in ASA-treated mice.

Supplementary figure S3 – COX-1 expression in clinical tumour samples does not correlate with the anti-metastatic effect of aspirin.

Supplementary figure S4 – Different modes of initial arrest of tumour cells in the pulmonary vasculature.

Supplementary figure S5 – Tumour cell adhesion to the endothelium is not affected by high shear stress.

Supplementary figure S6 – Comparison of different methods for the quantification of tumour cell intercalation.

Supplementary figure S7 – Immunofluorescence detection of proteins involved in TXA_2 signalling in lung sections.

CHAPTER 1

Introduction

1.1 METASTASIS

The term “metastasis” (from the Greek ‘change in the state’) was used for the first time in 1829 by the French gynaecologist JC Recamier to indicate the movement of tumour cells to the blood stream[1]. Nowadays, the definition of tumour metastasis is far more complicated and refers to the haematogenous or lymphatic dissemination of cells from the primary tumour to a secondary organ where they form tumour colonies, usually referred to as metastases or metastatic foci/tumours.

Per se, metastasis is a very inefficient process because few tumour cells develop into metastasis. It has been estimated that millions of tumour cells detach form the primary tumour and enter the circulation every day, but only a small percentage of them, likely no more than 0.01%[2], succeed in colonizing the host tissue[3,4]. The metastatic success of tumour cells depends on intrinsic and extrinsic factors[5]. On the one hand, the primary tumour is constituted by a genetically heterogeneous population of cells that are constantly selected by the tumour environment[6], which eventually leads to the emergence of highly malignant or invasive cell variants[7,8]. These variant genetic makeups constitute the intrinsic factor that allows the survival in the circulation and the colonisation of a secondary organ. On the other hand, the tumour microenvironment of the host tissue influences the potential of colonising tumour cells to form a metastasis. The tumour stroma consists of endothelial cells, fibroblasts, immune cells and extracellular matrix and their interaction with tumour cells considerably influence the behaviour of invading cells, either stimulating or inhibiting metastasis development. Thus, the establishment of metastasis is a selective and adaptive rather than a random process[1].

1.1.1 Metastasis organotropism

Different cancer types show distinct organ tropism patterns. Two theories have been proposed to explain the selectivity of metastatic dissemination: the 'anatomical and mechanical' hypothesis and the 'seed and soil' hypothesis. The 'anatomical and mechanical' theory was proposed in 1858 by Virchow, who believed that metastatic tropism relied on the physical arrest or entrapment of tumour cells in the vasculature[9]. This theory was further supported 70 years later by Ewing, who noted how circulatory patterns determined the specificity of colonization[10].

The 'anatomical and mechanical' theory was first challenged in 1889 by the British surgeon Paget with his 'seed and soil' theory. Paget noticed that breast cancer preferentially metastasized to specific organs although their blood supply was comparable to other organs, supporting the idea that spreading tumour cells (seeds) can grow only 'if they fall on congenial soil', distant organs with permissive features[11]. The 'seed and soil' theory has been confirmed by further experimental data, which demonstrated that the tissue-specificity of metastasis depends on both the genetic makeup of tumour cells, which are different intra- and inter-personally, and the molecular and cellular properties of the target stroma[12-14]. On the one hand, tumour cells possess specific gene signatures that allow their homing to the secondary site, such as the expression of matrix degradation enzymes, cytoskeleton remodelling factors and/or endothelium-adhesion molecules[15,16]. These features can be developed through spontaneous mutation in the primary tumour or induced by the microenvironment of the primary tumour or the blood circulation. On the other hand, the stroma provides signals that are necessary for metastasis. These signals can be released by the microenvironment of the primary tumour, such as transforming growth factor (TGF)-ß1 in breast cancer[17], during tumour cell dissemination, like platelet-derived TGF-ß1[18], or at the metastatic site, such as MMP-9 released from metastasis-associated macrophages and endothelial cells[16]. It is currently accepted that metastatic patterns may depend both on the 'seed and soil' and the

'anatomical and mechanical' theories: circulatory directions define the distribution of wandering cells but these cells can adhere only in compatible organs[19].

More recently, evidence has indicated that the receptiveness of the target tissue to spreading cells can be promoted by the primary tumour before metastatic seeding, a process that is usually indicated as pre-metastatic niche formation. The pre-metastatic niche is established through the release of growth factors, chemoattractants and exosomes by the primary tumour in the blood circulation[16,20-25]. These soluble molecules prime the stroma of the target organ to attract the engraftment of metastatic cells. This happens through the recruitment of bone marrow derived cells (BMDCs)[20,21,23,26,27] or the activation of local cells (such as platelets and fibroblasts)[26,28] that enhance tumour cell adhesion, immune evasion and invasion through the expression of adhesion molecules[20] and the secretion of pro-metastatic factors[21,22,27] or extracellular matrix remodelling enzymes[16,27].

1.1.2 Treatment of metastasis

Tumour metastases are the main cause of death from solid tumours, accounting for 90% of cancer mortality. This is primarily due to the fact that patients are diagnosed with a primary tumour at a time when it has already metastasized. Moreover, the existing anti-cancer therapies have generally been designed to limit tumour growth and might not be effective to contain metastatic disease[29,30]. The refractoriness of distant metastasis depends on a series of reasons. First, metastatic cells have a clonal origin from the primary site and are usually less phenotypically stable than the original tumour[31-34], which determines differences in their karyotype, growth, expression of surface proteins, immunogenicity and enzyme activities. These changes may result in resistance to normal chemotherapeutics or immune attacks[1]. Second, metastatic lesions are genotypically heterogeneous, both among different lesions (interlesional heterogeneity) and within the

same lesion (intralesional heterogeneity)[35,36]. As a consequence, the treatment may be efficient for some metastatic nodules but not for others[1]. Third, the metastatic stroma alters the effect of conventional chemotherapeutics on tumour cells and thus reduces the effectiveness of the therapy[1]. Finally, metastases often have a tortuous vasculature and high blood pressure, reducing drug penetration[30]. All together, cytostatic tumour-targeted therapies are usually not efficient at limiting the spread and growth of metastasis, and do not improve the overall survival or progression-free survival of patients[30,37,38].

Nevertheless, metastatic disease could be controlled through the development of drugs that prevent metastatic dissemination, in particular during the haematogenous transit of tumour cells[39]. Indeed, most therapeutic agents reach the highest concentration in blood, thus they have the potential to affect disseminating tumour cells more than extravasated ones. Therefore, the study of molecular mechanisms of metastasis dissemination is of paramount importance.

1.1.3 The haematogenous metastatic cascade

Tumour cells follow a series of sequential and interrelated steps in order to colonise a distant organ: tumour cells de-adhere from the primary tumour, intravasate in the blood and/or lymphatic vessels, interact with cells in the circulation, attach to the endothelium of the target organ, extravasate in the host tissue, where they can remain dormant or proliferate to form micrometastases or macrometastases[1] (Figure 1.1). During all of these steps, tumour cells interact with other cell types, either directly or through released factors, which influence the invasiveness of tumour cells.

The haematogenous route of metastasis is the focus of the present research project and therefore will be discussed in this section. In particular, we will focus on the intravascular transit of tumour cells.

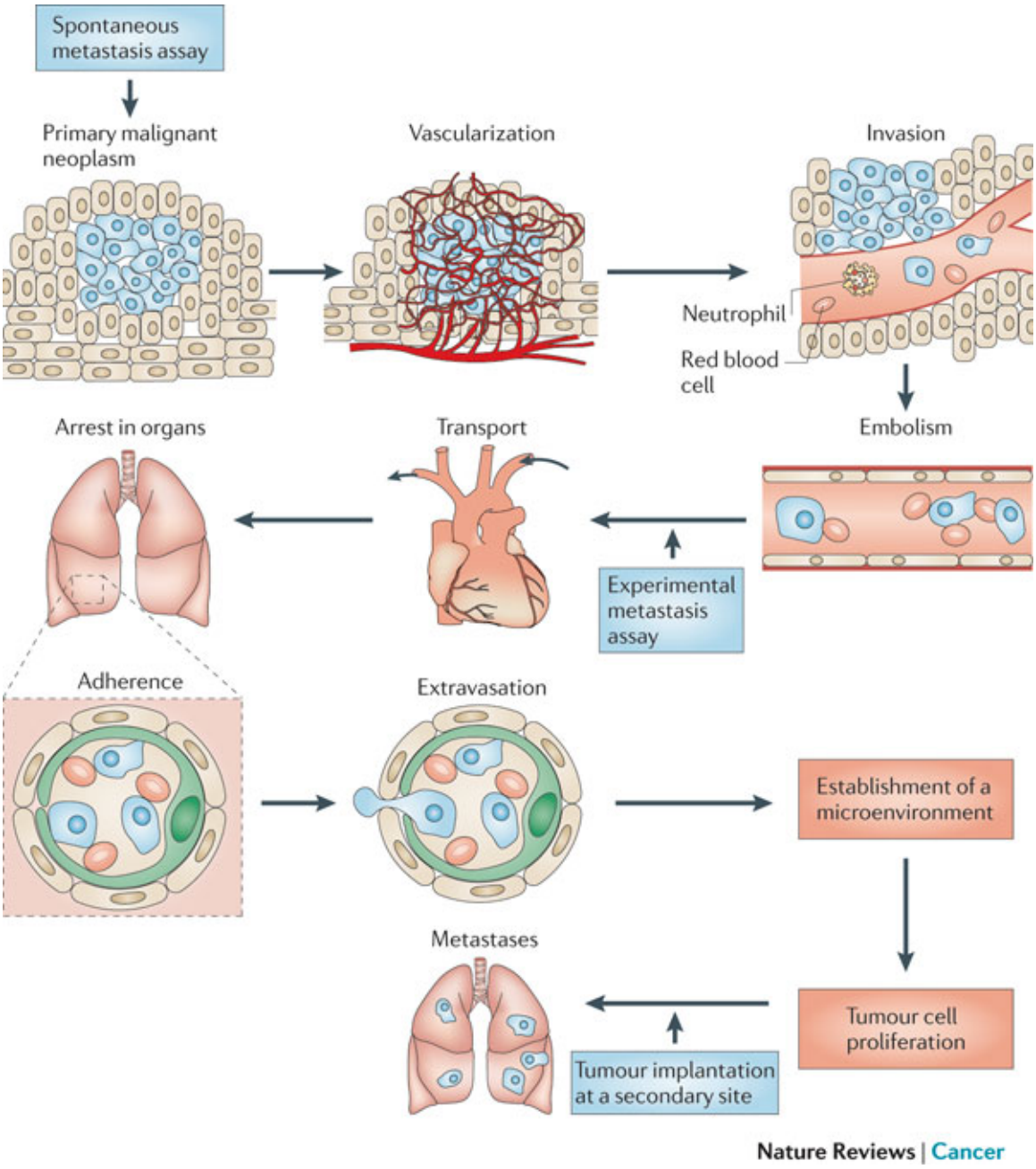

Figure 1.1 – The haematogenous metastatic cascade.

Cancer metastases develop through sequential and interlinked steps, collectively indicated as metastatic cascade. Tumour cells detach from the primary mass and embolise in the vasculature, where they interact with circulating cells such as platelets and leukocytes. After having survived in the circulation and adhered to the vasculature of a secondary organ, tumour cells extravasate and, upon persistent growth, they colonise the secondary site as micro- or macrometastases. Tumour cells can fail at each of these steps and be eliminated, contributing to metastatic inefficiency. Image obtained from Francia et al.[40] with permission.

1.1.3.1 Local invasion and intravasation

To invade the blood stream, tumour cells need to detach from the primary tumour and reach the proximal vessel.

In a tumour mass, tumour cells are constrained by junctions, such as adherens junctions (AJs), gap junctions, tight junctions (TJs) and desmosomes. In order to reach the vasculature, tumour cells disrupt these junctions by undergoing a transdifferentiation program called epithelial-to-mesenchymal transition (EMT)[41] through which cells with an epithelial phenotype, which is associated with cell-to-cell junctions, can acquire a mesenchymal and more invasive phenotype. The orchestration of the EMT program is driven by EMT-inducing transcription factors[42], such as Snail, Twist, Slug and zinc-finger E-box-binding (ZEB) factors[43,44], and the consequent deregulation of genes involved in tumour cell adhesion and motility (reviewed by [44]). For example, the downregulation or even repression of the expression of epithelial (E)-cadherin, a component of AJs, is considered a hallmark of EMT and is often accompanied by the overexpression of neuronal cadherin (N-cadherin). This phenomenon is termed cadherin-switch and is responsible for the acquisition of a mesenchymal phenotype. In this scenario, tumour cells lose the adhesion to epithelial cells expressing E-cadherin and acquire affinity to mesenchymal cells expressing N-cadherin[44].

Additionally, intravasating tumour cells undergo the rearrangement of actin cytoskeleton to assume a more round shape and form actin stress fibres, cellular structures that mediate the invasion and contractility of the cell[45]. Stress fibres and cytoskeleton rearrangement are controlled by RHO GTPases, a large family of proteins responsible for the activation of RHO-associated kinase (ROCK) and the subsequent actin polymerisation, myosin light chain phosphorylation, actomyosin contraction and cofilin (actin polymerisation inhibitor) inactivation. Due to their role in cell remodelling, RHO GTPases are tightly controlled during EMT and cell motility[44]. During EMT, the cadherin switch is responsible for the

activation of Rho GTPases Rac1 and Cdc41 and leads to a higher motility of tumour cells[46].

Several signalling pathways have been found to induce the activation of the EMT program, and the most characterised is TGF-ß family of proteins. These factors interact with their cognate type II TGF-ß family receptor (TßRII) and induce the assembly of SMAD complexes and their translocation into the nucleus, where they activate the expression of EMT-inducing transcription factors[44]. Additionally, TGF-ß proteins lead to the activation of RHO GTPases through the PAR6-mediated degradation of the inhibitor RHOA[44]. In this sense, the TGF-ß family acts as an orchestrator of cellular events involved in tumour cell intravasation and extravasation. It is believed that both signals from reactive stroma, either resident or recruited, and the presence of genetic and epigenetic makeup in receptive cells are responsible for the activation of latent EMT programs[42]. Macrophages are recruited to primary tumours through the release of colony stimulating factor 1 (CSF1) and are normally defined as Tumour Associated Macrophages (TAMs). These TAMs promote tumour cells intravasation both through soluble factors, such as TGF-ß, matrix remodelling proteases or tumour necrosis factor α (TNFα), or by direct contact, which induces the formation of invadopodia[47].

Tumour cells with a mesenchymal phenotype make their way towards neighbouring blood vessels. The entry of tumour cells in the vasculature is greatly promoted by angiogenic factors[48-50], which often lead to the generation of irregular and leaky vasculature that facilitates the direct entry of tumour cells in the circulation. Alternatively, tumour cells or associated stroma cells degrade the surrounding extracellular matrix (ECM) and basement membrane of the endothelium by expressing or releasing matrix remodelling enzymes, in particular matrix metalloproteinases (MMPs)[51,52]. Finally, tumour cells need to cross the endothelial barrier by disrupting cell-cell junctions in the endothelium. Although intravasation and extravasation take place at opposite sides of the endothelial barrier, it is

believed that similar mechanisms regulate transendothelial migration of tumour cells. Such mechanisms will be overviewed in the paragraph 1.1.3.1.

1.1.3.2 Circulating tumour cells

Once they enter blood vessels, tumour cells exist as circulating tumour cells (CTCs). The number of CTCs positively correlates with the advancement of cancer and development of metastasis[42,53-59].

CTCs have been detected both as single cells and, less frequently, as circulating tumour microemboli (CTM)[60,61], which could contain up to 50 CTCs. CTM derive from the concomitant intravasation of multiple cells at the primary site (collective cell invasion[62]), rather than aggregation in the circulation, and are characterised by the expression of plakoglobin, an adhesion molecule involved in tumour cell-cell adhesion[54]. CTMs are more likely to form metastasis than single CTCs. In fact, tumour cells in CTMs are protected against apoptosis and are more likely retained in capillaries, leading to the formation of metastasis[54]. Even when found as single cells, CTCs are usually associated with host cells such as platelets and immune cells. The interaction with these cells happens shortly after tumour cells intravasation and is known to support their survival and seeding of the secondary site (see section 1.1.4).

The majority of CTCs are characterised by a higher expression of mesenchymal markers[53], such as Twist1 and Snail1, and lower expression of E-cadherin than the primary tumour[63], consistent with their EMT transition during intravasation. However, in the blood of metastatic breast cancer patients, some CTCs were found to express just epithelial markers or a mixture of epithelial and mesenchymal markers. These cells were often present in clusters and associated with platelets[53]. It is believed that these cells undergo EMT within the circulation through the signalling of platelet-derived TGF-ß[18,53].

The half-life of CTCs is very short, estimated to be of 1 to 2.4 hours[64] and most intravenously injected CTCs die and are cleared during the first 24 hours[65,66]. Indeed, the circulatory system is a very hostile environment and circulating tumour cells are exposed to cell death through different mechanisms.

(1) CTCs contact with natural killer (NK) cells induces tumour cell death. The importance of NK anti-tumour response is shown by the fact that a high number of tumour infiltrating NK cells is associated with a better prognosis[67-69] and experimental NK depletion dramatically increases metastasis[70]. NK cells recognise tumour cells for their loss of major histocompatibility complex (MHC) class I ('missing self'), the expression of neoantigens ('non-self') or the upregulation of membrane proteins ('altered-self')[71]. NK-driven tumour cell death depends on the initiation of apoptosis or cytolysis through the release of cytotoxic granules[72,73], direct interaction of death receptors with their ligand on tumour cells[74 74-76] and secretion of IFN-γ, a known tumour suppressor molecule[77-79].

(2) CTCs can undergo cell death due to their presence in a suspension environment. Anoikis is a particular type of apoptosis induced by the absence of attachment to other cells or to the extracellular matrix (ECM), which culminates with the activation of caspase-3 and the subsequent cell death. The activation of the anoikis program can be triggered by the interruption of integrin interaction with ECM proteins or integrin receptors on other cells, which is necessary for the activation of pro-survival signalling cascades[80-83]. Concomitantly, the disengagement of cell contacts induces both an intrinsic pathway of anoikis, involving the release of cytochrome c from the mitochondria, and an extrinsic pathway of anoikis, involving the activation of apoptotic signalling downstream to tumour necrosis factor receptor (TNFR) superfamily[83]. The acquisition of an EMT phenotype and, particularly, the overexpression of EMT-inducing transcription factors has been implicated with anoikis resistance[84-86]. Moreover, the migration of

tumour cells in CTM might provide cell-cell adhesion signalling that protect tumour cells from anoikis, an observation that could motivate the higher apoptosis resistance of CTMs in comparison to CTCs.

(3) Haemodynamic shear forces can induce mechanical damage and tumour cell death[66,87]. The exposure of tumour cells to fluid shear stress increases their sensitivity to apoptosis induced by TNF-related apoptosis-inducing ligand (TRAIL), which is normally expressed by NK cells[88], and induced cell cycle arrest through a Smad-dependent mechanism[89].

The survival of CTCs in the circulation and the establishment of metastastatic lung nodules depend in part on intrinsic features of tumour cells. The comparison of gene expression profiles between CTCs and the primary tumour has revealed that metastatic clones possess a protein signature that makes them more adapted to colonise a distant organ. Such metastatic signatures are unlikely to develop during the haematogenous transit of CTCs and are most likely present (and then selected) in the primary tumour. Metastatic signatures comprise proteins involved in tumour cell response to growth factors (EGFR and HER2)[90], infiltrative functions (MMP1, fascin-1 and heparinase), metabolic pathways (PGC-1α)[63] and cytoskeletal remodelling (Myc/PI2KA, Ras and ROCK)[66]. Moreover, the expression of some integrins (i.e. αvß3[91,92] or αvß5[93]) and the downregulation of others (i.e. ß4[94] or αvß6[93]), a phenomenon known as integrin switch, might confer tumour cells an anoikis-resistant phenotype[83]. The interaction with the metastatic niche can also provide the survival signals necessary for tumour cell survival and colonisation, as discussed in the next sections.

1.1.3.3 Interaction with platelets

1.1.3.3.1 Platelet physiology

Platelets are small blood cell fragments of 2-3 μm in diameter and 7-9 fL in volume, with a distinctive discoidal shape and lack of nucleus, and represent the most abundant cell type in the circulation (150-1400x10^9 platelets per litre in humans and 1100x10^6 platelets per millilitre in mice[95]). Being anucleate, platelets have a very short life span of 8-10 days (in humans) and, in order to maintain the correct platelet count, new platelets need to be produced every day from myeloid precursor called megakaryocytes[96]. A distinctive trait of platelets is the presence of a high number of cytoplasmatic storage granules, classified as alpha- (α-) or dense-granules (Figure 1.2). α-granules are spherical structures with a diameter of 200-500 nm and are the most numerous type of vesicles. They contain essential proteins involved in platelet adhesion, recruitment of immune cells[97] and angiogenesis[98] Dense granules (also referred to as dense bodies or δ-granules) are smaller structures (250 nm in diameter) with highly dense cores that store low molecular weight molecules involved in activation and recruitment of other platelets to the site of damage[99].

The main function of platelets is to form an aggregate, defined as thrombus. Upon agonist stimulation, platelets undergo activation, a complex cellular process associated with a conformational change of membrane integrin $\alpha_{IIb}ß_3$ (also called glycoprotein [GP] IIa/IIIb) from a resting to an activated state ('inside-out signalling') and a Rho GTPase-dependent cytoskeletal rearrangement[100]. These events lead to the increase of platelets adhesion, the change of shape with production of filopodia and lamellipodia, and the release of the granules content in a process called degranulation. Agonists of platelet activation can be categorised as initial mediators (collagen and von Willebrand Factor, vWF) and second-wave mediators (such as adenosine diphosphate [ADP], thromboxane A_2, thrombin and epinephrine).

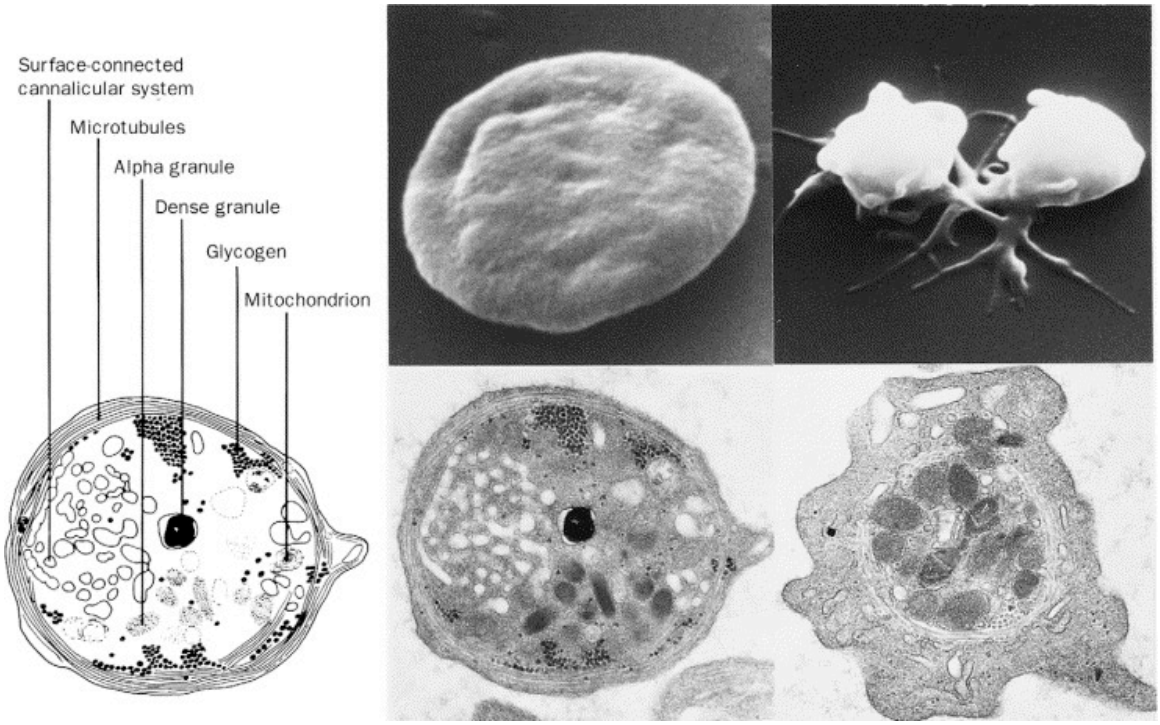

Figure 1.2 – Platelet structure.

Electron micrographs of platelets in their resting and activated state. Resting platelets (left) present a discoidal shape and numerous intracellular granules, classified as α-granules and dense-granules. Activated platelets (right) are characterised by the formation of long pseudopodia, the rearrangement of the cytoskeleton and the release of intracellular granules (degranulation). Image obtained from George et al.[101] with permission.

Platelets play a central role during haemostasis, a process through which vessel injury is repaired to maintain the integrity of the vascular system. Haemostasis involves two parallel and interrelated processes at the site of damage: thrombosis, which is the formation of a platelet aggregate (thrombus), and coagulation, a cascade of cell activation and proteolytic reactions involving different cell types (endothelial cells, platelets and leukocytes) and soluble proteins (coagulation factors). In particular, coagulation factors are enzymes with serine protease activity that exist in the circulation as inactive zimogens and undergo activation through proteolytic cleavage[102]. These processes lead to the formation of a (fibrin) clot, a plug of platelets and fibrin mesh (Figure 1.3).

1.1.3.3.2 Interaction of platelets with tumour cells

By mimicrying some steps of haemostasis, tumour cells are able to interact with circulating platelets during their haematogenous transit, a process referred to as Tumour Cell-Induced Platelet Aggregation (TCIPA). The association of platelets with tumour cells happens as early as after 1 minute from their intravasation[103], when they are in the circulation phase or shortly after entrapment in the capillary bed. The formation of platelet-tumour cell aggregates is very rapid, and aggregates decrease in size over the following 21 hours[103].

The interaction of tumour cells with platelets is driven by different mechanisms (Figure 1.3).

1.1.3.3.2.1 Expression of pro-coagulant factors

Tumour cells express haemostatic factors, such as tissue factor (TF), which is the main activator of the coagulation cascade *in vivo*[104]. TF (also known as CD142 or thromboplastin) is a 47 kDa transmembrane glycoprotein[105]. In physiological conditions, TF is expressed by cells adjacent to the vessel wall, such as smooth muscle cells, fibroblasts, pericytes, keratinocytes, astrocytes and myocytes, and is exposed by vessel injury[105,106]. Alternatively, its expression can be induced in monocytes and endothelial cells[107-111] upon different stimuli, such as tumour cell-derived inflammatory interleukin (IL)-1 and TNF-α[105,112], creating a pro-thrombotic environment.

When exposed to blood, TF initiates the extrinsic pathway of coagulation (Figure 1.3). TF binds to the coagulation factor VII and activates it to VIIa, forming a bimolecular complex

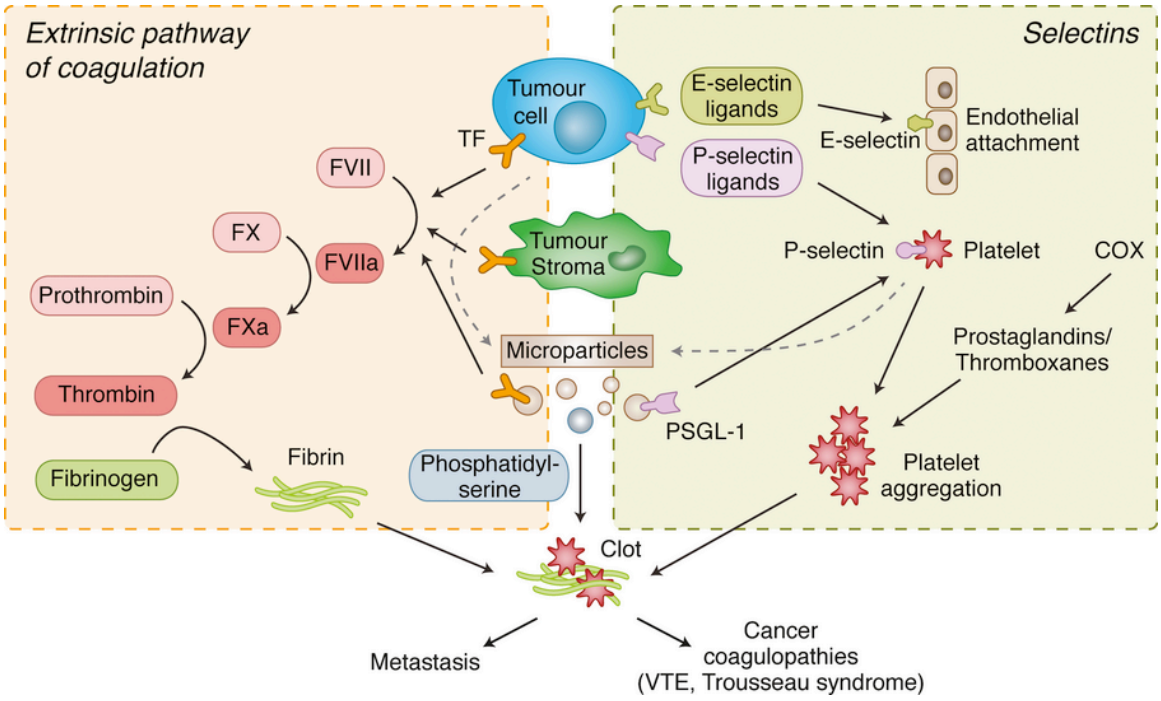

Figure 1.3 – Platelets interact with tumour cells through multiple mechanisms.

Tumour cells engage platelet aggregation through multiple pathways. On the left, TF on the surface of tumour cells, stroma or microparticles activates the extrinsic pathway of coagulation, which induces platelet aggregation and the deposition of a fibrin clot. On the right, tumour cells and microparticles express P-selectin ligands (e.g. PSGL-1) that promotes the direct interaction of tumour cells with platelets and platelet activation. Image obtained from Gil-Bernabé et al.[113] with permission.

(TF-VIIa). The complex TF-VIIa activates a cascade of proteolytic reactions and cell activation that ultimately leads to the activation of thrombin and fibrin deposition[102]. Thrombin cleaves protease activated receptor (PAR)-1 (in humans) and PAR-4 (in mice) on platelets and triggers platelets activation and change of shape[114]. Activated platelets express the high affinity form of integrin $\alpha_{IIb}ß_3$ and bind to fibrin, which also binds integrin $\alpha_v ß_3$ on tumour cells leading to the formation of platelets-fibrin microclots on tumour cells[106]. Thus, the expression of integrin $ß_3$ both on tumour cells and on platelets is necessary to form TF-dependent interactions[115]. Interestingly, $\alpha_v ß_3$ integrin exists in low-

and high-affinity states, but only the high-affinity form mediates the interaction of tumour cells with platelets and is found in tumour cells with higher metastatic potential[115].

1.1.3.3.2.2 Expression of adhesion molecules

Tumour cells express adhesion proteins that mediate the direct association with platelets. This is the case of P-selectin glycoprotein ligand-1 (PSGL-1), which interacts with P-selectin expressed on activated platelets[113,116]. *Per se*, PSGL-1 on tumour cells can interact with platelets but cannot directly activate them. However, evidence from P-selectin- or PSGL-1-null mice suggests that it is involved in fibrin generation[117] and couples with TF to initiate coagulation[118]. Thus, the direct association of tumour cells with platelets through P-selecting-PSGL1 interaction is sufficient to induce platelet activation[119]. It is believed that PSGL-1 stimulation on leukocytes induces their expression of TF and the release of TF-expressing microparticles, which takes part in PSGL-1 mediated platelet aggregation[118,120].

Additionally, different tumour cell lines, in particular carcinomas, present surface mucins that induce the formation of platelet microthrombi. This process seems to depend on the concomitant interaction of mucins with platelets P-selectin and neutrophil L-selectin and the induction of platelet activation by neutrophil-derived agonists[121].

1.1.3.3.2.3 Shedding of pro-coagulant microparticles

In addition to high expression of TF in tumour biopsies, cancer patients present high levels of circulating TF, in particular during advanced stages of disease and after chemotherapy or radiotherapy[122]. This phenomenon may be explained by the presence in the circulation of pro-coagulant microparticles (MPs), small membrane vesicles released by tumour cells and other stroma cells, such as activated monocytes and endothelial cells.

These particles express TF[123,124], PSGL-1[125] and phospahtidilserine[116] on their membranes and contribute to the hypercoagulable state by accumulating in proximity of tumour cells-platelets microemboli, where they further increase thrombin and fibrin generation.

Although pro-thrombotic MPs have been correlated with thrombotic risk and cancer progression, the mechanism of their contribution to metastasis and their potential use as biomarkers remain to be established.

1.1.3.3.2.4 Release of procoagulant factors

Tumour cells can also induce platelet activation, and subsequently aggregation, through the release of soluble pro-aggregant factors. For example, tumour cell-derived ADP can induce platelet activation and a conformational change of integrins to a high-affinity state towards fibrin, increasing the interaction with tumour cells. On the other hand, tumour cells release TNF-α, which induce the overexpression of TF by adjacent endothelial cells or monocytes and thus increase local coagulation[126].

1.1.3.4 Adhesion to the endothelium

As described in section 1.1.1, it is currently believed that the initial entrapment of tumour cells in the vasculature of a secondary organ is mainly dependent on the circulatory patterns downstream to the primary tumour. This is particularly true in the case of pulmonary circulation, where tumour cells, similarly to leukocytes, can get physically entrapped in the capillaries due to size restriction[127] (tethering), a process that is promoted by the formation of CTMs and tumour cells-platelets emboli. However, evidence indicate that tumour cells can arrest in vessels larger than their size, in particular in

pulmonary pre-capillaries arteries and portal venules[128], suggesting the existence of receptor-ligand interactions.

The initial arrest and subsequent adhesion of tumour cells is mediated by the expression of adhesion molecules by endothelial cells, in a process called endothelial (cell) activation. In basal conditions, the endothelium exists in a quiescent state where thrombotic, inflammatory and adhesive functions are repressed. Upon vascular injury, inflammation or infection, endothelial cells undergo activation and locally synthesise or expose adhesion molecules to generate local adhesion foci for platelets and leukocytes[129]. Hence, these proteins are collectively referred to as endothelial cell leukocyte adhesion molecules (ELAMs). In the context of metastasis, tumour cells have employed similar mechanisms to trigger endothelial activation and form stable adhesions. Factors derived from activated platelets, tumour cells and myeloid cells trigger ELAM expression and exposure.

Similarly to leukocytes, the adhesion of tumour cells to the vascular wall is a multistep process that involves the sequential expression of adhesion molecules and their ligands.

1.1.3.4.1 Initial arrest (selectins)

The initial arrest of tumour cells is mediated by the expression of selectins and selectin ligands. Selectins are a family of type-I transmembrane adhesion molecules with a conserved lectin domain and can recognise glycoconjugates containing constant moieties (Lewis x and Lewis tetrasaccharide sialyl groups)[130]. Specific selectins and selectin ligands are expressed by leukocytes, endothelial cells, platelets and some tumour cells; their expression is tightly regulated by both transcriptional regulation, exocytosis of intracellular granules and proteolytic cleavage in order to avoid deleterious thrombosis or leukocyte recruitment. There are three members of the selectin family, E-, L- and P-selectin. Endothelial cells (in mouse only) and platelets constitutively express P-selectin, which is rapidly translocated to their membrane upon exocytosis of Weibel-Palade bodies

(in endothelial cells) or α-granules (in platelets) during vascular injury, inflammation or tumour cell stimuli[131,132]. In this activated status, P-selectin on endothelial cells and platelets can interact with PSGL-1 and CD44 (in particular its variant CD44v) on tumour cells[133,134]. Additionally, the exocytosis of Weibel-Palade bodies in endothelial cells induces the exposure of vWF, which is bound by $\alpha_{IIb}ß_3$ and GPIb-IX-V on platelets associated with tumour cells[135].

On the other hand, E-selectin can be found exclusively on endothelial cells and its *de novo* transcription is induced upon pro-inflammatory stimuli (e.g. IL-1α, IL-1ß and TNF-α), shear stress or vascular injury[136-138]. Additionally, tumour cells and activated platelets induce E-selectin expression through soluble factors (TNF-α, CCL2, CCL3, CCL5, CCL7 and Gro-α)[139-142], thrombin generation[132] and other cytokines contained in tumour cell-conditioned medium[129]. Cancer cells express numerous ligands for endothelial E-selectin, including HCELL (a sialofucosylated glycoform of CD44), PSGL-1, E-selectin ligand 1, mucin 1 (MUC1) and galectin-3-binding protein (LGALS3BP)[143-145].

The expression of selectin ligands on leukocytes mediates their rolling along the vascular wall, a process necessary to reduce their velocity and arrest on the activated vascular wall. Rolling is achieved through the rapid establishment and disengagement of selectin-selectin ligands interactions under shear flow forces. Although tumour cell rolling can be visualised *in vitro*, proofs that a similar mechanism happens *in vivo* are still tenuous. In support of this, some of the adhesion molecules involved in tumour cells or leukocytes adhesion differ, suggesting the existence of alternative mechanisms[144].

1.1.3.4.2 Firm adhesion (integrins)

Selectin-mediated adhesion of leukocytes, platelets and tumour cells to the vascular wall is transient and susceptible to shear stress and more stable interaction need to be formed in order to undertake diapedesis. A firmer adhesion is achieved through the expression on

endothelial cells of a second set of ELAMs, mainly (but not exclusively[144,146]) represented by integrin ligands. The principal endothelial integrin ligands are vascular cell adhesion molecule 1 (VCAM-1) and intercellular adhesion molecule 1 (ICAM-1). VCAM-1 expression is limited to activated endothelial cells and some BMDCs and, during inflammation or vascular injury, it serves as a docking point for circulating leukocytes by directly binding their surface ligands integrin $\alpha_4ß_1$ (also called VLA-4) and integrin $\alpha_4ß_7$. Similarly, ICAM-1 mediates the binding of leukocytes via integrin $\alpha_Lß_2$, also called LFA-1[147].

Through a similar mechanism, tumour cells can directly interact with VCAM-1 through the expression of integrin $\alpha_4ß_1$/VLA-4[148-150] and ICAM-1 through integrin $\alpha_Lß_2$/LFA-1[147] and MUC1[151]. Other integrins (e.g. $ß_3$, $ß_6$, $\alpha_vß_3$, $\alpha_6ß_4$) are also essential for the interaction of tumour cells with the endothelium[152-154]. Thus, it appears the direct interaction of tumour cells with the vascular wall is responsible for the establishment of stable adhesion. However, the association of platelets and the subsequent recruitment of immune cells is still necessary for the successful engraftment of metastatic cells[103].

1.1.3.5 Interaction with myeloid cells

Early after the intravasation, tumour cells-platelets microemboli start interacting with circulating BMDCs belonging to the myeloid lineage, mainly neutrophils and macrophages. Both monocytes and neutrophils derive from a shared hematopoietic myeloid progenitor, the myeloblast, in response to different stimuli from the bone marrow niche[155-157].

1.1.3.5.1 Neutrophils

Neutrophils (also called polymorphonuclear neutrophils or PMNs) are circulating leukocytes that belong to the granulocyte branch of the innate immune system and oversee immune and pro-inflammatory functions. Upon inflammation or infection, neutrophils are rapidly recruited from the bone marrow and the circulation to the site of damage, where they tether and undergo diapedesis. Here they kill invading pathogens through multiple mechanisms[158] and activate an acute inflammatory response through the release of cytokines and the engagement of the adaptive immune system[159].

In the context of haematogenous metastasis, neutrophils are recruited to disseminating tumour cells[103]. Tumour cells and activated endothelial cells directly attract neutrophils by secreting pro-inflammatory IL-8/CXCL8[160-162]. Additionally, tumour cells recruit neutrophils through chemoattractants released by platelets aggregates on their surface, such as CXCL5 and CXCL7[103]. Neutrophils start rolling on activated endothelium through interaction of their L-selectin and PSGL-1 with PSGL-1 and E-/P-selectin, respectively, on endothelial cells[148133]. These bonds are transient and do not prevent the detachment of neutrophils by sheer stress, yet they bring CTCs and neutrophils in closer proximity. IL-8 induces the upregulation and activation of $ß_2$ integrins (such as $\alpha_M ß_2$ integrin, also called MAC1) in neutrophils, which allow the establishment of stronger and sheer-resistant bonds with ICAM-1 and VCAM-1 on tumour cells, activated endothelium and to components of the coagulation cascade[160,162-165]. Both physical interaction and soluble factors released by tumour cells potentiates IL-8 generation, and subsequently MAC1 expression by neutrophils[166]. Thus, tumour cells, endothelial cells and neutrophils interrelate through a positive feedback loop that potentiates activation and adhesion, mainly through IL-8 signalling.

1.1.3.5.2 Monocytes

1.1.3.5.2.1 Physiology of monocytes

Monocytes are a population of undifferentiated blood-borne BMDCs that belong to the mononuclear phagocyte system of the innate immunity. After a short time in the blood circulation (one day in mice[167]) monocytes infiltrate tissues where they differentiate into tissue macrophages or more specialised myeloid dendritic cells (DCs) lineages. Macrophages are tissue resident cells whose main role is to recognise and phagocyte pathogens. Apart from general tasks, tissue-specific macrophages oversee specialised functions that are induced by the specific microenvironment that they encounter: alveolar macrophages in lungs, Kupffer cells in liver, osteoclasts in bone and microglia in brain[168]. On the other hand, DCs are more specialised phagocytic cells with antigen-presenting abilities. DCs are recruited to areas of infection, where they differentiate into antigen presenting DCs, expressing MHC class II molecules and higher levels of CD11c. These cells subsequently migrate to draining lymph nodes where they stimulate naïve CD8+ T cells to proliferate, engaging the acquired immune response[169].

Macrophages and DCs derive from the differentiation of the same monocytic precursors. The recruitment to a particular organ and the direction of monocytes differentiation are dictated by the microenvironment that they encounter. Both human and mouse monocytes can be classified into two subsets according to marker expression. Resident monocytes ($CCR2^{-}CD26L^{-}Cx3CR1^{high}Ly6C^{-}$ in mouse and $CD14^{+}CD16^{+}$ in humans)[168,170] are longer-lived cells that home towards peripheral non-inflamed organs such as lung, liver, spleen and brain. This homing is dependent on the interaction with Cx_3CR1 ligand (fraktaline or Cx_3CL1)[171] or tissue-specific ligands adhesion molecules on endothelial cells[172]. Resident monocytes can differentiate into resident macrophages and DCs, both *in vitro* and *in vivo*[168], or remain in the circulation as patrolling monocytes[173].

Inflammatory monocytes ($CCR2^{+}CD62L^{+}Cx3CR1^{low}Ly6C^{+}$ in mouse and $CD14^{high}CD16^{-}$ in humans)[168,170] represent the second subset of blood borne monocytes. These cells migrate towards gradients of CCL2, also known as chemoattractant monocyte chemotactic protein (MCP-1), normally released in areas of local inflammation, and bind to CD34 on activated endothelial cells[168,171,174]. Once recruited to an inflamed tissue, these inflammatory monocytes are more likely to differentiate into DCs [171].

These two subtypes of monocytes do not independently differentiate from the myeloblast; instead $Ly6C^{-}$ resident monocytes derive from the phenotypic differentiation of $Ly6C^{+}$ inflammatory monocytes through an intermediate $Ly6C^{med}$ state[175]. It is believed that these intermediate monocytes are recruited to sites of inflammation and can differentiate into both macrophages and, primarily, DCs[168].

1.1.3.5.2.2 Interaction of monocytes with tumour cells

In the context of haematogenous metastasis, the recruitment of monocytes to disseminating tumour cells is the result of a network of cellular interactions and cytokine release. Tumour, endothelial and platelets can directly attract monocytes/macrophages by releasing MCP-1/CCL2[166,176], which interacts with CCR2 receptor expressed by monocytes/macrophages[176]. The importance of CCL2-CCR2 signalling for the recruitment of monocytes to tumour cells is highlighted by the fact that anti-CCL2 treatment dramatically reduces the formation of lung metastases[176]. It is believed that CCL2 synthesis by tumour cells happens after the arrest in the vasculature of the target organ, when the interaction of tumour cells with platelets induces the activation of the NF-κB pathway and the consequent release of CCL2[18].

Additionally, some tumour cells have the ability to secrete colony stimulating factor (CSF-1, also indicated as monocytes CSF or M-CSF). CSF-1 is a growth factor that recruits monocytes, and its interaction with CSF-1R on monocytes triggers a signalling cascade

involving phosphoinositide 3-kinase (Pi3K), extracellular-signalling-regulated kinase (ERK) and Sp1, leading to the regulation of different genes. In the context of metastasis, monocytes respond to CSF-1 stimulation by differentiating into an invasion-promoting phenotype (similar to tumour-associated macrophages or TAMs), which have multiple pro-metastatic functions[177]. Moreover, CSF-1 inhibits the maturation of monocytes to dendritic cells, which would activate an immune response against tumour cells. It is not surprising that a high expression of CSF-1 can be found in several tumour samples and CSF-1 expression levels correlate with tumour grade and poor prognosis[178,179]. Moreover, CSF-1 deficiency in mice impairs metastasis[180].

Circulating monocytes can also arrest in the proximity of tumour cells through adhesion mechanisms that are physiologically adopted by activated endothelial cells to recruit leukocytes. Tumour cells have adapted to abnormally express VCAM-1[181-185] and ICAM-1[183], which bind to integrins $\alpha_4ß_{1/7}$ expressed by monocytes and macrophages, and their levels on tumour cells correlate with long term growth of lung metastases[181]. However, the depletion of VCAM-1 on tumour cells does not affect the interaction with monocytes *in vivo*[181], suggesting that redundant mechanisms of interaction are in place.

Finally, tumour cells can indirectly attract monocytes through platelets aggregated on their surface[26], in part due to their role in the activation of the endothelium[146]. Platelets are known to drive the recruitment of monocytes/macrophages and neutrophils through the release of factors contained in their alpha-granules, such as CXCL5/7, CCL2/MCP-1, CCL5/RANTES, IL-8 and others[103,135,186,187]. Additionally, platelet can engage tumour cells[18] or endothelial cells[119] to release chemoattractants. After recruitment, immune cells expressing PSGL-1 directly bind to P-selectin expressing platelets[186,188-190], an association that is stabilised by the activation of $ß_2$ integrins on leukocytes and the subsequent interaction with fribrinogen on activated platelets[187].

1.1.3.5.2.3 Kinetics of monocytes recruitment

Monocytes at diverse differentiation stages interact with tumour cells at consequent phases of metastatic spread. Gil-Bernabé et al.[26] have described the recruitment of a subset of undifferentiated monocytes/macrophages ($CD11b^{+}F4/80^{+}CX_3CR1^{+}CD11c^{-}Ly6C^{-}$) to disseminating tumour cells. This recruitment depends on the TF-dependent engagement of the coagulation cascade, leading to the deposition of clots on the surface of tumour cells that establish direct interaction with the monocytes. The clustering of monocytes/macrophages with tumour cells-platelets aggregates takes place within the vasculature from 2 hours after tumour cell introduction and reaches its maximum at 8 hours. The recruitment of these myeloid cells is promoted by the release of CCL-5 by activated endothelial cells and their expression of the adhesion molecules VCAM-1, vascular adhesion protein-1 (VAP-1) and E-selectin, all induced by clots on tumour cells[119,146]. Tumour cell-clots-monocyte clusters are dissolved after 24 hours, suggesting that these patrolling monocytes support very early phases of metastasis[26]. During the time when tumour cells are adhered to the lung vasculature, a second wave of inflammatory monocytes are recruited by tumour cells through a CCL2-CCR2 signalling[176]. After diapedesis, these monocytes differentiate into metastasis-associated macrophages (MAMs), characterised by an inflammatory phenotype ($F4/80^{+}CSF1\text{-}R^{+}CD11b^{+}$ $Ly6C^{-}$ $CX_3CR1^{high}CCR2^{high}$)[29]. These MAMs localised on the other side of the vascular wall are recruited to the proximity of extravasating tumour cells within 24 to 72 hours after injection of tumour cells, correlating with their contribution to tumour cell extravasation and initial growth[29].

1.1.3.6 Transendothelial migration

After their intravascular arrest, tumour cells reach the secondary site by crossing the endothelial barrier in a process called transendothelial migration (TEM) or diapedesis,

which has many similarities to the extravasation of leukocytes during inflammatory responses[191]. Together with arrest and adhesion to the endothelium, TEM is normally considered a part of the extravasation process, which is essential for the escape of tumour cells from the hostile environment of blood circulation.

Tumour cell TEM can occur through two routes: paracellular and transcellular. Transcellular TEM involves the passage of tumour cells through the body of an endothelial cell. Although this process is employed by leukocyte during diapedesis[192], it seems that tumour cells employ this route only marginally and *in vitro*[193,194]. Paracellular TEM involves the passage of tumour cells between endothelial cells and requires the disruption of endothelium integrity. *In vivo*, the measurement of vascular permeability to imaging molecules[195] represents a surrogate method to measure endothelial integrity and correlates with tumour cell extravasation.

Several mechanisms have been proposed for the increase of vascular permeability in metastasis, including both traits of the tumour cells and the crosstalk with other cell types in the metastasis microenvironment.

(1) Tumour cells can induce the disruption of endothelial cell junctions. TJs are made up by numerous families of integral transmembrane, anchoring and regulatory proteins[196,197], which form adhesion plaques that mediate both adhesion and paracellular permeability[198]. Among others, the expression of Claudin 5 is restricted to endothelial TJs[199]. On the other hand, AJs serve to maintain physical association and cellular polarity of endothelial cells and are built by transmembrane, anchoring and regulating proteins[196,197]. In particular, VE-cadherin (also known as CD144 or CDH5), bound to ß-catenin, is a specific component of endothelial AJs junctions[197]. Tumour cells and other associated cells can affect the integrity of endothelial cells junctions. The release of soluble factors such as vascular endothelial growth factor (VEGF) and TGF-ß1 by tumour

cells or associated platelets and monocytes/macrophages induces the phosphorylation of the adhesion proteins zonula occludens (ZO)-1 and -2, occludin, claudin-5 and de-phosphorylation of VE-cadherin, leading to the opening of TJs and AJs[197,200]. Additionally, the release of angiopoietin-like protein 4 (Angptl4) by TGF-ß-induced tumour cells promotes the disruption of both TJs and AJs, leading to a higher tumour cells extravasation[17]. Also, tumour cell-[201-203] or platelet-derived[201] 12(S)-HETE, a product of arachidonic acid metabolism, induces endothelial cell retraction. It has been postulated that 12(S)-HETE might be directly transferred between tumour cells and endothelium through the formation of gap junctions shortly after their interaction[204]. Other cytokines, such as CXCL12 and CCL2[205], have been found involved in the increase of vascular permeability *in vivo*, although the underlying mechanisms have not been fully elucidated.

(2) Endothelial cell retraction can be induced by cytoskeletal rearrangement in endothelial cells. VEGF[200] and 12(S)-HETE[206], derived from tumour cells or associated cells, induce the phosphorylation of cytoskeletal proteins, the formation of stress fibers[206] and the redistribution of actin fibres towards the centre of the cells[200]. Moreover, direct contact of tumour cells with the endothelium activates ROCK, p38 and ERK MAPKs[207,208] in endothelial cells and induces the assembly of stress fibers[208,209], phosphorylation of myosin light chain (MLC)[208] and tropomyosin 1 (TPM1)[209] and disruption of VE-cadherin junctions, all processes associated with endothelial cell retraction and vascular permeability *in vivo*[205].

(3) Tumour cells induce the irreversible retraction of endothelial cells by stimulating apoptosis[210] and necroptosis[211] of adjacent endothelial cells. In particular, the stimulation of necroptosis is due to the interaction of amyloid precursor protein (APP) on tumour cells and its receptor DR6 (also called tumour necrosis factor receptor superfamily 21 [TNFRSF21]) on endothelial cells, leading to cell death signalling in endothelial cells[211]. This allows the opening of the endothelial cells

barrier to the passage of tumour cells and, hypothetically, the release of pro-migratory molecules to intravascular cells.

The dynamic change of tumour cell shape seems to be essential for efficient extravasation. Tumour cells can extend protrusions called invadopodia, which form through the polymerisation of actin fibers at the leading edge[212]. In contrast to other membrane extensions, invadopodia are proteolytically active, as they release microvesicles expressing matrix-degrading proteases (in particular membrane type 1 metalloprotease, or MT-MMP1)[213,214]. RHO-family GTPases and ROCK play a central role in the regulation of cytoskeleton contraction and production of invasive protrusions[212]. Indeed, the inhibition of RHO GTPase cell division control protein 42 (CDC24)[215] and Rac1[152,216] reduces TEM of prostate cancer cells, affecting metastasis.

1.1.3.7 Colonisation of the secondary site and early metastasis progression

The ability to colonise a distant organ is the second most important rate-limiting step in the development of metastasis and it depends on the ability to invade the secondary site and sustain tumour growth. This process goes along with the generation of a metastatic niche that supports the survival and outgrowth of disseminated tumour cells (DTCs).

After tumour cells have trespassed the endothelial barrier, they need to move through the basement membrane and the organ ECM. Tumour cells supervise the reorganisation of the existing ECM. On the one hand, existing ECM components are degraded through the release of active proteases (MMPs, hydrolases, collagenases and Angpt2), which mediate the disruption of the basement membrane and the penetration of the tissue[16,20,27,145,217]. On the other hand, the constitution of the pre-existing ECM is modified through the deposition of new components[20,218,219] or the crosslinking of collagen fibres to promote the recruitment of BMDCs and invasion[27,220,221]. Both degradation and remodelling are

overseen by tumour cells, stroma cells and BMDCs. The latter can be recruited during the establishment of the pre-metastatic niche.

During dissemination, CTCs show a mesenchymal phenotype. Although this morphology might be important for the resistance to shear forces and the generation of invasive protrusion between endothelial cells, it might not be ideal for the proliferation in the secondary site. It has been postulated that invasive tumour cells might be able to revert the EMT program through a process defined as mesenchymal-to-epithelial transition (MET). Overall, it seems that the re-acquisition of E-cadherin expression and the regulation of cancer cell shape are at the core of EMT reversion. The levels of E-cadherin were found higher in metastatic nodules than in the primary tumour of cancer patients[222,223], with a positive correlation between E-cadherin expression and metastasis size[222]. E-cadherin expression is induced in metastasis-initiating cells through multiple mechanisms[224-226] and is associated with a higher invasivity at the secondary site, but low efficiency of intravasation in the primary tumour, compatible with the reversion of the EMT program[224]. The MET program can be induced by the microenvironment at the metastatic site. For instance, the exposure of breast tumour cells to hepatocytes induces the loss of methylation of E-cadherin promoter, inducing its expression[222]. Moreover, it has been postulated that TGF-ß signalling, which is known to induce E-cadherin expression[224,226], could derive from circulating platelets during tumour cells dissemination. Collectively, these data suggest that the reversion of EMT program takes place through signalling at the metastatic niche, rather than selection of cells with a more epithelial phenotype at the primary tumour.

Not all extravasated tumour cells will form overt metastasis. Indeed, more than half of patients with diagnosed ‘localised’ non small cell lung cancer present with DTCs in the bone marrow. The presence of DTCs correlates with poor prognosis[227], suggesting that metastatic dissemination starts early after the onset of the primary tumour. DTCs can remain alive within the secondary site for a variable period of time, normally referred to as

tumour cell dormancy[228]. These DTCs persist in a growth-arrested state that is promoted, maintained or inhibited by the metastatic niche. In the peri-vascular niche the endothelial basement membrane is a source of thrombospondin-1 (TSP-1), which promotes the growth arrest of tumour cells, while sprouting neovasculature promotes the reinitiation of growth through the release of TGF-ß1 and periostin[229]. Noticeably, dormant DTCs are resistant to most anti-tumour treatments, both in clinical and experimental studies, and thus represent important factors in metastatic relapse[230-233].

1.1.4 Contribution of the 'intravascular metastatic niche' to metastasis

1.1.4.1 Platelets

Cancer patients have an increased incidence of coagulopathies, such as venous thromboembolism (VTE), hypercoagulable state, platelets dysfunction and Trousseau syndrome[234,235]. This higher incidence of thrombosis, which is a major cause of death, can be linked to the generation of a pro-thrombotic state by tumour cells[236]. In fact, TF and PSGL-1 have been found constitutively expressed by most tumour cell lines, and TF levels in cancer biopsies correlate with the incidence of VTE. Additionally, TF expression by tumour cells correlate with the advancement of cancer[237-242] and can be upregulated up to 1000 folds in highly metastatic cells[238], where the expression correlates with metastatic potential[237,238,240,241]. Pro-thrombotic MPs expressing TF have also been associated with advanced stages of cancer, poor survival and metastasis[122]. These observations suggest a link between coagulation and metastasis.

The contribution of platelet aggregation and coagulation to metastasis has been known since mid-nineteenth century, when Trousseau noticed the presence of excessive blood clotting in patients with occult carcinoma. More recently, two seminal papers by Gasic et al.[243,244] recognised the requirement of platelets for the efficient formation of experimental metastasis. Since then, multiple experimental and clinical studies have reported the

correlation between thrombosis and metastasis development, where thrombocytopenia and loss of platelet activation correlate with a reduction of experimental and spontaneous metastasis[18,26,103,146,243-249]. In these studies, platelet defects were achieved through different approaches. On the one hand a platelets are stably depleted in transgenic mice deficient in $G\alpha_q$[245,250], GPIbα[251] or PAR-4[249], which make platelets unresponsive to agonist stimulation, or in NF-E2, a transcription factor required for megakaryocytes maturation[249]. The genetic depletion of platelets is often associated with embryonic lethality[252] and haemorrhage[253]. Alternatively, a transient thrombocytopenia is obtained through the use of chemical agents, such as neuraminidase[244,254,255], or antibody-induced platelet depletion, such as anti-GPIbα[103,256]. More indirectly, the interference of tumour cell interaction with platelets reduced metastatic efficiency, an effect that can be achieved by the depletion/block of TF[237,238,257-260], α_vß$_3$ integrin[115] or PSGL-1 (on tumour cells), α_{IIb}ß$_3$ integrin[247,248,261-263] or P-selectin[264,265] (on platelets). Metastasis can also be inhibited by a range of anti-coagulant drugs, such as inhibitors of thrombin[26,146,266-269], fibrin(ogen)[245,247], fibronectin[247], vWF[247] and NSAIDs.

The abnormal association of platelets on tumour cells can support metastasis through multiple mechanisms (Figure 1.4).

1.1.4.1.1 Survival in the circulation

Platelets aggregates can physically shield tumour cells from shear stress-induced cell death[87]. Moreover, the formation of interactions between tumour cells and platelets might prevent anoikis by inducing survival signals in tumour cells[135].

On the other hand, platelets protect tumour cells from the interaction with cytolytic NK cells and limit their elimination of tumour cells[70,245,257,270], an effect that is fibrinogen dependent[245]. This protection seems to depend both on the physical shielding of tumour cells by bound platelets[113,271] and fibrin[245,257] and to the release of soluble factors such as

TGF-ß and platelet-derived growth factor (PDGF)[272-274] that induce NK quiescence. In particular, platelet- or tumour-derived TGF-ß is responsible for the down-regulation of NKG2D receptor on NK cells, the reduction of NK cells degranulation and the reduction of IFN-γ secretion by NK cells[77,275], which are known mechanisms of NK anti-tumour immunity[276]. The anti-metastatic effect of NK cells happens during the intravascular phase of metastasis, approximately at 1 to 6 hours after tumour cell injection[270]. However, the

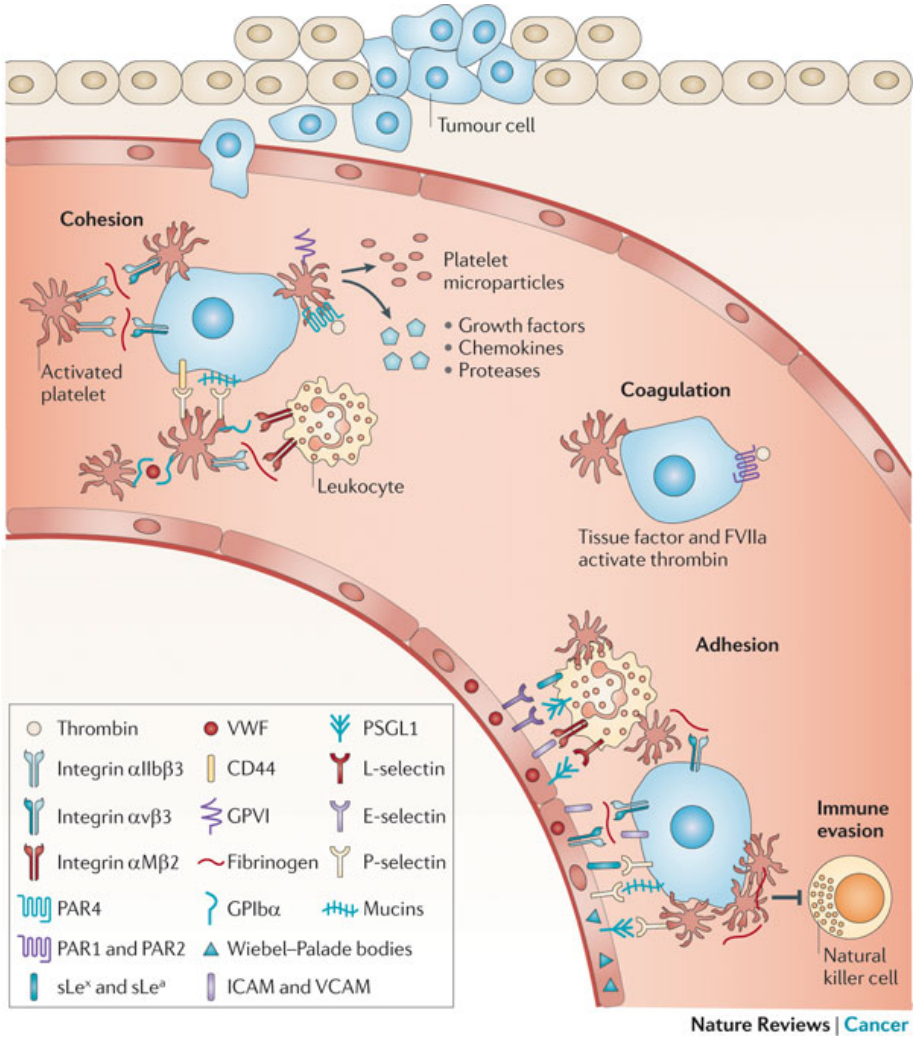

Figure 1.4 – The cross-talk between platelets and tumour cells supports metastasis.

Diagram depicting the cross-talk between platelets and circulating tumour cells during haematogenous transit. Platelets support metastasis through multiple mechanisms, such as physical protection, release of content of their granules and attachment to the endothelium. Subsequent steps of the haematogenous metastatic cascade are promoted by platelets, in particular survival, adhesion and immune cell recruitment. Image obtained from Gay et al.[135] with permission.

effect of platelets on the early survival of tumour cells does not only rely on their inhibition of NK cytotoxicity. Indeed, the knockdown of TF and thrombin in the absence of NK cell functions is sufficient to reduce the survival of tumour cells in the lung vasculature[245].

1.1.4.1.2 Initial arrest and adhesion

The initial arrest of tumour cells in the vasculature can be mediated by platelets. Indeed, platelets express adhesion molecules to the endothelium[277] and thus form adhesive bridges between tumour and endothelial cells. Interestingly, tumour cells expressing activated $\alpha_v ß_3$ integrin display a platelet-interactive phenotype and are more capable of arresting in a platelet-dependent manner and are thus positively selected from the primary tumour to form metastasis[115].

1.1.4.1.3 Interaction with monocytes/macrophages

Platelets promote the interaction of tumour cells with pro-metastatic myeloid cells. The direct link between platelet aggregates on tumour cells and the recruitment of immune cells in the lung vasculature has been shown by Gil-Bernabé et al.[26]. In this study, the inhibition of platelet aggregation on tumour was sufficient to abrogate the recruitment of a subset of monocytes/macrophages during the intravascular phase of metastasis. These monocytes/macrophages support tumour cell survival in the circulation and metastasis.

1.1.4.1.4 Tumour cell TEM

The extravasation of tumour cells is also facilitated by the interaction with platelets. Platelet activation and degranulation are associated with release of CCL2, PDGF, TGF-ß, 12(S)-HETE[201], EGF and VEGF[278] and insulin-growth factor 1 (IGF1), which are known triggers of endothelial cells retraction and vascular permeability[205,279]. In the case of

VEGF, this effect is due to the disruption of VE-cadherin-ß-catenin complex in AJs[278]. On the other hand, TGF-ß induces the disruption of TJs (ZO-1) and AJs (ß-catenin) of endothelial cells through the induction of ANGPTL4 in tumour cells[17]. The vascular leakage then exposes subendothelial matrix proteins like collagen and vWF, which are avidly recognised by platelets receptors $\alpha_2ß_1$, GPVI (for collagen) and GPIbα (for vWF)[135]. This interaction triggers another wave of platelet activation and release of pro-invasive factors. Platelet-derived TGF-ß also activates Smad signalling in tumour cells, inducing the engagement of EMT program by tumour cells[18].

1.1.4.1.5 Early colonisation of the secondary site

The interaction of tumour cells with platelets is temporary and extends for approximately one day, during the presence of tumour cells in the circulation[187]. However, platelets can activate signalling pathways that will promote metastasis after tumour cell extravasation, both dependent or independent on immune cells. Platelet-derived soluble factors or direct contacts induce tumour cell expression of pro-invasive factors, such as MMP9 and Serpin1[18,280]. Activated platelet also release factors involved in angiogenesis, such as VEGF, FGF, MMPs, TGF-ß and angiostatin[281].

1.1.4.1.6 TF-dependent pro-metastatic effects

Besides its role in inducing platelet aggregation, TF expression by tumour cells can also induce the activation of intracellular signalling cascades that support tumour cell adhesion[282,283], survival[284], migration[283,285,286] and angiogenesis[239,287], thus increasing metastatic potential. These pathways are activated by the TF-dependent generation of thrombin. In particular, thrombin generation leads to the cleavage of protease activated receptors (PAR), expressed on platelets (PAR-4), endothelial cells and tumour cells (PAR-1 and PAR-2)[113]. PAR-1 in tumour cells can also be activated in a thrombin-independent

manner through TF activation of factor VIIa/Xa and induction of an intracellular signalling which affects the early survival and arrest of tumour cells, even in the absence of active NK cells[257,288,289]. Thus, the expression of TF by tumour cells supports metastasis through multiple concomitant mechanisms, both dependent and independent on the haemostatic system.

1.1.4.2 Activated endothelium

The importance of endothelial activation to metastasis is highlighted by the fact that failure to establish interaction between tumour and endothelial cells affect metastasis. Indeed, the knockdown/depletion of CD44[290,291], integrin $\alpha_v ß_3$[90], integrin $\alpha_4 ß_1$/VLA-1[149,292,293] or cell surface mucins[264] on cancer cells reduced their metastatic ability and the expression of these molecules correlates with poor prognosis[294-296]. Similarly, the genetic depletion or pharmacological inhibition of P-selectin[133], E-selectin[121,297,298], VCAM-1, VAP-1[146] in host endothelial cells dramatically affect the onset of metastasis in different *in vivo* models. In particular, the disruption of VLA-4/VCAM-1 interaction affects metastasis from multiple tumour types, including melanoma, lymphoma, breast and lung carcinomas[146,149,292,293]. Moreover, heparin and their derivatives show a pronounced anti-metastatic effect due to both an anti-thrombotic effect and their activity in blocking P-selectin, VLA-4 and other integrins[299].

The inhibition of endothelial activation and the disruption of the interaction with tumour cells can affect metastasis through the impairment of tumour cells initial arrest and adhesion. Indeed, the inhibition of adhesion molecules on both tumour and endothelial cells reduces tumour cells arrest and adhesion[149,154,215,292,300-303]. More indirectly, the inhibition of platelet aggregation with tumour cells by different means reduced the adhesion of tumour cells to the endothelium[115,263,304,305].

However, activated endothelial cells can promote metastasis independently of their adhesion to tumour cells-platelets microemboli, by recruiting immune cells with pro-metastatic functions[119,146,181] (see next section). This recruitment depends on the expression of VCAM-1, vascular adhesion protein-1 (VAP-1) or E-selectin, which are known to mediate the homing of leukocytes[119,146,181,306,307], and on the release of chemoattractants (CCL5, CCL2/MCP-1) by activated endothelial cells[119]. CCL2-CCR2 signalling on endothelial cells has also been implicated in the enhancement of vascular permeability[205].

Additionally, the engagement of tumour cells on activated endothelium leads to the activation of intracellular signalling cascades that promote metastasis. VLA-4/VCAM-1 and E-selectin/E-selectin ligand interaction induces the release of MMP-2 and 9 by endothelial cells, followed by digestion of the tight junctions between endothelial cells, endothelial cell retraction and tumour cell extravasation[141].

1.1.4.3 Monocytes/macrophages

During their haematogenous transit, tumour cells interact with circulating precursors of macrophages, indicated as monocytes. Despite historical evidence that suggested an anti-metastatic effect of tumour cell-associated macrophages[308], there is now substantial evidence suggesting that the interaction of monocytes/macrophages with tumour cells in the circulation or at the metastatic site promotes metastasis. Evidence from animal models strongly supports this claim. The ablation of macrophages through genetic or pharmacological means affects the survival, seeding and growth of disseminating tumour cells[26,29,309-311], dramatically affecting metastasis. These observations are supported by clinical evidence indicating that a higher macrophage infiltration in tumours or regional lymph nodes negatively correlates with survival and prognosis[312,313] and is associated with the appearance of lung metastases[181]

Monocytes and macrophages at different differentiation stages support multiple steps of the metastatic cascade, through both soluble factors and direct contact with tumour cells and associated non-tumour cells. At the primary site, macrophages promote intravasation through the induction of a migratory phenotype in tumour cells [314,315], co-migration along invading tumour cells[316], deposition of collagen 'guides'[317] and secretion of proteases[318], which promote the movement of tumour cells towards the vasculature.

Within the circulation, monocytes/macrophages recruited to tumour cells promote tumour cell survival and metastatic seeding[26,119] and might support the invasion of the lung tissue by initiating a MET program in tumour cells[319]. Extravasating tumour cells recruit a subpopulation of inflammatory macrophages, distinct from resident macrophages, which maintain physical contact with tumour cells during TEM and initiation of growth. The recruitment of these MAMs is neutralised by the inhibition of CCL2-CCR2 signalling, which also promotes tumour cell seeding and growth[176]. The release of VEGF is thought to be responsible for the induction of vascular permeability and tumour cell extravasation[176]. Additionally, these inflammatory MAMs prevent early TRAIL-induced apoptosis of extravasated tumour cells through the interaction with VCAM-1 on tumour cells, which activates a PI3K/Akt pro-survival signalling pathway mediated by Ezrin[181]. The persistent growth of metastasis is further supported by MAMs expressing FLT1/VEGFR1 receptor, which is required for the expression of pro-metastatic CSF-1 and other pro-inflammatory mediators[311]. MAMs can also promote the invasion of the secondary organ through the release of MMP-9, which increase tissue permeability and the mobilisation of pro-angiogenic VEGF[16].

All together, these observations suggest a central role of monocytes and macrophages in the generation of a permissive microenvironment that promotes the establishment of metastasis, both during intravascular and extravascular phases. Thus, macrophages might represent promising therapeutic targets for the prevention or control of metastatic disease[320].

1.2 ASPIRIN

1.2.1 Aspirin, an historical perspective

Aspirin (commercial name of acetylsalicylic acid [ASA]) was first formulated in 1895 by the young chemist Felix Hoffman as a derivative of the white willow extract, salicylic acid. Salicylate had been used since the ancient Egypt in decoctions and, since 1874, as a drug with anti-pyretic, mild analgesic and anti-inflammatory properties[321]. However, this drug had a poor therapeutic efficacy and it was administered at relatively high doses, that were slowly metabolized and frequently led to the appearance of side effects[322]. In order to overcome the low efficacy of salicylic acid as a drug, Bayer research laboratories hired Felix Hoffman to develop a derivative of salicylate. In less than one year, Hoffman was able to synthetize an acetylated form of salicylic acid, where the acetyl group was added to the hydroxyl (-OH) group of the benzene ring. His commitment was due not only to a scientific interest, but also to personal reasons. In fact, Hoffman's father suffered from arthritis and could no longer be treated with salicylic acid due to its side effects. After the synthesis of aspirin, Hoffman's father became the first man to ever be administered aspirin, which proved to be effective and was brought to much larger clinical trials.

This new formulation was named as 'Aspirin' by Heinrich Dreser, the head pharmacologist of Bayer. Some reports maintain that this name derives from St Aspirinius, the patron saint against headaches, while others suggest that the name is the abbreviated version of the German 'Acetylspirsaüre', that indicates the acetylated form of the acid derived from meadowsweet (*Spirea* in the Linnaean system).[321]

After commercialization it became evident that aspirin shared similar pharmaceutical properties to salicylate, but it was 1.5 times more potent than its precursor and could be used at lower doses. Moreover, the metabolism of aspirin was faster and it was associated with lower levels of blood salicylate, an effect that was associated with less frequent side effects.[322]

Although it was introduced in clinical practice shortly after its commercialization, the mechanism of action of aspirin remained unknown until almost 100 years later, when Vane and colleagues noticed that aspirin inhibited the release of thromboxane A_2 (called at that time 'rabbit aorta contracting substance' or RCS) and other prostaglandins (PGs) in lungs of guinea pigs under anaphylaxis[323]. In 1971 these results were confirmed *in vitro* when Vane incubated lung tissue homogenate (known to produce PGs) with arachidonic acid and aspirin, finding that PG formation was reduced in a dose-dependent way by the drug[324]. In the same year, other seminal papers confirmed that aspirin inhibits PGs synthesis irrespective of species, tissue and administration route[325-327]. From the time of this discovery to the present the molecular details of aspirin mechanism of action have been elucidated and it is now clear that aspirin is a multifaceted drug, whose function go well beyond the anti-inflammatory purposes that drove Felix Hoffman's discovery.

1.2.2 Mechanism of action

Aspirin belongs to the family of non-steroidal anti-inflammatory drug whose effects are mediated by the inhibition of cyclooxygenase (COX). COX is an enzyme involved in the rate limiting steps of the biosynthesis of prostanoids, mediating the conversion of arachidonic acid into prostaglandin (PG) G_2 and then into PGH_2, the common precursor of prostanoids[328] (Figure 1.5). Prostanoids are a family of bioactive lipids that comprises prostaglandins (PGD_2, PGE_2, PGF_{2a}), thromboxane A_2 (TXA_2) and prostacyclin (PGI_2), and are synthesized by different PG synthases (PGS). Through their interaction with cognate receptors on target cells, prostanoids are mediators of many physiological and pathological functions.

There are two isoforms of COX, COX-1 and COX-2, and both of them are irreversibly inhibited by aspirin through the acetylation of serine residues in their catalytic site. The

affinity of COX-1 to aspirin is 10-100 times higher than that of COX-2[329], so higher doses are required to inhibit the latter.

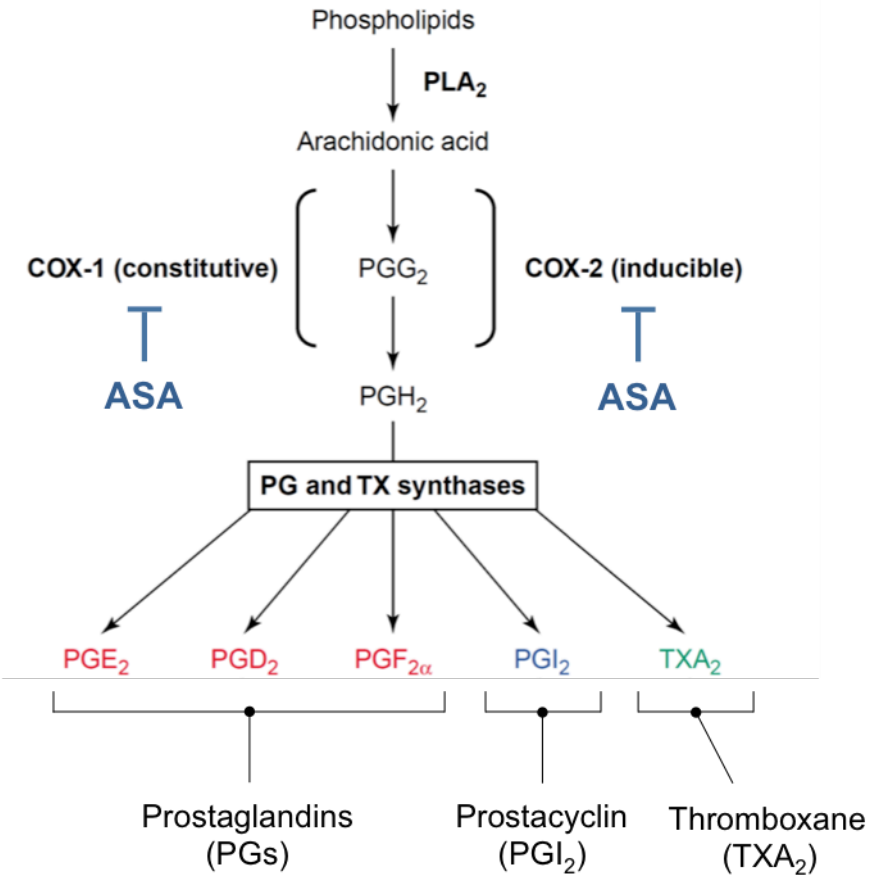

Figure 1.5 – Biosynthesis of prostanoids.

Upon platelet activation, arachidonic acid (AA) is released from the plasma membrane by phospholipase A_2 (PLA_2). AA is then converted into PGH_2 by COX-1 or COX-2 through a two-step catalytic reaction. PGH_2 is the common precursor of all prostanoids, a family of bioactive molecules including prostaglandins (PGs), prostacyclin (PGI_2) and thromboxane (TXA_2). The conversion of PGG_2 to PG, PGI_2 or TXA_2 products is mediated by selective synthases. Aspirin (ASA) irreversibly inhibits COX-1 and COX-2, thus reducing the synthesis of downstream prostanoids. Adapted from Iniguez et al.[330] with permission.

1.2.2.1 COX-1 and COX-2

1.2.2.1.1 Gene expression

COX-1 and COX-2, also indicated as Prostaglandin H Synthase (PGHS)-1 and -2, are encoded by different genes, called *PTGS1* and *PTGS2*.

PTGS1 is a 22 kb gene localised on chromosome 9[331]. Its TATA-less promoter contains multiple binding sites for transcription factors, which mediate its constitutive expression in a series of cell lines[332-334].

PTGS2 is a shorter gene (8.3 kb) localised on chromosome 1 which produces an mRNA product of 2.8 kb[331]. It works as an immediate-early gene and its expression is regulated by growth factors (IL-1, phorbol esters) and mediators of inflammation (TNFα, IL-6 and LPS)[332,335]. Several signalling pathways have been implicated in the regulation of *PTGS2* expression, for example NF-kB, C/EBP and P38/RK/Mpk2[331,332].

Due to the organisation of their promoters, COX-1 is constitutively expressed in many tissues and is the only isoform expressed in mature platelets[336]. On the contrary, COX-2 expression is constitutive only in some tissues (kidney and brain) and is induced by extrinsic stimuli (inflammation, wound healing, infections and cancer) in other cell types, such as monocytes[337,338].

1.2.2.1.2 Protein structure

COX-1 and COX-2 are active as homodimers. Each COX monomer consists of three independent folding units, an Epidermal Growth Factor (EGF)-like domain (N-terminal), a Membrane Binding Domain (MBD) and a Catalytic domain (C-terminal) (Figure 1.6).

The MBD allows the integration to one lipid monolayer of the endoplasmic reticulum membrane. It is constituted by 4 alpha helixes that surround an opening within the lipid bilayer of the endoplasmic reticulum or the nuclear envelope. This channel is in continuity

with the hydrophobic channel of the active site and allows the access of the substrate (arachidonic acid) or other inhibitors (NSAIDs)[335].

The catalytic site of COX is part of this enzymatic folding domain and consists of an internal pocket connected to the surface of the protein by a narrow hydrophobic passage called COX channel[336]. The aperture of the channel is located inside the lipid bilayer, thus allowing the direct access of the substrate arachidonic acid[328]. The catalytic site is responsible for two distinct enzymatic activities, cyclooxygenase and peroxidase, which are performed by distinct regions. The cyclooxygenase site is an hydrophobic channel located in the core part of the protein, while the peroxidase site is closer to the protein surface[335]. Both sites are functionally linked by a heme group that forms a bridge between them[339].

The amino acid homology of COX-1 and COX-2 is 60%, where most of the differences are localised at the N- and C-terminal[340]. Nevertheless, both isoforms share an equal molecular weight of 71 kDa, and the catalytic sites of the two isoforms are highly conserved as well as the critical residues for the catalytic reaction[340]. The only difference is that COX-2 has a secondary internal pocket and a larger central channel that allows larger substrates to enter the site[328], due to a single amino acid substitution in the active site (Figure 1.6)[331]. As a consequence arachidonic acid is still able to enter the active site of the enzyme, but is converted to an alternative product, 15-R-hydroxyeicosatetraenoic acid (15-R-HETE)[321].

COXs are highly conserved proteins, with a homology between species of 80-95%. Crystal structures of human, murine and sheep COX are superimposable[335].

1.2.2.1.3 Enzymatic activity

COXs convert arachidonic acid into PGH_2, the common precursor of prostanoids. The reaction happens in two steps that take place in the two interconnected catalytic sites

(Figure 1.6). First, a cyclooxygenase (bis-oxygenase) reaction happens in the cyclooxygenase site of the catalytic subunit, where arachidonic acid binds in proximity of Arg120 and Tyr355 (close to the channel aperture) and Ser530 (inside the hydrophobic core of the channel). In this position, two O_2 molecules are transferred to Tyr385 and then to AA, one after the other, to produce the cyclised intermediate PGG_2[339]. The heme group needs to be oxidised before this reaction takes place. Known oxidising agents are peroxynitrites (found in cells like monocytes) and hydroperoxides[332]. Second, PGG_2 is released and moves to the peroxidase site, where its 15-hydroperoxide group of PGG_2 is reduced by two electrons to PGH_2 in a peroxidase reaction[321].

It has been recently suggested that although they are structurally equal, only one of the two monomers of the COX-1/-2 homodimer is catalytically active, and is thus referred to as catalytic monomer. The other monomer has regulatory functions (allosteric monomer) and it is where the interaction with NSAIDs takes place[339].

1.2.2.1.4 Inhibition of COX by aspirin

Aspirin diffuses through the plasmatic membrane into the cytoplasm and penetrates the COX channel, where it docks to Arg120 and further acetylates Ser530 residue. The addition of an acetyl group generates a steric blockage of the active site that prevents the access of the substrate, arachidonic acid[336,339]. This reaction is irreversible and happens in two steps: a reversible non-covalent binding, which generates a transient complex with the enzyme, and an irreversible first order reaction. The first step consists of the formation of hydrogen bonds between the carboxyl group of aspirin and the hydroxyl groups of Tyr385 and Ser530 in the active site. This binding step takes place with the same efficiency for COX-1 and COX-2, as shown by similar absolute non-covalent binding energies. The second part of the reaction consists of the acetylation of Ser530 (Ac-Ser530) in the catalytic site of the enzyme, yielding acetyl-COX and salicylic acid (SA).

The activation free energy barrier of this reaction is higher for COX-2 (18.6 +- 0.1 kcal/mol) than for COX-1 (16.2 +- 0.1 kcal/mol), which depends on the presence of a different residue in position 513 (His513 for COX-1 and Arg513 for COX-2) (Figure 1.6). Due to the presence of a positively charged guanidinium group, Arg513 significantly increases the activation barrier of the acetylation reaction, disfavouring the covalent inhibition of COX-2[341]. The different activation barrier leads to an inactivation constant that is 50 times higher for COX-1 than COX-2, which makes aspirin 10-100 times more potent in inhibiting COX-1 than COX-2[329].

1.2.2.1.5 Function of COX-1 and COX-2

Although COX-1 and COX-2 share similar protein structure and catalytic activity, they mediate unique physiological functions. This is due to the fact that the two isoforms oversee the synthesis of distinct prostanoids in different cell types, which is achieved through different layers of regulation.

(1) COX-1 and COX-2 have a distinct spatial-temporal pattern of expression. As discussed earlier, COX-1 is a housekeeping gene constitutively expressed in most cell types. Conversely, COX-2 expression is stimulated in response to pro-inflammatory and mitotic stimuli, but remains localised to cells in the inflammatory niche.

(2) COX activity is functionally coupled with selective prostanoid synthases[342] through the co-expression in the same cell type and/or the subcellular co-localisation. For example, COX-1 and TXAS are localised in the membrane of the endoplasmic reticulum, where the spatial proximity allows the direct transfer of PGG_2 substrate from COX-1 to TXAS to produce TXA_2. Furthermore, the transcription of COX-2 and PGES is induced by the same stress-response promoters, such as cytokines and tumour-induced elements[343], in particular in monocytes.

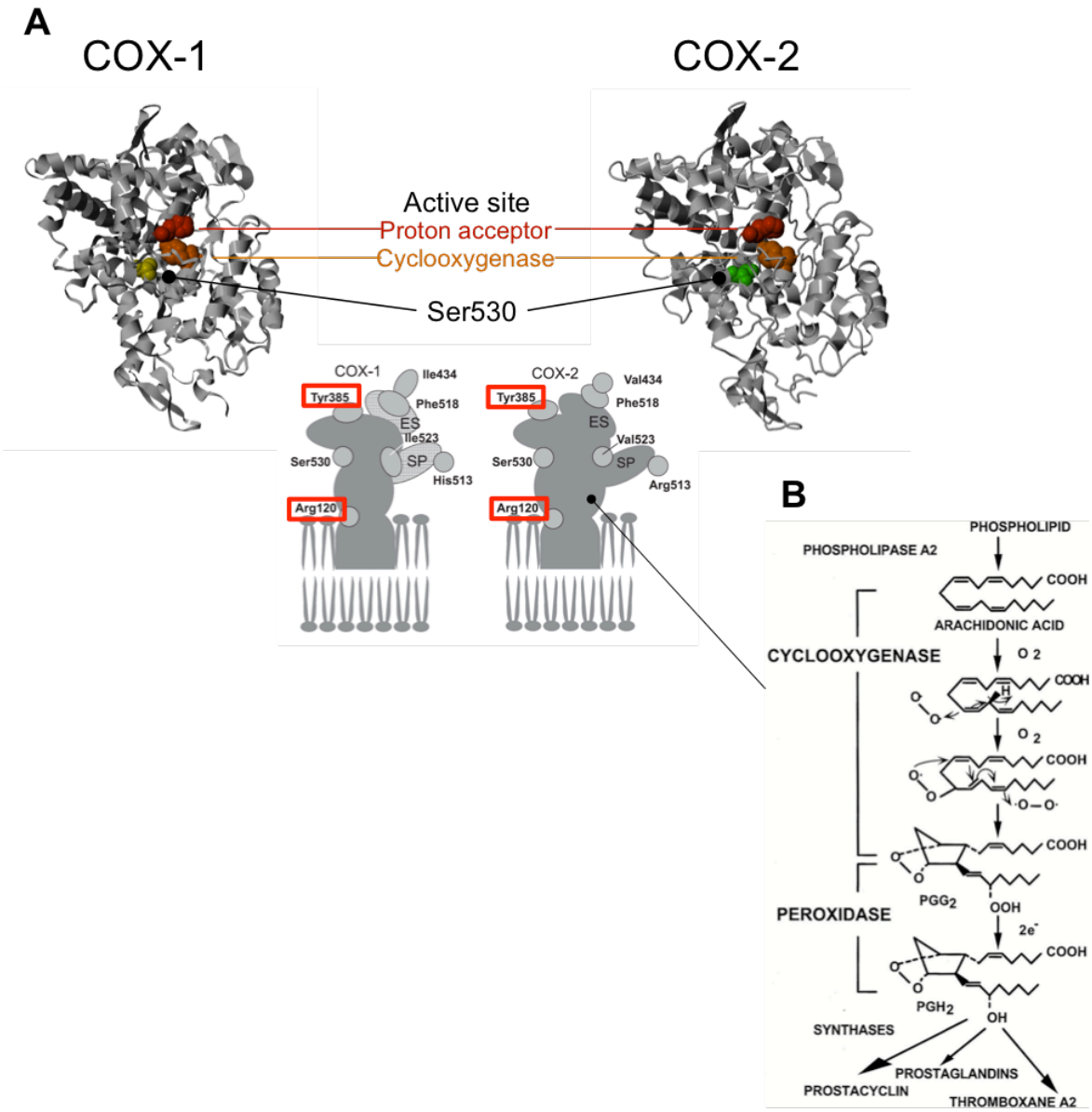

Figure 1.6 – Protein structure and catalytic reaction of COX enzymes.

(A) Tertiary protein structure of COX-1 and COX-2, highlighting the location of the active site. COX-2 presents a larger secondary site with a secondary internal pocket due to single amino acid substitutions. The existence of this side pocket is due to the presence of a smaller Val523 in COX-2 rather than Ile523 in COX-1, while the larger volume of the active site depends on the substitution of a Val434 in COX-2 to a Ile434 in COX-2 closer to the entrance of the active site, which increases the size of around 20%. The amino acids circled in red are responsible for the catalytic activity and for the docking of aspirin during inhibition.

(B) Two-step enzymatic reaction that converts arachidonic acid (AA) into the unstable product PGG_2 (cyclooxygenase reaction) and then into PGH_2 (peroxidase reaction).

Images adapted from Botting et al.[344] and Smith et al.[345] with permission.

(3) COX-1 and COX-2 catalysis is activated by different concentrations of their endogenous substrate. COX-1 is the main active form at high intracellular concentrations of AA, while COX-2 is the main active form at low concentrations.

(4) Prostaglandins are characterised by an extremely short half-life, which allows them to signal at short distances. The spatial pattern of expression of prostaglandin synthases and receptors ensures that only some cell types will respond to PG signalling.

All together, these features allow a separation of the functions overseen by COX-1 and COX-2. The main products of COX-1 activity are TXA_2 in platelets and PGI_2 in endothelial cells and gastric mucosa, where they oversee physiological functions. Conversely, COX-2 mediates the synthesis of PGE_2 during conditions such as inflammation, infection, mechanical or sheer stress.

1.2.2.2 Biosynthesis of prostanoids

1.2.2.2.1 Thromboxane A_2 (TXA_2)

TXA_2 is the main COX-1 derived prostanoid in blood. Its synthesis relies on the coupled activity of COX-1 and TXA_2 synthase (TXAS) in a number of cell types. The interaction of TXA_2 with the 7-transmembrane G-coupled TXA_2 receptor (TP) leads to the activation of different G proteins and various cellular responses, summarised in section 6.1.2.1 and Figure 6.1.

The most active site of TXA_2 synthesis is platelets, which start the *de novo* generation of TXA_2 from AA upon a pro-coagulant stimuli (e.g. collagen, thrombin and ADP). TXA_2 then interacts with TP receptor on the platelet plasma membrane, inducing platelet activation and aggregation in an autocrine and paracrine manner.

Additionally, TXA_2 can be synthesised by extra-platelet nucleated cells and can signal to a range of cells expressing TP receptor, which has a wide distribution in the cardiovascular system. In physiological conditions monocytes and alveolar macrophages express exclusively COX-1 and can synthesise small amounts of TXA_2, which is the most abundant prostanoid generated by non-stimulated monocytes[346,347]. TXA_2 synthesis by these immune cells is increased upon inflammatory stimuli, when COX-2 over-expression is believed to drive TXA_2 synthesis. Endothelial cells and vascular smooth muscle cells also respond to TXA_2 by leading to vasoconstriction and endothelial activation (see the Introduction to Chapter 6 for details). Finally, TXA_2 is involved in the contraction and proliferation of bronchial smooth muscle cells, thus overseeing functions in the respiratory system.

1.2.2.2.2 Prostacyclin (PGI_2)

PGI_2 is produced by both COX-1 and COX-2 through their coupling with PGIS activity. PGI_2 signals to its 7-membrane spanning G-protein coupled receptor IP on a variety of cell types, mediating mostly physiological functions.

In the cardiovascular system PGI_2 is a central regulator of homeostasis and its production is mainly localised in endothelial cells. Historically COX-2 was considered the only isoform responsible for PGI_2 production[348,349]. Recent evidence has challenged this belief by showing that under physiological conditions COX-1 drives the synthesis of PGI_2 by endothelial cells[333,350]. PGI_2 inhibits platelet activation and maintains platelets in a quiescent state[351]. Additionally, PGI_2 signals to vascular smooth muscle cells to induce vasodilation and inhibition of proliferation; PGI_2 signalling on leukocytes inhibits their adhesion to endothelial cells[352]. Thus, PGI_2 is a central regulator of vascular homeostasis and counterbalance the effects of pro-thrombotic TXA_2[353].

In the GI tract, PGI_2 prevents ulcers of the gastric mucosa through a process defined as gastric cytoprotection. Although the underlying mechanisms have not been elucidated, it appears that PGI_2-mediated cytoprotection depends on the increase of blood flow and the inhibition of leukocyte recruitment[354-356], possibly through a similar signalling to the cardiovascular system. Interestingly, a similar cytoprotective mechanism has been found in the brain, where PGI_2 prevents neuronal damage[357].

Although PGI_2 oversees mainly physiological and cardiovascular functions, in vivo studies have shown its implication in the progression of the inflammatory response[358]. Although the mechanisms are not yet understood, this effect might depend on the induction of vasodilation and the recruitment of immune cells to the site of inflammation.

1.2.2.2.3 Prostaglandin E_2 (PGE_2)

PGE_2 is the main product of COX-2 activity and derives from the coupled activity of COX-2 and PGE_2 synthase (PGES). Released PGE_2 interacts with its G-protein coupled receptor EP, which exists in 4 isoforms (EP_{1-4}). COX-2 is constitutively expressed by few cell types, mainly monocytes and their tissue-resident descendants (i.e. osteoclasts and microglia) and neurons, where it induces PGE_2 production to mediate physiological functions. For example, PGE_2 induces the hyperpolarisation nociceptive neurons, mediating the transduction of pain sensation[359]. Additionally, COX-2 expression and PGE_2 synthesis in these cells and other cell types (e.g. endothelial cells) is induced in pathological situations such as inflammation, wound healing and mitogens. In these situations, PGE_2 oversees primarily inflammatory functions.

The contribution of PGE_2 to the inflammatory response is substantiated by the genetically modified animal models, where the knockout of PGES prevents a variety of inflammatory diseases[360]. During the inflammatory response, PGE_2 plays a central role in the recruitment and modulation of immune cells[361]. On the one hand, PGE_2 induces

vasodilation and vascular permeability, thus promoting the influx of immune cells. More directly, PGE_2 signalling induces the release of IL-23 by DCs and, synergistically, activates CD4+ T helper cells to expand and differentiate to a IL-17-producing phenotype (Th17)[362-364]. In turn, IL-17 recruits more monocytes and neutrophils[364]. Additionally, PGE_2 regulates the production of pro-inflammatory IL-6 and TNF-α by monocytes/macrophages, DCs and T cells[365]. Concomitantly, PGE_2 induces IL-10 release by BMDCs, which is involved in the resolution of the inflammatory response[365].

1.2.3 Pharmacokinetics of aspirin

After oral administration, 50% of aspirin is absorbed in the stomach by passive diffusion[337]. Aspirin has a half-life of 15-20 minutes in plasma[337] because it is rapidly hydrolysed to salicylic acid (SA) by local esterases in the intestinal wall, liver and circulation. SA has a longer half-life of 3-20 hours, a time that positively correlates with the dosage[366]. SA is then directly excreted (~6%) or further metabolised and excreted as salicyluric acid (SUA, ~75%) or salicyl glucoronides (SGs, ~19%)[366,367]. ASA reaches much higher concentrations in the circulatory system than in the systemic tissues, hence blood cells are subject to higher doses. Since platelets are anucleate, they cannot synthesize new functional COX-1, thus aspirin effect on them is lifelong and new platelets must be generated to recover functionality[337].

Together, the pharmacology of aspirin explains why different doses have different effects on the body. At low doses (75-100 mg/day) aspirin acts mainly on platelets, triggering a COX-1-dependent, long lasting, anti-thrombotic response with extra-platelet targets minimally affected. At medium doses (325 mg/day) aspirin penetrates the gastro-intestinal mucosa and vascular endothelium, where COX-2-derived PGI_2 levels are reduced, resulting in analgesic, anti-pyretic and mild anti-inflammatory effects. The inhibition of PGE_1 induces anti-pyretic effects while the inhibition of PGE_2 is responsible for the anti-

inflammatory effects of the drug[344]. High doses of aspirin (generally no more than 1.2 g/day) are used to control chronic inflammatory diseases by inhibition of COX-2 and subsequent reduction of PGE_2 and PGI_2 in the inflammation site[337].

At clinical doses aimed at achieving an anti-inflammatory and analgesic effect, aspirin inhibits both COX-1 and COX-2, thus causing the common side effects such as gastric lesions and internal bleeding. These effects are due to the inhibition of COX-1 in platelets and in the gastric mucosa, leading to reduced levels of pro-thrombotic TXA_2 and cytoprotective PGI_2, respectively. In order to overcome this problem, a new class of selective COX-2 inhibitors (coxibs) was launched and used in clinical trials. However, some of those inhibitors (i.e. rofecoxib) were associated with a high rate of cardiovascular morbidity such as myocardial infarction. It has been postulated that such effects depend on the reduction of COX-2 dependent PGI_2 production, which acts as an anti-coagulant and vasodilator. Lower levels of PGI_2 and the disrupted balance with TXA_2 lead to thrombogenesis, elevated blood pressure and may lead to cardiovascular casualties[335], suggesting that aspirin might be a safer choice to maintain this balance.

1.3 EFFECTS OF ASPIRIN ON CANCER AND METASTASIS

During the past 50 years, a growing body of literature has shown that aspirin has a protective role towards cancer and metastasis development. Both experimental studies and clinical trials have contributed to such evidence, suggesting a universal effect of aspirin on cancer.

1.3.1 Experimental studies

A number of experimental studies have reported a reduction in the incidence[368,369] and in the growth of tumours[370-375] in mice treated with aspirin. These effect have been attributed to various mechanisms: decrease of tumour cells proliferation[371,373], angiogenesis[373], impairment of recruited immune cells[376,377] and an increase in apoptosis[368,372], although no effect on apoptosis, proliferation or recruitment of immune cells is achieved at low-doses of aspirin[378].

More relevantly to our project, aspirin has also been associated with the reduction of metastasis in experimental studies. The idea that aspirin could be inversely associated with metastasis was brought up for the first time in 1968 by Gasic[244], who observed that thrombocytopenic rats, treated with neuraminidase, formed a reduced number of lung metastases and this anti-metastatic effect could be rescued by the infusion of platelets-rich plasma (PRP), an early evidence of platelets contribution to metastasis. Five years later, Gasic and collaborators confirmed this finding by showing that the inhibition of platelet aggregation achieved through aspirin treatment dramatically reduced the number of lung metastases[243]. The anti-metastatic effect of aspirin was clear in both experimental and spontaneous metastasis models.

Following Gasic's seminal work, other studies on animal models demonstrated that aspirin reduced experimental metastasis development from different types of tumour cells or primary tumours[379-386 384,387,388]. Although some evidences did not show an association

between aspirin treatment and metastases reduction [247,389-391], the majority of studies indicate a clear effect of aspirin treatment on metastasis development, an effect that is conserved in different species and tumour cell models.

1.3.2 Clinical studies

1.3.2.1 Observational studies

Following up on experimental studies, a series of observational studies (case-control or cohort) have been made to understand the association between aspirin and cancer[392-407]. These studies evaluated the incidence of cancer diagnosis in cancer free participants undergoing aspirin/NSAIDs treatment for other diseases, mainly cardiovascular. Although these studies differed in their strategy, examined population, doses of aspirin (81 mg to 1200 mg/day) or type of cancer, the general trend was a 20-50% reduction in the risk of cancer and cancer-related mortality attributable to aspirin use, with a pooled odds ratio (OR) of 0.80 (95% CI 0.73-0.87, $p<0.0001$)[408]. This reverse association was seen for overall cancer and for prostate cancer[403,404,409], breast cancer[398,400,402,406,407], lung cancer[398,402,406] and, in particular, colorectal cancer [394,396,397,399,405,406], for which the pooled OR was 0.62 (95% CI 0.58-0.67, $p<0.0001$)[410]. No effect was seen for melanoma[411]. Overall, the data suggested that aspirin was effective since at low-medium doses (100-325 mg) per day and the increase of dose did not show additional benefit[400,402]. Moreover, the cancer prophylactic effect of aspirin correlated with the duration of treatment and, in most cases, was significant after 10-20 years of treatment[399,401,402].

1.3.2.2 Randomised clinical trials

The results from observational studies might be biased by confounding factors such as lifestyle, other diseases or diverse treatment regimes. Thus, more conclusive evidence of

the causal relationship between aspirin and cancer was determined through randomised controlled trials, where aspirin or placebo was allocated for the treatment of cardiovascular diseases, and patients were retrospectively monitored and followed-up for the diagnosis of cancer[412-420]. Since treatment of cancer was not the primary purpose of these trials, with the exception of the CAPP2 trial[420], the treatment regimes were not homogeneous.

Several randomised trials showed a protective effect of aspirin on the recurrence of colorectal adenomas (precursor of neoplastic adenomas) and advanced colorectal adenomas, even at 1 year after randomisation[415-418]. Additionally, aspirin treatment was associated with a reduced incidence of cancer-related deaths[413,419,421] and a significant reduction in the incidence of colorectal cancer, starting 5-10 years after randomisation[408,420]. Interestingly, there was no increase in efficacy between lower and higher doses in the same trials in terms of benefit on cancer prevention[418,419].

However, the two largest clinical trials failed to show an effect of aspirin on primary prevention of cancer, mainly colorectal. In the Physicians' Health Study (PHS)[414,422] and the Women's Health study (WHS)[412], which collectively recruited more than 60000 physicians and nurses, aspirin did not affect the risk of cancer appearance or cancer mortality over a period of 5 or 10 years, although an effect on colorectal cancer was seen after 16 years of treatment in the WHS post-trial follow up[423]. These results highlighted the fact that chemo-preventive effect of aspirin is expected to be seen after 10 years of follow-up. This latency is compatible with the whole genesis of adenoma-carcinoma sequence, expected to last 10-15 years[408]. Interestingly, in PHS and WHS studies aspirin was delivered every second day, a regime not commonly employed by other trials. Considering the short half-life of aspirin and the ability of cells to regenerate functional COX-1 and COX-2, this regime might not have been sufficient to achieve a sustained systemic inhibition of COX. Thus, the limitations of these studies could have been a short follow up or the lack of chronic treatment.

The inconsistency among clinical trials have been partially addressed by their meta-analysis, where multiple randomised trials are pooled together and analysed on the basis of common criteria, such as cancer type, treatment regime etc. These meta-analyses equally showed a significant prophylactic effect of aspirin on different cancer types, in particular in the GI tract[424,425].

In particular, Rothwell et al.[426] pooled together all eligible randomised trials on aspirin and found a reduction of cancer-related deaths (odds ratio, OR, 0.85, 95% CI 0.76-0.96, p=0.008) and of the incidence of all cancers (hazard ratio, HR, 0.88, 95% CI 0.80-0.98, p=0.017), with the highest benefit in patients receiving treatment for 5 years or longer. This meta-analysis confirmed that the reduction in incidence of colorectal cancer could be seen from after 10 years post-randomisation[408], suggesting an effect of aspirin on the carcinogenic process. In a concomitant meta-analysis, the same group showed that the effect of aspirin on mortality and cancer incidence (colorectal cases) was present since low doses (75 mg/day) and no benefit was associated to the allocation to medium (300 mg/day) or high doses (500-1200 mg/day)[427].

1.3.2.3 Clinical trials on the effect of aspirin on metastasis

The data from the observational studies and randomised clinical trials indicated that aspirin was effective in reducing the long-term cancer incidence, although additional benefits of aspirin treatment appeared short-term. Indeed, aspirin decreased the cancer-related mortality within 2-3 years from randomisation and, overall, the effect on cancer-related death was more pronounced than the effect on cancer appearance[428], which suggested an effect on cancers not diagnosed at the beginning of the study. These observations prompted Rothwell and collaborators to investigate the association of aspirin with other parameters such as tumour growth and metastasis. The systematic review of case-control studies showed that the regular use of aspirin reduced the proportion of

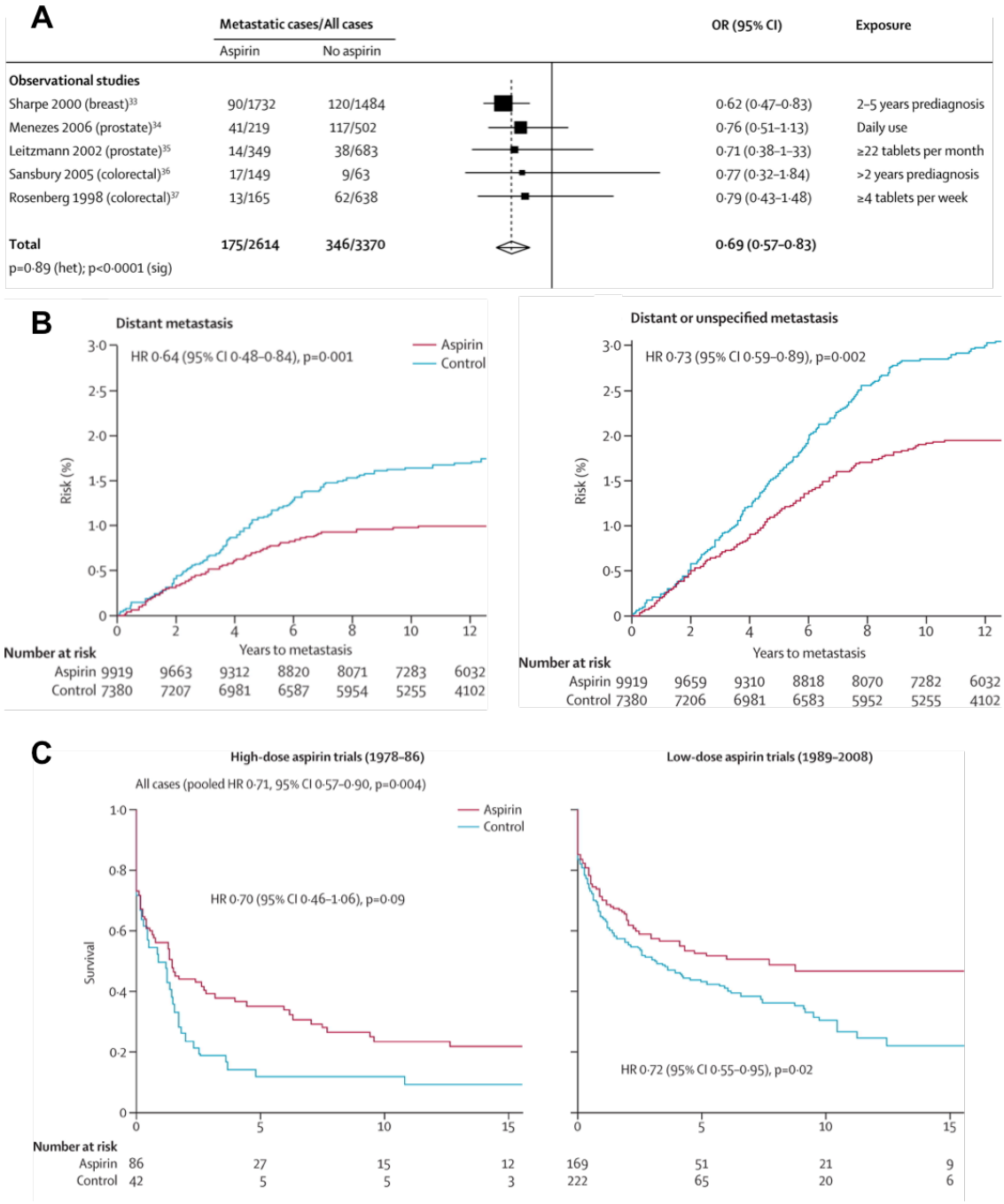

Figure 1.7 – Effect of aspirin on risk of distant metastasis in clinical trials.

(A) Proportion of metastatic cancers and risk of distant metastasis (odds ratio, OR) between aspirin users and non-users, evaluated in 5 observational studies. Adapted from Algra et al.[410], with permission.

(B) Risk of metastasis (hazard ratio, HR) from any in-trial diagnosed cancer, evaluated in the meta-analysis of five randomised trials of aspirin versus control. Metastasis are categorised as distant (definite blood-bourne metastasis in known distant tissues) or unspecified (metastasis with no record of the secondary site). Adapted from Rothwell et al. [428], with permission.

(C) Risk of cancer-related deaths (adenosarcoma) in five randomised trials of aspirin versus control, stratified as low dose (<300 mg/day) or high dose (≥300 mg/day) in all cases of metastasis, both evident or not at the initial diagnosis. Adapted from Rothwell et al.[428], with permission.

metastatic cancer (OR 0.69, 95% CI 0.57-0.83, p<0.0001) (Figure 1.7A)[410]. Similarly, the meta-analysis of 5 UK-based randomised trials showed an effect of aspirin in reducing the risk of metastatic cancer (HR 0.64, 95% CI 0.48-0.84, p=0.001, Figure 1.7B) and the risk of developing metastasis for in-trial cancer cases (HR 0.45, 95% CI 0.28-0.72, p=0.0009)[428]. This effect was homogeneous and significant on a range of distant metastasis, including brain, lung and liver metastasis from different types of primary tumours, with a more prominent effect in patients with adenocarcinoma and, in particular, colorectal cancer. Moreover, aspirin decreased the overall cancer- and metastasis-related mortality (HT 0.71, 95% CI 0.57-0.9, p=0.004), in particular for adenocarcinoma. To note, all considered trials had daily aspirin regimes and trials of high-dose aspirin (>300 mg) did not show a benefit over low-dose aspirin (<300 mg) in terms of overall survival rate of adenocarcinoma patients.

1.3.2.4 Risk-benefit evaluation of prophylactic aspirin

Together, the results from meta-analysis of randomised trials suggest a protective effect of aspirin on cancer incidence and metastasis, which reduce the overall cancer mortality, in particular due to colorectal cancer. These findings have important implications for the prevention and treatment of cancer. Hence, the overall risk-benefit of aspirin administration needs to be carefully evaluated.

The most severe side effects associated with aspirin treatment are internal bleeding, comprising haemorragic strokes and, more commonly, extracranial bleeds, especially in the gastrointestinal tract[429,430]. According to primary prevention trials, aspirin allocation would account for 0.10% increase of extracranial bleeding[431]. Gastrointestinal bleeding is also the most lethal side effects, accounting for 3.6 events per 10000 people treated with aspirin for a year. Other events, such as peptic ulcers, are associated with aspirin treatment although the rate and fatality are low below the age of 70[432].

On the other hand, allocation to aspirin results in an overall 7-9% reduction of cancer (women-man) and cardiovascular cases in people taking aspirin for 10 years[430]. Among people who benefit from aspirin allocation, 61-80% would have a reduction of cancer incidence, particularly in the case of colorectal cancer[430]. Moreover, mortality would decrease of 9-13% (women-men), with higher benefits from treatments longer than 5 years[430,433]. This reduction is almost completely dependent on a reduction of cancer-related deaths (89-96%). According to the available data, aspirin would also reduce the risk of developing distant metastasis, in particular for colorectal cancer (70% reduction), and decrease the risk of cancer-related death for both patients with and without metastasis at initial diagnosis (50% reduction for the latter)[428]. Concomitantly, aspirin reduces the risk of cardiovascular events (12% reduction), mainly strokes, myocardial infarction and coronary heart disease[431].

Are we then ready to prescribe aspirin as a prophylactic or adjuvant therapy? The overall benefit-harm balance of aspirin in the prevention of cancer is favourable, in particular for patients between 55 and 65 years of age[430]. However, the latency of this effect (5-10 years of more) would imply a long term treatment of patients with low-medium doses of aspirin, which would hypothetically lead to a 15.4% increase in risk of upper gastrointestinal symptoms in aspirin-allocated patients[434]. The cancer incidence in the UK is 0.73% of the general population (http://publications.cancerresearchuk.org/cancerstats/statsincidence/dtincrates.html). To date, no predictive biomarkers are available for patients at risk of developing side effects, who will not benefit from aspirin prophylaxis. Moreover, it would be challenging to address the effect of aspirin in cancer prevention through Phase III trials, mainly because of the number of participants required and the length of follow-up. Hence, aspirin is still not generally recommended as prophylactic therapy for the prevention of cardiovascular disease and cancer in the general population.

Nevertheless, aspirin treatment could be beneficial as adjuvant therapy in higher risk groups, in particular people with cancer. On this line, a series of phase III clinical trials, started or upcoming, will help to understand the role of aspirin treatment in stratified groups of cancer patients[434]. In particular, an international Phase 3 trial coordinated by the Medical Research Council (MRS) has been recently started (ADD-ASPIRIN, http://www.addaspirintrial.org), which will recruit 10000 patients with several common cancers (colorectal, breast, prostate, gastro-oesophageal) across the UK and India. This double-blind placebo controlled trail will test the effects of low (100 mg/day) and 'high' (300 mg/day) doses of aspirin on the recurrence of cancer after surgery, chemotherapy or radiotherapy and the appearance of metastasis.

1.3.3 Understanding the anti-metastatic effect of aspirin through experimental studies

A wide range of experimental studies, both *in vitro* and *in vivo*, have attempted to give a mechanistic explanation of the anti-metastatic effect of aspirin. Despite the large number of published papers, the mechanism underlying the anti-metastatic effect of aspirin remains elusive. Here we review the challenges encountered in designing relevant experimental studies and the obtained results aimed at understanding metastasis prevention by aspirin.

1.3.3.1 Doses of aspirin in animal studies

Aspirin was first synthesised and introduced in the clinic in 1897[321], in a time when its clinical effects, but not its pharmacology, were known. The first insights into the mechanism of action of aspirin were obtained by Vane in 1971[324], almost a century after its commercialisation. In the years following Vane's discovery, other evidence contributed to the understanding of the mechanism of action, and side effects, of aspirin and this

knowledge is still expanding in the present day. In this sense, aspirin represents one of the few drugs where the clinical trial preceded the investigation of its mechanism of action.

Aspirin has a rather complex pharmacology, where different doses achieve distinct pharmacological effects. Therefore, *in vivo* models, rather than *in vitro* ones, are often more informative of its systemic and multi-organ effects. The most challenging part of aspirin dosage has not been the determination of the human equivalent dose (HED)[435], but rather the animal equivalent dose ("AED"). Considering the importance of dose stratification in the clinic, the choice of an AED is of particular importance in order to draw valuable conclusions. It has been a common practice to use linear dosage conversion factors based on body weight conversion[435-437] or to select an arbitrary dose not associated with toxic effects[379,380]. As a consequence, in the past 50 years aspirin has been used in experimental studies at a wide range of doses (1.25-1000 mg/kg per day) mainly in mice[243,375,379,385,436-441]. However, the rate of drug absorption, metabolism and excretion, as well as the required frequency of treatment and delivery route can dramatically differ between species.

One valuable approach for the allometric translation of drug doses between species is the use of body surface area (BSA) normalisation method, which advocates the use of mg/m^2 instead of mg/kg as dose unit. Such method derives from the observation that basal metabolism and biological parameters (such as blood volume, plasma proteins and renal function) are similar between mammalian species if normalised for their body surface. Thus, scaling drug doses on the basis of BSA method takes in consideration the size-related differences in physiology[435]. For example, according to the BSA conversion, mice (0.007 m^2) should take a 13 times higher dose of a drug in order to achieve the same dosage to humans (1.6 m^2), providing that the same administration regime is maintained. However, the suitability of this translation method relies on the assumption that the pharmacokinetics and mechanism of action of a drug is conserved between species. Taking for example aspirin, COX-1 and COX-2 have identical catalytic residues in mice

and humans but share a 90% homology, which could potentially be translated into a different rearrangement of the COX channel, leading to a different efficiency of aspirin inhibition. Moreover, it is not known if the absorption, distribution, metabolism and excretion (abbreviated as ADME)[442] parameters of aspirin are conserved between man and mouse. In this situation, the mere use of BSA conversion to extrapolate a dose from human to mice might be inappropriate or lead to incorrect assumptions.

1.3.3.2 Confounding targets

Aspirin shows different pharmacological properties at different doses, mainly dependent on the inhibition of COX-1 and COX-2. Additionally, COX-independent targets have been identified *in vitro* and *in vivo*. For instance, aspirin is known to inhibit the activity of IκB kinase (IKK) ß, preventing the degradation of IκB and the activation of the transcription factor NF-κB[443-445]. The repression of NF-κB activity by aspirin has been associated with the reduced expression of E-cadherin, ICAM-1 and VCAM-1, which are adhesion molecules involved in metastasis, with the repression of apoptosis and with the development of chemoresistance. Additionally, aspirin was found to induce apoptosis of cultured tumour cells through the permeabilisation of the mitochondrial membrane, which induces the release of cytochrome c and the activation of caspases[446,447], the regulation of pro- and anti-apoptotic proteins[448-450], and the inhibition of ERK[451] and Wnt/ß-catenin pathways.

Several experimental studies have investigated the molecular mechanisms of aspirin anti-metastatic effect, showing that aspirin could interfere with different steps of the metastatic cascade[380,383,384,452-456]. In most of these studies, the effect of aspirin was attributed to COX-independent targets. Although these mechanisms of action could contribute to the anti-metastatic effect of aspirin, some evidence suggests that COX-dependent targets could be more relevant.

(1) Both chemopreventive and anti-metastatic effects of aspirin have been observed in cardiovascular trials (75-300 mg/day) and the increase of dose did not show any further benefit[427,428], compatible with a sustained inhibition of COX-dependent targets. According to the BSA conversion system, these doses would correspond to 12.5-50 mg/kg/day of aspirin administered to mice. Moreover, oral administration of 100-300 mg of aspirin in humans leads to plasmatic peak of 4-50 μM[337,457,458], which are expected to be the highest systemic doses.

(2) COX-independent inhibition of NF-κB and ERK signalling pathway and the induction of apoptosis have been reported *in vitro* at millimolar concentrations of aspirin[443,444,459], which are at least 5 times above the peak plasmatic concentration in patients.

(3) Lower doses of NSAIDs, used at concentration that inhibit COX-1/-2, are not sufficient to inhibit apoptosis *in vitro*[459] or *in vivo*[378].

These observations suggest that COX inhibition remains the most plausible mechanism of metastasis prevention by aspirin.

1.3.3.3 Contribution of COX-1 and COX-2 to experimental metastasis

COX-1 and COX-2 can contribute to the development of metastasis through different mechanisms.

COX-2 has a well-documented pro-tumorigenic role. In fact, COX-2 has been found overexpressed by several tumour cells and tumour samples, particularly of colorectal origin,[460-465] and has been found involved in the early progression of colorectal adenocarcinoma. Moreover, the overexpression of COX-2 in the mammary tissue is sufficient to induce the development of tumours[466]. COX-2 has also a documented pro-metastatic role and its expression levels correlates with poor prognosis[467] and

experimental metastasis[468]. The inhibition of COX-2 decreases metastasis in a number of models[469-471]. Both the pro-tumorigenic and pro-metastatic effect of COX-2 might be attributed to its main product PGE_2. COX-2:PGE_2 expression by tumour cells mediates evasion from apoptosis[472], increased survival[473-476], sustained growth[477], vascular permeabilisation[460], angiogenesis[478-480], evasion of the immune response[361,481,482], migration[483] and invasion[460,484]. More generally, PGE_2 mediates the engagement of the inflammatory response, which has been recently recognised as one hallmark of cancer, and can promote metastasis through multiple mechanisms[485,486].

To the best of our knowledge, COX-1 has not been directly implicated in the development of metastasis, possibly due to its constitutive expression in most cell types. Nevertheless, COX-1 expression by platelets is involved in their aggregation and association with tumour cells, and its inhibition by aspirin reduces TCIPA in a series of tumour cell lines[243,386,487,488]. The pro-metastatic role of TCIPA thrombosis is well established (see section 1.1.4.1). In favour of COX-1 contribution to metastasis, the anti-metastatic effect of aspirin was seen at low-dose clinical trials (75-300 mg), consistent with an anti-thrombotic effect and low systemic bioavailability. This treatment regime is not compatible with a sustained systemic inhibition of COX-2, which could only be achieved by higher doses and more frequent intake of aspirin (e.g. 650 mg of aspirin, three or four times a day)[337].

In conclusion, the relationship between aspirin and cancer/metastasis is not as linear as it had been initially thought. The uncertainty regarding the basis of the anti-metastatic effect of aspirin relies on the wide range of molecular targets of aspirin, a range that varies depending on the employed dose. Thus, the mechanism of metastasis prevention by aspirin should be investigated at clinically relevant doses.

1.4 AIM OF THE PROJECT

The aim of this project is to investigate the molecular mechanisms underlying the anti-metastatic effect of aspirin, an effect seen in several clinical trials. We hypothesize that this effect depends on the inhibition of COX-1 and/or COX-2, both of which can play a permissive role in metastasis development. The relative contribution of COX-1 and COX-2 to metastasis will be addressed in an experimental model of metastasis through the use of aspirin or selective COX inhibitors or, alternatively, genetically modified mouse models. In particular, we will examine the dose, kinetics and downstream effectors of metastasis inhibition by aspirin. Overall, this investigation will help to gain new mechanistic insights into the metastatic cascade. Moreover, by tentatively extrapolating our results to the clinic, it will contribute to understanding the possible application of aspirin or alternative selective drugs as prophylactic or adjuvant therapy in the prevention of metastasis.

CHAPTER 2

Materials and Methods

2.1 *IN VITRO* ASSAYS

2.1.1 Cell culture

2.1.1.1 Cell lines and culture conditions

B16F10 murine melanoma cells were cultured in RPMI 1640 medium (Sigma-Aldrich) supplemented with 10% heat-inactivated fetal bovine serum (FBS) (Gibco), 2 mM L-glutamine, 25 mM HEPES, 50 U/mL Penicillin and 5 µg/mL Streptomycin (all from Thermo Fisher Scientific). 4T1 murine breast cancer cells, MC-38-GFP murine colorectal cancer cells and MDA-MB-231 human breast cancer cells were cultured in Dulbecco's Modified Eagle Medium (DMEM, Sigma-Aldrich) supplemented with 10% FBS, 50 U/mL Penicillin and 5 µg/mL Streptomycin, in a 5% CO_2 humidified atmosphere at 37˚C. MC-38-GFP cells were grown under selection with 5 µg/mL puromycin. B16F10 cells were obtained from Dr Ali Amirkhosravi from Prof J.L. Francis's lab, Florida Hospital Cancer Institute, Orlando[258]. 4T1 and MC-38 cells were purchased from the American Type Culture Collection (ATCC). MDA-MB-231 cells were a kind gift from Prof A.J. Ridley's lab, King's College London. For passaging, cells were washed twice with PBS, incubated for 5 minutes with Versene (B16F10) (Thermo Fisher Scientific) or Trypsin-EDTA 0.05% solution (all other cell lines) (Sigma-Aldrich) in a 5% CO_2 humidified atmosphere at 37˚C and then harvested with complete growth medium. All cell were used within 20 passages from thawing and were routinely tested for mycoplasma contamination by using MycoAlert Mycoplasma Detection Kit (Lonza Group, Ltd.).

2.1.1.2 Tumour cell staining

Exponentially growing B16F10 cells were stained with Celltracker blue CMAC, orange CMRA or green CMFDA dyes (Thermo Fisher Scientific), following the manufacturer's indications. Briefly, CMAC, CMFDA and CMRA were resuspended in DMSO at 10 mM. B16F10 at 50-60% confluence were incubated for 30 minutes in a 12.5 μM solution of the dye in FBS-free RPMI medium in a 5% CO_2 humidified atmosphere. Following the removal of staining solution, cells were incubated for additional 30 minutes in FBS-free RPMI medium. Medium was then changed to complete RPMI and cells were used for the intended experiment.

2.1.1.3 Drug treatment

B16F10 tumour cells were grown for 24 hours and incubated with the indicated doses of ASA, added to the medium as DL-lysine acetylsalicylate (AspégicTM injectable, Sanofi Aventis), SC-560, NS-398 (Cayman Chemical). Equal volumes of vehicle (H_2O for ASA, DMSO for SC-560 and NS-398, ethanol for PICO) were used as controls. The doses of drugs for *in vitro* studies were chosen on the basis of the expected plasmatic concentration in mice, calculated according to the bioavailability and excretion parameters in humans. Since the same pharmacokinetic measurements are not available for mice, we assumed that these parameters would be comparable in mice and humans.

		Dose used *in vitro*
ASA	Low	0.075 mg/mL
	Medium	0.217 mg/mL
	High	1.171 mg/mL
SC-560		0.06 mg/mL
NS-398		0.0304 mg/mL

Table 2.1 – Doses of COX inhibitors used *in vitro*.

Doses of ASA, SC-560 and NS-398 for *in vitro* studies were calculated as expected plasmatic dose on the base of aspirin pharmacokinetic parameters in humans.

2.1.1.4 Isolation and culture of lung microvascular endothelial cells

Lung microvascular endothelial cells were isolated as previously described[489], with a modified protocol. In brief, lungs were isolated from 3 C57BL/6 mice (as described below) under sterile conditions and placed under a laminar flow hood. Lungs were dissected into 2-mm^3 blocks and digested in a 0.5 mg/mL collagenase solution (Thermo Fisher Scientific) for 1 hour at 37°C, with intermittent agitation. Digested lungs were filtered through a 70 µm cell strainer (Thermo Fisher Scientific) with PBS to remove undigested debris. Cell suspension was centrifuged at 210 xg for 5 minutes and washed twice with PBS supplemented with 2.5% (v/v) FBS (PBS-2.5%FBS) at RT. For sorting, cells were counted and incubated in blocking solution (10 µg/mL murine IgG in ice-cold PBS-2.5%FBS) for 30 minutes at 4°C. After one wash in PBS-2.5%FBS, cells were stained for 30 minutes at 4°C with labelled primary antibodies diluted to 1 µg/mL in ice-cold PBS-2.5%FBS: anti-Isolectin-B4-FITC (L2895, Sigma-Aldrich), anti-CD31-PE (102408, Biolegend) and anti-CD105-APC (120414, Biolegend). Cells were then washed in ice-cold PBS supplemented with 0.5% (v/v) FBS (PBS-0.5%FBS) and filtered through a 35 µm mesh (BD Bioscience) to prepare a single cell suspension. After setting fluorescent compensation with single-stained controls, Isolectin-$B4^+CD31^+CD105^+$ cells were sorted (sorting was performed by Dr A. Worth) and seeded in a T-25 flask coated with gelatin 2% (Sigma-Aldrich) in an enriched DMEM medium [20 mM HEPES, 50 U/mL Penicillin and 5 µg/mL Streptomycin, 1x MEM Non-essential Amino Acid Solution, 1 mM Sodium pyruvate, 50 µM 2-mercaptoethanol, 12 U/mL heparin, 20% v/v FBS and Endothelial Cell Growth Supplement (Sigma Aldrich)] (all from Thermo Fisher Scientific, if not differently specified). Before the first passage, LMVECs were grown for 3 weeks, changing medium every 2-3 days. LMVECs were then passaged when they reached 90% confluence and kept in culture for no longer than 10 passages.

2.1.1.5 Western blotting

Cells were harvested as described above and washed twice with PBS. The cell pellet was then snap frozen in liquid nitrogen and stored at -80°C. Cell lysates were obtained by resuspending the cell pellet in RIPA buffer (Sigma-Aldrich, 80 µL/10^6 cells) supplemented with Halt Protease Inhibitor Cocktail (Thermo Fisher Scientific). Cells were incubated with lysis buffer for 30 minutes on ice and vortexed every 5 minutes. Cell lysates was centrifuged at 10000 xg for 10 minutes at 4°C and the supernatant was collected for the quantification of protein concentration through Pierce™ BCA protein assay (Thermo Fisher Scientific), following the manufacturer's instructions. Proteins (20 µg) were resuspended in 1x loading buffer (RunBlue, Expedeon Protein Solutions), denaturated at 100°C for 5 minutes and separated by SDS-PAGE on NuPage Novex™ 4-12% Bis-Tris gels (Thermo Fisher Scientific). Gels were electroblotted on Immobilion®-P PVDF membranes (Merck Millipore), previously activated in 100% methanol (Sigma Aldrich) following the manufacturer's instructions. Membranes were then blocked and blotted with the primary antibodies: anti-COX-1 (ab109025, Abcam, 1:1000 in 5% milk, overnight at 4°C), ant-TP (sc-30036, Santa Cruz biotechnology, 1:500 in 5% milk, overnight at 4°C), anti-TXAS (ab39362, Abcam, 1:500 in 5% milk, overnight at 4°C) and anti-beta actin (ab8227, Abcam, 1:10000 in 5% BSA [Sigma], 1½h at RT). Between steps, membranes were washed with TBST, which consists in TBS (Tris-buffered saline) [50 mM Tris.HCl, pH 7.4 and 150 mM NaCl, prepared in house] supplemented with 0.05% TWEEN® 20 (Sigma Aldrich). Bands were revealed by incubation with species-specific secondary antibodies conjugated with HRP (Thermo Fisher Scientific, 1:2000-1:10000 dilution, 1h at RT), followed by detection of chemiluminescent signal through ECL kit (Amersham) and imaging at LI-COR Odyssey Fc system.

2.1.2 Platelets assays

2.1.2.1 Blood collection

For studies requiring platelet isolation, mice were sacrificed with an overdose of pentobarbital (intravenously) and blood was collected by cardiac puncture with syringes containing freshly prepared 3.2% (w/v) sodium citrate (Thermo Fisher Scientific) or ACD buffer [83 mM trisodium citrate, 111 mM dextrose, 71 mM citric acid] (all from Sigma-Aldrich or Fisher Thermo Scientific), at 1:10 ratio to blood volume. Anticoagulated blood was kept under agitation until platelet isolation.

2.1.2.2 Isolation of PRP

Citrated blood was diluted 1:2 with Modified Tyrode's Hepes (MTH) buffer [134 mM NaCl, 0.3 mM $NaH_2PO_4 \bullet 2H_2O$, 3 mM KCl, 5 mM HEPES, 5 mM Dextrose, 2 mM $MgCl_2$] (all from Sigma-Aldrich or Fisher Thermo Scientific) supplemented with 0.02 U/mL apyrase (Sigma Aldrich) and 0.25 μM PGE_1 (Alprostadil, Sigma Aldrich). The suspension was centrifuged at 180 xg for 10 minutes at 22'C and the supernatant was collected as Platelet Rich Plasma (PRP). To isolate Platelet Poor Plasma (PPP), a portion of the remaining red blood cell pellet and interphase was centrifuged at 12000 xg for 2 minutes at RT and the supernatant was collected.

2.1.2.3 Isolation of washed platelets

Washed platelets were isolated prior to staining. Briefly, PRP was diluted with washing buffer [10%MTH v/v in dH_2O, supplemented with 0.10% w/v $NaHCO_3$, 0.20% w/v BSA and 1 mM EGTA] and centrifuged at 1300 x g at 22˚C for 10 minutes. Platelet pellet was washed twice with washing buffer containing 0.25 μM PGE_1 by centrifuging PRP at 1300 x

g at 22˚C for 10 minutes. Platelets were then counted in a Coulter counter (Beckman; 50 µm aperture tube, 3-30 fL particles).

2.1.2.4 Staining of platelets

Platelets were adjusted to a concentration of $8x10^5$ cells/µL in Washing buffer. Platelets were stained with PKH26 (Sigma) according to the manufacturer's protocol. They were subsequently centrifuged at 1200 xg at 22˚C for 20 minutes and adjusted to the required concentration in PPP (adhesion and TEM assays) or Resuspension buffer [10%MTH v/v in dH_2O, supplemented with 0.10% w/v $NaHCO_3$ and 0.20% w/v BSA]. Concentrations of $1.5x10^6$ (*ex vivo* TCIPA assays)[26,113], $9x10^6$ (*ex vivo* whole lung imaging assays)[26,113], $1.2x10^6$ (tumour cell adhesion assay) or $6x10^5$ (tumour cell intercalation assay) platelets/µL were used in order to achieve a consistent ratio of platelets to tumour cells per unit of volume (1.2-1.5 platelets : tumour cells/µL).

2.1.2.5 *Ex vivo* platelet aggregation on tumour cells (TCIPA)

CMFDA-stained B16F10 cells were seeded at 10^4 cells/chamber in collagen I biocoated multichambers (BD Bioscience). The following day, $30x10^6$ PKH26-stained platelets and ASA, SC-560 or NS-398 were added and incubated with tumour cells for 2 hours, fixed with 2% PFA (in PBS; Sigma) and mounted with Vectashield mounting medium containing DAPI (Vector Laboratories). When tumour cells were treated separately, they were incubated in RPMI supplemented with the drugs for 2 hours at 37°C, then they were washed twice with PBS and incubated with platelets. When platelets were treated separately, they were incubated in washing buffer supplemented with the drugs for 30 minutes at 30°C. Platelets were washed twice in washing buffer and then added to tumour cells.

2.1.2.6 Agonist-induced platelet aggregation and quantification by flow cytometry

Platelet aggregation was evaluated through a previously described method[490] (Figure 2.1). Briefly, citrated PRP was incubated with the agonists AA (1 µM, Sigma-Aldrich), U46619 (0.3 µM, Tocris) and ADP (1 µM, ChronoLog) or their vehicles in half-area-96-well microtiter plates, for a total volume of 50 µL/well. Immediately after agonist addition, platelet aggregation was achieved through the incubation PRP at 37'C for 5 minutes under 1 mm orbital shaking (Infinite m200 plate reader, Tecan). Aggregated PRP was diluted 1:8 with ACD buffer and labelled with anti-CD41-APC antibody (Biolegend, 1:160 in PBS) for 30 minutes at 4'C. Samples were then diluted with formalin 0.1% in PBS (Sigma-Aldrich) and supplemented with 10^4 CountBright absolute counting beads (Thermo Fisher Scientific). Labelled platelet suspension was analysed at a FACSCalibur flow cytometer (BD Biosciences). Beads (FL1/SSC-H) were gated and platelets (FL4-H/SSC-H) were acquired until the count of 100 beads was reached.

Acquired data were analysed using FlowJo software version 7.6.5, through the generation of a gate around the population of single platelets in the FL4-H/SSC-H or or FL4-H/FSC-H plot. The total number of events was quantified and normalised to the number of beads, used as a surrogate measure of volume (Figure 2.1). The depletion of single platelets population is representative of platelet aggregation, and can be visualised through the appearance of a comet tail of platelet aggregates[490].

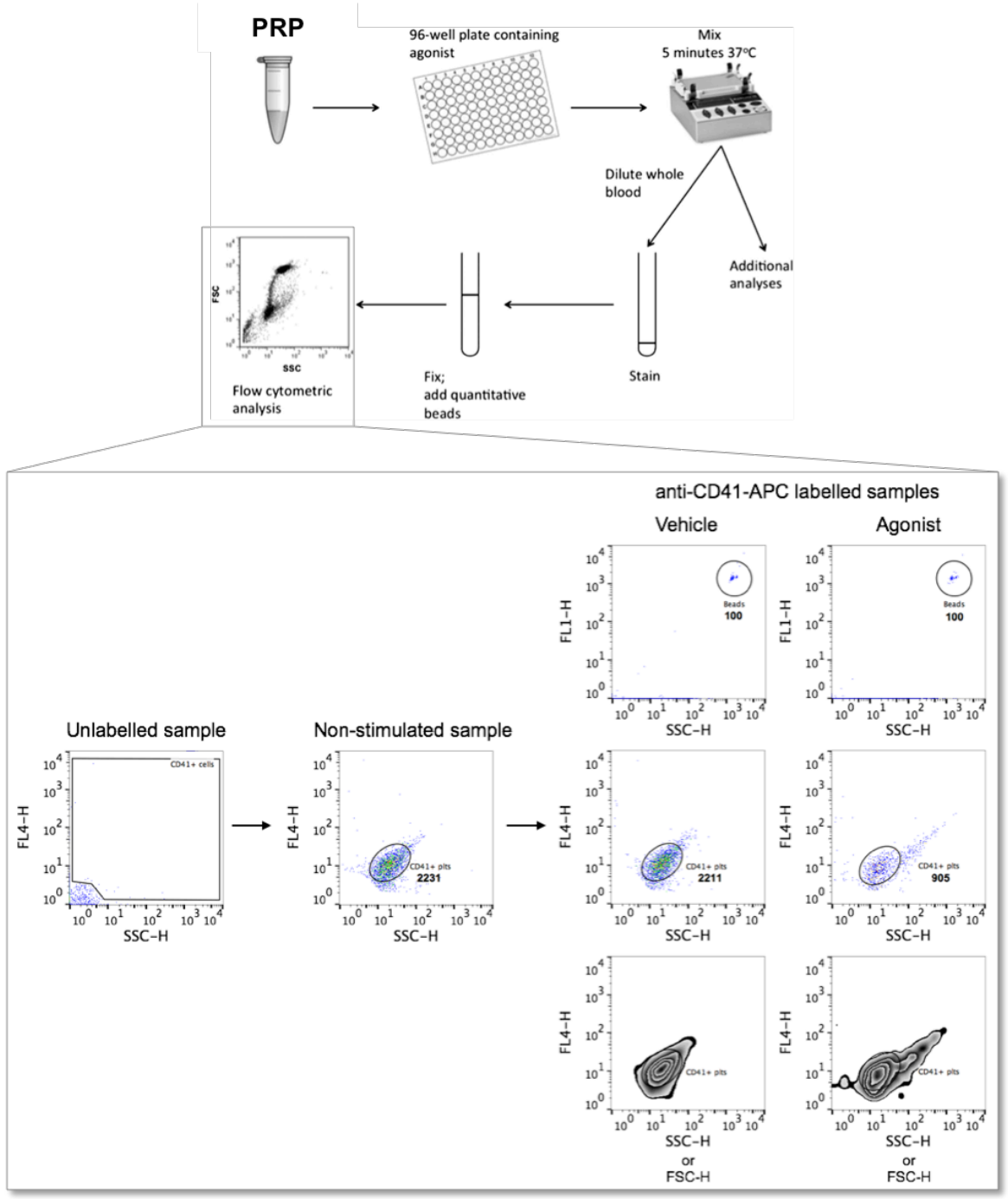

Figure 2.1 – Schematic representation of the measurement of platelet aggregation through FACS.

Platelet Rich Plasma (PRP) was aliquoted in 96-well microplates and mixed for 5 minutes at 37°C. Then, a sample of aggregated PRP was stained with anti-platelet CD41-APC antibody, fixed in formalin and supplemented with quantitative beads. Platelet suspension was analysed using a flow cytometer. To analyse platelet aggregation, the population of CD41+ cells was selected from an unlabelled sample. Platelets were gated in the non-stimulated sample, then counted and normalised to the number of enumeration beads. Platelet aggregation was evaluated as decrease of single platelet number. Notice the appearance of comet tail of platelet aggregates, as shown by zebra dot plots. Image adapted from Armstrong et al.[490].

2.1.2.7 Intracellular Ca^{2+} mobilisation analysis

The mobilisation of intracellular Ca^{2+} in platelets was performed as previously indicated[491], with some modifications. Briefly, PRP was incubated for 45 minutes at 30°C in the presence of 3 μM Fura-2 AM (Thermo Fisher Scientific), previously dissolved in DMSO to a concentration of 1 mM, following the manufacturer's instruction. Platelets suspension was supplemented with 0.25 μM PGE_1. Then, platelets were spun down at 1300 xg for 10 minutes and resuspended in MTH at $2x10^6$ platelets/μL and aliquoted in a 96-well microplate (50 μL per well, for a total of $1x10^8$ platelets per well). The plate was placed in a pre-warmed plate reader (37°C) and acquired for a total of 30 cycles of 9 seconds of 1 mm orbital shaking, followed by fluorescence reading with excitation at 340/380 nm and emission at 520 nm. After 5 cycles the plate was ejected and 1 μM U46619 or vehicle (MTH buffer) were added in a volume of 1 μL per well, then reading was continued for the remaining 25 cycles. The concentration of intracellular Ca^{2+} was calculated from the ratio of 340/380 nm readings.

2.1.3 Tumour cell adhesion and intercalation assays

2.1.3.1 Tumour cells adhesion assay under flow

$1.5x10^4$ LMVECs were seeded in each channel of a 6-channel μ-Slide $IV^{0.4}$ (IBIDI), previously coated with 2% gelatin, and fresh growth medium was replaced at 30 minutes and 24 hours post-seeding. After two days, washed platelets were isolated from C57BL/6 mice, labelled with PKH26 and treated with ASA (Medium dose), SC-560, NS-398 (Table 2.1) or their vehicles for 30 minutes. Platelets were then washed with MTH buffer and resuspended in PPP. Concomitantly, LMVECs and exponentially growing B16F10 cells were treated with ASA, SC-560, NS-398 or their vehicles for 2 hours, washed twice with growth medium and resuspended with complete growth medium. B16F10 cells were then labelled with CMFDA and harvested. $3x10^5$ CMFDA-labelled B16F10 and $60x10^6$ PKH26-

labelled platelets were introduced in the flow channel under a shear pressure of 0.05 dyn/cm^2, which corresponds to the shear stress rate in brain capillaries[492], controlled by a PHD2000 apparatus (Harvard). Real time adhesion was imaged for 10 minutes in one field of view (FOV) per channel through an epifluorescence microscope, equipped with an incubator that maintained a 5% CO_2 humidified atmosphere at 37˚C. Then shear stress was increased to 1 dyn/cm^2 and adhesion was acquired for additional 2 minutes. Pictures of 10 fixed fields of view were acquired before and after the increase of shear pressure.

2.1.3.2 Tumour cells intercalation assay in static conditions

3x10^5 LMVECs were seeded in each well of a 24-well plate, previously coated with gelatin 2%, and fresh growth medium was replaced after 30 minutes and 24 hours. At 2 days after seeding, washed platelets were isolated from C57BL/6 mice, labelled with PKH26 and resuspended with PPP. Concomitantly, exponentially growing B16F10 cells were labelled with CMFDA and harvested. Before acquisition, vehicles or drugs were added to the medium of LMVECs, just before the introduction of 5x10^4 CMFDA-B16F10 and 30x10^6 PKH26-platelets. Intercalation was monitored in 3 fields of view per well for 15 hours through an epifluorescence microscope equipped with an incubator that maintained a 5% CO_2 humidified atmosphere at 37˚C. Tumour cell intercalation was quantified visually from microscopic fields or through reconstruction of tumour cells surface and ellipticity (oblate) measurement at Imaris software (v8.2, Bitplane).

2.2 *IN VIVO* ASSAYS

All animal procedures were carried out in accordance with the United Kingdom Animals (Scientific Procedures) Act 1986 and following local ethics review.

2.2.1 Animal strains

C57BL/6, BALB/c and SCID mice were purchased from Charles River Laboratories. *Cx3cr1*$^{gfp/+}$ mice (B6.129P-*Cx3cr1*^{tm1Litt}/J) were obtained from The Jackson Laboratory[493]. *COX-1*$^{-/-}$ mice are a kind gift from Prof T.D. Warner, The William Harvey Research Institute, Barts and the London School of Medicine and Dentistry, London. 8-10 week old female mice were used for *in vivo* experiments involving drug treatment and/or tumour cell injection, while older naïve mice with a C57BL/6 background were employed for blood withdrawal and platelet isolation.

2.2.2 Drug treatment

All drugs were administered through drinking water, given ad libitum and changed every second day. ASA was resuspended in sterile dH_2O administered as DL-lysine acetylsalicylate. SC-560 was resuspended in DMSO and dissolved in water supplemented with 0.2% (v/v) polyethylene glycol 200 (PEG200) and 0.01% (v/v) Tween-20 (both from Sigma-Aldrich). NS-398 was resuspended in DMSO and dissolved in water supplemented with 0.9% w/v sodium chloride (Sigma-Aldrich). PICO and OZA were dissolved in ethanol (Sigma-Aldrich) and dissolved in water. All drinking water solutions were supplemented with 2% w/v sucrose (Sigma-Aldrich).

2.2.3 Experimental lung metastasis assay

$2.5x10^5$ B16F10 cells and $3.0x10^5$ MC-38-GFP cells were intravenously injected into C57BL/6 mice. $1.5x10^5$ 4T1 cells were intravenously injected in BALB/c mice. $1x10^6$ MDA-MB-231 cells were intravenously injected in SCID mice. A total volume of 100 µL of cell suspension was injected for all cell types. After 2 weeks (4T1 cells), 3 weeks (B16F10 and MC-38-GFP cells), or 4 weeks (MDA-MB-231 cells), mice were anesthetized with Pentobarbital (70 mg/kg, intraperitoneally), and lungs were artificially ventilated through a tracheotomy. Mice were killed by exsanguination and lungs were exposed and perfused through the pulmonary artery with Krebs-Ringer Buffer (KRB) [4.74 mM KCl, 1.17 mM $MgSO_4 \cdot 7H_2O$, 1.27 mM $CaCl_2 \cdot 2H_2O$, 1.18 mM KH_2PO_4, 118.4 mM NaCl, 24.87 mM $NaHCO_3$, 10 mM glucose, 5% w/v dextran] (all from Sigma-Aldrich or Thermo Fisher Scientific). Once cleared of blood, lungs were dissected and immersed in 10% formalin solution (Sigma-Aldrich). Metastatic lung nodules were counted or assessed by MRI scan.

2.2.4 MRI scan of lungs

MDA-MB-231 metastasis could not be assessed visually in lungs cleared of blood. In order to assess the metastatic load, formalin-fixed lungs were embedded in 4% agarose in dH_2O. MRI on embedded lungs was performed at 4.7T or 7.0T (Agilent, VNMRS) using a 25-mm inner diameter quadrature birdcage coil (Rapid). T2-weighted fast spin echo 3D scan was acquired (echo spacing 9.35 msec, echo train length 8, effective TE 37.41 msec, TR 200 msec) with a FOV of (32x32x32) mm^3 to ensure complete volume coverage of the coil (and sample). Scan time was approximately 27 min per sample for an isotropic resolution of 125 µm. Ten samples were queued for unsupervised MRI measurement using an in-house developed carriage system utilising a stepper motor driven by an Arduino controller (http://www.arduino.cc). Tumour burden was quantified by ImageJ (v.1.46r) and ITK-SNAP software (v.3.4.0).

2.2.5 Urine collection and SUA measurement

Urine was collected upon restraining C57BL/6 mice and indomethacin (10 µg/mL in DMSO, both from Sigma-Aldrich) was immediately added. Urine was clarified through centrifugation at 10000 x g for 15 minutes at 4°C. SUA concentration was assessed through a HPLC and absorbance detection by Dr M. Stratford. Briefly, 5 µL of urine were mixed with 50 µL of 10 µM 6-methoxysalicylate (internal standard) and 1 mL of 10 mM formic acid. 5 µL of the sample were injected onto the HPLC for analysis. Samples were analysed by HPLC (Waters 2695, Watford, UK) equipped with a Micromass Quattro Micro Mass spectrometer (Waters). Separation was achieved using a kinetix XB (2.6 µm, 2.1 x 50 mm) column maintained at 35 °C with eluent A: 10 mM formic acid; eluent B: acetonitrile, using a flow rate of 0.25 mL/ min and a gradient of 8–50 % B over 4 min. Salicyluric acid was detected using electrospray in negative mode with MS/MS with a capillary voltage of 1.2 V at 194 – 150 (cone voltage 20V) and IS at 166.9-123 (cone voltage 20 V). Sample concentrations were calculated based on a calibration curve prepared with commercially available salicyluric acid.

2.2.6 *Ex vivo* whole lung imaging assay

$5x10^5$ CMAC-stained B16F10 cells and $9x10^8$ PKH26-stained platelets were injected into the opposite tail veins of *Cx3cr1*$^{gfp/+}$ mice. The chosen number of platelets corresponds to ½ of the total number of platelets in an adult mouse of approximately 20 g, resulting in the incorporation of labelled platelets in at least half of the formed clots. After 8 hours, lungs were isolated as described above and placed in a specially designed chamber with a coverslip window at its bottom. The chamber was designed and manufactured by Dr J. Beech and Dr S. Smart. The lungs were inflated with 0.5 mL of air and remained inflated during the imaging[26,267].

2.2.7 Endothelial cell labelling for whole lung imaging

To address the extravasation state of tumour cells, we have employed an established techniques to visualise fluorescently labelled blood vessels in intact lungs[215,267,494]. Briefly, mice were artificially ventilated as described above. Before lung isolation, endothelial cells were labelled with an anti-CD31-APC antibody (50 µL, Biolegend) injected in the vena cava and left to circulate in the lung vasculature for 5 minutes, after vena cava ligation. Lungs were then perfused and harvested as usual and imaged as intact organs under a confocal microscope. Tumour cell extravasation was evaluated visually from microscopic fields or through reconstruction of tumour cells and vessel surface at Imaris software (v8.2, Bitplane).

2.2.8 Immunofluorescence staining of lung sections

For the preparation of lung sections, lungs were harvested and perfused as indicated above and then perfused with 50 mL of ice-cold PFA 4% through the pulmonary artery. Lungs were then inflated with 1 mL PFA and immerged in sucrose 25% (Sigma-Aldrich) at 4°C for 48 hours, changing sucrose every day. Lungs were snap frozen using Cryo Freeze spray (Agar Scientific) and 18 µm sections were cut at a cryostat microtome and collected on positively charged glass slides (Superfrost® Plus, Thermo Thermo Scientific). Slides were left to air-dry overnight at 37°C and then stored at -80°C/-20°C.

For immunofluorescence staining, sections were rehydrated in PBS and permeabilised with 0.2% Triton-X in (Sigma Aldrich) in TBS, for intracellular epitopes. Then, sections were blocked for endogenous peroxidase in PBS supplemented with 30% w/v hydrogen peroxide (1:100; Thermo Fisher Scientific). Endogenous streptavidin and biotin were blocked with a blocking kit (Vector) following the manufacturer's instruction. Next, slides were incubated with Image-iT® FX to block autofluorescence background. Slides were then blocked with 0.5% Roehinger milk buffer (TNB, PerkinElmer).

Immunostaining of proteins was performed using the Tyramide Signal Amplification-biotin kit (PerkinElmer), following the manufacturer's instructions. Briefly, sections were incubated overnight with the following primary antibodies: COX-1 (ab109025, Abcam, 1:250), TP (sc-30036, Santa Cruz, 1:250), TXAS (ab39362, Abcam, 1:250), VCAM-1 (MAB6434, Millipore, 1:100). IgGs from the same species were used at the same concentration as isotype controls. All antibodies were diluted in TNB and incubated overnight at 4°C. Next, primary antibodies were detected using biotinylated secondary antibodies (all from Thermo Fisher Scientific), diluted 1:500 in TNB. Tissues were then incubated with Streptavidin-HRP complex (1:200 in TNB) and, subsequently, Tyramide Signal Amplification-biotin complex (1:100 in amplification buffer) (all from PerkinElmer). Finally, signal was revealed through streptavidin-fluorophore conjugates (1:100, Streptavidin-AF488 or streptavidin-AF633, Thermo Fisher Scientific). vWF did not need amplification and was immunostained by incubating the sections with the primary antibody (ab11713, Abcam, 1:500 in TNB, overnight at 4°C) or isotype control and then secondary AF488-labelled antibody (A-11015, Thermo Fisher Scientific).

All incubation steps were done in a dark humidified chamber and were followed by 5-minutes washes with PBS. After staining, slides were mounted with ProLong® Gold antifade reagent (Thermo Fisher Scientific) and covered with a coverslip.

2.2.9 Analysis of prostanoids in biological fluids

2.2.9.1 Serum and plasma TXB_2

Blood was collected from terminally anaesthetized C57BL/6 mice through vena cava cut with (plasma) or without (serum) ACD buffer (1:10 v/v). For serum preparation, blood was left to clot for 30 minutes at room temperature and centrifuged at 850 xg for 15 minutes at 4'C. For plasma preparation, anticoagulated blood was centrifuged at 1000 xg for 15 minutes at 4'C. Both supernatants, corresponding to serum and plasma, were collected and stored at -80'C. Serum and plasma TXB_2 were measured through a Thromboxane B_2 EIA kit (Cayman chemicals).

2.2.9.2 Plasma PGE_2

For *ex vivo* PGE_2 generation assay, blood was collected from terminally anaesthetised C57BL/6 mice in syringes containing ACD buffer (1:10 v/v). Whole anti-coagulated blood was incubated with 10 µg/mL LPS (Sigma-Aldrich) or saline for 24 hours at 37°C. Plasma was isolated through whole blood centrifugation at 1000 xg for 15 minutes at 4°C and the supernatant was stored at -80"C. Plasmatic PGE_2 was measured through PGE_2 Metabolite EIA kit (PGE_2M, Cayman Chemicals), which allows the quantification of 13,14-dihydro-15-keto PGA_2 and 13,14-dihydro-15-keto PGE_2 metabolites.

For *in vivo* PGE_2 generation assay, C57BL/6 mice were injected with 5 mg/kg LPS or saline and blood was collected through vena cava at 4 hours after injection, in syringes containing ACD buffer. Whole anti-coagulated blood was centrifuged at 1000 xg for 15 minutes at 4°C and plasma was collected in the supernatant and stored at -80°C. Plasmatic PGE_2 was measured through PGE_2 ELISA kit (Abcam).

2.3 MICROSCOPY

2.3.1 Epifluorescence microscopy

For tumour cell adhesion assay, images were acquired at the Nikon Eclipse TE2000-E microscope, fitted with Solent Scientific cabinet for cell growing and equipped with a Nikon Plan Fluor 10x/0.30 Ph1 DL objective. Pictures were acquired every 5 seconds for 10 minutes (0.05 dyn/cm^2) and 2 minutes (2 dyn/cm^2) with a Hamamatsu ORCA-ER digital camera. For tumour cell intercalation assay, images were acquired at the Nikon NIS-Elements AR 4.30.02 64-bit microscope, equipped with a Nikon Plan Fluor 10x/0.30 Ph1 DL objective. Pictures were acquired every 10 minutes for 15 hours.

2.3.2 Confocal microscopy

Z-stack images were acquired with an inverted confocal microscope (LSM-710 and LSM-880; Carl Zeiss Microimaging) equipped with a Plan-Apochromat 20x/0.8 M27 objective. CMAC, GFP and PKH26/CMRA were excited by 405 nm, 488 nm and 561 nm laser lines, respectively. PKH26 and CMAC were acquired simultaneously, while GFP and CMRA were acquired separately. All images were acquired line by line. Image stacks of 15-40 slices with an interval of 1.15-2 μm of at least 15 random fields per lung or 5 per lung section were acquired. Whole left lung were acquired through tile scan of approximately 750 single images (20x) with 10% overlapping for stitching.

2.4 STATISTICAL ANALYSIS

Statistical analysis was performed with GraphPad Prism (version 5.02). D'Agostino and Pearson omnibus normality test was applied to data sets to assess data distribution. For normally distributed data, unpaired t-test (two groups), one-way ANOVA with Tukey's test (more than two groups) or Pearson test (correlation analysis) were used. For non-normally distributed data, Mann Whitney (two groups) or Kruskal-Wallis with Dunn's multiple comparison post-hoc tests (more than two groups) or Spearman test (correlation analysis) were used. For non-linear regression analysis, a substrate inhibition equation and extra sum of squares F test were employed to assess statistical difference between curves.

Data represents mean +/± SD unless specified otherwise. Differences are considered significant with a p value lower than 0.05. * denotes $0.01<p\leq0.05$, ** $0.001<p\leq0.01$ and *** $p\leq0.001$.

CHAPTER 3

Aspirin affects metastasis through the inhibition of COX-1

3.1 INTRODUCTION

3.1.1 Aspirin, COX inhibition and metastasis

As described in detail in section 1.2, aspirin is a widely used drug that inhibits the activity of COX-1 and COX-2. Both isoforms mediate the conversion of arachidonic acid (AA) into PGH_2, the common precursor of all prostanoids.

In the clinic, aspirin is administered at low (75-100 mg/day), medium (325 mg/day) and high (1-3 g/day) doses. Due to the pharmacology of the drug, low-dose aspirin inhibits almost exclusively COX-1 in the pre-systemic compartment. Thus, platelets are the cells most affected by low-dose aspirin treatment, which reduces their aggregation triggering an anti-thrombotic effect. At medium and high doses both COX-1 and COX-2 are affected. Being COX-2-derived prostanoids (mainly PGE_2) key players in the inflammatory response, medium and high doses of aspirin trigger both an anti-thrombotic and anti-inflammatory responses.

Evidence from experimental and clinical studies indicates an effect of aspirin on metastasis prevention. In particular, low-medium dose of aspirin (<300 mg/day) was responsible for a 30-70% reduction in the risk of developing distant metastasis from a range of primary tumours, in particular colorectal cancer. Although the mechanism of action of aspirin has been extensively described, the reasons of its metastasis prevention remain elusive. We have employed *in vivo* models of metastasis to address this issue.

3.1.2 Choice of aspirin doses for *in vivo* studies

Aspirin has been associated to a wide range of mechanisms of action, both COX-dependent and COX-independent, and the pharmacological properties of the drug vary depending on the dose. Thus, a careful selection of aspirin dosage is required for the design of experimental studies aimed at understanding molecular basis of the anti-metastatic effect of aspirin shown by clinical trials. From my point of view, the best approach for choosing an equivalent dose of aspirin in mice based on the dose in man should incorporate two steps. First, the BSA normalisation method[435] should be used to select the starting dose of aspirin for the animal experiment. Second, the pharmacological effects of the chosen dose should be tested through the evaluation of COX-1 and COX-2 inhibition *in vivo*. In addition, the relative contribution of COX-1 and COX-2 can be investigated by employing selective inhibitors.

3.1.2.1 Evaluation of aspirin activity *in vivo*

The assessment of COX-1 and COX-2 activity after the oral administration of aspirin or other NSAIDs is important to evaluate the treatment efficacy and understand the outcome, both in clinical and experimental studies. Over the last 50 years considerable efforts have been made to develop reliable methods to evaluate COX-1 and COX-2 activity, which have taken into account several variables.

The first consideration was the choice of biomarkers for the activity of the two COX isoforms. COX-1 and COX-2 catalyse the same subsequent reactions that lead to the synthesis of PGG_2, the common precursor of all prostanoids. Thus, in principle COX-1 and COX-2 are able to synthesise all prostanoids. In practice, however, their activity is rarely redundant. For example, TXA_2 is mainly (but not exclusively) produced by COX-1, while PGE_2 is preferentially produced by COX-2[342]. Thus, TXA_2 and PGE_2 have been chosen as biomarkers of COX-1 and COX-2 activity, respectively.

The second challenge has been the choice of metabolite to be used for the measurement of prostanoids. Prostanoid undergo a very rapid metabolism in most biological fluids or they are rapidly bound by cell receptors in target organs, which makes it impossible to measure their circulating levels. Thus, metabolites of the primary prostaglandins have been chosen as biomarkers for COX-1/-2 activity. For example, TXA_2 half-life in blood and other aqueous solutions is of around 30 seconds[495], thus its metabolites TXB_2 in plasma/serum and 11-dehydro-TXB_2 or 2,3-dinor-TXB_2 in urine are used as surrogates. Similarly, PGE_2 half-life is 30 seconds and it is rapidly taken up by target cells after its secretion, thus metabolites such as 13,14-dihydro-15-keto PGA_2 are used to evaluate PGE_2 systemic synthesis. However, the physiological levels of PGE_2 metabolites in plasma are very low (3-12 pg/mL)[496] and below the limit of detection. Since PGE_2 synthesis is largely induced by inflammatory conditions, a widely used approach is to incubate anti-coagulated whole blood with LPS, which induces the expression of COX-2 in monocytes and increase the concentration of plasmatic PGE_2[497].

The choice of biological sample is also of pivotal importance. This is for example the case of serum and plasma samples in the measurement of TXB_2. Serum corresponds to the soluble fraction of coagulated blood, while plasma is obtained as the non-cellular fraction of anti-coagulated blood. In the isolation of serum, the activation of the coagulation cascade leads to thrombin deposition, which activates platelets to generate *de novo* TXA_2, thus increasing TXB_2 concentration. This is why plasmatic TXB_2 concentration is not higher that 1-2 pg/mL, while serum TXB_2 levels can reach up to 400 ng/mL, a 1000 fold increase[498]. In this perspective, the measurement of TXB_2 in serum is representative of the *ex vivo* synthesis of TXA_2 by platelets. Since this process is dependent on COX-1 activity, the quantification of serum TXB_2 is a gold standard technique to measure the efficacy of anti-thrombotic therapies on the activity of COX-1 in platelets. On the other hand, the levels of TXB_2 in plasma and of 11-dehydro-TXB_2 in urine reflect the systemic

and, in the case of 11-dehydro-TXB_2, cumulative production of TXA_2 *in vivo* by platelets, endothelial cells and other cell types, but cannot discriminate the source of TXA_2.

Different considerations need to be made in the case of COX-2 activity. PGE_2 levels do not change between plasma and serum and the quantification of PGE_2 metabolites in either plasma/serum or urine is representative of its systemic biosynthesis. On the contrary, the levels of PGE_2 in LPS-stimulated plasma reflect the *ex vivo* activity of COX-2 in monocytes exclusively[497].

Indirect measurements of aspirin efficacy *in vivo* are also available, which take into consideration the anti-thrombotic and anti-inflammatory effects of COX-1 and COX-2 inhibition, respectively.

The use of light transmission (LTA) aggregometry is a gold standard technique used in the clinic to evaluate platelet functions, such as the residual COX-1 activity. LTA methods consist in the turbidimetric (or flow cytometric) measurement of platelet rich plasma following stimulation with an agonist. A wide range of agonists can be used to achieve COX-1-dependent or -independent aggregation. In particular, AA, TP agonist U46619 (stable analogue of TXA_2) and thrombin are agonists that induce platelet aggregation through a COX-1-dependent pathway and can be used to assess the extent of COX-1 inhibition. On the contrary, adenosine diphoshpate (ADP), collagen and epinephrine trigger platelet aggregation through a COX-1-independent activation of integrin GPIIb/IIIa, thus are categorised as COX-1-nonspecific methods.

Equally, the extent of COX-2 inhibition can be indirectly evaluated through the measurement of circulating pro-inflammatory cytokines and chemokines, such as TNF-α[436,499], CCL15[500] and hs-CRP[499].

To summarise, several methods exist that allow the evaluation of COX-1 and COX-2 activity *in vivo* and parameters such as the choice of sample and PG metabolite, as well

as sample processing, should be taken into careful consideration to avoid deceiving results.

3.1.2.2 Selective inhibitors of COX-1 and COX-2

The development of selective inhibitors of COX-1 or COX-2 has been challenging, due to the similarity of the two isoforms and the >90% homology of their catalytic/allosteric site. Nevertheless, selective drugs exist and their selectivity relies on the existence of single amino acid substitutions in the COX channel and catalytic site.

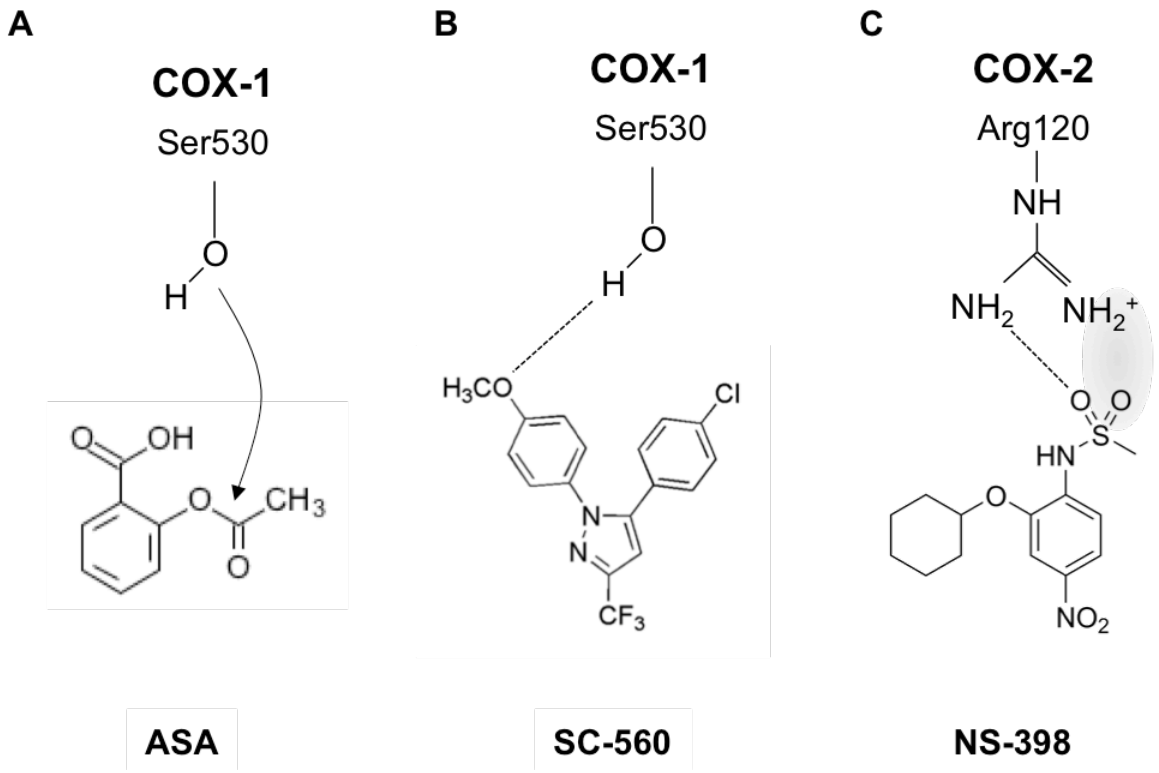

Figure 3.1 - Structure of COX inhibitors.

(A) Aspirin or acetylsalicylic acid (ASA), non-selective inhibitor of COX-1 and COX-2.

(B) SC-560, selective inhibitor of COX-1. Note the 4-methophenyl ring with a phenyl group, responsible for the H-bonding to Ser530 in COX-1 active site.

(C) NS-398, selective inhibitor of COX-2. NS-398 forms a ionic and a hydrogen bond with two nitrogen atoms of Arg120 in the active site of COX-2.

All drug structures were adapted from KEGG Drug database.

In general, most COX-2 selective inhibitors cannot access COX-1 catalytic site due to steric blockage. Of particular importance is the substitution of Ile523 (COX-1) in Val523 (COX-2), where the difference in one methyl group allows the generation of a side opening in the wall of the channel, known as COX-2 pocket[501]. Drugs that can access COX-2 pocket and not COX-1 catalytic site are classified as coxibs and their selectivity depends on steric blockage rather than isoform-specific mechanisms of inhibition[332,501]. Other inhibitors, such as NS-398, rely on their chemical features to selectively bind residues in the COX-2 catalytic site[335,340]. This selectivity has been empirically derived from inhibition curves but the molecular mechanisms of the interaction are still not known[502].

Due to the presence of the COX-2 pocket, size exclusion cannot be employed for COX-1 selective inhibitors. Hence, all COX-1 selective inhibitors rely on the presence of structural elements that allow the specific docking to the COX-1 active site. Several classes of COX-1 inhibitors have been recognised, although Arg120 and, similarly to aspirin, Ser530 are the most common docking residues in COX-1 catalytic site[503].

In this Chapter two selective inhibitors have been used, SC-560 (COX-1 inhibitor) and NS-398 (COX-2 inhibitor).

SC-560 is a highly selective inhibitor of COX-1 that belongs to the class of diarylheterocycles with pyrazole heteroaromatic ring (Figure 3.1B). SC-560 inhibition of COX-1 depends on the H-bonding of one oxygen atom of the 4-methophenyl ring with the hydroxyl group of S530 on COX-1[503]. In an *ex vivo* assay, Smith et al.[504] calculated that the IC50 of SC-560 is 9 nM for COX-1 and 6.3 μM for COX-2, thus the selectivity of SC-560 to COX-1 is 700-fold higher than to COX-2.

NS-398 (N-[2-(cyclohexyloxy)-4-nitrophenyl] methanesulfonamide, Figure 3.1C) belongs to the methanesulfonanilide class of COX-2 inhibitors. This molecule is the result of a

structural modification of nimesulide that allows a selective access of the COX-2 site[505] and the docking of its oxygen atom to His90 in the COX-2 active site[506,507].

3.2 AIMS

The aim of this Chapter is to set up an *in vivo* model in which aspirin affects the development of experimental metastasis and to understand the contribution of COX-1 and COX-2 to this process. This has been done through the following workflow:

1) Dose-setting: a range of doses of aspirin have been chosen and rigorously tested for their *in vivo* efficacy, which includes the assessment of COX-1/COX-2 inhibition and the effect on thrombosis and inflammation.

2) Treatment of metastasis with aspirin: we have investigated the effect of the selected doses of aspirin on the establishment of metastasis in several experimental models.

3) Selective inhibition of COX-1 or COX-2: we have employed selective inhibitors of COX-1 and COX-2 or genetically engineered mice to understand the molecular mechanisms of metastasis inhibition by aspirin.

3.3 RESULTS

3.3.1 *In vivo* dose-setting of aspirin

3.3.1.1 Doses of aspirin and intake assessment

To characterise the effects of aspirin on metastasis, we chose different doses of aspirin (ASA)[a] (30 mg/L, 180 mg/L and 625 mg/L), which had been previously used to achieve similar effects to the low, medium and high doses in humans[243,436,437]. By applying a BSA dose conversion from the average daily intake of ASA, the selected doses correspond to a HED of 63, 349 and 986 mg/day, respectively (Table 3.1), which fall in the expected range of low-, medium- and high-dose regimes in human adults. Hence, these doses are here indicated as Low, Medium and High (Figure 3.2A).

Aspirin or vehicle (Control) was administered to C57BL/6 mice through drinking water, supplemented with sucrose and freshly changed every other day. The expected daily water consumption per mouse in the different groups was comparable (Supplementary figure S1). The intake of aspirin per mouse was evaluated by measuring the levels of its stable metabolite in urine (salicyluric acid or SUA) (Figure 3.2B). SUA was preferred to plasmatic salicylic acid (SA) because it accumulates in urine, representing the most abundant metabolite of ASA[366], and because plasmatic SA undergoes a much more rapid metabolism in blood giving more variable results (Supplementary figure S2).

[a] From now on, 'aspirin' is used to indicate the treatment regime, while its abbreviation ASA is used to indicate the compound used in drinking water for *in vivo* experiments and in figures.

	Control	Low	Medium	High
ASA concentration in drinking water *(mg/L)*	0	30	180	625
Volume of drinking water per day *(mL/day)*	5.017	5.624	5.001	4.500
Ingested ASA per day *(µg/day)*	0	209	1149	3244
Excreted SUA per day *(µg/day)*	0	63.24	433.74	1010.10
ASA consumption per body weight (*mg/(kg/day)*)	0	10.45	57.45	162.2
Expected HED from literature (*mg/day*)	0	33 - 174	184 - 958	519 - 2700
BSA-based HED (*mg/day*)	0	63	349	986

Table 3.1 – **Descriptive parameters of ASA intake.**

C57BL/6 mice were treated with vehicle (Control) or Low, Medium and High doses of ASA for 3 weeks and water intake was measured every other day. The concentration of ASA in drinking water and the volume of consumed water per day per animal were used to calculate different drug intake measurements (n≥50 mice per group). The concentration of urinary SUA was measured through HPLC analysis (n ≥16 mice per group).

ASA= acetylsalicylic acid; SUA=salicyluric acid; HED= human expected dose; BSA= body surface area (allometric conversion method).

The urinary levels of SUA (Figure 3.2B) were consistent with the daily ASA intake extrapolated from drinking water volumes (Figure 3.2C). Aspirin intake was constant for the duration of the experiment (Figure 3.2D), as expected from a chronic treatment, and was significantly different in the three treatment groups (Figure 3.2B and C).

A

Dose name	Concentration of ASA in drinking water	Effects	Ref
Low	30 mg/L	Anti-thrombotic	436
Medium	180 mg/L	Anti-thrombotic and anti-inflammatory (expected)	437
High	625 mg/L	Anti-thrombotic and anti-inflammatory	243

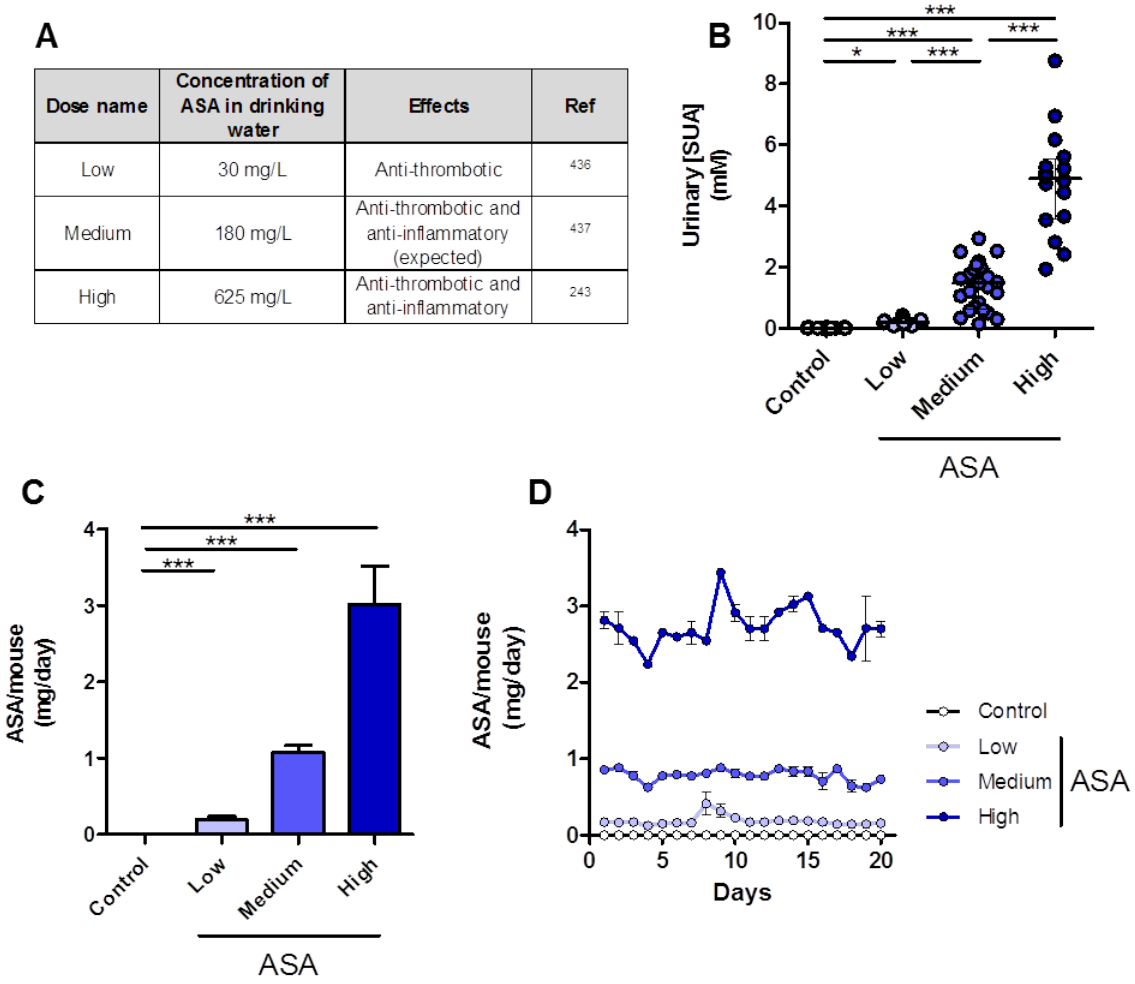

Figure 3.2 – Evaluation of aspirin intake.

(A) Table summarising the chosen doses of ASA and their expected effects, as reported in the literature.

(B) Concentration of salicyluric acid (SUA), a stable metabolite of ASA, measured in urine of C57BL/6 mice treated with vehicle (Control, n=27 mice) or ASA (Low, Medium or High, n=26, 25 and 16 mice, respectively) for 2 weeks (mean ± SD, 1-way ANOVA with Tukey's Multiple Comparison test).

(C-D) Expected average daily intake (C) (n=21 days per group; median + interquartile range (IQR), 1-way ANOVA with Kruskal-Wallis test with Dunn's Multiple Comparison post-hoc test) or daily intake over time (D) (n=2 cages for all time points; mean ± SD) of ASA per mouse, extrapolated from the drinking water consumption of C57BL/6 mice over a period of 3 weeks.

3.3.1.2 Analysis of COX-1 inhibition by aspirin

In order to verify the efficacy of the chosen doses, specific biomarkers of COX-1 or COX-2 activity were chosen to assess the extent of COX-1 and COX-2 inhibition following aspirin treatment (see diagram in Figure 3.3A). TXB_2 is a stable metabolite of COX-1-derived TXA_2 and it is representative of *ex vivo* COX-1 activity in platelets. Serum levels of TXB_2 were highly and significantly reduced by ASA at all doses (Figure 3.3B). *In vivo*, very small amount of COX-1 activity are sufficient to generate TXA_2 to a level that triggers platelet aggregation[508], thus it has been established that the inhibition of TXB_2 generation *ex vivo* in coagulated blood should be greater than 95% to reflect a substantial inhibition of platelet activation *in vivo*[498]. Only Medium and High doses reduced TXB_2 by more than 95%.

To further understand the extent of COX-1 inhibition in platelets, agonist-induced platelet aggregation was assessed in blood from ASA-treated mice through a modified light transmission aggregometry approach. AA, U46619 and ADP were used as agonists to induce platelet aggregation in a COX-1-dependent (AA and U46619) or -independent (ADP) manner. Medium and High doses decreased COX-1 mediated platelet aggregation induced by AA and U46619, but not by ADP (Figure 3.3C and D). Low dose ASA did not significantly affect platelet aggregation at all conditions, although a trend could be seen (Figure 3.3C).

Taken together, these results suggest that aspirin inhibits COX-1 activity and platelet aggregation at the Medium dose, indicating that in our model this is the minimum effective dose to achieve an anti-thrombotic effect.

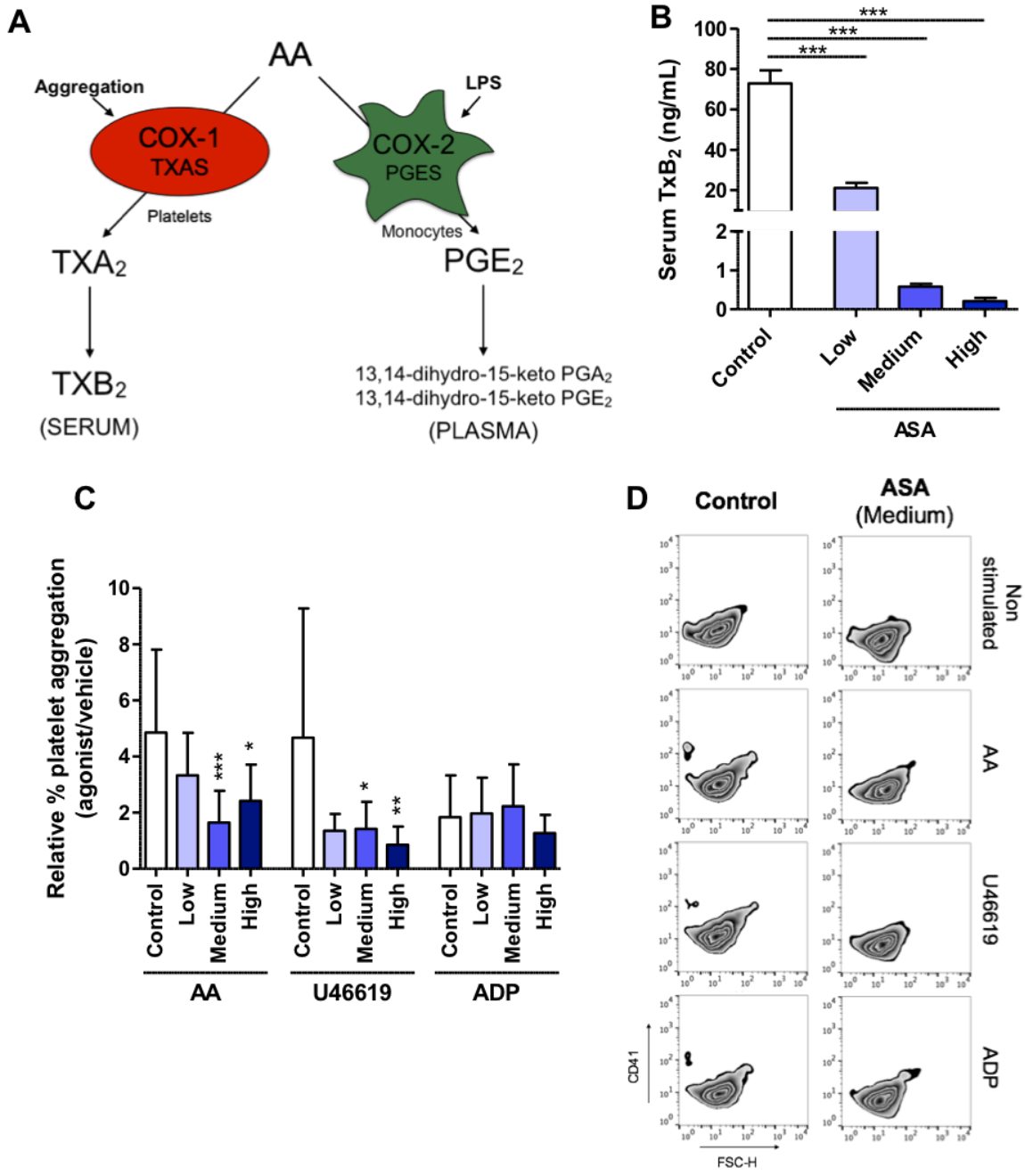

Figure 3.3 – Inhibition of COX-1 and platelet aggregation by aspirin.

(A) Diagram of COX-1 and COX-2 products chosen as biomarkers of their activity. Serum TXB_2 is representative of *ex vivo* COX-1 activity in platelets and plasma PGE_2 is representative of COX-2 activity in monocytes (*ex vivo*) or systemically (*in vivo*).

(B) Concentration of TXB_2 in serum from mice treated with vehicle (Control) or ASA at Low, Medium and High doses (n=3 mice per group). The serum concentration of TXB_2 is representative of COX-1 residual activity in platelets.

(C-D) Quantification (C) and representative zebra dot plots (D) of agonist-induced platelet aggregation, measured through FACS analysis of CD41-stained platelets. AA (1 mM), U46619 (0.3 μM) and ADP (1 μM) were used as agonists to trigger a COX-1-dependent (AA and U46619) or independent platelet (ADP) aggregation (n=4 mice per group).

All data are represented as mean + SD, 1-way ANOVA with Tukey's Multiple Comparison test.

3.3.1.3 Analysis of COX-2 inhibition by aspirin

PGE_2 is the most abundant product of COX-2 activity. However its metabolism is very fast,. For this reason, plasma levels of PGE_2 are generally very low and beneath the limit of detection. In order to evaluate the extent of COX-2 inhibition after ASA treatment we used an established assay in which LPS increased *ex vivo* production of PGE_2 by monocytes[497]. 10 ug/mL LPS induced overexpression of COX-2 when added to anti-coagulated whole blood *ex vivo*[497], leading to higher plasmatic levels of PGE_2 (Figure 3.4A), although the difference was not significant. When anti-coagulated blood was withdrawn from ASA-treated mice, the levels of plasmatic PGE_2 were significantly reduced at the Medium and High doses (Figure 3.4B), indicating in inhibition of COX-2 at these doses.

To verify that COX-2 was inhibited also at a systemic level, we employed a similar approach *in vivo*. Briefly, we set up a model where the injection of LPS in naïve C57BL/6 mice induced the systemic overexpression of COX-2 and increased plasmatic PGE_2 synthesis, measured as PGE_2 metabolite (PGE_2M, equivalent to 13,14-dihydro-15-keto PGA_2 and 13,14-dihydro-15-keto PGE_2) (Figure 3.4C and D). Next, the effect of aspirin on COX-2 activity was determined by treating mice with ASA for 2 days before the injection of LPS, blood withdrawal and PGE_2 extraction from plasma (Figure 3.4C). Plasmatic PGE_2 levels were significantly reduced by all doses of ASA (Figure 3.4E).

Taken together these results indicate that aspirin induces an anti-thrombotic and anti-inflammatory effect at the Medium and High doses, while no substantial inhibition of COX-1 was seen by the Low dose.

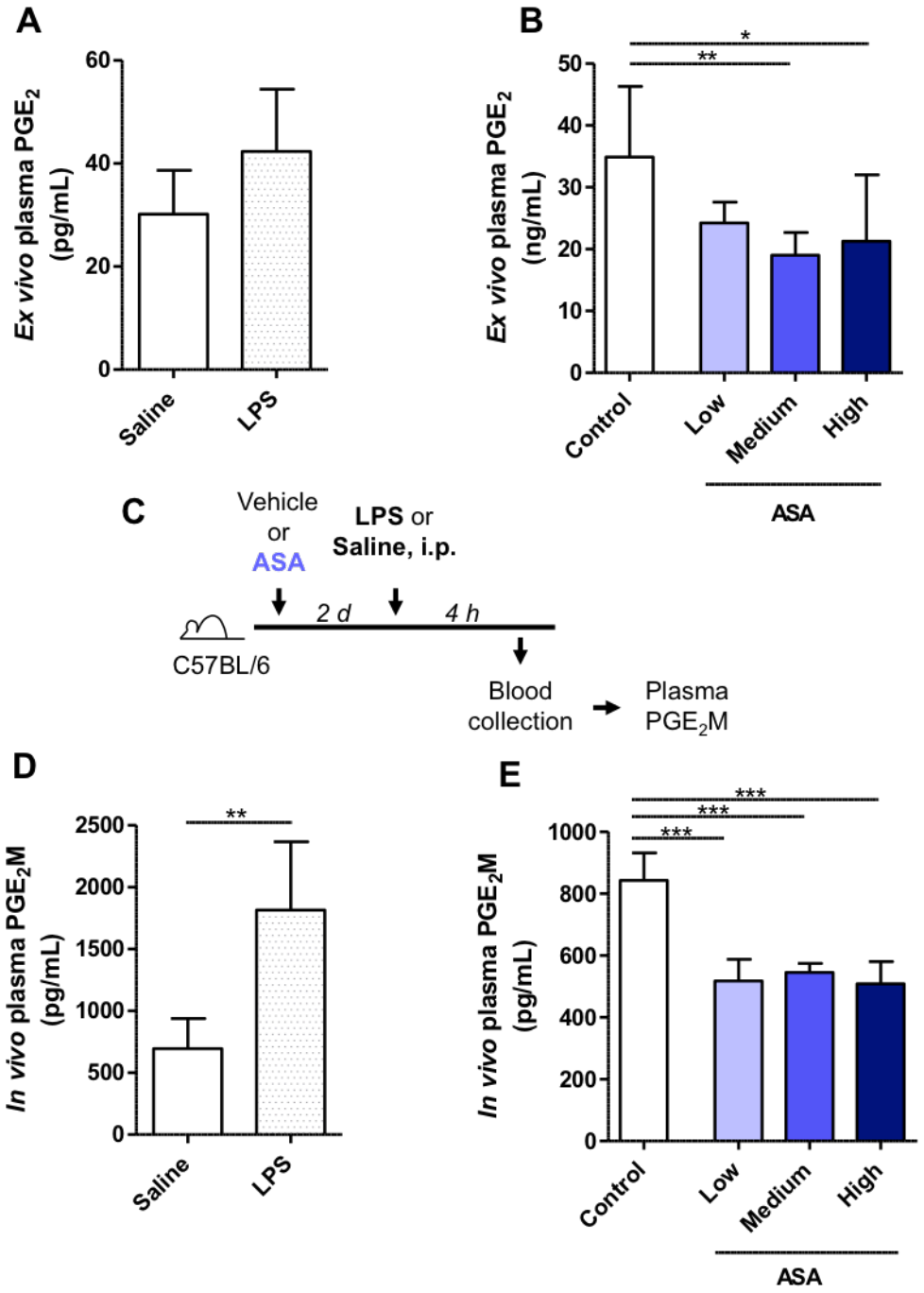

Figure 3.4 – Inhibition of COX-2 activity by aspirin.

(A) Concentration of PGE_2 in plasma stimulated with LPS (10 µg/mL) or saline *ex vivo* for 24 hours (n=4 mice per group). PGE_2 generated through this method is representative of COX-2 residual activity in monocytes (mean + SD, unpaired t test).

(B) Concentration of PGE_2 in LPS-stimulated plasma derived from mice treated with vehicle (Control, n=8 mice) or Low, Medium and High doses of ASA (n= 4 mice for all ASA groups; mean + SD, 1-way ANOVA with Tukey's Multiple Comparison test).

(C) Experimental design. Mice were treated with vehicle or ASA. After two days from the start of the treatment, mice were injected with saline or LPS (5 mg/kg) through the intraperitoneal (i.p.)

route and blood was harvested after 4 hours for the isolation of plasma and measurement of PGE_2 Metabolite (PGE_2M, equivalent to 13,14-dihydro-15-keto PGA_2 and 13,14-dihydro-15-keto PGE_2).

(D) Concentration of PGE_2M in plasma from saline- or LPS-injected mice (n=4 mice per group) treated with vehicle for two days (mean + SD, unpaired t test). PGE_2M is representative of systemic COX-2 activity.

(E) Concentration of PGE_2M in plasma derived from LPS-injected mice treated with vehicle or ASA at Low, Medium or High doses (n=3 mice per group; mean + SD, 1-way ANOVA with Tukey's Multiple Comparison test).

3.3.2 Effect of aspirin on experimental metastasis

3.3.2.1 Aspirin reduces experimental metastasis from melanoma cells

As detailed in Figure 3.5A, C57BL/6 mice were treated with ASA (Low, Medium and High) for two days before the intravenous injection of syngeneic B16F10 melanoma tumour cells. Aspirin treatment at the Medium and High doses reduced the number of metastatic lung nodules by more than 50% (Figure 3.5B and C). Noticeably, the number of nodules negatively correlated with the intake of ASA, measured through the levels of SUA (Figure 3.5D). These data confirmed the preventive effect of aspirin on metastasis, as previously shown[243,380,384].

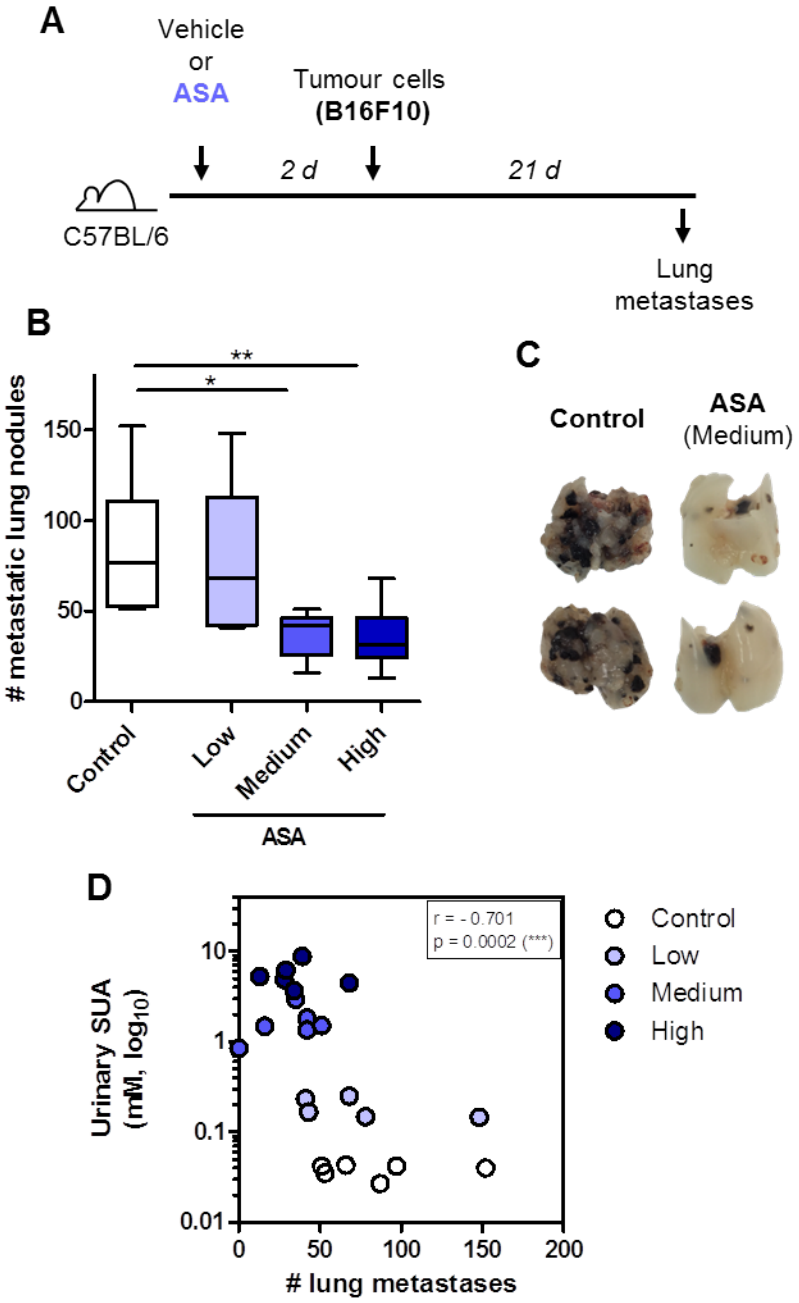

Figure 3.5 – **Aspirin reduces experimental metastasis from B16F10 cells.**

(A) Experimental design to establish the effect of aspirin on lung metastasis. C57BL/6 mice were administered vehicle (Control) or ASA in drinking water and intravenously injected with B16F10 cells two days after the start of the treatment. Lungs were isolated at day 21 for the count of metastatic lung nodules.

(B-C) Number (B) and representative images (C) of metastatic lung nodules at 3 weeks after intravenous injection of B16F10 cells in mice treated with vehicle (n=6 mice) or ASA (Low, Medium and High, n=5, 5 and 6 mice, respectively; median ± range, 1-way ANOVA with Tukey's Multiple Comparison test).

(D) Correlation plot of the intake of aspirin, measured as urinary concentration of SUA, versus the number of metastatic lung nodules per mouse (n=6 mice for Control and High groups, n=5 mice for Low and Medium groups; Spearman rank correlation).

3.3.2.2 Aspirin reduces metastasis in alternative experimental models

In order to verify the universality of these results, we assessed the effect of aspirin on lung nodules in alternative experimental models of metastasis: MC-38-GFP (murine colorectal cancer cells, syngenic to C57BL/6 mice), 4T1 (breast cancer cells, syngeneic to BALB/c mice) and MDA-MB-231 (human breast cancer cells, xenograft into SCID mice)[b]. Aspirin administered at the Medium dose decreased the number of MC-38-GFP- (Figure 3.6A), 4T1- (Figure 3.6B) and MDA-MB-231- (Figure 3.6C and D) derived metastatic lung nodules to a similar extent than B16F10 cells (Figure 3.6E). Interestingly, lung foci from both murine and human breast cancer cells were similarly affected by aspirin. These data suggest a widespread effect of aspirin on metastasis development that is not dependent on tumour origin or species.

3.3.3 Analysis of COX-1 and COX-2 contribution to metastasis

3.3.3.1 Dose-setting of selective COX-1 and COX-2 inhibitors

Aspirin at the Medium dose reduces metastasis, when both COX-1 and COX-2 are inhibited. In order to understand the relative contribution of COX-1 and COX-2 to metastasis, we have employed selective inhibitors of COX-1 (SC-560) and COX-2 (NS-398). We chose doses that had been previously reported to show selective inhibition of COX-1[509,510] or COX-2[511]. SC-560 and NS-398 were delivered through drinking water and the drug intake was regular for the duration of the experiment (Figure 3.7A and B). In agreement with expectations, the levels of serum TXB_2 (Figure 3.7C) and plasma PGE_2 (Figure 3.7D, *ex vivo*, and E, *in vivo*) confirmed the isoform selectivity of the chosen regime of treatment.

[b] MDA-MB-231 formed edematous lung nodules that cannot be visibly assessed in perfused lungs. In this case we have employed MRI imaging to detect the differences in nuclear magnetic moment between lung soft tissue (displayed as white in the MRI scan) and hypo-intense lung nodules (displayed as black in the MRI scan), even in the absence of contrast agents.

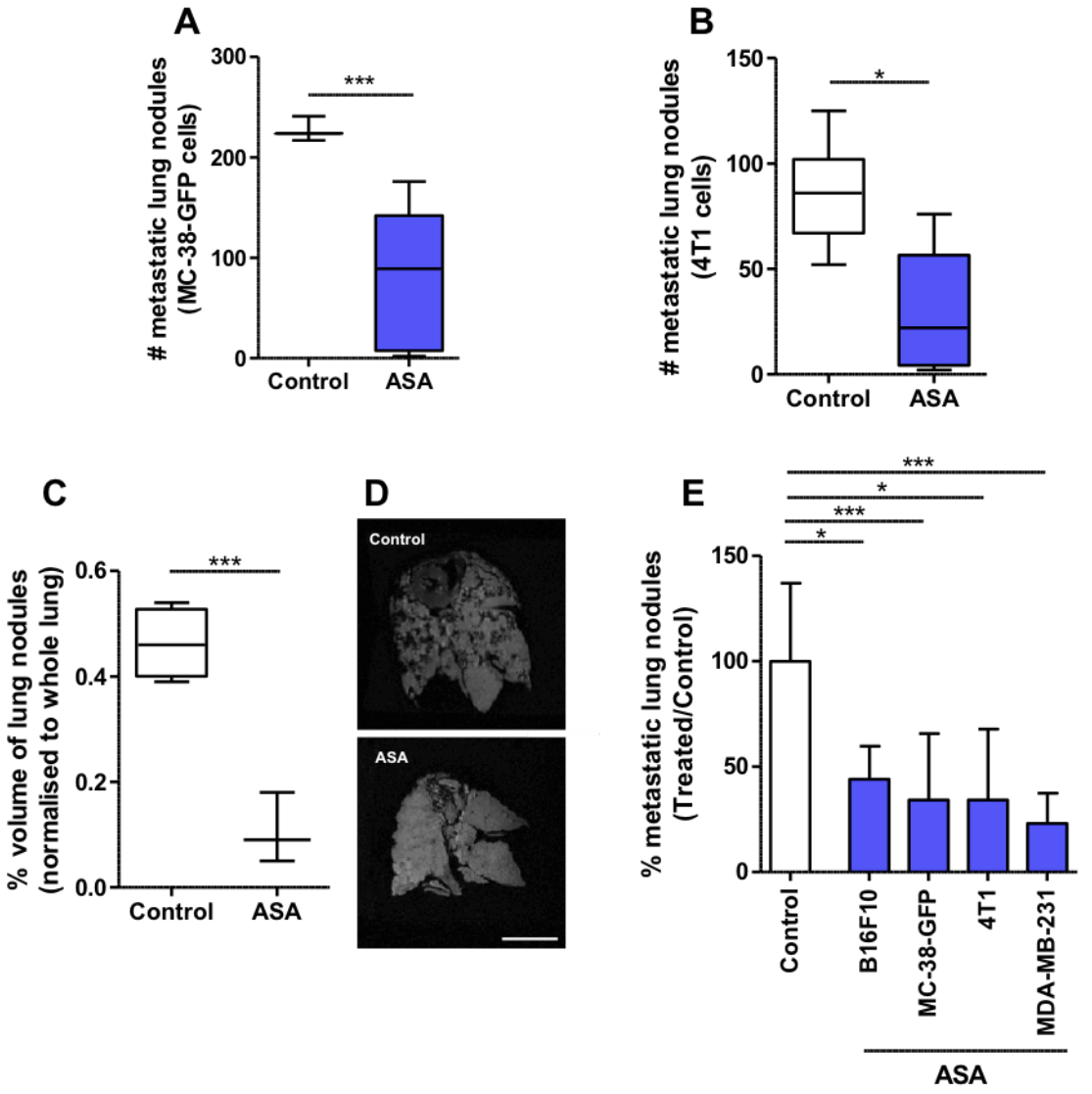

Figure 3.6 – Aspirin reduces metastasis in alternative experimental models.

(A) Number of metastatic lung nodules, assessed in C57BL/6 mice at 3 weeks after the injection of MC-38-GFP cells. Mice were treated with vehicle (Control, n=3 mice) or ASA (Medium dose, n=5 mice) starting 2 days before the injection (median ± range, 1-way ANOVA with Tukey's Multiple Comparison test).

(B) Number of metastatic lung nodules, assessed in BALB/c mice at 2 weeks after the injection of 4T1 cells. Mice were treated with vehicle (n=7 mice) or ASA (Medium dose, n=6 mice) starting 2 days before the injection (median ± range, 1-way ANOVA with Tukey's Multiple Comparison test).

(C-D) Volume of lung nodules, normalised to total lung volume (C), and representative images of lungs scans (D) acquired by MRI on *ex vivo* lungs from SCID mice at 4 weeks after the injection of MDA-MB-231 cells, upon treatment with vehicle (n=4 mice) or ASA (n=3 mice; median ± range, 1-way ANOVA with Tukey's Multiple Comparison test). Scale bar represents 5 mm.

(E) Comparison of the number of metastatic lung nodules, normalised to the relative control, between all tested experimental metastasis models (data from Figures 3.6A-C) (mean + SD, 1-way ANOVA with Tukey's Multiple Comparison test).

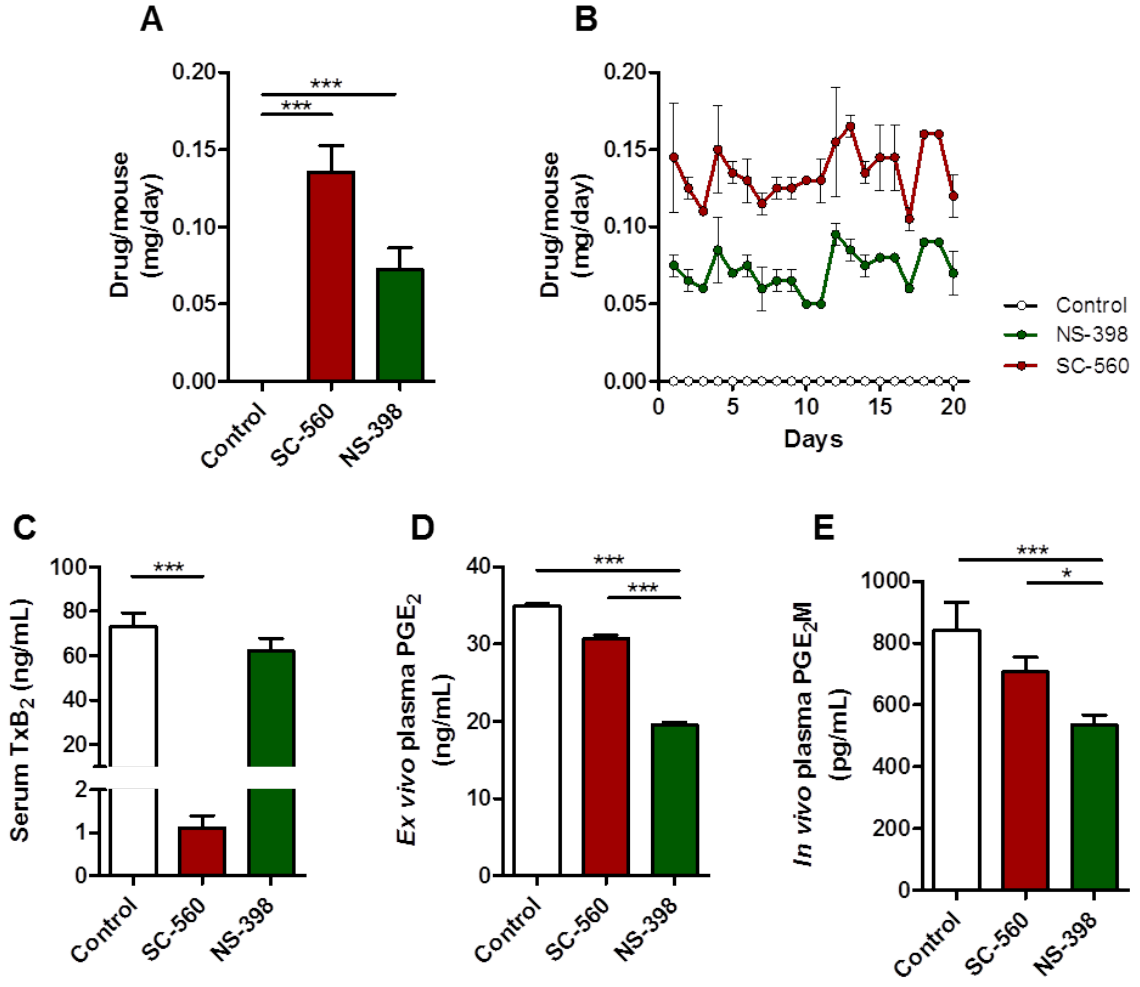

Figure 3.7 – Dose setting of selective COX-1 or COX-2 inhibitors.

(A-B) Average intake per day (A) (n=21 days per group) and over 3 weeks (B) (n=2 cages for all time points) of vehicle (Control), SC-560 (24 mg/L) and NS-398 (12 mg/L), extrapolated from drinking water volumes.

(C) Concentration of TXB_2 in serum from mice treated with vehicle, SC-560 or NS-398 (n=3 mice per group).

(D) Concentration of PGE_2 in LPS-stimulated plasma derived from mice treated with vehicle (Control), SC-560 or NS-398 (n=8, 4 and 3 mice, respectively).

(E) Concentration of PGE_2M in plasma derived from LPS-injected mice treated with vehicle (Control), SC-560 or NS-398 (n=3 mice per group).

All data are represented as mean +/± SD; 1-way ANOVA with Tukey's Multiple Comparison test.

3.3.3.2 The inhibition of COX-1 is sufficient to inhibit experimental metastasis

Similarly to Figure 3.5A, mice were treated with SC-560 or NS-398 and challenged with B16F10 cells. SC-560 significantly reduced the number of metastatic lung nodules (Figure 3.8A) to a similar extent to Medium and High doses of ASA (Figure 3.8B, data re-plotted from Figure 3.5B and 3.8A). On the contrary, NS-398 did not reduce the number of lung foci, suggesting that the effect of aspirin on metastasis is dependent on the inhibition of COX-1.

To determine the validity of these results, SC-560 and NS-398 were also employed in alternative metastasis models. SC-560 inhibited metastatic lung nodules from MC-38-GFP (Figure 3.8C), 4T1 (Figure 3.8D) and MDA-MB-231 (Figure 3.8E) cells, while NS-398 also reduced metastasis from MC-38-GFP cells (Figure 3.8C).

Taken together these data indicate that anti-metastatic effect of aspirin is mediated by the inhibition of COX-1 activity and suggest a role of this isoform in the metastatic process. To our knowledge, the data presented here constitute the first report showing that the inhibition of COX-1 by aspirin is sufficient to reduce metastasis.

3.3.3.3 Metastasis inhibition in COX-1 deficient mice

In order to further dissect the contribution of COX-1 to metastasis development, COX-1 deficient mice (*Ptgs1*$^{-/-}$, indicated here as COX-1$^{-/-}$) were used for the metastasis assay. The number of B16F10-derived metastatic lung nodules in COX-1$^{-/-}$ mice was dramatically reduced compared to their wild type counterparts (C57BL/6, indicated here as COX-1$^{+/+}$) (Figure 3.9A). This effect was accompanied by a decrease of TXB_2 in plasma and serum (Figure 3.9B and C) and a decreased platelet aggregation (Figure 3.9D and E). These results suggest that the expression of COX-1 in the host environment is important for the successful development of metastasis.

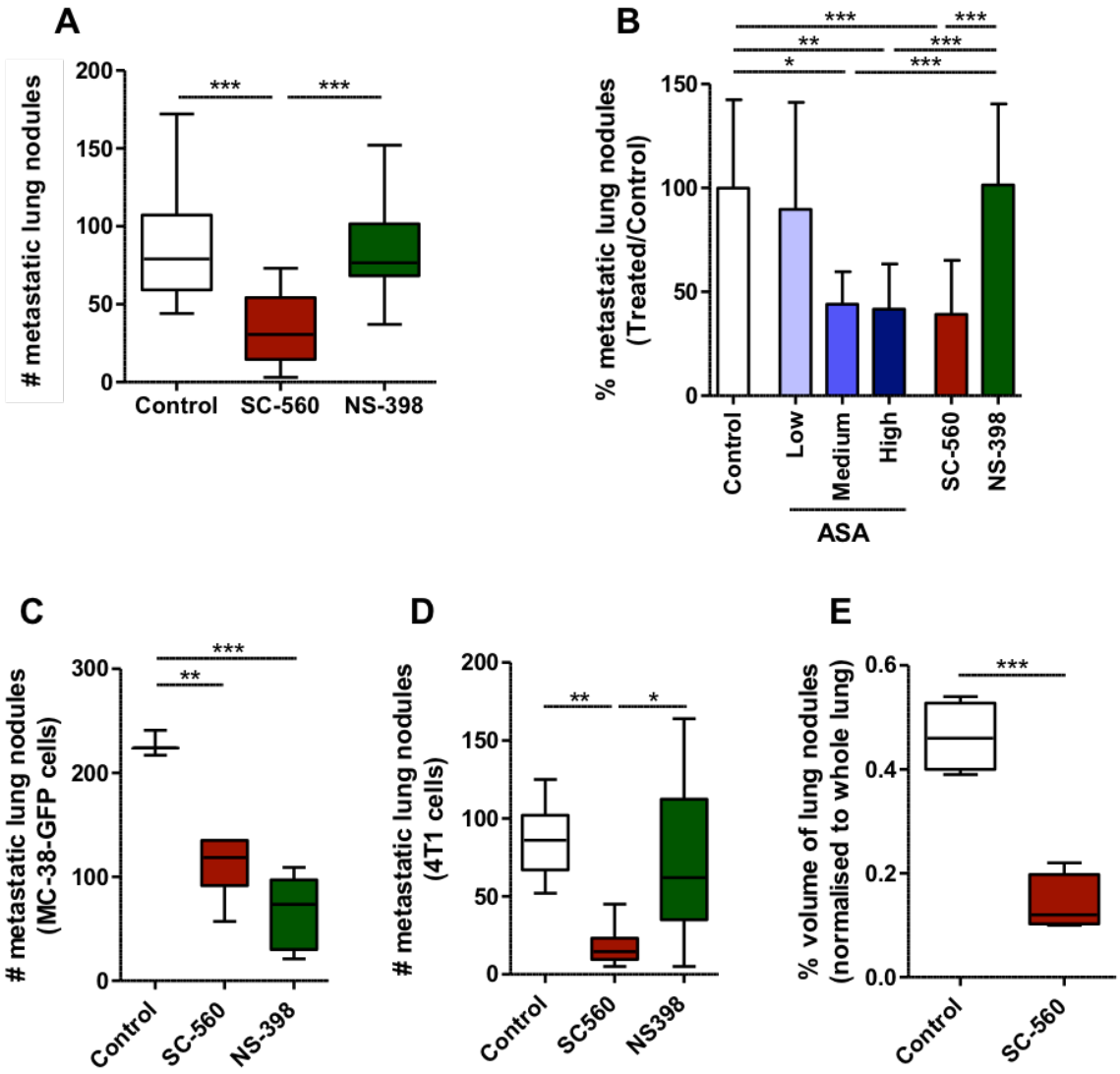

Figure 3.8 – The inhibition of COX-1 by SC-560 reduces metastasis.

(A) Numbers of metastatic lung nodules at 3 weeks after intravenous injection of B16F10 cells in C57BL/6 mice treated with vehicle (Control), SC-560 or NS-398 (n=16, 12 and 16 mice, respectively) for 3 weeks, starting 2 days before tumour cell injection (median ± range, 1-way ANOVA with Tukey's Multiple Comparison test).

(B) Comparison of the number of metastatic lung nodules, normalised to the relative control, in mice treated with ASA (all doses, data from Figure 3.5B), SC-560 or NS-398 (data from Figure 3.8A) (mean + SD, 1-way ANOVA with Tukey's Multiple Comparison test).

(C) Number of metastatic lung nodules in C57BL/6 mice at 3 weeks after the injection of MC-38-GFP cells, upon treatment with vehicle, SC-560 or NS-398 (n=3, 6 and 6 mice, respectively; median ± range, 1-way ANOVA with Tukey's Multiple Comparison test).

(D) Number of metastatic lung nodules in BALB/c mice at 2 weeks after the injection of 4T1 cells, upon treatment with vehicle, SC-560 or NS-398 (n=7, 6 and 6, respectively; median ± range, 1-way ANOVA with Tukey's Multiple Comparison test)).

(E) Volume of lung nodules, normalised to total lung volume, calculated from MRI scan on lungs from SCID mice at 4 weeks after the injection of MDA-MB-231 cells, upon treatment with vehicle or SC-560 (n=4 per group; median ± range, 1-way ANOVA with Tukey's Multiple Comparison test)).

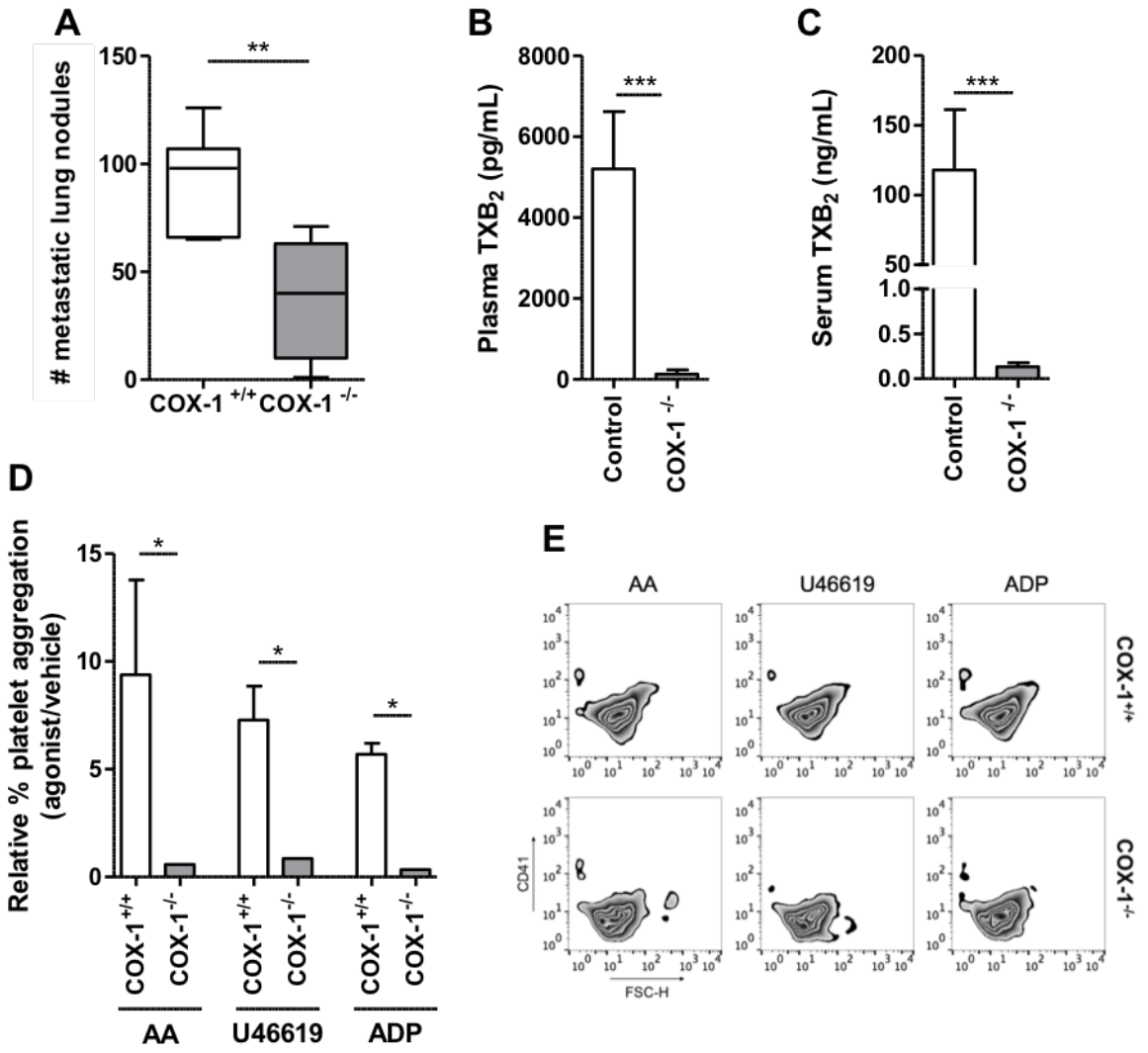

Figure 3.9 – Metastasis establishment is impaired in COX-1 deficient mice.

(A) Numbers of metastatic lung nodules, assessed at 3 weeks after intravenous injection of B16F10 cells in COX-$1^{+/+}$ mice (C57BL/6) or COX-$1^{-/-}$ mice (*Ptgs1*$^{-/-}$) (n=7 mice per group; median ± range, unpaired t test).

(B-C) Concentration of TXB_2 in plasma (B) and serum (C) from COX-$1^{+/+}$ or COX-$1^{-/-}$ mice (n=4 mice per group; mean + SD, unpaired t test).

(D-E) Quantification (D) and representative zebra dot plots (E) of agonist-induced platelet aggregation of PRP from COX-$1^{+/+}$ or COX-$1^{-/-}$ mice (n=8 and 4 mice, respectively), measured through FACS analysis of CD41-stained platelets (mean + SD, 1-way ANOVA with Tukey's Multiple Comparison test). AA (1 mM), U46619 (0.3 μM) and ADP (1 μM) were used as agonists to trigger a COX-1-dependent (AA and U46619) or independent (ADP) platelet aggregation.

3.4 DISCUSSION

3.4.1 Aspirin dose-setting

In order to understand the mechanism of the anti-metastatic effect of aspirin in clinical trials, we have chosen three doses of aspirin that were previously used in the literature[243,436,437]. These doses were expected to correspond to the low, medium and high dose regimes in humans, expectations that were supported by the theoretical HED calculated through a BSA conversion system (Table 3.1). Additionally, we have chosen to deliver aspirin through drinking water, as previously reported[380,436,437,512]. This administration route is the closest to the oral tablet administration in the clinic and is associated with less distress for the experimental animals, in comparison with oral gavage. Moreover, this delivery route allows the maintenance of a chronic treatment regime, where the targets of aspirin should be constantly inhibited during the whole duration of the experiment. However, animals have free access to the drug and the actual intake per animal could fluctuate between days or animals in the same cage.

To overcome all these challenges, we have performed a rigorous analysis of the intake and *in vivo* efficacy of the selected doses. First, we have checked the daily intake of aspirin per mouse through different methods. We have measured the daily drinking volume per cage and extrapolated the expected daily dosage of aspirin per animal. This method provides a simple and quick quantification of the cumulative drug consumptions over time but it is not accurate in evaluating the drug intake of each animal in the cage. To address this issue we have quantified the excretion of salicyluric acid (SUA) in the urine of individual animals (Figure 3.2B). It appeared that, in a given day, the intake of aspirin was similar between mice in the same treatment group, suggesting that the intake of water is equally distributed within a cage. It follows that drinking volumes can be used as a quick approximation of the real drug intake per animal.

Moreover, the measurement of SUA levels in urine provides some information regarding aspirin metabolism in mice. Based on the MGI average urinary output per day (http://www.informatics.jax.org/), 30% of ingested ASA is excreted as SUA each day, a rate that is well conserved among increasing doses (Table 3.1). In humans, approximately 75% of orally ingested aspirin is excreted as SUA, a percentage that decreases at higher dosages[366]. Thus, the pharmacokinetics of ASA differs in humans and mice and the simple BSA-based translation might not be sufficient to choose an equivalent dose among species.

To overcome this problem, efforts have been made to evaluate the extent of COX-1 and COX-2 inhibition, and their physiological effects, at the selected doses. In our model, COX-1 was inhibited at all doses (Figure 3.3B). However, the Low dose reduced the *ex vivo* synthesis of TXA_2 by only 71%. As expected, such inhibition did not correspond to a significant reduction in the agonist-induced aggregation of platelets, even if a trend was visible (Figure 3.3C and D). Although 30 mg/L of aspirin in drinking water had been previously associated with a reduction of excreted TXB_2 and platelet aggregation[436], in our hands this dose did not show strong anti-thrombotic effects. In our experiments, the Medium dose was the minimum dose to effectively inhibit COX-1 activity and reduce COX-1 dependent platelet aggregation. To note, the High dose further decreased the *ex vivo* synthesis of TXA_2 (~3 times) in comparison to the Middle dose but did not further affect platelet aggregation, suggesting a plateau effect.

All doses of aspirin that we have used inhibited COX-2 *ex vivo* and *in vivo* (Figures 3.4B and E). This result is not completely unexpected. Previous evidence have shown that low-dose aspirin inhibits PGE_2 *in vitro*, although more transiently than higher doses[513], and decreases inflammatory cytokines *in vivo*[436]. Nevertheless, to our knowledge this is the first comprehensive characterisation of the effect of a range of aspirin doses on the activity of COX-2 in mice. The nature of COX-2 inhibition by low-dose aspirin is not known

and it might be related to an additional species-related difference in the drug bioavailability and/or pharmacology.

All together, the chosen Medium and High doses of aspirin resemble the corresponding doses in humans and are associated with an anti-thrombotic and anti-inflammatory effect. In our hands, the Low dose was predominantly anti-inflammatory with minimal anti-thrombotic effects, suggesting a different pharmacology of aspirin in mice.

3.4.2 Aspirin exerts an anti-metastatic effect in experimental models

We have applied the selected doses of aspirin to a well-established experimental model of lung metastasis, extensively used in our lab[26,146]. Mice were pre-treated with aspirin for two days before intravenous injection of tumour cells. This regime was chosen with the intention that the anti-platelet or anti-inflammatory effects of aspirin would be achieved by the time of tumour cell challenge. Accordingly, we have found an inhibition of the activity of COX-1 (Figure 3.3B) and COX-2 (Figure 3.4B and E) at 48 hours after the start of the treatment. Therefore, we can assume that aspirin has reached a full inhibitory effect at the moment of tumour cells introduction in the vasculature.

After three weeks of chronic treatment, the number of metastatic lung nodules was reduced by more than 50% at the Medium and High doses (Figure 3.5B), while the Low dose did not significantly affect the numbers of metastases. Interestingly enough, the 5-times increase of dose between the Medium and High regimes did not further decrease the number of metastatic lung nodules. Since the Medium dose showed close to the maximum anti-metastatic effect of aspirin, we used this dose in most *in vivo* experiments in the next Chapters. These findings are in agreement with the epidemiological data that found a protective effect of aspirin on distant metastasis at low-medium doses of <300 mg/day, an effect that was not further enhanced at higher doses (>300 mg)[428].

The anti-metastatic effect of aspirin negatively correlated with the drug intake (Figure 3.5D), a result that confirms the well-established effect of aspirin in preventing experimental metastasis[379-385]. However, it is interesting to note that such effect takes place at a much lower dose than what was expected from the literature[243,380,381].

In order to exclude that the effect of aspirin on metastasis was restricted to melanoma cells and/or C57BL/6 mice, we have tested the effect of aspirin on alternative cell lines (MC-38-C57BL/6), mouse strains (4T1-BALB/c) and species of origin of the cell line (MDA-MB-231-SCID). Aspirin impaired metastasis establishment in all models to a similar extent (Figure 3.6E). Together with previous experimental evidence on alternative cell lines[379-385], these results suggest the widespread inhibitory effect of aspirin on metastasis. Clinical studies have shown that the metastasis-preventive effect of aspirin is particularly pronounced on adenocarcinomas such as colorectal and other gastrointestinal cancers[410,428]. The effect of aspirin on MC-38 cells is in agreement with these data. We have also found that aspirin reduces experimental metastasis from non-adenocarcinoma cancers (breast and melanoma), for which no effect of aspirin on metastasis appearance was observed in clinical studies[411,428]. This discrepancy might be partially explained by the lack of primary tumour in our model, assuming that the early dissemination of different tumour types might be differentially decreased or enhanced by aspirin treatment. Moreover, Rothwell et al.[418] have found that aspirin reduces the appearance of lung metastasis irrespectively of the primary tumour (HR 0.34, 95% CI 0.14–0.83). Our model of experimental metastasis reproduce the intravascular steps leading to lung colonisation, which are equally affected by aspirin over a range of tumour cell types, suggesting a general effect on tumour cell seeding in the lung vasculature. Considering the technical versatility of B16F10-C57BL/6 model and the extensive use in our lab[26,146], we have chosen to employ the B16F10-C57BL/6 experimental model for the experiments of the next Chapters, although the most crucial findings were also confirmed in other cell models (data not shown).

Importantly, we observed a reduction of metastatic lung nodules only when COX-1 and COX-2 activity was inhibited (Medium and High doses), whereas the inhibition of COX-2 alone (Low dose) was not sufficient. These observations might indicate a prominence of COX-1, rather than COX-2, in the metastatic process. In particular, metastasis inhibition was associated with a decrease of platelet-derived TXA_2 and platelet aggregation, suggesting that COX-1 expressed by platelets supports metastasis. Although the role of COX-1 in other cell types cannot be ruled out, these evidences suggest that aspirin affects metastasis at least through an anti-coagulant effect derived from the inhibition of COX-1.

3.4.3 COX-1 inhibition is sufficient to reduce metastasis

The data collected so far have shown an anti-metastatic effect of Medium and High doses of aspirin that is associated with the inhibition of both COX-1 and COX-2. In order to dissect the contribution of each isoform to metastasis, we have employed selective inhibitors of COX-1 (SC-560) or COX-2 (NS-398). The selectivity of the chosen doses was confirmed though the evaluation of the residual activity of COX-1 and COX-2 *ex vivo* and *in vivo* (Figures 3.7C-E).

When employed in our experimental model, NS-398 did not show any anti-metastatic effect on B16F10 and 4T1-derived lung metastasis, but it significantly inhibited MC-38-GFP metastatic success (Figures 3.8), suggesting a certain extent of cell line-specificity (but not host-specificity). In support of this, previous evidence has shown an inhibition of metastasis in some cell lines but not in others, even at much higher doses of NS-398 [383,514]. The reason for this difference is not known but we can hypothesise that it depends on the cell-specific phenotype and consequent drug sensitivity and interaction with the microenvironment. For instance, COX-2 is overexpressed in numerous tumour cell lines and solid tumours, particularly in the case of colorectal cancer[460-465]. Moreover, the inhibition of COX-2 decreases tumour cells proliferation[515] and tumour growth[516,517], an

effect that correlates with the level of COX-2 expression[516-518]. We have found that MC-38 cells express much higher levels of COX-2 in comparison to B16F10 cells (data not shown), therefore they would be more sensitive to COX-2 inhibition. In this scenario, the nature of metastasis decrease by COX-2 inhibitors would be mostly tumour-centred and tumours that express low levels of COX-2 would be less affected by COX-2 inhibition.

In contrast, SC-560 was found to inhibit metastasis in a wider range of experimental models, irrespective of mouse strain or tumour type (Figures 3.8B and D-F). Interestingly, SC-560 and ASA decreased the number of lung metastasis to a similar extent, suggesting that the inhibition of COX-1 by aspirin is sufficient to affect metastasis. COX-1 inhibition was effective on cell lines with high (MC-38) or no (B16F10) expression of COX-1 (data not shown and Figure 6.6B), suggesting that the inhibition of COX-1 in cancer cells has no impact on the anti-metastatic effect of ASA/SC-560. This observation is supported by ONCOMINE gene expression data (Supplementary figure S3), which shows that several cancer types (both adenocarcinoma and non-adenocarcinoma) express COX-1 to a comparable extent to normal tissue (Supplementary figure S3A). Additionally the level of COX-1 expression does not correlate with lower odds of metastatic cancer in randomised clinical trials of aspirin versus control (Supplementary figure S3B)[428]. This observation holds true for colorectal and gastric cancer, which are mostly affected by the anti-metastatic effect of aspirin. These data suggest that the tumour-specific sensitivity to aspirin does not depend on COX-1 expression by tumour cells. If tumour COX-1 is not a target of metastasis prevention, then microenvironmental COX-1 could be involved. SC-560, but not NS-398, reduced *ex vivo* TXA_2 generation by platelets (Figure 3.7C), leading us to hypothesise that the inhibition of COX-1 in platelets contributes to the anti-metastatic effect of ASA and SC-560. In favour of this idea, Lewis Lung Carcinoma (LLC) cells, which are around 50% less prone to induce platelet aggregation than B16F10[385], are less sensitive to SC-560 anti-metastatic effect[383]. This perspective would imply that platelets, rather than tumour cells, are the target of COX-1 inhibition. Thus, tumour types that

depend more on platelet aggregation for their dissemination would benefit more from the anti-metastatic effect of aspirin, providing a rationale for the tumour-specific sensitivity to the drug.

The importance of COX-1 in the host microenvironment is further demonstrated by the reduction of metastasis in COX-$1^{-/-}$ mice (Figure 3.9A). In this model, COX-1 activity is inhibited in host cells, but not in tumour cells. The fact that COX-$1^{-/-}$ mice bore a similar number of lung metastasis to ASA- or SC-560-treated animals suggests that tumour cells are not the target of pharmacological inhibition. Together with the previous results, these observations suggest that COX-1 inhibitors reduce metastasis through a microenvironment-centred mechanism. This hypothesis will be further dissected by assessing the metastatic potential of MC-38 (high COX-1 expression) in COX-$1^{-/-}$ mice under vehicle or SC-560 treatment.

The strong anti-metastatic effect associated with COX-1 inhibition is a novel finding, especially in a context where the contribution of COX-1 to cancer remains poorly understood. The little attention given to COX-1 derives from the constitutive nature of its expression and from its homeostatic functions, such as platelet aggregation and gastric cytoprotection. Over the past decades, these observations have made of COX-1 a less plausible candidate in tumour progression and have also complicated its use as pharmacological target. Since the inhibition of COX-1-derived prostanoids is responsible for the appearance of gastric ulcers and gastrointestinal bleeding, the most severe side effects of aspirin treatment, it follows that a further understanding the role of COX-1 in the dissemination of tumour cells could potentially help to design more efficient therapies for the prevention of metastasis.

3.4.4 Conclusions

In this Chapter we have shown the development of an *in vivo* model of pharmacological inhibition of metastasis that will be employed in the next Chapters. Additionally, we have shown that the inhibition of metastasis by aspirin is associated with the inhibition of COX-1, in particular in the microenvironment, suggesting a central role of this isoform in the development of metastasis. This finding represents the key point of this project and will be the focus of following dissertations.

CHAPTER 4

Aspirin reduces metastasis through the inhibition of COX-1 during the intravascular phase

4.1 INTRODUCTION

In the previous Chapter we showed that aspirin decreases experimental metastases through a COX-1 dependent mechanism. So far, it seems that the inhibition of COX-1 affects the behaviour of tumour cells through an indirect mechanism that involves the effect on the microenvironment. After the detachment of tumour cells from the primary tumour and the intravasation, the metastatic cascade can be generally divided into an intravascular, extravasation and extravascular phases. Luckily enough, the nature of the tumour cells-host interaction changes during these sequential phases (see section 1.1.2 of Chapter 1), so the time-stratification of treatment can help understand the mechanisms of COX-1 contribution to metastasis.

In this Chapter we suggest an effect of aspirin on early steps of metastasis, in particular the intravascular phase of tumour cell dissemination. This observation has important clinical outcomes for metastasis preventive therapies. Here I review the current state of art of the pharmacological treatment of metastasis and the available models to study the haematogenous transit of tumour cells.

4.1.1 Metastatic (in)efficiency

Metastasis is a very inefficient process and only approximately 0.01% of cancer cells released in the circulation can form metastasis. There are two main rate-limiting processes for the establishment of metastasis, seeding and growth[311]. Seminal work by Fidler[65] showed that ^{125}IUDR-labelled B16 melanoma cells arrest in the lungs shortly after intravenous introduction, but most of the arrested cells started to die and only 1.5% of the

injected tumour cells survived in the lungs during the first 24 hours. These findings have been confirmed in other models[29,267,389,519-523]. This evidence identified that metastatic inefficiency happens mainly during the intravascular phase of tumour cell dissemination. As described in section 1.1.2.2, circulating tumour cells are exposed to haemodynamic forces, anoikis and anti-tumour immune response, leading to cell death. In particular, the induction of apoptosis is an important determinant in metastatic inefficiency and apoptosis-resistant cells are more efficient in forming metastatic colonies[524]. However, most of the cells that succeed in completing the initial seeding will form overt metastasis which will kill the patient[30], an idea supported by the negative correlation between the number of CTCs and prognosis in cancer patients[60,525]. Additionally, evidence suggests that tumour cells in established metastatic colonies can restart the metastatic cascade and invade tertiary distant sites. This is the case of metastasis-to-metastasis spread[526,527] or the re-colonisation of the primary tumour (self-seeding)[528], which increases the aggressive phenotype of the tumour.

In all these cases, the intrinsic metastatic inefficiency is not sufficient to abrogate the appearance of distant metastases. Thus, therapies that target the intravascular steps of metastasis would be beneficial for the prevention of metastasis appearance (either primary or secondary) and the overall progression of the disease. Possible targets could be phenotypic traits of disseminating tumour cells that allow the completion of the early metastatic cascade, however these features might differ among cancer types, stages of cancer and distinct disseminating cells. On the other hand, the host stroma is much more genetically stable than metastatic cells, hence targeted therapies against the metastatic microenvironment can be the best approach for anti-metastasis therapy[39].

4.1.2 Animal models of the intravascular phase of metastasis

Preclinical models represent a great tool to model the early steps of tumour cell dissemination, in particular experimental metastasis assays. 'Experimental metastasis' refers to a model where tumour cells are directly introduced in the systemic circulation[529] and differ to 'spontaneous metastasis' for the lack of a primary tumour[529,530]. Experimental metastases can be induced in different secondary organs: liver (intrasplenic or portal vein injection), brain (intracarotid injection), brain and bone (intracardiac injection) or lungs (tail vein injection). This organ tropism pattern depends both on the anatomical organisation of the vasculature downstream to the injection site and on the features of both tumour cells and secondary organ[11,531-534]. Although the relative contribution might change between cell lines, it is believed that both physical entrapment and selective recognition of target organ drive the metastatic pattern of tumour cells.

In this project we have employed an experimental model of pulmonary metastasis to address the effect of COX inhibition on tumour cell spread. After intravascular introduction, tumour cells travel through the vena cava, reach the right atrium and are pumped by the right ventricle through the pulmonary artery into the pulmonary vasculature and they get entrapped in alveolar capillaries (Figure 4.1). In this sense, lung capillary beds work as size restriction filters for the initial arrest of tumour cells, making the lungs one of the most vulnerable organs for the development of metastasis. However, tumour cells can arrest also in vessels of larger size then their diameter (for example arterioles[523]), which suggests that the physical entrapment of tumour cells is not sufficient to allow extravasation and tumour cells need to establish more stable interactions with endothelial cells. Once extravasated in the lung parenchyma, tumour cells can stay quiescent for a various amount of time and in some cases they start the initial growth that will lead to the establishment of small lung nodules, called micrometastasis. If proliferation is sustained, micrometastasis will exponentially growth to form macrometastasis, the first form of clinically/experimentally detectable metastasis[128].

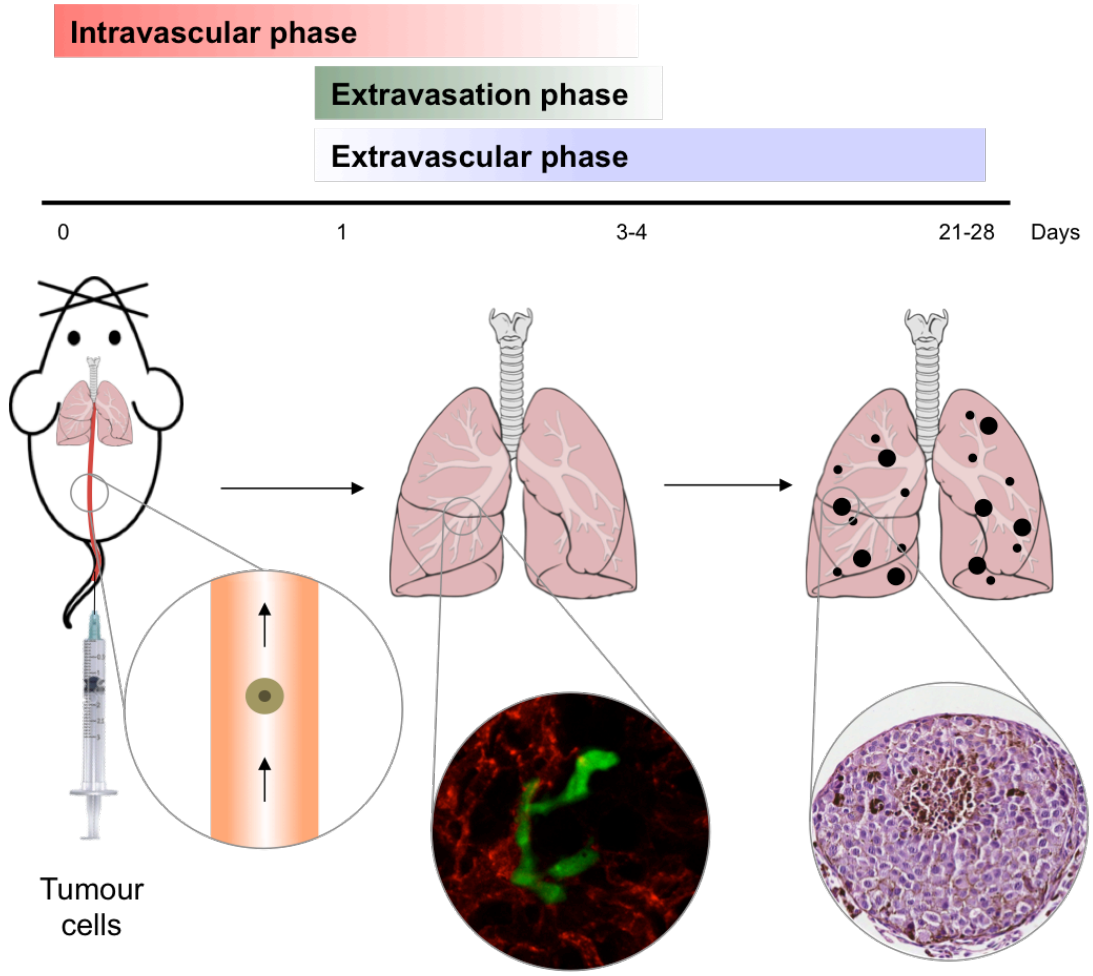

Figure 4.1 – Experimental model of pulmonary metastasis.

Tumour cells are introduced intravenously through tail vein injection. Tumour cells travel through the caudal veins and vena cava and reach the heart within seconds after the injection, then they are pumped through the pulmonary artery into the lung vasculature. Lung alveoli are surrounded by ramified networks of short capillaries with a diameter of 3-8 μm (in humans), a space sufficient for the transit (and oxygenation) of a single line of red blood cells. Tumour cells arrest in alveolar capillaries due to physical entrapment or receptor-ligand binding. Tumour cells then start to extravasate, a process that is completed between 1 and 4 days post-injection. A small percentage of cells will then progress into micro- and macro-metastases during the following 2 to 4 weeks, depending on the cell line. The collection of lungs at different time points allows the visualisation of tumour cells during their intravascular, extravasation or extravascular phase.

The efficiency of initial seeding can be evaluated on the base of the number of macrometastasis, assessed through different methods[264,265,310,530,535-540]. Lungs can also be harvested at earlier time points and represent one of the most suitable organs for the direct visualisation of tumour cells in the circulation of the whole fresh tissues (Figure 4.1). In comparison to tissue sectioning, whole lung imaging is less subject to technical artefacts because it preserves cell-cell and cell-ECM interactions and maintains the tri-dimensional structure of the pulmonary vasculature[523]. We have employed a model of isolated-perfused whole lung[541] and adapted it to visualise labelled tumour cells on the lung surface by *in situ* fluorescence imaging. This method has been extensively employed to visualise biochemical processes[542,543] and tumour cells at different steps of the metastatic process[26,29,215,494,523,544].

More recently, the use of high-resolution intravital microscopy techniques (IVM) has been employed to analyse different steps of the intravascular phase of metastasis in living animals. These techniques rely on the implantation of imaging window chambers that allow the exposure of optically inaccessible tissues and the imaging of tumour cell seeding, invasion and early proliferation in the lungs[545,546]. This system represents a promising alternative to *ex vivo* whole lung microscopy and will allow a better understanding of the intravascular phases of metastasis.

Overall, although the experimental pulmonary assay does not recapitulate earlier phases of the metastatic cascade, it represents an ideal method for the analysis of the haematogenous transit of tumour cell and early metastatic seeding. In this and the next Chapter, we have applied this method to evaluate tumour cell persistence in the lung vasculature and their interaction with other cell types in the circulation.

4.2 AIMS

In this Chapter we have attempted to pinpoint the phase(s) of haematogenous metastasis where the contribution of COX enzymes is most prominent. In order to do so, we have

1) characterised the early kinetics of metastasis engraftment in our model
2) addressed the contribution of COX activity to the early persistence of tumour cells in the vasculature
3) tested the effect of timely controlled treatment with aspirin and COX inhibitors on the establishment of metastatic lung nodules.

4.3 RESULTS

4.3.1 Effects of COX inhibition on early phases of metastasis

4.3.1.1 Kinetics of B16F10 extravasation in lungs

Disseminating tumour cells remain in the blood stream for one to four days prior to extravasation, a time that varies depending on the type of primary tumour[187]. To understand the kinetics of tumour cells extravasation in our model, we injected fluorescently labelled B16F10 cells in C57BL/6 mice and monitored their extravasation status for 4 days in whole lungs. Endothelial cells were labelled shortly before lung isolation and perfusion. The number of non-extravasated, partially extravasated and extravasated tumour cells (Figure 4.2A) revealed that B16F10 cells were localised mainly intravascularly during the first 24 hours after tail vein injection and underwent extravasation between day 1 and 3. All remaining cells had extravasated at 4 days post-injection (Figure 4.2B).

We also evaluated the average number of tumour cell per FOV and the number of tumour cells per cluster, as representative of tumour cell survival and proliferation, respectively. The number of B16F10 cells rapidly decreased in the first day after injection, suggesting that only 25% of the total adhered tumour cells survive in the vasculature within this early time window. Then, the number of tumour cells reached a plateau at the following time points (Figure 4.2C, black curve). Concomitantly, tumour cells started proliferating from day 3 and the first micrometastases were visible on day 4 (Figure 4.2C, blue curve, and D).

Together these data suggest that, in our experimental metastasis model, the seeding phase ends at 3-4 days after the injection and is immediately followed by the initial growth of tumour cells, most likely carried out by the first cells to have completed extravasation.

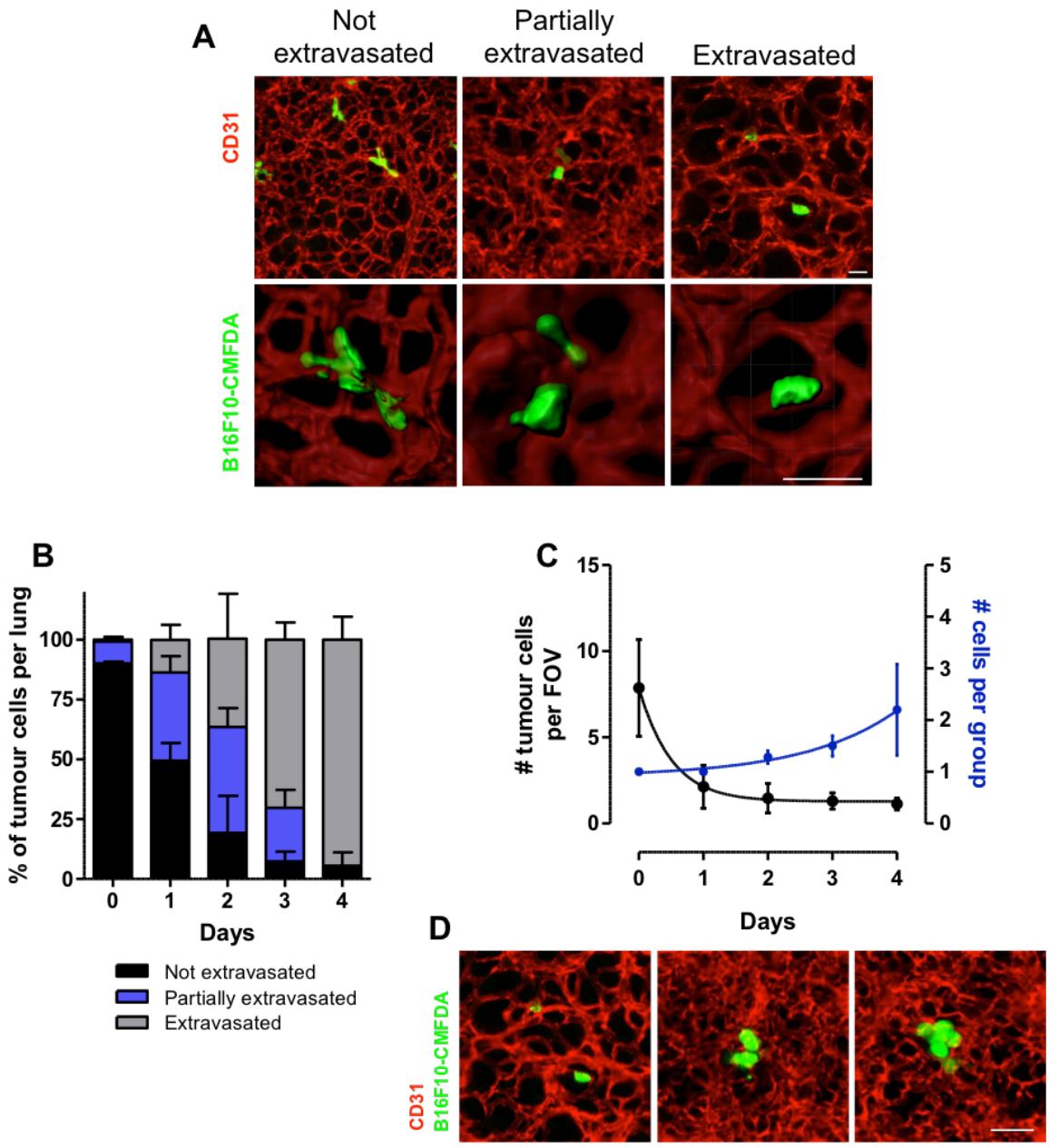

Figure 4.2 – Kinetics of B16F10 cells extravasation in lungs.

(A) Representative maximum intensity projection (MIP) of 3D confocal stacks (20x, top) and surface reconstruction (bottom) of tumour cells (B16F10-CMFDA, green) in whole lungs of C57BL/6 mice intravenously injected with CD31-APC antibody to stain endothelial cells (red). Tumour cells were scored as Not extravasated (left panels), Partially extravasated (middle panels) or Extravasated (right panels) according to their localisation relatively to the labelled vasculature. Scale bars represent 10 µm.

(B) Quantification of the number of Not extravasated, Partially extravasated and Extravasated B16F10-CMFDA cells, imaged in whole lungs up to 4 days after intravenous injection (n=3 mice per group, ≥6 tumour cells per lungs were analysed).

(C) Number of tumour cells (black curve) and number of tumour cells per group (blue line) counted in microscopic FOV from whole lungs up to 4 days after intravenous injection of B16F10-CMFDA cells (n=3 mice per group, ≥6 FOVs per lungs were analysed).

(D) Representative MIP of 3D confocal stacks (20x) of tumour cells (green) at different stages of proliferation, imaged in whole lungs of C57BL/6 mice with labelled endothelial cell (red). Scale bar represents 30 µm.

4.3.1.2 Early persistence of tumour cells in the pulmonary vasculature is reduced by COX-1 inhibition

To address the effect of COX-1 and/or COX-2 inhibition on tumour cells within the vasculature, we assessed the presence of tumour cells during the first 24 hours after injection with ASA, SC-560 or NS-398 treatment (Figure 4.3A). Both ASA and SC-560, but not NS-398, resulted in a reduction of the total number of tumour cells in the left lung one day after the injection (Figure 4.3B and C). A similar reduction was obtained when cells were injected in COX-$1^{-/-}$ mice (Figure 4.3D), suggesting that COX-1 is required for the persistence of tumour cells within the lung vasculature and the subsequent establishment of metastatic lung nodules.

4.3.1.3 Early COX-1 inhibition affects metastatic lung nodules

The data so far suggest that the inhibition of COX-1 affects tumour cells survival during the first 24 hours of their presence in the circulation. In order to determine the effect of early COX inhibition on the establishment of metastatic lung nodules, mice were treated with ASA, SC-560 or NS-398 for 3 weeks (ASA, SC-560 and NS-398 groups) or until one day after the intravenous injection of B16F10 cells (ASA-*2→+1*, SC-560-*2→+1* and NS-398-*2→+1* groups) and the number of metastasis was assessed after 3 weeks (Figure 4.4A). We observed a similar reduction of metastatic lung nodules in the ASA and SC-560 groups compared to the *-2→+1* treatment groups, while no NS-398 treatment regime affected metastasis (Figure 4.4B-D). These findings suggest that early steps of metastasis, in particular the haematogenous transit of tumour cells, are affected by COX-1 inhibition and this effect is sufficient to reduce the onset of metastasis.

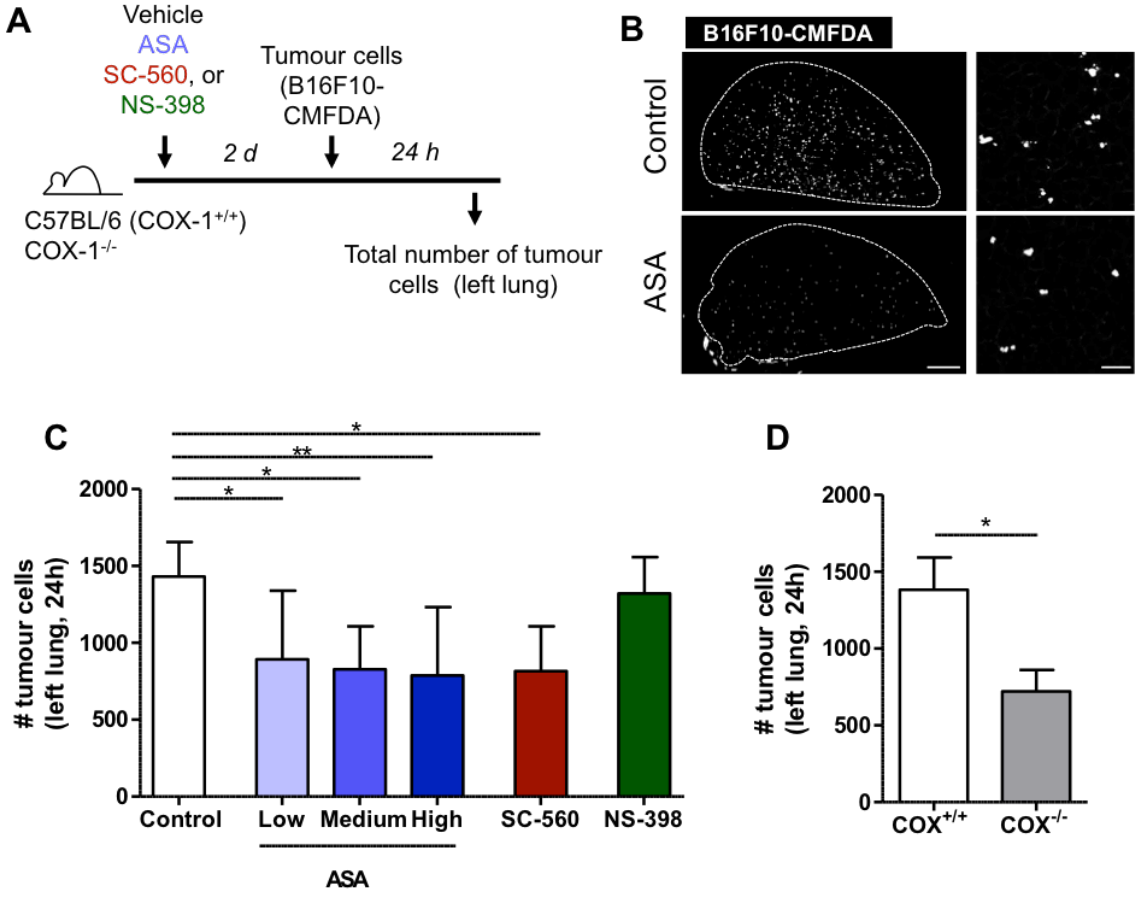

Figure 4.3 – COX-1 inhibition affects the early persistence of tumour cells in the lungs.

(A) Experimental design to study the early persistence of tumour cells in lungs. Tumour cells (B16F10-CMFDA) were injected in the tail vein of C57BL/6 mice two days after the start of treatment with vehicle (Control), ASA, SC-560 or NS-398, delivered through drinking water. Lungs were harvested 24 hours after the injection and imaged as intact organ. The total number of tumour cells was counted on the surface of the left lung.

(B) Representative confocal tile scans (left panels) and magnifications (20x, right panels) of the intact left lung of C57BL/6 mice at 24 hours after the injection of tumour cells (white), upon treatment with vehicle (top panels) or ASA (Medium dose, bottom panels). Scale bars represent 1 mm (left panels) and 100 µm (right panels).

(C) Total number of tumour cells in the intact left lung of C57BL/6 mice treated with vehicle, ASA (Low, Medium and High doses), SC-560 or NS-398 (n=6, 6, 7, 6, 4 and 5 mice, respectively), imaged at 24 hours after the injection of tumour cells (mean + SD, 1-way ANOVA with Tukey's Multiple Comparison test).

(D) Total number of tumour cells in the intact left lung of wild type (COX-$1^{+/+}$) or COX-$1^{-/-}$ mice (n=6 and 5 mice, respectively), imaged at 24 hours after the injection of tumour cells (mean ± SD, unpaired t test).

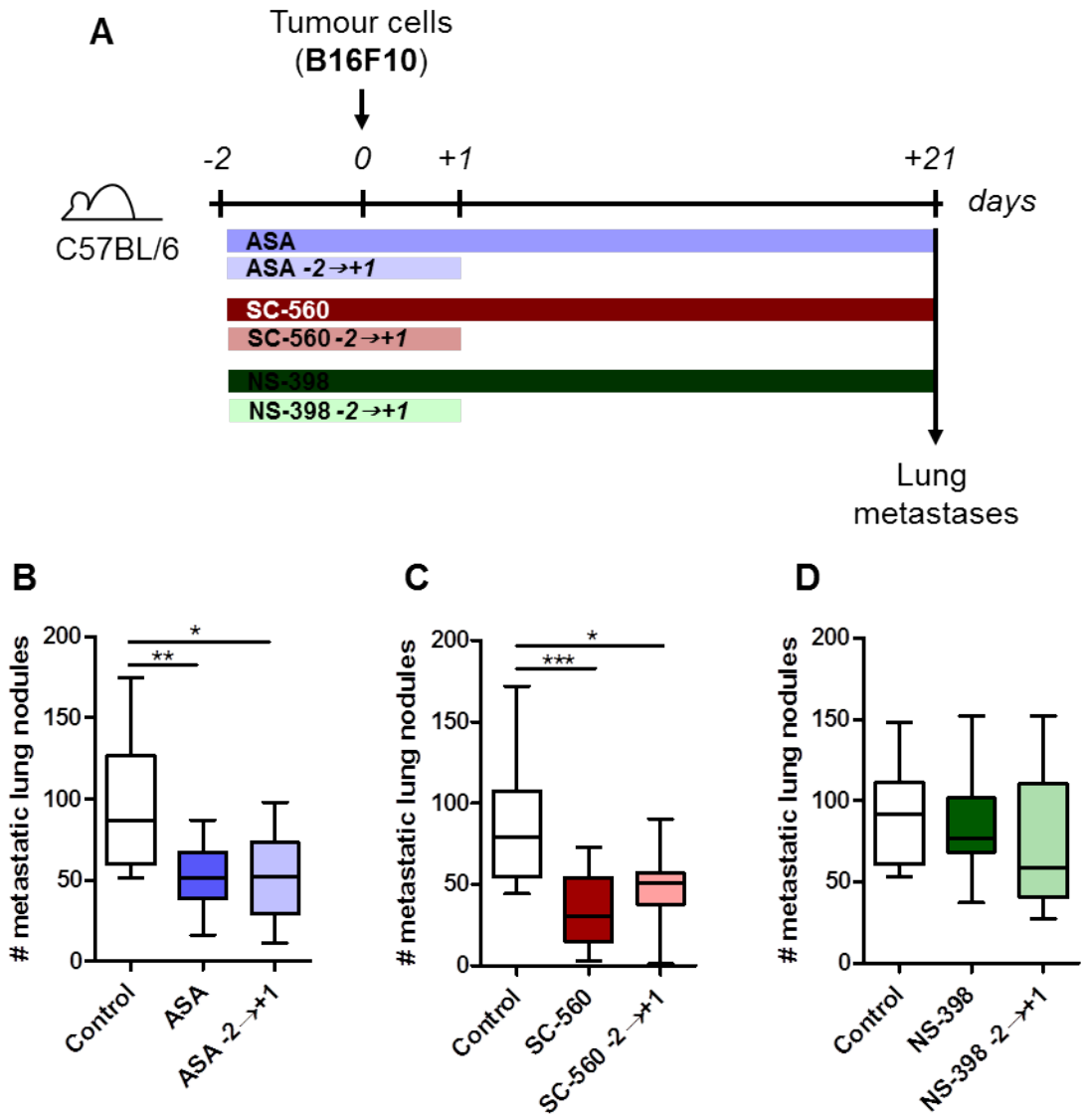

Figure 4.4 – COX-1 inhibition affects the intravascular phase of metastasis.

(A) Experimental design to address the effect of COX inhibition on the intravascular phase of metastasis. C57BL/6 mice were treated with vehicle (Control), ASA (Medium dose), SC-560 or NS-398 starting 2 days before the intravenous injection of B16F10 cells (day -2). Treatment was carried out until 21 days after injection (ASA, SC-560 or NS-398 groups) or up to one day after injection (*-2→+1* groups, intravascular phase). For all groups, lungs were harvested at 3 weeks after tumour cells injection.

(B) Number of metastatic lung nodules at 3 weeks after intravenous injection of B16F10 cells in mice treated with vehicle, ASA or ASA *-2→+1* (n=13, 13 and 6 mice, respectively).

(C) Number of metastatic lung nodules at 3 weeks after intravenous injection of B16F10 cells in mice treated with vehicle, SC-560 or SC-560 *-2→+1* (n=12, 12 and 10 mice, respectively).

(D) Number of metastatic lung nodules at 3 weeks after intravenous injection of B16F10 cells in mice treated with vehicle, NS-398 or NS-398 *-2→+1* (n=10, 16 and 10 mice, respectively).

All data are represented as median ± range, 1-way ANOVA with Tukey's Multiple Comparison test.

4.3.2 Effect of COX inhibition on the extravasation phase of metastasis

We have previously shown that in our model tumour cells extravasate between day 1 and day 3 after their intravenous injection. We wanted to address whether the extravasation phase of metastasis is also affected by COX inhibition. Mice were treated for 3 weeks (ASA, SC-560 or NS-398 groups), until day 4 (ASA *-2→+4*, SC560 *-2→+4*, NS-398 *-2→+4*) or from day 1 to day 4 (ASA *+1→+4*, SC560 *+1→+4*, NS-398 *+1→+4*) after intravenous injection and lungs were collected at day 21 (Figure 4.5A). While *-2→+4* treatment should affect both intravascular and extravasation phases of metastasis, the *+1→+4* treatment was planned to only affect the extravasation process, without interfering with the adhesion of tumour cells to the lung vasculature. The number of lung nodules was decreased by ASA and SC-560 *-2→+4* treatment, but not when treatment was delivered from day 1 to day 4 (Figures 4.5B and C). NS-398 did not affect metastasis at all treatment schedules (Figure 4.5D). When compared with the results of Figure 4.4, there is a trend indicating that *-2→+4* treatment further inhibited metastasis in comparison to *-2→+1* treatment, although not in a significant way. These results indicate that metastasis is prevented by COX-1 inhibition carried out until the completion of tumour cells extravasation, but the inhibition of the extravasation phase alone is not sufficient to reduce metastasis establishment. This observation suggests that COX-1 might play a pivotal role during the intravascular phase of the metastatic process, in particular at the survival, adhesion and initial extravasation steps.

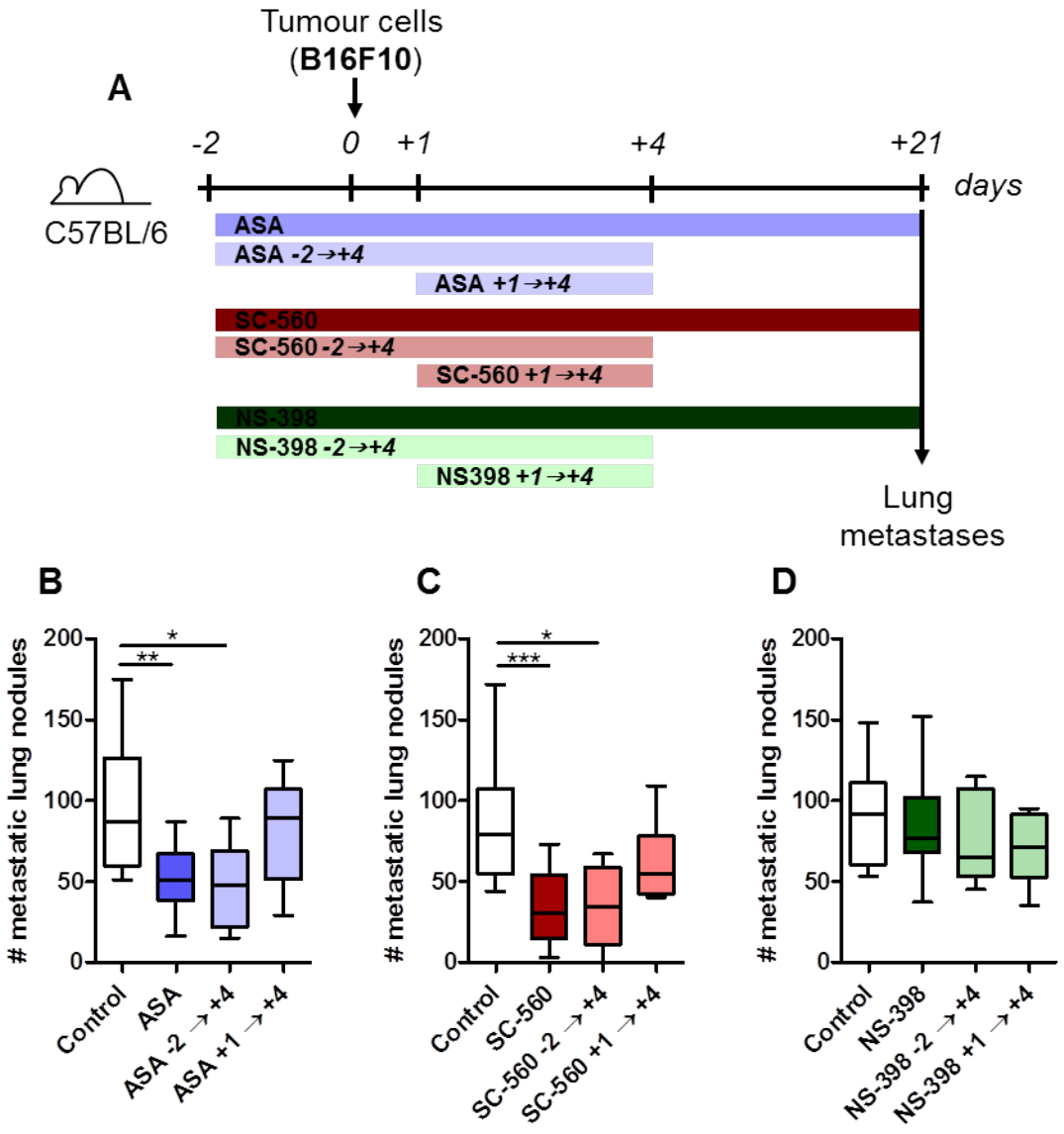

Figure 4.5 - Effects of COX inhibition on the intravascular and/or extravascular phase of metastasis.

(A) Experimental design to address the effect of COX inhibitor on the intravascular and/or extravasation phases of metastasis. C57BL/6 mice were treated with vehicle (Control), ASA (Medium dose), SC-560 or NS-398 and intravenously injected with B16F10 cells on day 0. Treatment was carried out starting 2 days before until 3 weeks after injection (ASA, SC-560 or NS-398 groups), starting 2 days before up to 4 days after injection (*-2→+4* groups, intravascular and extravasation phase) or between 1 to 4 days after injection (*+1→+4* groups, extravasation phase). For all groups, lungs were harvested at 3 weeks after tumour cells injection.

(B) Number of metastatic lung nodules at 3 weeks after intravenous injection of B16F10 cells in mice treated with vehicle, ASA, ASA *-2→+4* or ASA *+1→+4* (n=13, 13, 5 and 6 mice, respectively).

(C) Number of metastatic lung nodules at 3 weeks after intravenous injection of B16F10 cells in mice treated with vehicle, SC-560, SC-560 *-2→+4* or SC-560*+1→+4* (n=12, 12, 5 and 6 mice, respectively).

(D) Number of metastatic lung nodules at 3 weeks after intravenous injection of B16F10 cells in mice treated with vehicle, NS-398, NS-398 *-2→+4* or NS-398*+1→+4* (n=10, 16, 6 and 5 mice, respectively).

All data are represented as median ± range, 1-way ANOVA with Tukey's Multiple Comparison test.

4.3.3 COX-1 inhibition does not affect the extravascular phase of metastasis

As represented in Figure 4.2, B16F10 tumour cells complete the extravasation process 4 days after their intravenous injection, a time point when all cells can be localised in the lung parenchyma. ASA, SC-560 or NS-398 treatment was delivered for 3 weeks or from day 4 until day 21 (ASA *+4→+21*, SC560 *+4→+21*, NS398 *+4→+21*) (Figure 4.6A). The count of lung nodules revealed that this late treatment did not affect metastasis for all three drugs tested (Figure 4.6B-D). These findings support the idea that COX-1 inhibition affects metastasis when tumour cells are in the vasculature or extravasating, but not when the extravasation process has completed. In this perspective, COX-1 seems to have a role during the presence of tumour cells in the vasculature or in the extravasation process, but could not have an effect after the extravasation of tumour cells.

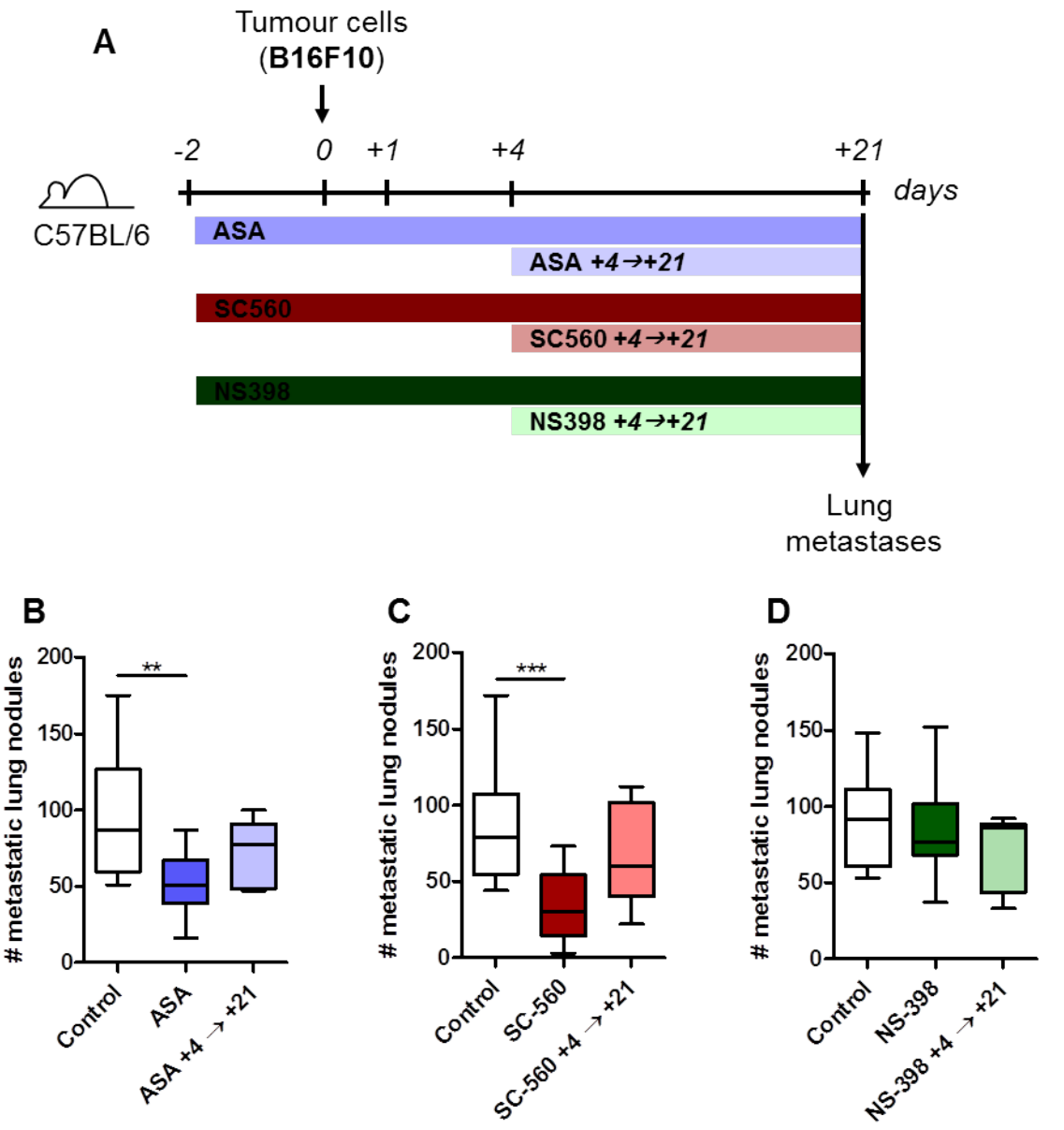

Figure 4.6 - COX-1 inhibition does not affect metastasis after tumour cells extravasation.

(A) Experimental design to address the effect of COX inhibitor on the extravascular phase of metastasis. C57BL/6 mice were treated with vehicle (Control), ASA (Medium dose), SC-560 or NS-398 and intravenously injected with B16F10 cells on day 0. Treatment was carried out starting 2 days before until 21 days after injection (ASA, SC-560 or NS-398 groups) or starting 4 days until 21 days after injection (*+4→+21* groups, extravascular phase). For all groups, lungs were harvested at 3 weeks after tumour cells injection.

(B) Number of metastatic lung nodules at 3 weeks after intravenous injection of B16F10 cells in mice treated with vehicle, ASA or ASA *+4→+21* (n=13, 13 and 6 mice, respectively).

(C) Number of metastatic lung nodules at 3 weeks after intravenous injection of B16F10 cells in mice treated with vehicle, SC-560 or SC-560 *+4→+21* (n=12, 12 and 5 mice, respectively).

(D) Number of metastatic lung nodules at 3 weeks after intravenous injection of B16F10 cells in mice treated with vehicle, NS-398 or NS-398 *+4→+21* (n=10, 16 and 6 mice, respectively).

All data are represented as median ± range, 1-way ANOVA with Tukey's Multiple Comparison test.

4.4 DISCUSSION

In the previous Chapter we have shown that the inhibition of metastasis by aspirin is associated with the inhibition of COX-1 activity. In order to understand the cellular and molecular mechanism through which COX-1 contributes to metastasis, we have started to investigate the kinetics of metastasis inhibition by aspirin.

4.4.1 Analysis of B16F10 extravasation kinetics

Tumour cells can take a variable number of days to complete the extravasation phase[537]. The efficiency and kinetics of the early phases of metastasis are different depending on the model, tumour cell lines and site of injection. These differences are determined by physical factors, such as the size and blood pressure of the target organ or the size and deformability of the tumour cells[128]. Moreover, cell- and organ-specific expression of adhesion molecules and their ligands or release of chemokines would influence the efficiency of homing.

In order to characterise the timing of adhesion, extravasation and early proliferation of B16F10 cells, we have employed a well-established model of whole lung imaging technique. This model allows the visualisation of labelled tumour cells within the superficial lung vasculature in the intact lungs (Figure 4.2). In our model, the very initial arrest of tumour cells in the lungs is probably due to multiple mechanisms. On the one hand, around 20% of tumour cells were physically entrapped in lung capillaries due to size restriction (Supplementary figure S4). Microscopic pictures of lungs collected immediately after injection show tumour cells squeezed into the vasculature, within capillaries of smaller diameter than tumour cells. Moreover, the presence of the tumour cell restricted the access of the labelling anti-CD31 antibody to endothelial cells around and downstream the tumour cells, which is an indication of capillary trapping[546]. These

observations suggest that passive mechanisms of adhesion take place early after the injection of B16F10 cells.

On the other hand, some indications suggest the early presence of adhesion mechanisms between tumour and endothelial cells. First, endothelial cells were labelled in proximity of the majority of tumour cells (around 80%), suggesting that enough space was present between tumour cells (and possibly not imaged associated platelets) and luminal surface of the endothelium for the access of anti-CD31 antibody (Supplementary figure S4). Second, the imaged tumour cells resisted the lung perfusion process, which likely happens at higher sheer rates than the normal blood flow. Finally, the surface reconstruction of tumour cells and lung vasculature showed that the diameter of the vessel was visibly larger than the one of most tumour cells. Together, these observations suggest that some retained tumour cells do not reach the capillaries but localise in pre-capillary arterioles due to specific adhesion to the luminal surface of the endothelium. It is well established that circulating tumour cells interact with platelets early after the intravasation and are surrounded by platelets clots within few minutes[103]. Activated platelets express adhesion molecules and can work as bridges for the interaction between tumour cells and endothelium, in particular in capillary beds[547]. It is possible that the early adhesion of tumour cells to the lung vasculature is mediated by the interaction with platelets and it should then be targeted by anti-thrombotic therapies. This hypothesis will be tested in the next Chapters.

Although the initial arrest of tumour cells in the lung vasculature is considered to be very efficient, the further steps in the cascade are less successful[128]. It has been previously shown that 98% B16F10 cells injected into the tail vein are found in the lungs one hour after injection[537]. We found that the number of tumour cells in the lung vasculature exponentially decreased in the first 24 hours and further diminished until the second day post-injection, reaching a nadir (Figure 4.2C). Only around 25% of the initially arrested

cells were found in the lungs one day after the injection, suggesting that the majority of cells are cleared due to apoptosis or immune surveillance.

We have also observed the initial step of tumour cells seeding in the lung parenchyma. At day 4 post-injection, around 17% of the tumour cells detected in the lungs were part of multicellular foci, which indicates the reinitiation of their growth. All these cells were localised in the extracellular space, suggesting that the intravascular proliferation is a rare event for B16F10 cells[523]. Proliferating cells represented the 1.4% of all cells detected immediately after injection. Considering that only 0.04% of all total cells would form metastatic lung nodules, the initial proliferation of extravasated cells does not guarantee their development into metastatic lung nodules.

4.4.2 COX-1 inhibition affects the intravascular phase of metastasis

In this Chapter we have tested the effect of COX inhibition on the early permanence of tumour cells within the lung vasculature. At one day after the injection, 85% of B16F10 cells are localised within the lung vasculature, either adhered or at early stages of extravasation (Figure 4.2B). Hence, we have employed the isolated-perfused lung model to image the total number of tumour cells in the left lung, which has been previously shown to correlate with early tumour cells survival[26,29,146]. The data here presented show that the inhibition of COX-1, achieved through pharmacological treatment (ASA or SC-560) or genetic depletion (COX-1$^{-/-}$ mice), was associated with a reduced number of tumour cells in the lungs at early stages (Figure 4.3D). This effect could be due to a number of factors.

First, COX-1 inhibition might affect tumour cells survival due to a direct cytotoxic effect of COX-1 inhibitors on tumour cells. However, a similar reduction in the number of tumour cells at 24 hours post-injection was found in lungs from COX-1$^{-/-}$ mice (Figure 4.3D), where COX-1$^{-/-}$ inactivation takes place in host cells only. This observation suggests that

any effect on tumour cells survival would be due to the inhibition of COX-1 in the microenvironment. During the first 24 hours after injection, the majority of B16F10 cells is localised within the lung vasculature, where platelets and endothelial cells are the most prominent source of micro-environmental COX-1. In particular, previous evidence suggests that the inhibition of platelet aggregation could result in a reduced survival of tumour cells in the circulation (see section 1.1.3.1 for details).

Another possible explanation for the reduction of early tumour cells persistence in the lungs could be an effect of COX-1 inhibition on adhesion to the endothelium. This hypothesis implies that if tumour cells cannot establish stable interactions with endothelial cells, they would be washed away by perfusion, experimentally, or shear stress, physiologically. As commented previously, around 80% of B16F10 cells seem to be localised in pre-capillary arterioles and adhere with the endothelium shortly after their introduction in the circulation. Considering that the interaction of tumour cells with platelets happens shortly after their introduction in the vasculature, we can hypothesise that the presence of COX-1-inactive or -deficient platelets in the circulation would dramatically decrease their ability to form adhesive bridges between tumour cells and endothelial cells.

Finally, around 30% of tumour cells have started to extravasate at 24 hours post-injection (Figure 4.2B). It is possible that COX-1 inhibition affects TEM, thus reducing the initial lung seeding.

All together, the most likely scenario is that the decrease in the number of tumour cells at 24 hours is due to a combination of reduced survival, adhesion and TEM. This hypothesis will be addressed in the next Chapters.

The inhibition of tumour persistence in the lungs at early time points has long-term effects on the establishment of metastasis. In fact, metastatic lung nodules were reduced by COX-1 inhibition to a similar extent irrespectively whether treatment was carried out for 3 weeks or until one day after tumour cell injection (Figure 4.4B and C). Moreover, we have

seen a similar relative reduction in the number of tumour cells in the lungs at one day post-injection (Figure 4.3B) and the number of lung nodules at three weeks post-injection (Figure 3.5B). These observations suggest that the anti-metastatic effect of aspirin is mostly effective during the presence of tumour cells in the circulation, corresponding to the seeding phase of metastasis.

4.4.3 COX-1 is not essential for the extravasation phase of metastasis

The data presented so far suggest that COX-1 has a pivotal role during the first day of tumour cell presence in the circulation, but it does not exclude an effect on subsequent phases of metastasis beyond their intravascular localisation. The extravasation process of B16F10 cells extends over a period of three days and all viable cells have extravasated at four days after the injection (Figure 4.2B). On this basis, we have analysed the effect of COX inhibitors on these phases of metastasis.

The inhibition of COX-1 did not reduce metastasis when mice were treated during their extravasation (from day 1 to day 4 after injection, Figure 4.5), although a trend without significance was seen in the case SC-560. These findings would imply that COX-1 activity is not essential for the extravasation phase *per se*.

Consistent with this, metastatic lung nodules were found reduced when COX-1 was inhibited during both intravascular and extravasation phases of metastasis (Figure 4.5B and C). The extent of this anti-metastatic effect was similar to a treatment carried out for the whole length of the experiment or interrupted one day after the injection of tumour cells. Thus, extending COX-1 inhibition after the first 24 hours did not significantly improve the anti-metastatic outcome. All together, these findings suggest that COX-1 inhibitors (ASA and SC-560) exert their anti-metastatic effect when administered during the first day of tumour cells dissemination, when tumour cells are still circulating.

Nevertheless, these data do not totally exclude an effect of COX inhibition on extravasation. A fraction of B16F10 had already started the extravasation process during the first day after injection (Figure 4.2B). In theory, the first tumour cells that engage in TEM possess a more invasive phenotype and re-initiate proliferation shortly after their extravasation. Considering the anti-metastatic effect of early COX-1 inhibition, it is possible that COX-1 would partly contribute to the extravasation phase, a hypothesis that will be tested in the Chapter 5.

4.4.4 COX-1 inhibition does not affect the progression of metastasis after tumour cells extravasation

We sought to understand the effect of COX inhibition on later stages of the metastatic process, in particular after the extravasation of tumour cells. In order to do so, mice were treated with ASA, SC-560 or NS-398 starting at 4 days after tumour cells challenge, a time point where all B16F10 were extravasated in lungs (Figure 4.2B). The number of metastatic lung nodules was not affected by this late treatment (Figure 4.6), suggesting that COX-1 and COX-2 do not contribute to the establishment of metastatic lung nodules after the extravasation of tumour cells. The extravascular phase would include early survival of tumour cells in the extravascular space, initiation of proliferation (micrometastasis) and persistent growth (macrometastasis).

It is important to note that, just based on the data presented, we cannot exclude an effect of COX inhibition on the proliferation of disseminated cells. According to the experimental metastasis model employed here, the number of metastatic lung nodules is representative of tumour cell survival and seeding efficiency, in particular during the haematogenous and perivascular phases of metastasis. On the contrary, the measurement of the nodules size is representative of the proliferation of tumour cells in the metastatic site. The visual examination of lungs from ASA, SC-560 and NS-398-treated mice has suggested that

metastatic foci are smaller in presence of COX-2 inhibition (data not shown), suggesting an anti-proliferative effect. In the future, the calculation of the metastatic index (total metastasis volume/whole lung volume) from lung sections will help to further understand the role of COX inhibition on metastasis progression.

4.4.5 Clinical outcomes

We have shown that the inhibition of COX-1 affects the initiation and early progression of metastasis, but not its sustained growth. These observations have important clinical outcomes. Primary tumours constantly shed tumour cells in the circulation and it is believed that tumour cell dissemination starts at very early stages in some types of cancer[548,549]. Since the anti-metastatic action of aspirin is achieved shortly after the entrance of tumour cells in the circulation, it follows that cancer patients should be administered adjuvant low-dose aspirin treatment at the moment of cancer diagnosis.

This treatment would be particularly beneficial for patients with localised cancer at the moment of diagnosis but it could also improve the overall survival of patients with metastatic disease. On the one hand, numerous evidences have shown an effect of aspirin on the growth of the primary tumour[370-375]. This would suggest that, irrespectively from the stage of cancer, aspirin would be a valuable therapy to prevent tumour expansion and, hypothetically, metastasis growth. On the other hand, established metastases can behave like primary tumour and shed disseminating tumour cells, which can then re-colonise the primary site ("tumour self-seeding")[528] or engraft new sites ("metastasis-to-metastasis seeding")[526,527]. In both cases, aspirin would still prove beneficial to limit tumour spread across the body.

Together with our findings, these considerations suggest that low-dose aspirin could represent a cost-effective means to control tumour cells spread in cancer patients, especially when early cancer diagnosis is available. However, the balance between

therapeutic and side effect needs to be carefully evaluated. When treatment with aspirin is not an option, the employment of more selective inhibitors (such as SC-560) could be an alternative. Additionally, the further understanding of COX-1 contribution to tumour spread could help to design more efficient therapies for the prevention of metastasis.

4.4.6 Conclusions

Overall, in this Chapter we have described the kinetics of metastasis inhibition by aspirin and selective COX inhibitors. After the empirical description of the dynamics of tumour cell extravasation, we have differentiated the treatment in time slots that would affect tumour cells within the lung vasculature, during the extravasation and in the lung extravascular space. Our results suggest that COX-1 inhibition primarily affects the intravascular phase of metastasis and this effect is sufficient to reduce the number of metastatic lung nodules at later time points.

During these early stages tumour cells undergo a series of steps of the metastatic cascade, such as interaction with platelets and immune cells, initial entrapment in capillaries and adhesion to the endothelium. Moreover, a fraction of tumour cells start the extravasation process. Chapter 5 will be focusing on the contribution of COX-1 to each of these steps, with the purpose of investigating the molecular mechanisms behind COX-1-dependent impairment of metastasis.

CHAPTER 5

COX-1 contributes to multiple steps of the intravascular phase of metastasis

5.1 INTRODUCTION

5.1.1 Role of the metastatic niche during the haematogenous transit of tumour cells

The metastatic cascade is a multi-step process that goes from the dissociation from a primary tumour to the formation of distant metastases in the secondary organ. During the intravascular phase, CTCs transit in the blood stream until they arrest in a distant vascular bed. The blood circulation represents a very hostile environment, where tumour cells are exposed to cell death by shear stress and cytotoxic immune cells (see section 1.1.2.2). Both intrinsic features of the tumour cells and their interaction with other cell types within the circulation allow them to survive and seed a distant organ. In particular, circulating tumour cells with advantageous traits are able to trigger the generation of a pro-thrombotic 'early metastatic niche'[103] that supports their seeding and progression. This niche is constituted by platelets, immune cells and endothelial cells and their soluble factors.

Overall, platelets are a central orchestrator for the generation of microemboli containing tumour cells, platelets and immune cells, localised in close proximity to endothelial cells in the microvasculature. The formation of these aggregates promotes metastasis through multiple mechanisms, involving increased survival, adhesion and invasiveness of tumour cells (see section 1.1.3.1). Moreover, local paracrine signalling activates expression programs in tumour cells that would affect their ability to invade the secondary organ after the dissolution of the heteroaggregates and extravasation.

The inability of tumour cells to trigger platelet aggregation on their surface had been extensively linked to metastatic inefficiency and the expression of pro-coagulant factors by

CTCs is positively selected for metastasis. Thus, platelets represent a selection driver for metastatic phenotype.

5.1.2 Contribution of COX-1 to the interaction of tumour cells with platelets

Tumour cells can interact with platelets through multiple mechanisms, which include the expression of pro-coagulant TF and of the adhesion molecule PSGL-1 (see section 1.1.2.3). TF-mediated TCIPA has been documented in numerous cell lines and the expression of TF and ß$_3$ integrins by tumour cells correlates with metastatic potential[115]. In our model, it is believed that the main mechanism of TCIPA initiation by B16F10 is the expression of TF[26] and not PSGL-1[267]. While PSGL-1 mediates the direct interaction with P-selectin on platelets, TF requires the activation of the coagulation cascade. In fact the formation of TF-VIIa complex leads to the activation of thrombin, which plays a central role in the formation of thrombus. On the one hand, thrombin binds to PAR receptors on platelets and induces platelet activation[550]. This process involves a G_q and G_{13}-mediated signalling cascade that leads to the inside-out activation of integrin $\alpha_{IIb}ß_3$ to its high-affinity state and the phosphorylation of myosin light chain, which induces platelet change of shape and degranulation[114]. On the other hand, thrombin cleaves soluble fibrinogen to fibrin monomers (fibrinopeptide A and B), which polymerise to form fibres[551]. The high-affinity forms of integrins $\alpha_v ß_3$ on tumour cells and $\alpha_{IIb}ß_3$ on platelets bind to fibrin and mediate the deposition of fibrin clots on the surface of tumour cells[106]. This process is referred to as initiation of thrombus formation.

The initial generation of thrombin by TF-VIIa complexes is highly inefficient because of the low concentration of other coagulation factors[106]. Hence, the initial thrombus is rather small and it may contain non-activated platelets[106]. The expansion of the thrombus requires the recruitment and activation of other platelets, which will provide additional coagulation factors for the expansion and stabilisation of the clot[106,552]. This process is

mediated by the activation of integrin $\alpha_{IIb}ß_3$ and the release of adhesion molecules contained in the α-granules of platelets, such as vWF. Thus, the initial layer of activated platelets in the clot serves as adhesive surface for the tethering of other platelets. This binding is stabilised by the release of activation agonists (e.g. ADP and serotonin), contained in the dense-granules of platelets[106,553]. TXA_2 is also a secondary mediator of the amplification of thrombus formation, being a potent agonist of platelet aggregation. In contrast with other agonists, its generation relies on the *de novo* synthesis from lipid precursors[554]. Thrombin activation of platelets induces the increase of cytosolic Ca^{2+}, which activates phospholipase A_2 (PLA_2) and its translocation into the plasma membrane. PLA_2 then releases AA in the cytoplasm, which is converted by COX-1 and TXAS into TXA_2 (see section 1.2).

The inhibition of COX-1 by low-dose aspirin is associated with a sustained inhibition of TXA_2 synthesis by platelets. Since the initial aggregation of platelets on TF-expressing tumour cells is mediated by other mechanisms, aspirin is able to reduce the expansion of platelets-fibrin clots but not the initial formation. Thus, aspirin is normally referred to as a weak platelet inhibitor.

5.2 AIMS

The data collected so far suggest that the preventive effect of aspirin on metastasis relies on the inhibition of COX-1, in particular during the intravascular phase of pulmonary metastasis. In this chapter we have employed *in vitro* and *in vivo* assays to investigate the effects of COX inhibition on multiple steps of the haematogenous transit of tumour cells. In particular, we have focused on exploring COX contribution to:

1) the interaction with host circulating cells (platelets and monocytes/macrophages)
2) the adhesion of tumour cell to the endothelium and TEM.

5.3 RESULTS

5.3.1 Effects of COX inhibition on the interaction of tumour cells with blood elements

5.3.1.1 The inhibition of COX-1 reduces platelet aggregation on tumour cells

Platelets can aggregate on the surface of B16F10 cells through a TF-dependent mechanism[26]. The inhibition of COX-1 activity is sufficient to inhibit platelet aggregation *ex vivo* (Figure 3.3C and D) and concomitantly decrease the number of metastatic lung nodules (Figure 3.5B and C). We hypothesise that COX-1 inhibition results in a decreased aggregation of platelets on tumour cells (TCIPA), which leads to a lower metastatic capacity of tumour cells. To test this, labelled B16F10 cells (B16F10-CMAC) and platelets (Plts-PKH26) were injected into the opposite tail veins of $Cx_3CR1^{gfp/+}$ mice treated with ASA, SC-560 and NS-398 (Figure 5.1A). The interaction of tumour cells and platelets within the vasculature was analysed in whole lungs 8 hours after the injection. In particular we measured the percentage of tumour cells associated with platelets, the number of platelet aggregates per tumour cells and the size of platelet clots, which are representative parameters of the efficiency of the initiation (percentage of tumour cells with aggregates) or expansion (number and size of aggregates) phases of thrombus formation. No treatment affected the interaction of platelets on B16F10 cells, since all cells were associated with platelet clots in untreated or treated mice (Figure 5.1B and C). This observation confirmed that the initiation of platelet aggregation on tumour cells does not rely on COX isoforms. Nevertheless, ASA and SC-560, but not NS-398, decreased the number (Figure 5.1B and D) and the size (Figure 5.1B and E) of clots per tumour cell. These findings were validated *in vitro*, where labelled tumour cells (B16F10-CMFDA) and platelets (Plts-PKH26) were co-incubated in the presence of the different treatments

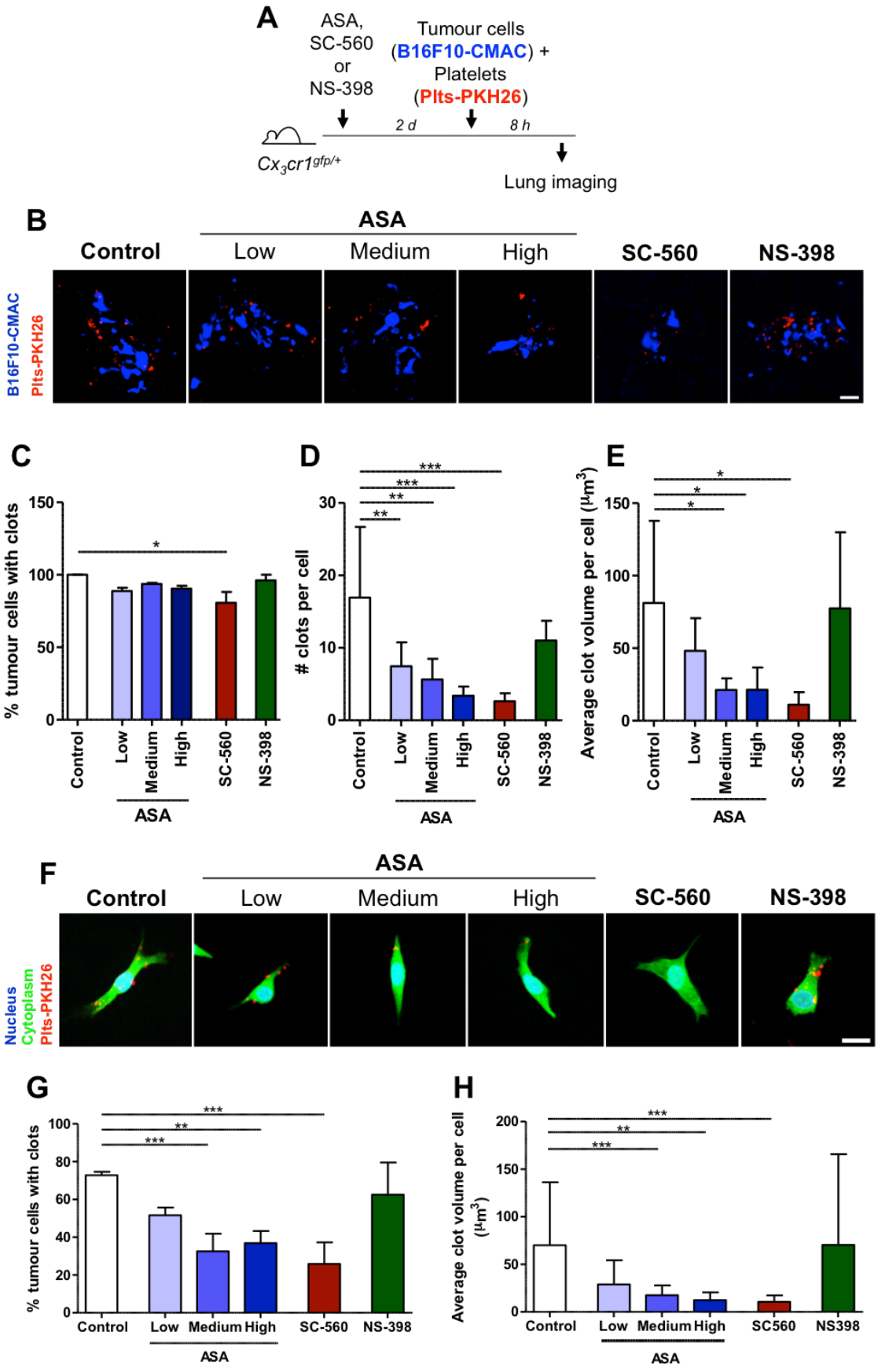
A
ASA, SC-560 or NS-398
Tumour cells (B16F10-CMAC) + Platelets (Plts-PKH26)
2 d
8 h
Cx3cr1gfp/+
Lung imaging
B
ASA
Control
Low
Medium
High
SC-560
NS-398
B16F10-CMAC
Plts-PKH26
C
% tumour cells with clots
D
clots per cell
E
Average clot volume per cell (µm3)
F
Nucleus
Cytoplasm
Plts-PKH26
G
% tumour cells with clots
H
Average clot volume per cell (µm3)
SC560
NS398

Figure 5.1 – The inhibition of COX-1 reduces the aggregation of platelets on tumour cells.

(A) Experimental design to visualise tumour cells interaction with platelets within the pulmonary vasculature. Labelled tumour cells (B16F10-CMAC) and platelets (Plts-PKH26) were injected in the opposite tail veins of *Cx$_3$cr1$^{gfp/+}$* mice, two days after the start of treatment with vehicle (Control), ASA (all doses), SC-560 or NS-398. Lungs were harvested at 8 hours after the injection and imaged as intact organs.

(B) Representative MIP of 3D confocal stacks of tumour cells (blue) and platelets (red) in whole lungs of *Cx$_3$cr1$^{gfp/+}$* mice, treated with vehicle, ASA, SC-560 or NS-398. Scale bar represents 30 µm.

(C-E) Percentage of tumour cells associated with platelets (C) (n=3 mice, 15 FOVs per lung were analysed; median ± IQR, 1-way ANOVA with Kruskal-Wallis test with Dunn's Multiple Comparison post-hoc test), number of clots per tumour cells (D) (n=3 mice, 3 cells per lung were analysed; mean ± SD, 1-way ANOVA with Tukey's Multiple Comparison test) and cumulative volume of clots per tumour cell (E) (n=3 mice, ≥3 clusters per lung were analysed; mean ± SD, 1-way ANOVA with Tukey's Multiple Comparison test) in lungs from mice treated with vehicle, ASA, SC-560 or NS-398, quantified from confocal microscopy images (20x and 40x) of whole lungs.

(F) Representative MIP of 3D confocal stacks of tumour cells (B16F10-CMFDA, green) seeded on culture slides and incubated with platelets (Plts-PKH26, red) in the presence of vehicle, ASA, SC-560 or NS-398. The nuclei of tumour cells were stained with DAPI after fixation (blue). Scale bar represents 30 µm.

(G-H) Percentage of tumour cells associated with platelets (G) and cumulative volume of platelet clot per tumour cells (H) upon vehicle, ASA, SC-560 or NS-398 *in vitro* treatment, quantified from confocal microscopy images of culture slides (n=2 independent experiments, ≥4 cells per group were analysed; mean ± SD, 1-way ANOVA with Tukey's Multiple Comparison test).

(Figure 5.1F-H). These findings confirmed that the inhibition of COX-1, but not of COX-2, affects the exponential phase of platelet aggregation and the recruitment of new platelets, decreasing the size and number of platelets aggregates on tumour cells.

5.3.1.2 COX-1 inhibition in platelets reduces TCIPA

The inhibition of platelet aggregation on tumour cells could be equally due to an effect of COX-1 inhibition on tumour cells or platelets. Platelets or tumour cells were pre-incubated with ASA, SC-560 or NS-398, then drugs were washed away and cells were co-incubated to analyse platelet aggregation on tumour cells (Figure 5.2A-C). The percentage of tumour cells associated with platelets was decreased by ASA and SC-560 when platelet and tumour cells were treated together (Figure 5.2A) or when platelets alone were pre-treated (Figure 5.2B), but not when tumour cells were pre-treated (Figure 5.2C).

These data confirm that the inhibition of COX-1, but not of COX-2, impairs the aggregation of platelets on tumour cells and this is due to an effect on platelets rather than on tumour cells. Together with the previous data, this evidence suggests that aspirin inhibits COX-1 in the microenvironment, rather than in tumour cells.

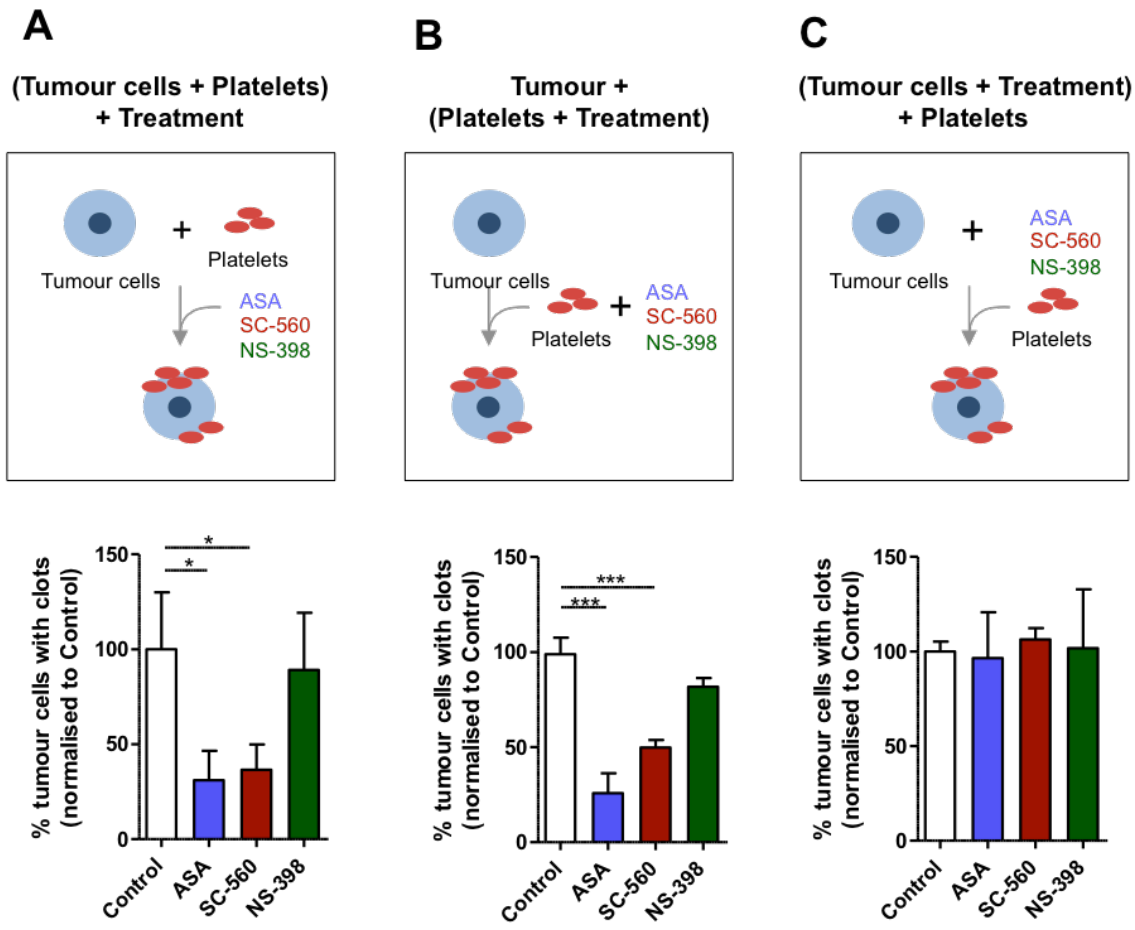

Figure 5.2 – The inhibition of COX-1 in platelets is responsible for the decreased aggregation on tumour cells.

(A) (Top panel) Experimental design: tumour cells (B16F10-CMFDA) were incubated with platelets (Plts-PKH26) in the presence of vehicle (Control), ASA (Medium dose), SC-560 or NS-398. (Bottom panel) The percentage of tumour cells associated with platelets was quantified from confocal microscopy images (20x) (n=3 independent experiments, ≥14 cells were analysed).

(B) (Top panel) Experimental design: tumour cells were incubated with platelets that had been pre-treated with vehicle, ASA, SC-560 or NS-398. (Bottom panel) The percentage of tumour cells associated with platelets was quantified from confocal microscopy images (20x) (n=3 independent experiments, ≥12 cells were analysed).

(C) (Top panel) Experimental design: tumour cells were pre-treated with vehicle, ASA, SC-560 or NS-398 and incubated with platelets. (Bottom panel) The percentage of tumour cells associated with platelets was quantified from confocal microscopy images (20x) (n=3 independent experiment, ≥14 cells were analysed).

All data are represented as mean + SD, 1-way ANOVA with Tukey's Multiple Comparison test.

5.3.1.3 COX-1 inhibition reduces the recruitment of monocytes/macrophages to tumour cells

As described in sections 1.1.2.5 and 1.1.3.3, tumour cells interact with immune cells, which can alternatively play a permissive or anti-tumour role. Previous work in our lab has shown that clots on the surface of tumour cells recruit a population of monocytes/macrophages that promotes the survival of disseminating cells and further development into metastasis[26]. To analyse if aspirin interferes with this recruitment, we injected fluorescently labelled tumour cells and platelet in *Cx3cr1*$^{+/gfp}$ mice treated with ASA, SC-560 and NS-398 (Figure 5.1A). In this mouse strain circulating monocytes/macrophages express GFP[26,493]. Although most tumour cells were still surrounded by clots (Figure 5.1B and C), ASA and SC-560 reduced the number and size of clots within the cluster (Figure 5.3A-C). As a consequence, all tumour cells were surrounded by monocytes/macrophages clusters (Figure 5.3A), but the size of clusters was reduced upon ASA and SC-560 treatment (Figure 5.3D), suggesting that the magnitude of recruitment positively correlate with the mass of platelets clot (Figure 5.3E).

Together, these results suggest that the anti-thrombotic effect of aspirin leads to a reduced recruitment of monocytes/macrophages to tumour cells. Previous evidence has shown that monocytes/macrophages support the survival and metastatic efficiency of tumour cells[26]. These data imply that one possible mechanism through which COX-1 inhibition affects metastasis could be the impairment of the recruitment of pro-metastatic monocytes/macrophages to tumour cells during the first hours of metastatic dissemination.

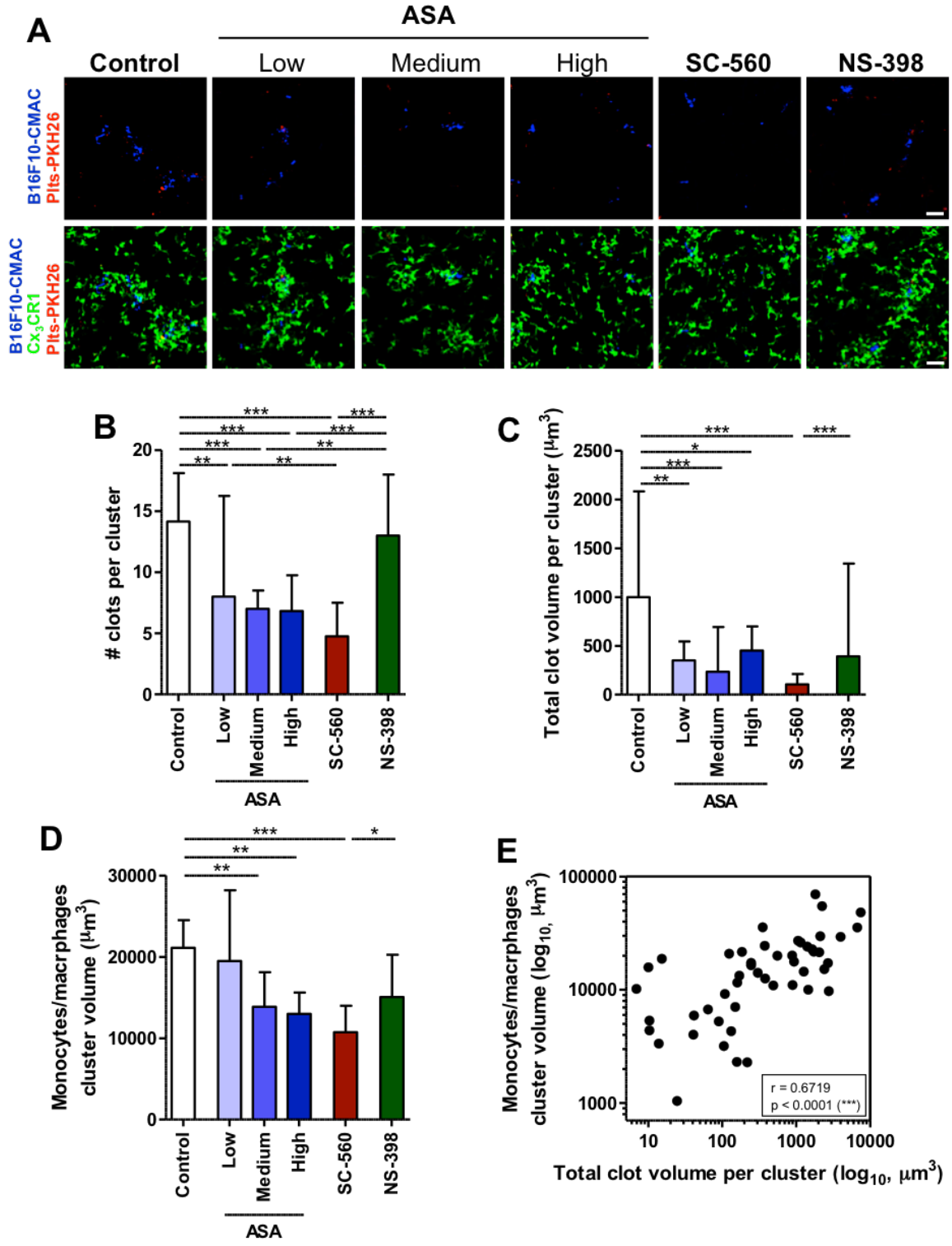

Figure 5.3 – COX-1 activity is required for the recruitment of monocytes/macrophages to tumour cells.

(A) (see Figure 5.1A for the experimental design) Representative MIP of 3D confocal stacks of tumour cells (B16F10-CMAC, blue), platelets (Plts-PKH26, red) and Cx_3CR1^+ monocytes/macrophages (GFP, green) imaged in whole lungs from *Cx3cr1*$^{gfp/+}$ mice at 8 hours after the intravenous injection of tumour cells. Mice were pre-treated with vehicle (Control), ASA (all doses), SC-560 or NS-398 starting 2 days before the injection. Scale bars represent 50 µm.

(B-C) Number (B) and cumulative size (C) of clots of platelets in clusters of monocytes/macrophages and tumour cells, calculated from confocal microscopy images (20x and 40x) (n=3 mice per group, ≥9 clusters per lungs were analysed; median ± IQR, 1-way ANOVA Kruskal-Wallis test with Dunn's Multiple Comparison post-hoc test).

(D) Total volume of monocytes/macrophages cluster, calculated from confocal microscopic images (20x) (n= 3 mice, ≥4 clusters per lungs were analysed; median ± IQR, 1-way ANOVA Kruskal-Wallis test with Dunn's Multiple Comparison post-hoc test).

(E) Correlation plot of the monocytes/macrophages volume versus the cumulative size of clots within the cluster (n=49; Spearman rank correlation).

5.3.2 Effects of COX inhibition on tumour cell interaction with the vasculature

5.3.2.1 COX-1 inhibition decreases vasoconstriction

In physiological conditions, vascular smooth muscle cells express TP (Supplementary figure S7) and respond to TXA_2 stimulation by contracting, leading to vasoconstriction[555]. COX-1 inhibition decreases the synthesis of TXA_2 by platelets (Figure 3.3B). It has been suggested that a fraction of circulating cells arrest in the lung vasculature due to physical entrapment rather than receptor-ligand interaction (Supplementary figure S4). In order to verify if aspirin affects the diameter of vessels lumen through the inhibition of COX-1, lung sections from mice treated with ASA, SC-560 or NS-398 were immunostained for endothelial cells (vWF) and the diameter of vessels was measured. As expected, the inhibition of COX-1 by ASA and SC-560 was associated to a higher calibre of lung vessels, while the inhibition of COX-2 by NS-398 did not alter their diameter (Figure 5.4A and B). Moreover, the overall percentage of capillary-sized vessels (≤60 µm diameter[556]) was decreased by ASA and SC-560 treatment (Figure 5.4C). These results suggest that the inhibition of TXA_2 release, mainly by platelets associated with tumour cells, decreases the contraction of vascular muscle cells, leading to vasoconstriction. This effect might be responsible for a lower number of tumour cells entrapped in the lung vasculature and to a decrease of metastatic efficiency.

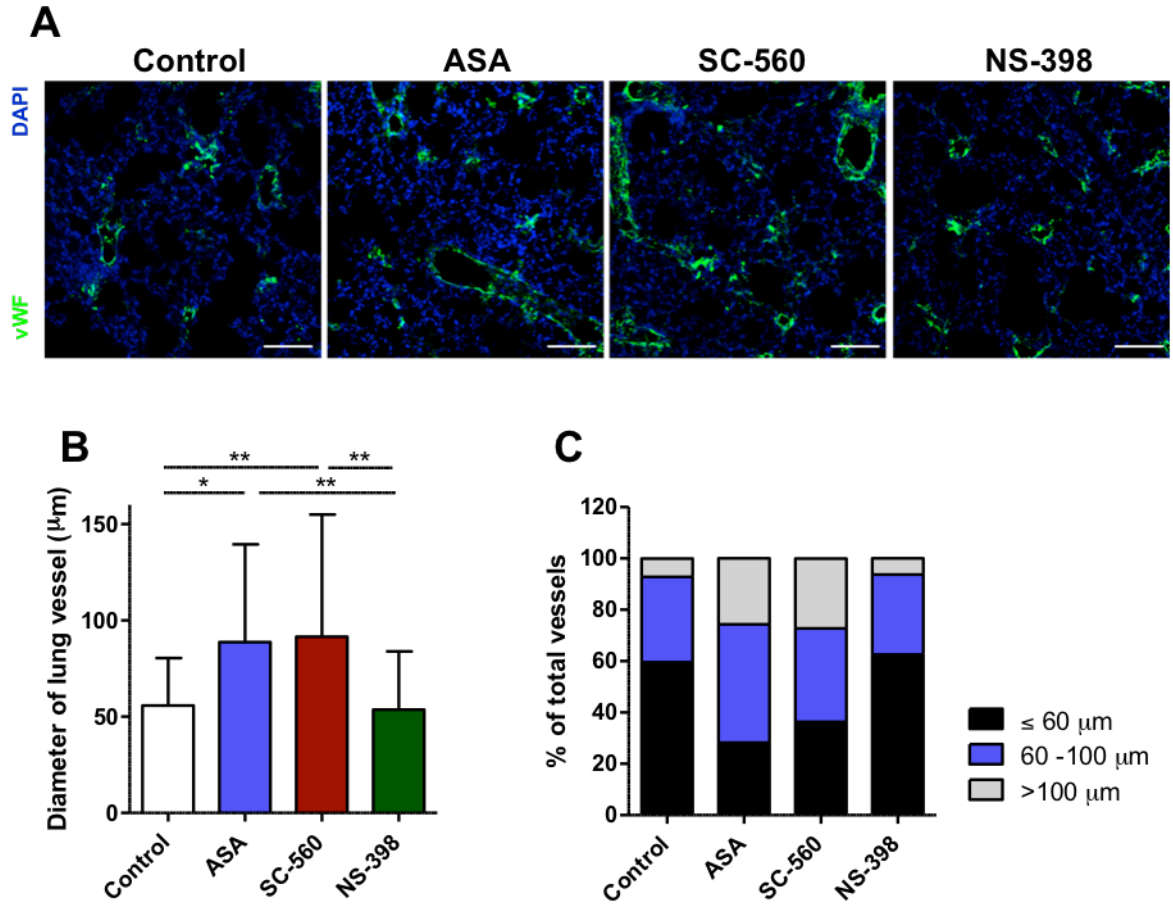

Figure 5.4 – COX-1 inhibition is associated with reduced vasoconstriction.

(A) Representative MIP of 3D confocal stacks of lung sections from *Cx$_3$cr1$^{gfp/+}$* mice treated with vehicle (Control), ASA (Medium dose), SC-560 or NS-398, starting 2 days before the intravenous injection of tumour cells. Endothelial cells were labelled by immunofluorescence staining with an anti-vWF antibody (green) and nuclei were stained with DAPI (blue). Scale bars represent 100 µm.

(B) Quantification of the luminal diameter of pulmonary vessels in lung sections from mice treated with vehicle, ASA, SC-560 or NS-398 (n=3 mice per group, ≥7 vessels per lung were analysed; mean + SD, 1-way ANOVA with Tukey's Multiple Comparison test).

(C) Percentage of vessel classified on the basis of diameter size as capillaries (≤60 µm), arterioles/venules (60-100 µm) arteries/veins (>100 µm) (according to [556]) and normalised to the total number of vessels per FOV (n=3 mice per group, ≥7 vessels per mouse were analysed; mean values).

5.3.2.2 COX-1 activity contributes to endothelial activation

Upon stimuli, endothelial cells can undergo activation and express adhesion molecules such as E-selectin, ICAM-1 and VCAM-1. These markers are not expressed in physiological conditions and assist the adhesion of leukocytes during inflammatory response[129]. Additionally, it has been shown that endothelial activation can be triggered by the presence of clots on the surface of tumour cells in the lung vasculature and allow firmer adhesion of tumour cells to the vasculature in the metastatic process[146]. We investigated whether aspirin affects endothelial activation by evaluating the expression of an endothelial activation marker (VCAM-1) in lung sections. Our data show that the ASA reduced the percentage of tumour cells associated with VCAM-1 expressing vessel (Figure 5.5A and B) and the level of expression of VCAM-1 by endothelial cells (Figure 5.5C). These data suggest that the activity of COX-1 is required for tumour cell-induced endothelial activation. To support this observation, in future plans we will assess the expression of VCAM-1 in lung sections from mice treated with SC-560 or NS-398.

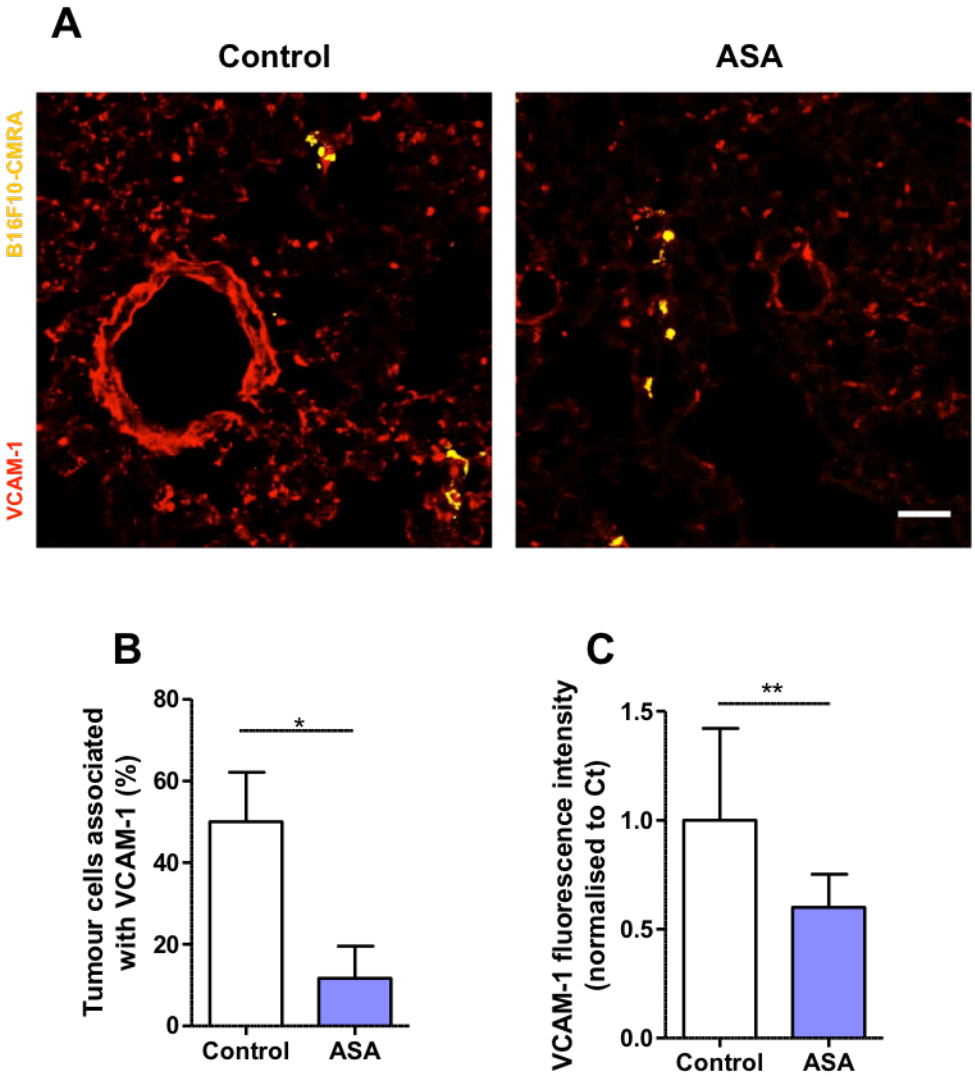

Figure 5.5 – ASA decreases the activation of endothelial cells.

(A) Representative MIP of 3D confocal stacks of lung sections from *Cx$_3$cr1$^{gfp/+}$* mice treated with vehicle (Control) or ASA (Medium dose), starting 2 days before the intravenous injection of B16F10-CMRA tumour cells (orange). Activated endothelial cells were labelled by immunofluorescence staining with an anti-VCAM-1 antibody (red). Scale bar represents 50 µm.

(B-C) Quantification of the number of tumour cells associated with VCAM-1 expressing vessels (B) and fluorescence intensity of VCAM-1 in endothelial cells (C), assessed in confocal microscopy images (20x) (n=3 mice, ≥6 tumour cells per lung were analysed; mean + SD, unpaired t test). Tumour cells were considered associated with a VCAM-1 expressing vessel if localised at a distance of 80 µm or less, as previously indicated[146].

5.3.2.3 COX-1 inhibition reduces the adhesion of tumour cells to the endothelium

Decreased endothelial activation has been correlated with a lower number of metastatic lung nodules[146]. This effect is possibly due to a disruption of receptor-ligand interaction between tumour cells-platelet aggregates and endothelium, leading to a reduced adhesion. We have tested this hypothesis by employing a tissue culture microfluidic system with time lapse imaging to model *in vitro* tumour cell arrest and adhesion under flow. Briefly, lung microvascular endothelial cells (LMVECs) were isolated from C57BL/6 mice, as previously shown[489], and grown in culture. Then labelled tumour cells (B16F10-CMFDA) and platelets (Plts-PKH26), all derived from a syngeneic host, were infused onto a monolayer of LMVECs under flow with a physiological shear stress of 0.05 dyn/cm^2 and adhesion was acquired in real time (Figure 5.6A). All cells were pre-treated with vehicle, ASA, SC-560 or NS-398 prior to the flow experiment. As depicted in Figure 5.6B and C, all drug treatments affected the number of adhered tumour cells to the endothelium. Additionally, the interaction between tumour cells and endothelium was resistant to the challenge with an increased shear stress pressure (1 dyn/cm^2 for 2 minutes, Supplementary figure S5). These data suggest that both COX-1 and COX-2 contribute to the early arrest/adhesion of tumour cells.

Additionally, we have quantified the percentage of tumour cells associated with platelets at the end of the flow experiment. We saw that ASA and SC-560, but not NS-398, decreased platelet aggregation on tumour cells (Figure 5.6D), consistent with an effect of COX-1 inhibition on TXA_2 generation. These observations suggest that TCIPA has a permissive role for tumour cell adhesion to the endothelium and point out the importance of COX-1 in the tumour- or stroma-to-platelets signalling. Since COX-2 inhibition did not affect platelet aggregation, its effect on adhesion might be tumour-dependent.

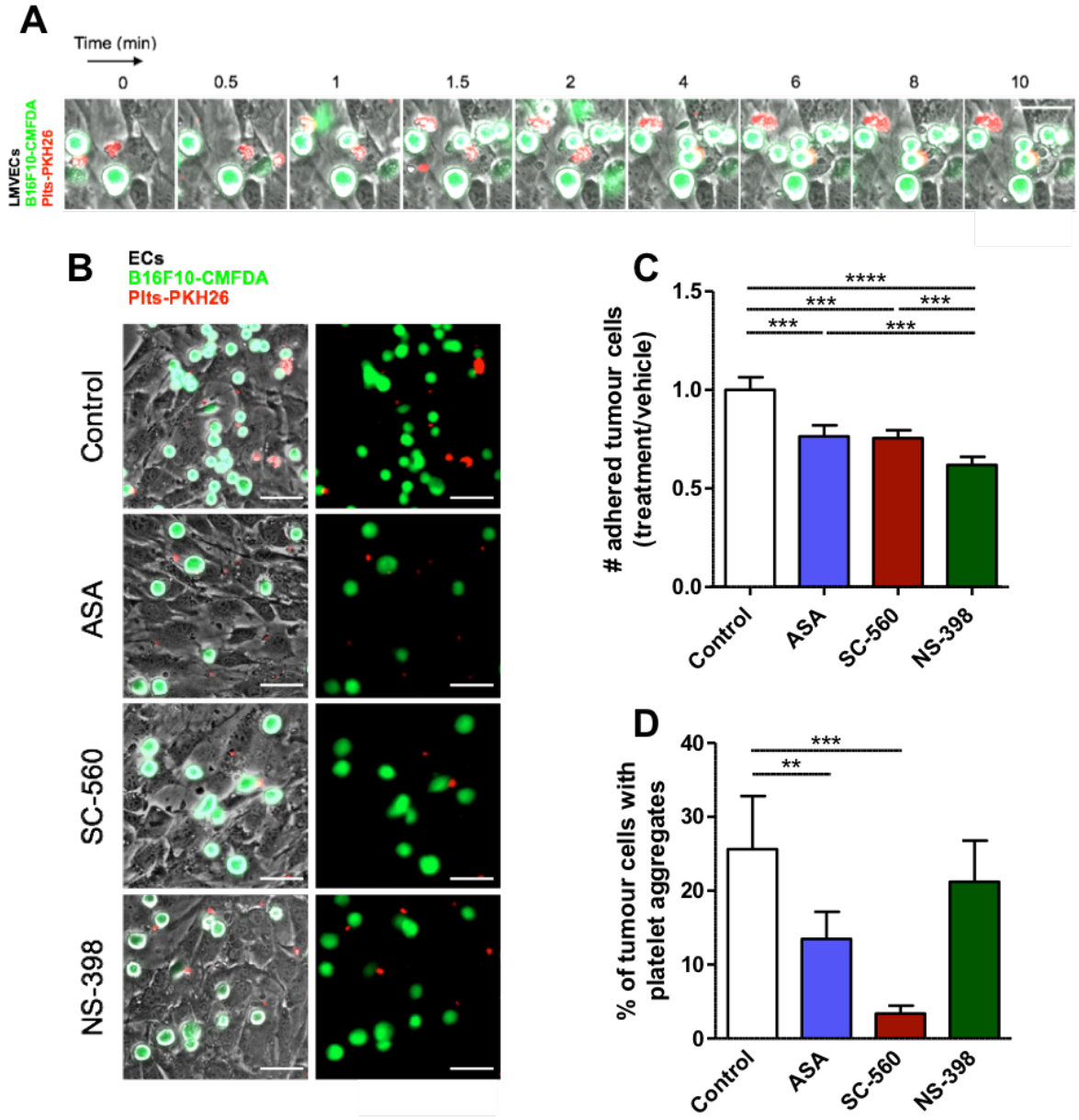

Figure 5.6 – COX-1 inhibition reduces the adhesion of tumour cells to the endothelium and decreases tumour cell-platelet interaction under shear stress.

(A) Selected still images of time-lapse microscopy analysis of tumour cells (B16F10-CMFDA, green) adhering to lung microvascular endothelial cells (LMVECs, DIC) in the presence of platelets (Plts-PKH26, red) under 0.05 dyn/cm^2 shear stress. The sequence shows the association of tumour cells to platelets and the adhesion to the endothelium. Scale bar represents 20 µm.

(B) Representative epifluorescence images (10x) of tumour cells, platelets and endothelial cells after 10 minutes of 0.05 dyn/cm^2 shear stress upon vehicle (Control), ASA, SC-560 or NS-398 pre-treatment. Scale bars represent 100 µm.

(C-D) Quantification of the relative number of adhered tumour cells, normalised to vehicle (C) (n= 4 independent experiments, 10 FOVs per repetition), and the percentage of tumour cells associated with platelets (D), calculated from epifluorescence images acquired after 10 minutes of 0.05 dyn/cm^2 shear stress. Tumour cells, platelets and endothelial cells were pre-treated with vehicle, ASA, SC-560 or NS-398 treatment (n=4 independent experiments, ≥4 FOVs per repetition).

All data are represented as mean ± SD, 1-way ANOVA with Tukey's Multiple Comparison test.

5.3.2.4 COX-1 inhibition affects transendothelial migration (TEM)

A high number of B16F10 cells arrest in the lung vasculature shortly after their introduction in the circulation or their passage over lung microvascular endothelial cells (Figure 5.6), either through physical trapping, direct contact or platelet-mediated adhesion. However, only few of those cells will form overt metastasis. Our previous data suggest that COX-1 inhibition might affect the early extravasation of tumour cells. In order to explore this hypothesis, we analysed the effect of COX inhibition on TEM of tumour cells in the presence of platelets through a surrogate assay. Briefly, labelled tumour cells (B16F10-CMFDA) and platelets (PKH26-Plts) were added to a monolayer of LMVECs and their intercalation within the monolayer was analysed in real time under static conditions. Upon intercalation, tumour cells change from a round shape to an elongated one, with the formation of invadopodia during intermediate stages (Figure 5.7A). Hence, tumour cells were scored as not intercalated (round-shaped), intercalating (round-shaped with protrusions) and intercalated (spindle-shaped) through the measurement of their ellipticity with Imaris software. We confirmed that numerical measurement corresponded to the visual classification (Supplementary figure S6). In order to address the contribution of COX-1 and COX-2, ASA, SC-560 and NS-398 were added to the medium shortly before the start of image acquisition. We saw that ASA and, to a lesser extent, SC-560 affected the efficiency of transmigration (Figure 5.7B). In particular, tumour cells initiated intercalation and extracalation (reverse transmigration) multiple times in the presence of ASA (see asterisks in Figure 5.7C), but few cells were able to permanently intercalate. In contrast, NS-398 did not affect the intercalation of tumour cells. These data suggest that COX-1, but not COX-2, contribute to the extravasation of tumour cells.

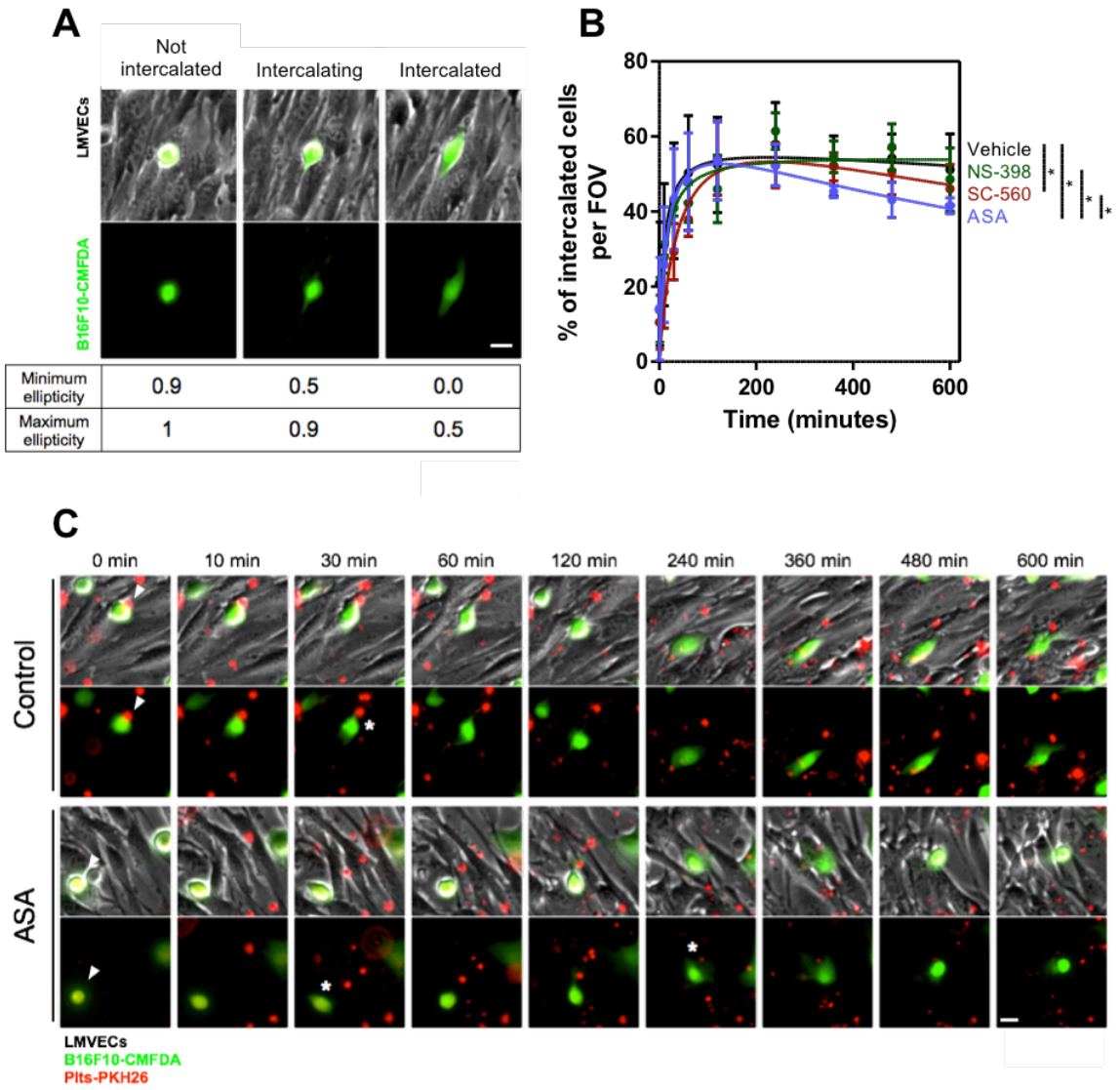

Figure 5.7 – COX-1 inhibition is associated with a reduced TEM efficiency.

(A) Representative epifluorescence images and ellipticity (oblate) quantification of tumour cells (B16F10-CMFDA, green) intercalation within an endothelial cells monolayer (LMVECs, DIC). Tumour cells were scored as not intercalated, intercalating or intercalated according to cell shape and ellipticity thresholds. Scale bar represents 20 µm.

(B) Percentage of intercalated tumour cells upon vehicle (Control), ASA, SC-560 and NS-398 treatment, monitored for 10 hours (n=3 independent experiments, ≥22 cells per FOV were analysed; mean ± SD, Nonlinear fit with extra sum-of-square F test).

(C) Selected still epifluorescence microscopy images (10x) of time-lapse microscopy analysis of tumour cells (B16F10-CMFDA, green) intercalating within a monolayer of LMVECs (DIC) in the presence of platelets (Plts-PKH26, red). The co-culture was treated with vehicle or ASA shortly before image acquisition. Arrows indicate the contact of tumour cells with platelets; asterisks indicate the start of intercalation. Scale bar represents 10 µm.

5.3.2.5 Platelets interaction with tumour cells contributes to TEM

We sought to further understand the mechanism through which COX-1 inhibition affected tumour cells extravasation. We have established that the aggregation of platelets on tumour cells is reduced by COX-1 inhibition (Figure 5.1 and 5.6D). We thus hypothesised that the reduction of tumour cell intercalation by ASA and SC-560 was a platelet-dependent mechanism. To test this hypothesis we used different approaches.

First, non-intercalated tumour cells travel for longer tracks and at higher speed than intercalated cells (Figure 5.8B, where cell 1 is not intercalated and cell 2 is intercalated). Thus the movements of tumour cells associated (at a distance ≤2 μm from adjacent platelets) or not associated (at a distance >2 μm from adjacent platelets) with platelets were tracked over time through an algorithm generated on Imaris software. We found that the speed (Figure 5.8B) and track length (Figure 5.8C) of tumour cell movement was significantly higher if they were not associated with platelets, suggesting that they were less likely to intercalate.

Second, we monitored the intercalation of tumour cells incubated with endothelial cells alone or in the presence of platelets. As depicted in Figure 5.8D, the absence of platelets reduced the efficiency of intercalation by affecting the percentage of intercalated cells and by inducing reverse transmigration of tumour cells. The effect of platelets depletion was more pronounced than the treatment of tumour cells, platelets and endothelial cells with ASA (Figure 5.7B).

To confirm a direct effect of platelet contact with tumour cells, we monitored the intercalation state (ellipticity) of tumour cells during or immediately after the interaction with platelets. We found that vehicle- and NS-398-treated tumour cells initiated intercalation 10 minutes after the interaction with one ore more platelets (Figure 5.8E and F). In contrast, platelet interaction with tumour cells did not induce any significant change of shape in the presence of ASA and SC-560, suggesting that the contact of tumour cells

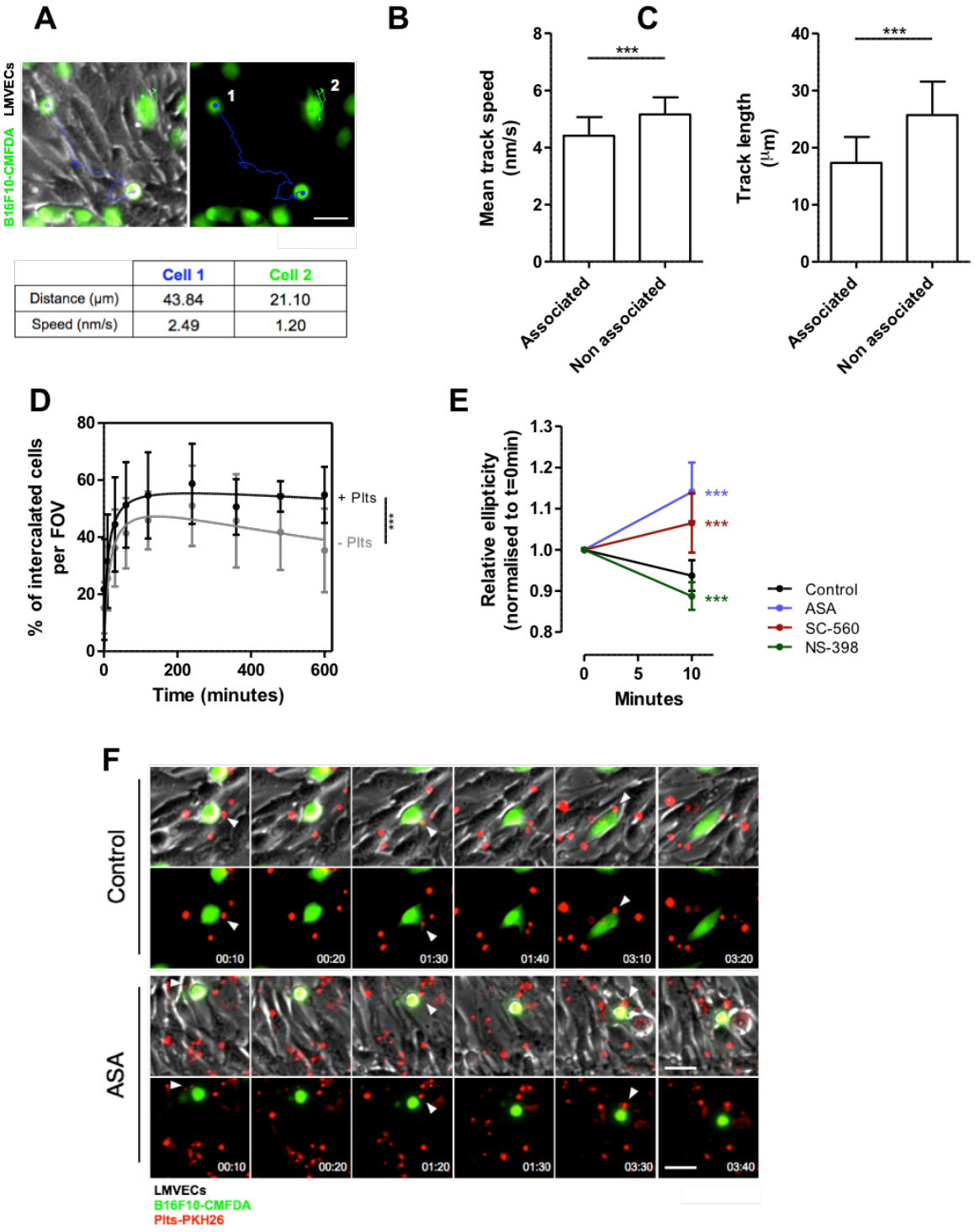

Figure 5.8 – The association of platelets with tumour cells supports tumour cell TEM.

(A) Representative epifluorescence images of tumour cells (B16F10-CMFDA, green) movement on endothelial cells (LMVECs, DIC) for an intercalated (green track) or non-intercalated (blue track) tumour cells. Distance and speed of tumour cell movement were analysed through ImageJ software (v1.46r). Scale bar represents 20 µm.

(B-C) Velocity (B) and distance (C) of tumour cell movement when associated or not associated with platelets (n=3 independent experiments, ≥150 cells per repetition were analysed; median ± IQR, Mann Whitney test).

(D) Percentage of intercalated tumour cells incubated with endothelial cells in the presence (+Plts) or absence (-Plts) of platelets, monitored for 10 hours (n=3 independent experiments, ≥150 cells per repetition were analysed; mean ± SD, Nonlinear fit with extra sum-of-square F test).

(E) Relative ellipticity (normalised to t=0) of tumour cells during (t=0 min) or after (t=10 min) contact with one or more platelets, calculated from epifluorescence images of time-lapse microscopy. Tumour cells, platelets and endothelial cells were co-cultured in the presence of vehicle (Control), ASA, SC-560 or NS-398 (n= 3 independent experiments, 10 cells per repetition were analysed; mean ± SD, unpaired t test).

(F) Selected still epifluorescence microscopy images (10x) of time-lapse microscopy analysis of tumour cells, endothelial cells, and platelets in co-culture treated with vehicle (Control) or ASA shortly before image acquisition. Arrows indicate the contact of tumour cells with platelets. Scale bars represent 20 µm.

with platelets is not sufficient to induce intercalation in the absence of COX-1 activity (Figure 5.8E and F).

All together, these data suggest that the interaction of platelets with tumour cells supports tumour cells transmigration. In particular, the presented results suggest a role of platelets as chaperones for the initiation of tumour cells intercalation in the endothelium, a function that is abrogated by COX-1 inhibition.

5.4 DISCUSSION

In the previous Chapter we have pinpointed the effect of aspirin and COX-1 inhibition on the intravascular phase of metastasis and in particular on the first day of the presence of tumour cells in the circulation. During their haematogenous transit tumour cells undergo a series of interrelated steps that lead to the colonisation of the secondary organ and are mainly associated with the vasculature, either adhered to the endothelium or extravasating.

In this Chapter we have attempted to analyse the effects of COX inhibitors on the early dissemination of tumour cells, with the aim of explaining the mechanism underlying metastasis inhibition by aspirin.

5.4.1 COX-1 activity in platelet is important for their aggregation on tumour cells

It is well established that tumour cells trigger the aggregation of platelets on their surface through several mechanisms (see section 1.1.2.3.2). This process is normally referred to as TCIPA (Tumour Cell-Induced Platelet Aggregation). Considering that the activity of COX-1 in platelets is essential for their aggregation (Figure 3.3 and 3.9), we have investigated the effects of COX inhibition on the interaction between tumour cells and platelets, both *in vivo* and *in vitro*. Our data indicate that the inhibition of COX-1, but not of COX-2, reduced TCIPA (Figure 5.1). As expected, thrombosis was not completely abrogated by COX-1 inhibition but tumour cells were surrounded with fewer aggregates of smaller size. In our model, the expression of TF, but not P-selectin ligand[267], is necessary for TCIPA initiation by B16F10 cells[26]. Moreover, the interaction between B16F10 cells and platelets can be abolished by hirudin, an inhibitor of thrombin activity[26,267]. Thus, the initial activation of platelets and interaction with B16F10 cells can be mediated by TF-dependent thrombin generation, which leads to the formation of fibrin clots on the surface of tumour cells. By inhibiting COX-1, ASA and SC-560 did not affect the initial interaction

of platelets with tumour cells but significantly reduced the TXA_2-driven thrombus growth. This confirms the role of *de novo* synthesised TXA_2 as second-wave agonist of platelet aggregation.

Alternatively, the protective effect of platelets towards tumour cells would motivate the fact that all tumour cells were surrounded by clots, even in the presence of anti-coagulant therapy. Since the ability of tumour cells to induce TCIPA is an adaptive mechanism enabling survival in the hostile circulatory microenvironment[113], it is possible that only tumour cells associated with platelets clots are able to persist, and be imaged, in the lungs. In this sense, the first line of metastasis inhibition by aspirin would be the reduction of tumour cells interaction with platelets. This observation is in agreement with our previous findings where the persistence of tumour cells in the lung vasculature was reduced by ASA and SC-560 by one day after injection (Figure 4.3). Thus, the decreased number of tumour cells would be partially due to the initial inhibition of platelet interaction with tumour cells through a COX-1 dependent mechanism.

Interestingly, the reduction of TCIPA was due to COX-1 inhibition in platelets, but not in tumour cells. Consistent with the reduction of metastasis in COX-$1^{-/-}$ mice, this observation suggests that the metastatic process is affected by COX-1 inhibition in the microenvironment. In particular, the effect of COX-1 in platelets seems to be a central hub in aspirin anti-metastatic effect. In the future, the analysis of tumour cell-platelets interaction in COX-$1^{-/-}$ mice or in mice where platelets have been selectively targeted with COX-1 inhibitors will help to clarify the contribution of platelet COX-1 to metastasis.

5.4.2 Adhesion to the endothelium

Another possible reason for the reduced presence of tumour cells in the lungs at early time points could be the impairment of tumour cells adhesion to the endothelium. Here,

we have tested this hypothesis and found that COX-1 inhibition affects tumour cells adhesion through multiple mechanisms.

First, inhibition of COX-1 decreases vasoconstriction (Figure 5.4). This effect is likely due to the reduced levels of TXA_2 in ASA and SC-560-treated mice, whereby TXA_2 signals to vascular smooth muscle cell and induces their contraction. Taking into account that the percentage of capillary-sized vessels in the lungs is reduced by 50% by COX-1 inhibition, the chances of tumour cells getting physically entrapped are diminished. Also, the inhibition of platelet aggregation on tumour cells upon COX-1 inhibition may decrease the entrapment in the lung capillaries.

Nevertheless, lungs are one of the organs where melanoma tumour cells preferentially home in mice, suggesting that specific receptor-ligands interactions contribute to the adhesion process. We have gathered some evidence that COX-1 inhibition impairs endothelial activation by reducing the expression of the adhesion molecules VCAM-1 in vessels adjacent to tumour cells (Figure 5.5). Previous studies have indicated that the abrogation of endothelial activation reduces the establishment of metastasis by affecting both tumour cell adhesion and later progression of the nodule[146]. Indeed, melanoma cells express VLA-4, the ligand for VCAM-1, and can firmly adhere to activated endothelium[557]. Additionally, VLA-4-VCAM-1 activates an “outside-in” signalling cascade in endothelial cells that induces endothelial cell retraction[558] and MMPs secretion[559], thus allowing tumour cell TEM. Thus, COX-1 inhibition can affect metastasis in part through the inhibition of endothelial activation.

The mechanisms driving the induction of endothelial cell activation are not completely understood. It has been previously shown that endothelial cells are activated by clots on the surface of tumour cells and the use of the thrombin-inhibitor hirudin decreases tumour cell-induced endothelial activation[119,146]. By reducing the number and size of platelet clots on tumour cells, ASA and SC-560 might affect endothelial activation through an anti-

thrombotic effect. Additionally, the reduced size of clots on tumour cells could explain the lower expression levels of VCAM-1 in vessels associated with tumour cells upon ASA treatment and could also account for a reduced adhesion of tumour cells to the endothelium.

In order to further clarify which mechanisms underlie the contribution of COX-1 to tumour cells adhesion *in vivo*, we have started to investigate the effect of COX inhibitors on an *in vitro* microfluidic model, where tumour cells and platelets were placed under flow on a monolayer of endothelial cells under physiological shear stress. By using this approach we were able to show that the adhesion of tumour cells to microvascular endothelial cells was affected by COX-1 and COX-2 inhibition, although we hypothesise that this depends on different mechanisms.

On the one hand, COX-2 inhibition did not affect platelet aggregation on tumour cells and might affect adhesion by targeting primarily tumour cells. Previous evidence show that COX-2-derived PGE_2 induces VEGF expression[560], which promotes tumour cell adhesion to the vasculature[561]. Nevertheless, we did not detect any *in vivo* effect of NS-398 on the early permanence of tumour cells in the lung vasculature, suggesting that the effect on tumour cells adhesion might only be evident *in vitro* where tumour cells are more directly exposed to the drug.

On the other hand, the inhibition of COX-1 reduced the adhesion of tumour cells to the microvasculature and, concomitantly, decreased the association of tumour cells with platelets (Figure 5.6C and D), compatible with the inhibition of TXA_2 signalling. Platelets form adhesive bridges for the adhesion of tumour cells to the vasculature[547], providing evidence that the effect of COX-1 on adhesion might be platelet-mediated.

It is worth noticing that the effect of COX inhibition on tumour cell adhesion is not very pronounced, suggesting that it might only be a minor component to the anti-metastatic effect of aspirin. Consistent with this observation, previous *in vivo* studies have shown that

the absence of platelets did not decrease the initial adhesion of tumour cells, but it affected the establishment of metastatic lung nodules at later time points[103]. Accordingly, in our microfluidic model the immobilisation of tumour cells to the endothelium happened quickly, with no evident rolling (similar to the *in vivo* behaviour[151]), and the majority of adhered tumour cells were not associated with platelets (Figure 5.6). These observations suggest that the adhesion can take place through direct interaction of tumour cells with the endothelium mediated by adhesion molecules and cognate ligands that are expressed beforehand by tumour and endothelial cells. For instance, VCAM-1/ICAM-1 on endothelial cells can interact with $\alpha_4ß_1/\alpha_Lß_2$ integrins on tumour cells[147,148]. Also, TF-expressing tumour cells can form direct and stable interactions by binding TFPI on endothelial cells[562]. The establishment of direct receptor-ligands interactions could explain why a higher shear stress did not disrupt the adhesion of tumour cells on the endothelium (Supplementary figure S5).

All together these evidences suggest that COX-1, *in vivo* and *in vitro*, and COX-2, only *in vitro*, can reduce tumour cell arrest in the lung microvasculature. To our knowledge, this is the first evidence directly linking COX-1 to the inhibition of tumour cell immobilisation. The inhibition of TXA_2 signalling by/to platelets and endothelial cells seems to be the most plausible underlying mechanism, due to its effect on tumour cell-platelet interaction and endothelial activation. This hypothesis will be discussed in Chapter 6.

5.4.3 Recruitment of monocytes/macrophages

Monocytes/macrophages are recruited to platelet aggregates on tumour cells arrested in the lung vasculature and promote their survival and progression into metastatic nodules[26]. We have hypothesized that one of the possible mechanisms through which aspirin inhibits metastasis is through the reduction of myeloid cells recruitment to tumour cells. The data here presented showed that the pharmacological treatment with COX-1 inhibitors affected

the efficiency of monocytes/macrophages recruitment to tumour cells by reducing the number of immune cells per cluster (measured as cluster size in Figure 5.3D). Previously, Gil-Bernabé et al.[26] found a similar effect in CD11b-DTR model, where the formation of smaller clusters was sufficient to reduce the survival and metastatic capacity of tumour cells. It follows that although COX-1 inhibition did not abrogate the recruitment of monocytes/macrophages to tumour cells, the reduction of the cluster size would be sufficient to reduce metastasis.

Interestingly, the size of the cluster positively correlated with the size of platelets clot (Figure 5.3E), suggesting that the extent of monocytes/macrophages recruitment depends on the efficiency of platelet aggregation on the surface of tumour cells. In particular, the initial interaction of platelets with B16F10 cells, which is mainly driven by a TF-dependent mechanism, was not reduced by ASA and SC-560 and could allow a limited recruitment of monocytes/macrophages. Instead, the expansion phase of thrombus growth was reduced by COX-1 inhibition thus affecting the number of myeloid cells in the cluster. The correlation between clot size and macrophage recruitment could be due to different but interrelated mechanisms. On the one hand, activated platelets can directly recruit monocytes/macrophages through the release of soluble factors contained in their granules[103,135,186,187], a mechanism employed to attract immune cells to the site of vascular lesion or inflammation. On the other hand, Laubli et al.[119] have shown that tumour cells associated with platelets and leukocytes induce the release of CCL5 by endothelial cells, which in turn recruits pro-metastatic monocytes. Finally, monocytes express VLA-4[141], the endogenous VCAM-1 ligand. Thus, the induction of endothelial activation by clots on the surface of tumour cells might contribute to the arrest of monocytes/macrophages in the proximity of tumour cells.

Collectively, these observations suggest that clots on the surface of tumour cells promote the recruitment of monocytes/macrophages through multiple mechanisms, both direct (release of chemoattractants by platelets) or indirect (endothelial activation and release of

chemokines). Thus, the effect of ASA and SC-560 on monocytes/macrophages recruitment could depend on both the decrease of the critical mass of platelet clots and the subsequent reduction of endothelial activation. Besides the role of thrombosis, in the next Chapter we will discuss the possible effect of TXA_2 signalling in the recruitment of monocytes/macrophages.

5.4.4 Transendothelial migration

Our previous data suggested that around 30% of total tumour cells in the lungs have started extravasating at one day after the injection, suggesting the TEM process starts early after the entry of tumour cells in the circulation. Considering that treatment with ASA and SC-560 during these early time points reduces metastasis, we have decided to test the effect of COX inhibition on TEM. The study of TEM *in vivo* through intravital microscopy can be very challenging, especially due to the short time window of its manifestation. As a starting point, we have chosen an *in vitro* surrogate model based on the ability of tumour cells to intercalate within a monolayer of endothelial cells. Although this model has some limitations, such as recapitulating TEM under static conditions and the lack of an extravascular space, it has previously shown a good correlation with the metastatic success of tumour cells *in vivo*[215,494].

We found that the inhibition of COX-1 led to a less efficient tumour cell intercalation within the endothelial monolayer (Figure 5.7). In fact, upon ASA and, to a lesser extent, SC-560 treatment tumour cells underwent repeated attempts to intercalate, followed by reverse transmigration, but only few cells remained intercalated for the whole experiment. Although COX-1 could affect TEM through alternative mechanisms, here we have taken in consideration the effects of COX-1-dependent inhibition of platelet aggregation on TEM.

We have shown that tumour cells bound to platelets are more prone to undergo intercalation and the presence of platelets in the system enhances tumour cell

intercalation (Figure 5.8). Interestingly, the initial contact of tumour cells with platelets induced an immediate shape change towards a more invasive phenotype in the presence of functional COX-1 (Figure 5.8E and F). These results are in agreement with previous reports suggesting that the direct contact of tumour cells with platelets promotes tumour cell extravasation and metastasis. In particular, Labelle et al.[18] have shown that the activation of NF-κB pathway in tumour cells exposed to platelet interaction, which in turn induces EMT and the adoption of an invasive phenotype.

Nevertheless, we have gathered some preliminary evidence that tumour cell-platelet contact alone is not sufficient for TEM. In fact, platelet interaction with tumour cells upon COX-1 inhibition did not induce the initiation of TEM (Figure 5.8E and F). These observations suggest that COX-1 activity is required for platelet-induced TEM, indicating that COX-1-derived soluble factors, additionally to physical contact, prime tumour cells for extravasation. Although other platelet-derived soluble factors have been found to stimulate a pro-invasive phenotype[18], this is the first report of the contribution of COX-1 products in priming tumour cells for extravasation. All together, the combination of fewer interactions between tumour cells and platelets and the inhibition of COX-1 derived soluble mediators can account for the inhibitory effect of COX-1 inhibition on TEM.

Our system did not allow the discrimination of the source of COX-1 metabolites responsible for TEM induction. In future plans, the use of COX-$1^{-/-}$ depleted platelets or the independent treatment of tumour cells, platelets and endothelial cells with COX inhibitors will greatly help to determine the role of COX-1 in the intercalation process.

5.4.5 Conclusions

In this Chapter we have shown the effect of pharmacological inhibition of COX on some steps of the haematogenous transit of tumour cells. It appears that the inhibition of COX-1 activity decreases the aggregation of platelets on tumour cells, which *per se* is sufficient to

impair metastasis[18,26,103,146,243-249]. Nevertheless, it also affects multiple consequent steps in the metastatic cascade (see section 1.1.3.1). Here we have identified the contribution of COX-1 to endothelial cell activation, adhesion of tumour cells to the endothelium, recruitment of monocytes/macrophages and TEM, all steps involved in the initial metastatic seeding. So far, it appears that these processes are affected by the reduced aggregation of platelets on tumour cells. Next Chapter will focus on understanding the source and contribution of COX-1-derived TXA_2 in our model and the effect of TXA_2 inhibition on metastasis.

CHAPTER 6

The inhibition of TXA_2 generation by platelets is responsible for the anti-metastatic effect of aspirin

6.1 INTRODUCTION

Together, the data collected so far highlight a pivotal role of the COX-1 isoform during the haematogenous transit of tumour cells. Cells in the vascular or peri-vascular niche can synthesise and/or respond to several prostanoids in both a paracrine and autocrine manner. In general, prostanoids have a very short half-life, so they act at very short distances. The main COX-1-derived prostanoids associated with the vascular system are thromboxane A_2 and prostacyclin (PGI_2). Additionally, under pro-inflammatory conditions, the synthesis of COX-2 derived PGE_2 may be induced in immune cells and endothelial cells. Considering the contribution of platelets in the metastatic niche in our system, we have focused on the signalling pathway of TXA_2 in the context of tumour metastasis.

6.1.1 TXA_2 signalling during haematogenous metastasis

Several cell types can be responsible for TXA_2 generation. Activated platelets are the main site of TXA_2 production, both in the circulation and systemically, although monocytes/macrophages, endothelial cells and vascular/bronchial smooth muscle cells can also release TXA_2. Therefore, highly vascularised tissues such as lungs, kidney and heart show a high expression of proteins involved in TXA_2 metabolism[563].

TXA_2 is a very potent agonist of platelet activation and its synthesis is tightly regulated physiologically to avoid excessive thrombosis and vasoconstriction, conditions associated with stroke and myocardial infarction. In this sense its short half-life in the circulation is an auto-regulatory mechanism to limit its range of action to the site of injury[564]. However, TXA_2 metabolism and signalling is often imbalanced in pathological conditions such as

atherosclerosis, arthritis, asthma and cancer. TXAS has been found overexpressed in a series of cancer cell lines and cancer samples in comparison to adjacent normal tissues[565-571], which results in higher TXA_2 concentration in tissue samples[567,569,572-575]. TXAS expression is a prognostic marker of reduced survival, invasion[566,570,571] and metastasis[576]. Additionally, platelet aggregates on tumour cells contribute to the generation of TXA_2, even in the absence of TXAS/COX-1 expression by tumour cells.

Many cells in the vascular niche express TP receptor, suggesting that TXA_2 signalling might go well beyond the activation of platelet aggregation. Indeed, recent evidence suggests that TXA_2 is an orchestrator of physiological responses to vascular damage and might be involved in metastatic seeding.

6.1.1.1 TXA_2 signalling on platelets

Historically, the signalling of TXA_2 in platelets is the best-characterised downstream cascade of TXA_2. Platelets express high levels of TP, both the TPß and (preferentially, in humans) TPα isoform. The interaction TXA_2:TP leads to various cellular responses on the basis of the G proteins activated by receptor agonism (Figure 6.1).

The activation of G_q proteins leads to the release of Ca^{2+} and the activation of PKC and PI3K, leading to granule secretion, activation of integrin $\alpha_{IIb}ß_3$ and change of shape with the production of pseudopodia[564,577-579]. Additionally, the increase of intracellular Ca^{2+} activates PLA_2 to release AA, leading to the *de novo* synthesis of more TXA_2 and the further expansion of the thrombus[564,580]. On the other hand, the activation of $G_{12/13}$ leads to the activation of RhoA GTPase[581] and ROCK[564] and following phosphorylation of myosin light

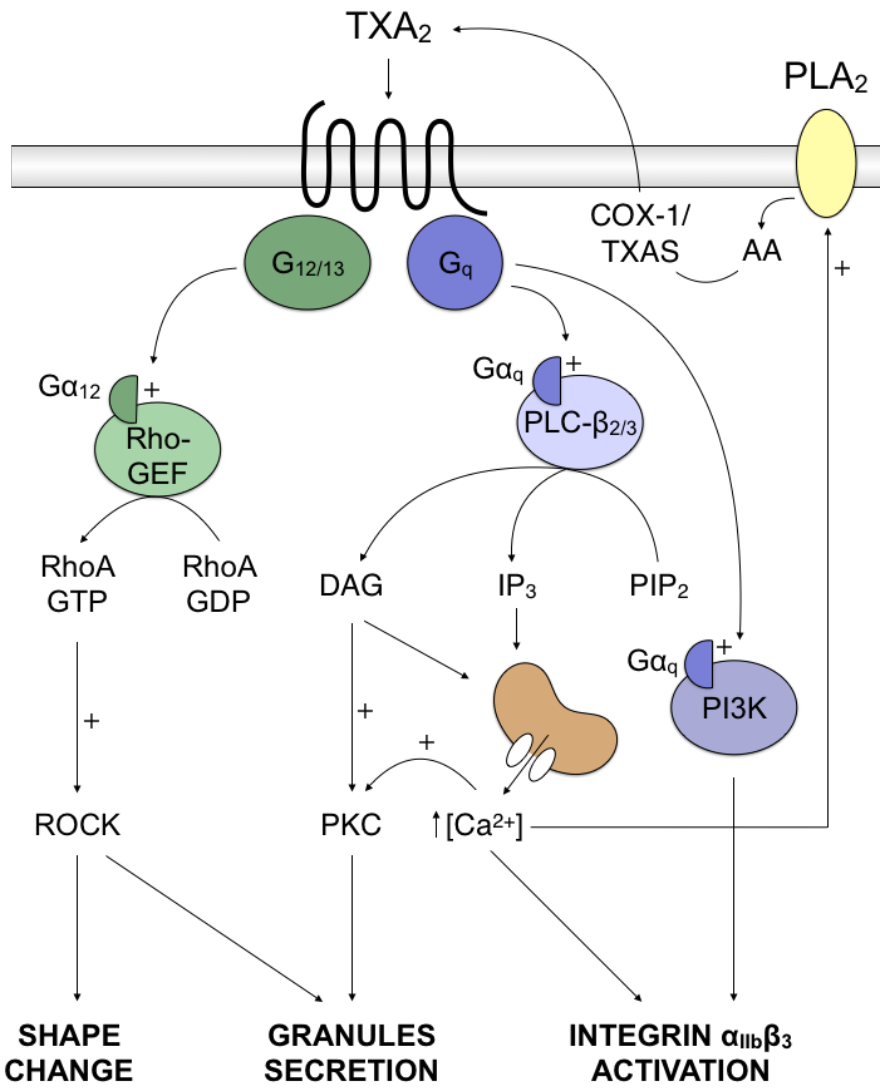

Figure 6.1 – TXA_2 signalling cascade in platelets.

Diagram depicting the intracellular signalling cascade downstream to TXA_2:TP interaction on the membrane of platelets. TP is a 7-transmembrane G-protein coupled receptor and activates $G_{12/13}$ and G_q. Upon TXA_2 agonism, G_q dissociates and releases $G\alpha_q$, which activates PLC-$\beta_{2/3}$, which hydrolyses membrane PIP_2 into DAG and IP_3. Both DAG and IP_3 induce the increase of intracellular Ca^{2+}, a central event that mediates the inside-out activation of $\alpha_{IIb}\beta_3$ integrin to its high affinity state and platelet degranulation. Additionally, DAG induces granules secretion through the activation of PKC. The mobilisation of intracellular Ca^{2+} activates membrane PLA_2 to release AA, which is then converted into TXA_2 by the coupled activity of COX-1 and TXAS. Concomitantly, the release of $G\alpha_{12}$ from $G_{12/13}$ dissociation induces Rho-GEF to exchange GDP to GTP bound to RhoA. In this activated state, RhoA-GTP activates ROCK, which phosphorylates (and inhibits) myosin light chain phosphatase and thus enhances the phosphorylation of myosin light chain (MLC), leading to the change of shape and degranulation of the platelet. [582,583]

AA= arachidonic acid; COX-1= cyclooxygenase-1; DAG= diacylglycerol; IP_3= inositol 1,4,5-triphosphate; PI3K= phosphoinositide 3-kinase; PIP_2= phosphatidylinositol 4,5-bisphosphate; PKC= protein kinase C; PLA_2= phospholipase 2; Rho-GEF= Rho guanine nucleotide exchange factor; ROCK= Rho-associated protein kinase; TXA_2= thromboxane A_2; TP= TXA_2 receptor; TXAS= thromboxane synthase.

chain (MLC), inducing the change of shape and the release of granules. The existence of such pathway explains why TXA_2 signalling can trigger shape remodelling independently to the increase of cytosolic Ca^{2+}[100]. In most cases, the G_q- and $G_{12/13}$-dependent signalling pathways are linked to specific platelet activation events, where G_q activation mediates TXA_2-induced platelet activation and $G_{12/13}$ mediates platelet change of shape[584,585]. However, these signalling pathways can trigger overlapping cell responses in some situations such as agonist concentration[586,587] or G-protein deficiency[588], so the linkage between TP-G coupling and the downstream platelet activation events is not univocal. In general, the integrated activation of both G_q and $G_{12/13}$ is needed to achieve the complete activation of platelets.

6.1.1.2 TXA_2 signalling on vascular cells

TXA_2 signals both to endothelial cells and vascular smooth muscle cells.

Endothelial cells express TP, preferentially TPß in humans. TXA_2:TP signalling on endothelial cells induces the overexpression of adhesion molecules like ICAM-1[589-593], VCAM-1[591,592] and endothelial leukocyte adhesion molecule (ELAM-1)[590], through a PKC-, NF-κB- or ROCK-dependent mechanism[592], E-selectin[591], leukocyte adhesion molecule (LAM)[591] and TF[594]. TXA_2 also increases the release of soluble chemokines, such as MCP-1/CCL2, TNF-α and platelet-activating factors (PAF)[595,596]. Thus, TXA_2-driven endothelial activation induces the recruitment and adhesion of platelets (through TF and PAF), monocytes (through adhesion molecules, MCP-1 and TNF-α)[593], and, putatively, cancer cells (through VCAM-1 and ICAM-1)[146]. In this scenario, TXA_2 is both a pro-thrombotic and pro-inflammatory factor and might play a role in tumour metastasis.

Additionally, TXA_2 signalling promotes migration[597,598] and proliferation[598] of endothelial cells *in vitro* and permeabilisation[599] and neovascularisation[597,600] *in vivo*, which could lead to tumour cell extravasation and angiogenesis. Interestingly, VEGF- and FGF2-driven

angiogenesis[598] and TNF-α stimulation[594] increase the production of TXA_2 by endothelial cells, triggering a positive feeback loop of autocrine endothelial cells activation. On the contrary, activated platelets induce the overexpression of COX-2 in endothelial cells both through a direct TXA_2-mediated signalling[592,601,602], a ROCK and NF-κB-dependent mechanism[592], and through the release of AA-containing microparticles[603]. It is believed that in both cases this stimulation results in the generation of PGI_2 by endothelial cells, which in turns inhibit platelet aggregation. Thus, platelets and endothelial cells take part into a dynamic interplay, aimed at controlling the thrombotic response.

Vascular smooth muscle cells show high expression levels of TP, whose interaction with TXA_2 triggers their proliferation[555], contraction and subsequent vasoconstriction. This latter effect is due to the increase of intracellular Ca^{2+}, which leads to the activation of Ca^{2+}-dependent myosin light chain kinase (MLCK), the phosphorylation of myosin light chains and the contraction of the muscular cells[583,604].

6.1.1.3 TXA_2 signalling on monocytes

TXA_2 is the main prostanoid produced by unstimulated monocytes[346,347,605] and it derives from their constitutive COX-1 activity. However, during inflammatory responses or interaction with platelets[606], COX-2 expression is induced in monocytes by stimulation with LPS[607] or platelet derived TGF-ß1[606]. In these circumstances, COX-2 contributes to the synthesis of additional TXA_2[606,608]. Interestingly, LPS, TGF-ß1 and TXA_2 take part into a self-potentiating loop where LPS and TXA_2 induce overexpression of TF[608], thus increasing platelet aggregation, TGF-ß1 release and COX-2-dependent TXA_2 generation by monocytes, which further potentiates TF expression.

Human monocytes express TP receptor[609] and the expression of TP (along with COX-1) increases during the differentiation to macrophages[607]. This suggests that COX-1-TXA_2 axis acquires more importance during inflammatory responses. Although the molecular

mechanisms have not been fully elucidated, TXA_2:TP interactions induces an elevation of intracellular Ca^{2+}, which is associated with phagocytic and chemotactic functions[609]. Moreover, TXA_2 stimulation of monocytes results in the overexpression of TF[608], which increases their direct procoagulant acitivity[346].

More indirectly, the TXA_2-dependent release of MCP-1/CCL2 by endothelial cells induces the recruitment of monocytes/macrophages and the concomitant endothelial activation, which promotes monocytes adhesion. All together, even if TXA_2 acts at short distances, it might affect the recruitment of monocytes circulating systemically, by targeting multiple cell types to produce secondary messengers. This evidence reinforces the idea that TXA_2 is not only a pro-aggregant molecule, but it also takes a central part in orchestrating pro-inflammatory and wound healing responses.

6.1.1.4 TXA_2 signalling on tumour cells

Several types of tumour samples[565,566,571,610,611] and cell lines[612,613] express higher levels of TP receptor, suggesting the existence of a selective advantage of TXA_2 signalling. In most cases, tumour cells express both high levels of TXAS and TP, suggesting that they sense TXA_2 in an autocrine manner. Interestingly, in the case of breast cancer TXAS and TP are expressed in different regions of the tumour tissue, suggesting that tumour cells can benefit from TXA_2 produced by platelets or other stroma cells in a paracrine manner[614].

Although the mechanisms are not completely understood, it is believed that TXA_2 signalling on tumour cells increases tumorigenicity and invasion. TXAS or TP overexpression is associated with higher motility[570,572], proliferation[615] and invasiveness[572,615,616]. More directly, the treatment of tumour cells with TXA_2 stable analogues increases proliferation[565,566,617,618], and treatment with TXAS inhibitor or TP antagonists decreases cell proliferation[565,566,615] and migration[566,570,574,575,615,616].

The effect on tumour cells proliferation is due to several mechanisms. In lung cancer cells, TXA_2 signalling induces the expression of Nurr1, which in turn stimulates the expression of cyclin D1 and the progression through cell cycle[618], and inhibits apoptosis through a p27-dependent mechanism[619]. Additionally, TXA_2 induces the overexpression of COX-2 in tumour cells[620], which is known to promote tumour cells proliferation.

In most cancer types, TXA_2 induces invasion through a RhoA-dependent mechanism. Briefly, TXA_2:TP binding activates protein-kinase C-related kinase (PRK1)[621] and Gα12 heterotrimeric G protein[622], leading to the activation of RhoA[574,613] and the consequent cytoskeleton reorganisation that enhances migration and metastasis.

In vivo, colon adenocarcinoma cells overexpressing TXAS[623] or TP[612] formed tumours that grew more rapidly and were more vascularised, due to the overexpression VEGF by tumour cells stimulated with TXA_2[612]. Moreover, TXA_2 released by tumour cells can directly stimulate angiogenesis *in vivo*[597,623]. Thus, the pro-tumorigenic effect of TXA_2 signalling does not only depend on the direct stimulation of tumour cell behaviour, but also to effects on the surrounding environment. The involvement of TXA_2 in tumour cells invasion could explain the anti-metastatic effect of TXAS[598,624] inhibitors and $TP^{-/-}$ mice[625].

6.1.2 Inhibitors of TXA_2 pathway

Due to its effect in the cardiovascular and respiratory system, unbalanced TXA_2 levels have been found associated with a series of pathological conditions[563], including cancer. Although low-dose aspirin is sufficient to abrogate COX-1-dependent generation of TXA_2 by platelets[626], it might results in the inhibition of other prostanoids associated with gastro-protective functions and is thus associated with gastrointestinal complications. This is why aspirin might not be the best choice to selectively control TXA_2 synthesis. Over the past 30 years efforts have been made to develop inhibitors that target TXA_2 synthesis (TXAS inhibitors) or signalling (TP antagonism).

Selective inhibitors of TXAS are the oldest class of TXA_2 inhibitors, having been developed in the 80s. The efficacy of TXAS inhibitors does not only rely on the inhibition of TXA_2 synthesis, but also on increased levels of precursors PGG_2 and PGH_2. These precursors can be actively transferred from platelets to endothelial cells at sites of interaction (a process known as endoperoxide rediversion or "steal")[627,628], which induces the synthesis of anti-thrombotic PGI_2 by endothelial cells[629]. However, PGG_2 and PGH_2 are also agonists of TP and can induce platelet aggregation, which might reduce the efficacy of TXAS inhibitors on TXA_2 signalling[629,630]. Despite efficacy in blocking platelet activation, most TXAS inhibitors have shown generally disappointing results brought to clinical trials[628].

The first and only TXAS inhibitor to be released on the market is Ozagrel (OKY-046), which has been proved effective in clinical trials for cardiovascular[631-634] and respiratory conditions[635,636]. Due to its efficacy, Ozagrel was introduced in the clinical practice for the prevention of asthma and stroke in Japan in 1992.

More clinical interest has been aroused by TP antagonist. These drugs bind (either reversibly or irreversibly) to the TP receptor on numerous cell types and prevent the interaction of all TP ligands such as TXB_2, PGG_2 and PGH_2[637]. This makes TP inhibitors more effective than TXAS inhibitors and aspirin. Despite these high expectations, very few TP antagonists are currently on the market because most of them have failed during clinical trials due to lack of benefit over aspirin[638].

The most recent and promising class of TXA_2 inhibitors is dual-acting drugs with both TXAS inhibitor and TP antagonist functions. Although some drugs have not shown more efficacy than aspirin[639], dual inhibitors still represent a promising alternative due to their stronger and more prolonged anti-thrombotic effect than aspirin and other NSAIDs[637,640].

In our experiments, we have employed the dual-action inhibitor Picotamide, which goes under the commercial name of Plactidil. Picotamide (Figure 5.1) is a derivative of 4-

hydroxy-isophthalic acid (N,N'bis(3-picolyl)-4-methoxy-isophthalamide)[641]. Its mechanism of action involves the inhibition of TXAS and the irreversible binding to TP, possibly followed by the internalisation of the bound receptor[642]. It has been reported that picotamide reduces AA-induced platelet aggregation and platelet TXA_2 synthesis[642,643] and interfered with smooth muscle cells migration and proliferation[644]. Picotamide has also been used in a series of clinical trials where it reduced cardiovascular complications[645] and mortality, more effectively than aspirin,[646] in peripheral vascular disease (PVD) patients, in particular in those with diabetes[646,647]. Due to its efficacy, picotamide is registered in Italy for the treatment of peripheral arterial disease (PAD)[637], although higher statistical power and sample size would be needed to introduce the drug for treatment of cardiovascular adverse events elsewhere[648].

All together, most TXA_2 inhibitors have failed to show evident benefit over aspirin in clinical trials or have been perceived to be too closely related in terms of pharmacological output, which has encouraged the preference of the inexpensive aspirin on more selective drugs. Nevertheless, lines of evidence would suggest the superiority of TXA_2 inhibitors over aspirin on the inhibition of TXA_2 generation. First, some TXA_2 inhibitors have a higher efficacy at inhibiting TXA_2 signalling and have shown a superior anti-thrombotic profile, in particular in high-risk groups[648]. Second, TXA_2 inhibitors affect both COX-1 and COX-2-derived TXA_2, an effect that is not achieved by low-doses of aspirin. Additionally, TXA_2 inhibitors with a TP antagonist activity prevent TP stimulation by all agonists, including PGG_2 and PGH_2 precursors and isoprostanes[648]. Finally TXA_2 inhibitors do not affect the synthesis of cardio- and gastro-protective PGI_2 and are thus associated with fewer out-of-target side effects, suggesting that they could represent a better choice than aspirin.

In conclusion, TXA_2 inhibitors have the potential to be introduced in the clinic for the prevention of vascular events due to the signalling of TXA_2 to both platelets and extraplatelets targets. In order to do so, clinical studies with higher statistical power are needed in order to evaluate effective dose, efficacy and side effects.

6.2 AIMS

In Chapter 5 we have isolated several sequential steps of the metastatic cascade that are affected by aspirin through COX-1 inhibition. It is well established that TXA_2 is the main COX-1 derived prostanoid in the circulation. In this Chapter we have started to dissect the molecular mechanism underlying the effect of COX-1 on metastasis by considering the contribution of TXA_2. In particular, our aims are:

1) To define the effect of TXA_2 inhibition on the establishment of metastasis.
2) To test the hypothesis that TXA_2 is the downstream effector of the anti-metastatic effect of aspirin.
3) To identify the source and the target of TXA_2 signalling in the context of haematogenous metastasis.

6.3 RESULTS

6.3.1 Effect of TXA_2 inhibition on metastasis

6.3.1.1 Dose-setting of TXA_2 inhibitors

The results described in Chapter 5 point out a central role of COX-1 during the haematogenous transit of tumour cells. Considering that TXA_2 is the main COX-1 derived prostanoid in the circulatory system, we started to investigate the contribution of TXA_2 to metastasis.

Picotamide (PICO, a dual inhibitor of TXAS and agonist of TP, Figure 6.2A) was delivered in drinking water at 30 mg/L, as previously shown[649]. At this dose the plasma levels of TXB_2 were significantly decreased by 70% (Figure 6.2B), suggesting an inhibition of TXAS activity in platelets and extra-platelets targets. Moreover, platelet aggregation was decreased by PICO, suggesting a reduction of TP signalling on platelets (Figure 6.2C). These data confirm that, at the chosen dose, PICO inhibited both TXAS activity and TXA_2:TP signalling.

In order to dissect the role of TXAS inhibition and TP agonism into more details, a more selective inhibitor was also employed. Ozagrel (OZA, Figure 6.2D) is a selective inhibitor of TXAS and was found to inhibit serum TXB_2 in a dose-dependent manner (Figure 6.2E), suggesting the inhibition of platelet TXAS. A dose of 400 mg/L was the minimum effective dose to trigger a substantial inhibition of TXAS activity, so it was chosen for functional experiments.

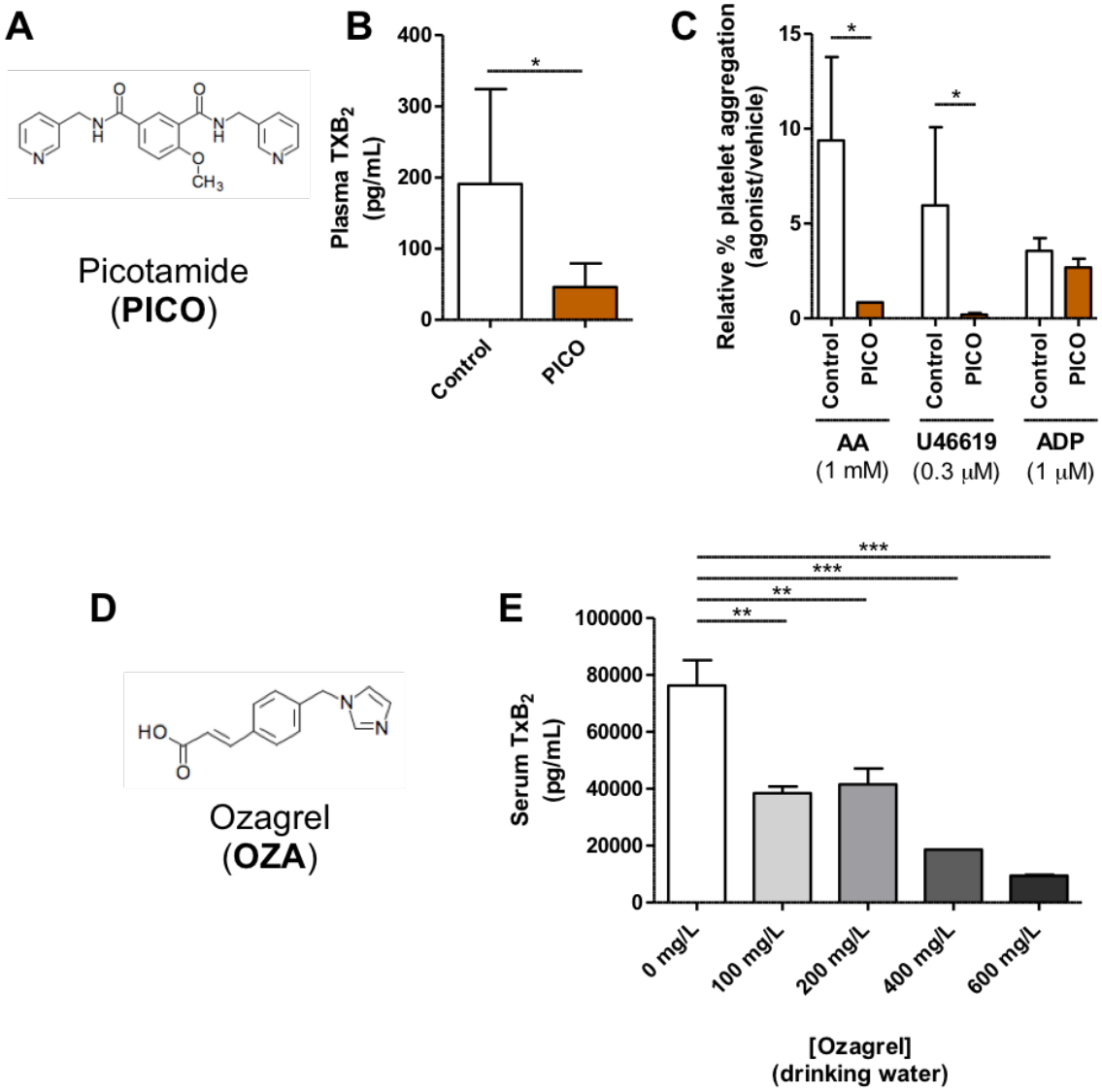

Figure 6.2 – Dose setting of TXA_2 inhibitors.

(A) Structure of Picotamide (abbreviated as PICO), adapted from KEGG Drug database.

(B) Concentration of TXB_2 in plasma from mice treated with vehicle (Control) or PICO for 48 hours (n=4 mice per group; mean + SD, unpaired t test).

(C) Quantification of agonist-induced platelet aggregation, measured through FACS analysis of CD41-stained platelets. AA (1 mM), U46619 (0.3 μM) and ADP (1 μM) were used as agonists (n=6 mice for Control and 4 mice for PICO; mean + SD, 1-way ANOVA with Tukey's Multiple Comparison test).

(D) Molecular structure of Ozagrel (abbreviated as OZA), adapted from KEGG Drug database.

(E) Concentration of TXB_2 in serum isolated from mice treated with vehicle (0 mg/L) or OZA (100-600 mg/L) for 48 hours (n=4 mice per group; mean ± SD, 1-way ANOVA with Tukey's Multiple Comparison test).

6.3.1.2 Inhibition of TXA_2 reduces experimental metastasis

To examine the role of TXA_2 in the establishment of metastasis, mice were treated with picotamide and challenged with tumour cells two days after the start of the treatment, as previously described (see Figure 3.5A). PICO significantly reduced the number of metastatic lung nodules (Figure 6.3A and B) to a similar extent to ASA and SC-560 (Figure 6.3C). This result strongly suggests an involvement of COX-1 derived TXA_2 in the aspirin-mediated inhibition of metastasis and further points out the importance of COX-1 in metastasis development.

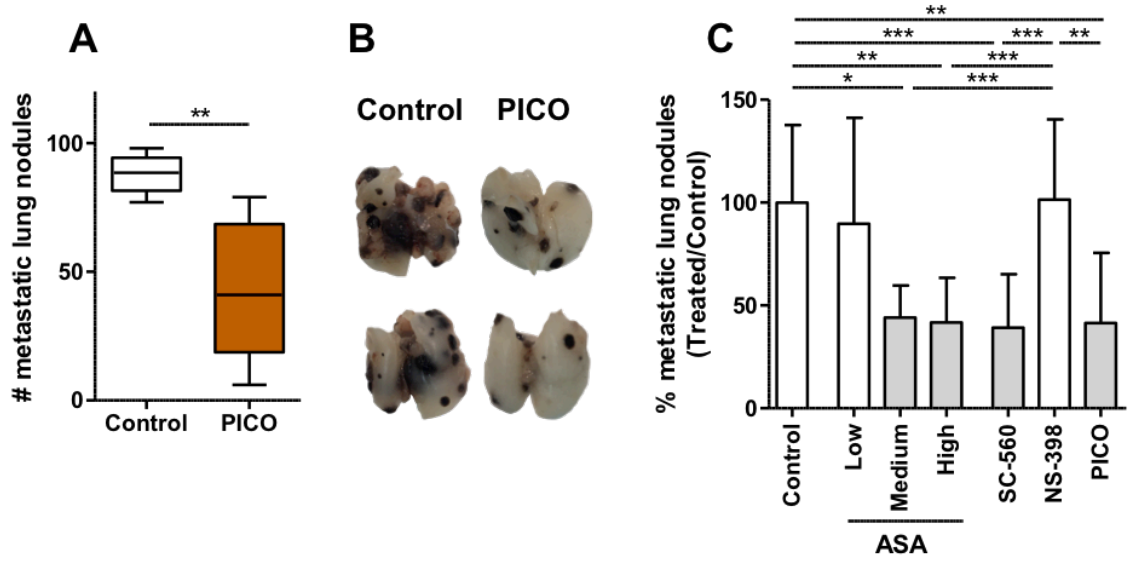

Figure 6.3 – The inhibition of TXA_2 signalling impairs the establishment of metastasis.

(A-B) Numbers (A) and representative images (B) of metastatic lung nodules at 3 weeks after intravenous injection of B16F10 cells in mice treated with vehicle (Control) or PICO (n=6 mice per group; median ± range, unpaired t test).

(C) Comparison of the number of metastatic lung nodules, normalised to the relative control, between all tested drugs (ASA, SC-560, NS-398 and PICO, data from Figure 3.5B, 3.8A and 6.3A; mean ± SD, 1-way ANOVA with Tukey's Multiple Comparison test).

6.3.1.3 TXA_2 inhibition reduces early phases of metastasis

We sought to understand the kinetics of TXA_2 inhibitors on the decrease of metastasis. The number of tumour cells in the left lung at 24 hour after injection was inhibited by OZA as well as by PICO (Figure 6.4A), suggesting an effect of TXA_2 signalling on the haematogenous transit of tumour cells. Consistent with its dual action, PICO was found to be more effective than OZA in reducing the retention of tumour cells, thus it was chosen for further experiments.

To corroborate the notion that TXA_2 was required for the intravascular phase of metastasis, mice were treated with PICO during the intravascular phase (PICO *-2→+1*), intravascular and extravasation phases (PICO *-2→+4*), extravasation phase (PICO *+1→+4*) or extravascular phase (PICO *+4→+21*) of metastasis. In all cases lungs were harvested at 3 weeks and the number of metastatic lung nodules was compared to mice treated for the whole experiment (PICO) (Figure 6.4B). A reduction in the number of metastatic lung nodules was seen at PICO, PICO *-2→+1* or PICO *-2→*+4 treatment regimes, but not at PICO *+1→+4* or PICO *+4→+21* (Figure 6.4C). These results support the idea that TXA_2 promotes metastasis at early steps of the metastatic cascade, in particular during the intravascular phase of tumour cells dissemination. Accordingly, TXA_2 inhibition did not exert any effect after the complete extravasation of tumour cells.

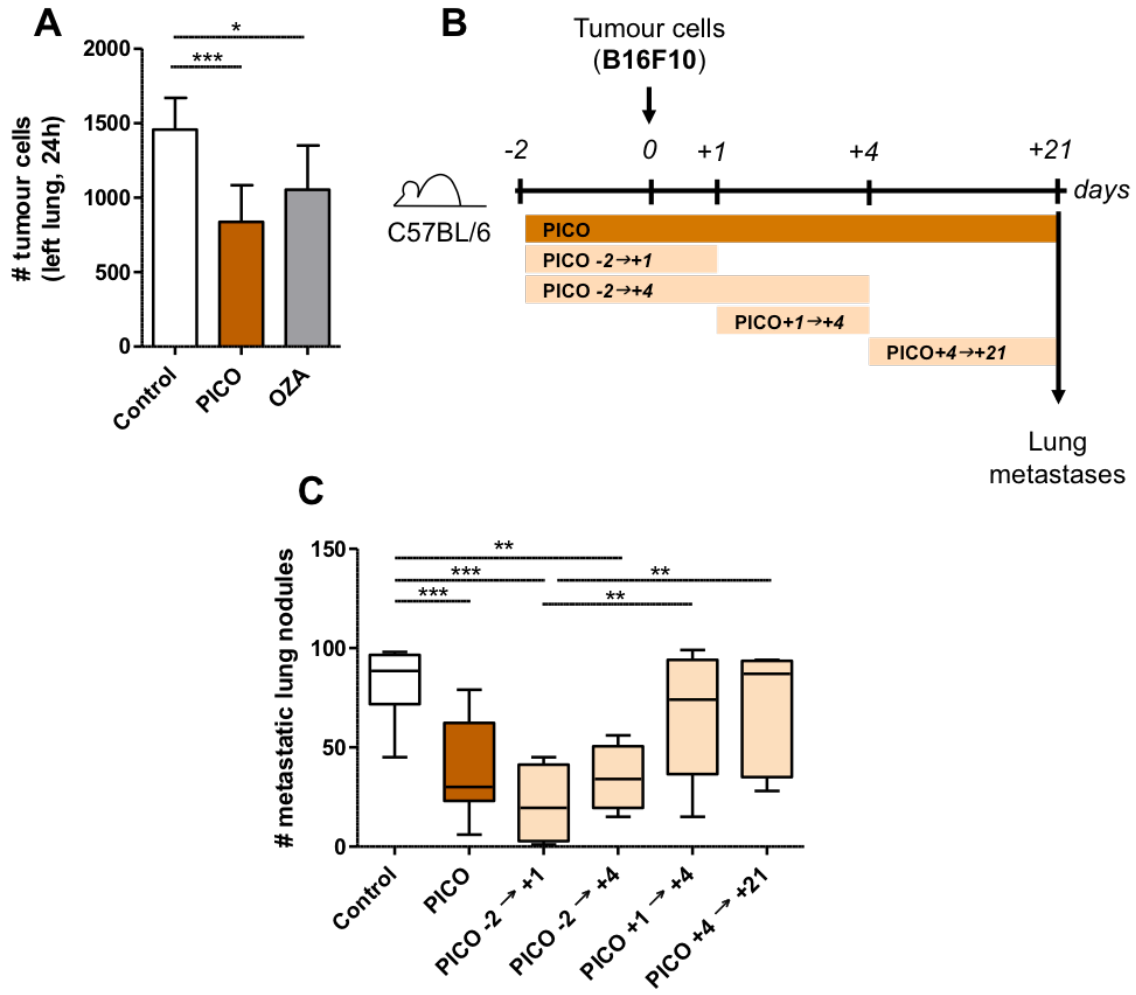

Figure 6.4 – The inhibition of TXA_2 signalling affects the intravascular phase of metastasis.

(A) Total number of tumour cells (B16F10-CMFDA) in the intact left lung of C57BL/6 mice treated with vehicle (Control), PICO or OZA (n=7, 8 and 7, respectively; mean + SD, 1-way ANOVA with Tukey's Multiple Comparison test), imaged at 24 hours after the injection of tumour cells.

(B) Experimental design to address the effect of PICO on different phases of metastasis. C57BL/6 mice were treated with vehicle or PICO starting 2 days before the intravenous injection of B16F10 cells (day -2). Treatment was carried out until 21 days after injection (PICO), until one day after injection (PICO *-2→+1*, intravascular phase), until 4 days after injection (PICO *-2→+4*, intravascular and extravasation phase), between 1 to 4 days after injection (PICO *+1→+4*, extravasation phase) or between 4 days until 21 days after injection (PICO *+4→+21*, extravascular phase). For all groups, lungs were harvested at 3 weeks after tumour cells injection.

(C) Number of metastatic lung nodules at 3 weeks after intravenous injection of B16F10 cells in mice treated with vehicle or PICO, according to the regimes described in (B) (n=10 mice for Control, 16 mice for PICO, 10 mice for PICO *-2→+1*, 5 mice for PICO *-2→+4*, 5 mice for PICO *+1→+4*, 5 mice for PICO *+4→+21*; median ± range, 1-way ANOVA with Tukey's Multiple Comparison test).

6.3.2 TXA_2 analogue U46619 abrogates the inhibition of metastasis by aspirin

We have shown that TXA_2 contributes to the successful establishment of metastasis during the intravascular/extravasation phase, leading to the hypothesis that the anti-metastatic effect of aspirin derives from the inhibition of COX-1 and its downstream effector TXA_2, in particular during early time points. In order to validate this hypothesis, we employed U46619, a stable analogue of TXA_2, at 50 mg/kg in combination with aspirin (ASA + U46619 group) to re-establish basal levels of plasmatic TXA_2 (Figure 6.5A) and platelet aggregation (Figure 6.5B) in ASA-treated mice. Next, mice were treated with vehicle (Control), ASA alone or ASA supplemented with U46619 for 3 weeks (ASA+U46619) or until one day after the intravenous injection of tumour cells (ASA+(U46619 *-2→+1*)) (Figure 6.5C). Noticeably, the addition of U46619 to ASA was able to restore the number of metastasis back to control values, irrespective of U46619 being delivered for the entire duration of the experiment or discontinued one day after tumour cell injection (Figure 6.5D). Since U46619 alone abrogated the anti-metastatic effect of ASA, these results suggest a central role of TXA_2 in the inhibition of metastasis by aspirin. Moreover, the presence of U46619 during the first 24 hours of metastasis was sufficient to abolish the inhibitory effect of aspirin, suggesting that TXA_2 preferentially acts during the permanence or early extravasation of tumour cells in the lung vasculature.

Taken together, these data more conclusively indicate that aspirin impairs metastasis through the inhibition of COX-1-derived TXA_2. In particular, the first 24 hours of metastasis are affected the most by ASA treatment, an effect that is completely abrogated by the presence of basal levels of TXA_2 in plasma.

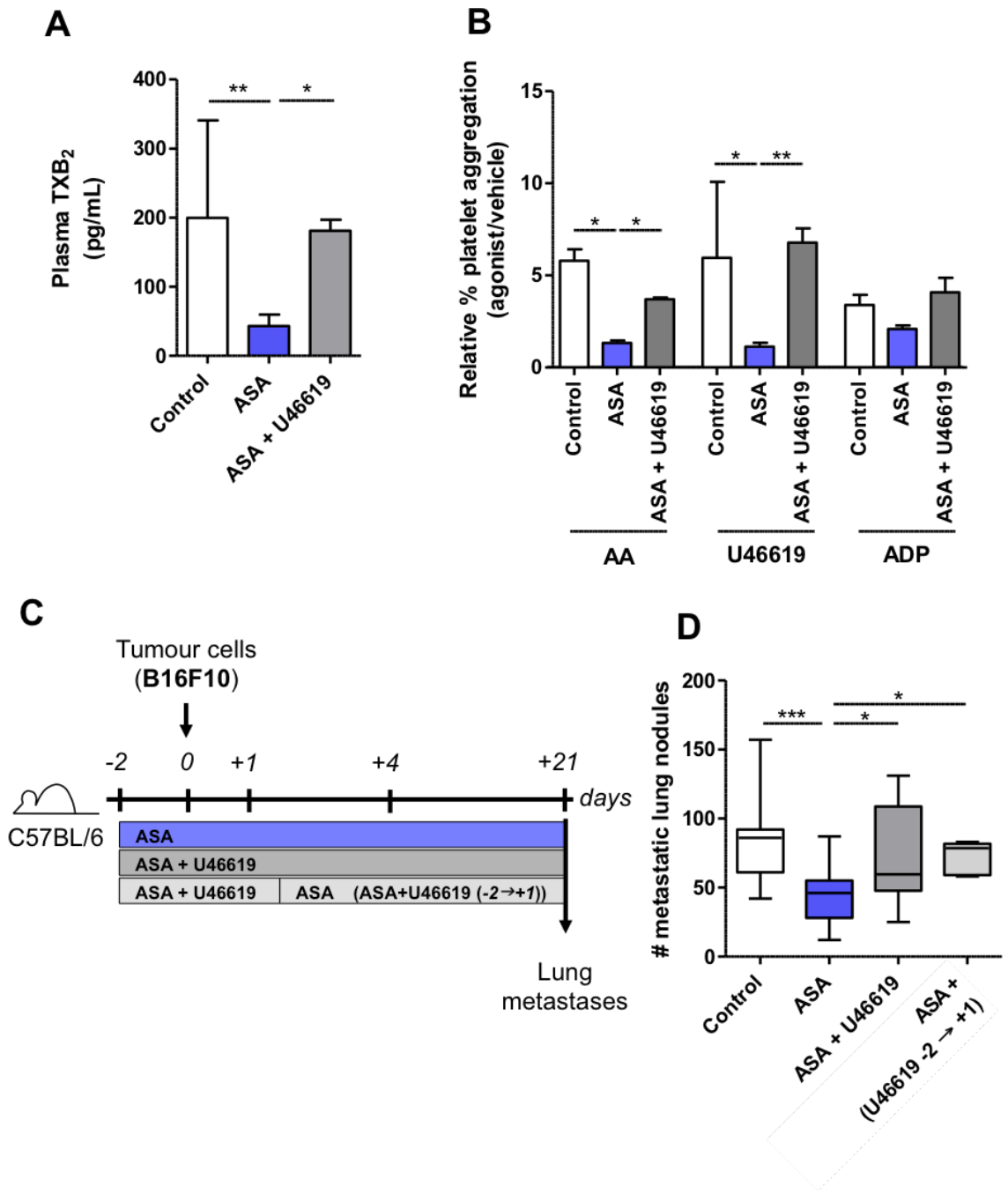

Figure 6.5 – U46619 rescues the anti-metastatic effect of ASA.

(A) Concentration of plasmatic TXB_2, derived from C57BL/6 mice treated with vehicle (Control), ASA or ASA supplemented with U46619 (stable analogue of TXA_2) (ASA+U46619) (n=3 mice per group; mean + SD, 1-way ANOVA with Tukey's Multiple Comparison test). Mice were treated through drinking water for 48 hours before blood collection.

(B) Quantification of agonist-induced platelet aggregation, measured through FACS analysis of CD41-stained platelets derived from vehicle, ASA or ASA+U46619 treated mice (n=6, 3 and 3 mice, respectively; mean + SD, 1-way ANOVA with Tukey's Multiple Comparison test). AA (1 mM), U46619 (0.3 μM) and ADP (1 μM) were used as agonists.

(C) Experimental design to study the effect of ASA+U46619 treatment on metastasis. C57BL/6 mice were injected with B16F10 cells and lungs were harvested at 21 days after injection for the

count of metastatic lung nodules. Starting 2 days before injection, mice were treated with vehicle, ASA or ASA supplemented with U46619 for 3 weeks (ASA+U46619) or until one day after injection (ASA+(U44619 *-2→+1*)).

(D) Number of metastatic lung nodules at 3 weeks after intravenous injection of B16F10 cells in mice treated with vehicle, ASA, ASA+U46619 or ASA+(U44619 *-2→+1*) (n=15, 19, 8 and 8 mice, respectively; median ± range, 1-way ANOVA with Tukey's Multiple Comparison test).

6.3.3 TXA_2 signalling from/to platelets is impaired by aspirin and is associated with metastasis reduction

6.3.3.1 COX-1 expressing platelets are the main source of TXA_2

During their haematogenous transit, tumour-host cell interactions take place. In order to dissect the molecular mechanism underlying the effect of TXA_2 inhibition on metastasis, we have analysed the expression pattern of proteins involved in the biosynthesis and signalling of TXA_2, focusing on cell types that interact with tumour cells early after their intravasation.

Tumour cells (B16F10), endothelial cells (LMVECs) and platelets (Plts), all from C57BL/6 mice, were used for Western Blot analysis of COX-1, TXAS and TP expression (Figure 6.6A). B16F10 cells did not show detectable expression of either COX-1, TP, and TXAS (Figure 6.5B), suggesting that their production and response to TXA_2 can only be minimal. Conversely, we found that LMVECs express COX-1 and TP, but not TXAS, and platelets express COX-1, TP and TXAS (Figure 6.6B). These results suggest that endothelial cells can sense, but not produce, TXA_2 while platelets express all proteins necessary to generate and respond to TXA_2.

The expression pattern of these proteins was also partially examined *ex vivo*, by immuno-staining lung sections for TXAS, TP and COX-1 (Supplementary figure S7). This preliminary analysis suggested that the pattern of protein expression in platelets, B16F10 and LMVECs was similar to the *in vitro* culture. Additionally, COX-1 was strongly

expressed by alveolar macrophages and TP was found in vascular smooth muscle cells, as expected. These results suggest that during early pulmonary metastasis platelets, and possibly alveolar macrophages, are the source of TXA_2, which can then signal to platelets, endothelial cells, and smooth muscle cells.

To further understand the source of TXA_2, the release of TXB_2 was assessed in conditioned media from B16F10 cells, LMVECs and platelets and their co-cultures. B16F10 and LMVECs produced very low levels of TXB_2 when cultured both separately and together (Figure 6.6C), which is in line with the results from Western Blot analysis (Figure 6.6B). On the contrary, platelets produced TXB_2 both in single culture and particularly in co-culture with tumour cells and endothelial cells or both (Figure 6.6C). The highest TXA_2 synthesis was seen when platelets, B16F10 and LMVECs were cultured together. These data suggest that platelets are the main producer of TXA_2, either alone or interacting with tumour and, particularly, endothelial cells.

In order to further dissect the source of TXA_2 in our system, platelets from $COX^{-/-}$ mice were isolated and cultured alone or in combination with B16F10 and/or LMVECs and TXB_2 levels were measured in the conditioned medium. TXA_2 synthesis was completely abrogated in cultures of COX-$1^{-/-}$ platelets alone or in combination with B16F10 and/or LMVECs (Figure 6.6C). These data suggest that platelets are the main source of TXA_2 in our system and their synthesis of TXA_2 heavily depends on COX-1 expression. TXA_2 release by platelets is stimulated by the interaction with tumour and endothelial cells and can be abrogated by COX-1 inhibition.

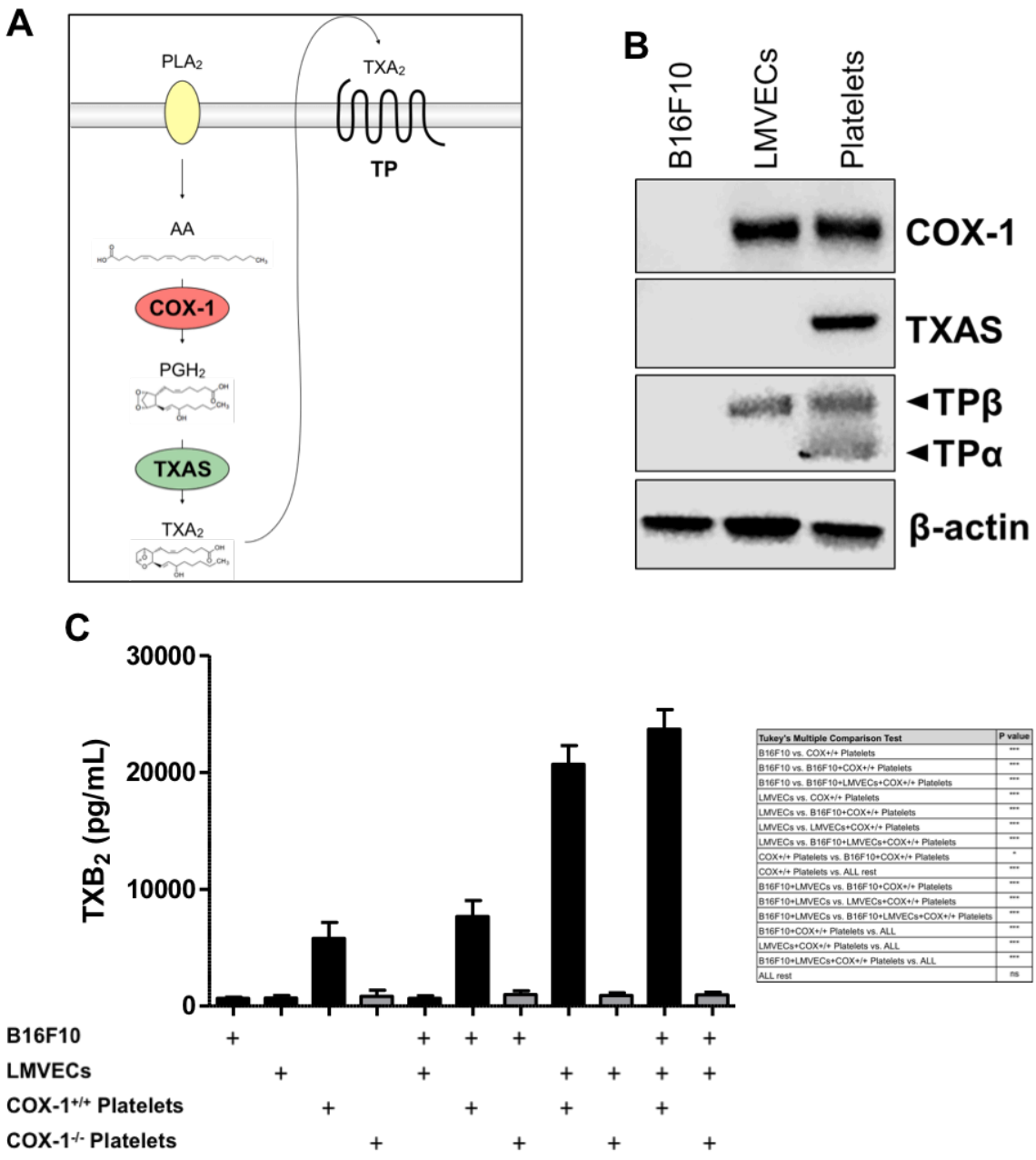

Figure 6.6 – The activity of COX-1 in platelets is responsible for TXA_2 synthesis in a simplified model of the intravascular metastatic niche.

(A) Diagram depicting the synthesis and signalling pathway of TXA_2 and the proteins involved. After the release from the cell membrane by PLA_2, AA is processed by COX-1 (and COX-2) into PGG_2 and PGH_2, the common precursor of all prostanoids. Thromboxane synthase (TXAS) then converts PGH_2 into TXA_2, which perfuses out of the cell and binds to its receptor (TP) in autocrine or paracrine manner.

(B) Detection of COX-1, TXAS, TP and β-actin (loading control) by immunoblotting in tumour cells (B16F10), lung microvascular endothelial cells (LMVECs) and platelets, all isolated from C57BL/6 mice. The two isoforms of TP receptor (TPα and TPβ) are detected. One out of 4 independent experiments is shown.

(C) Concentration of TXB_2 in conditioned medium of single culture or co-culture of B16F10, LMVECs and platelets, the latter derived from wild type (COX-$1^{+/+}$) or COX-$1^{-/-}$ mice. Statistically

significant differences are listed in the table on the right side (n=3 independent experiments; mean + SD, 1-way ANOVA with Tukey's Multiple Comparison test).

6.3.3.2 Aspirin impairs the synthesis and signalling of TXA_2 in platelets

In order to understand the effect of aspirin treatment on TXA_2 signalling in our system, TXB_2 levels were assessed in the conditioned medium of co-cultures of B16F10, LMVECs and COX-$1^{+/+}$ platelets treated with ASA. Figure 6.7A shows that ASA reduced the synthesis of TXA_2 in the co-cultures of B16F10, LMVECs and COX-$1^{+/+}$ platelets to a similar extent to the co-culture of B16F10, LMVECs and COX-$1^{-/-}$ platelets. These data indicate that ASA treatment dramatically affects TXA_2 synthesis and suggest that this effect depends on the inhibition of COX-1 in platelets. However, the different concentration of TXB_2 in the presence of COX-$1^{-/-}$ platelets and ASA treatment suggest that the inhibition of COX-1 by ASA is not complete.

We have shown that platelets synthesise TXA_2 after interaction with tumour cells and activated endothelial cells. Platelets can be the source but also the target of TXA_2 signalling, thanks to the expression of TP on their cell surface (Figure 6.6B). We have verified the effect of TXA_2 on platelets by stimulating PRP with U46619 and measuring the initiation of downstream signalling pathways. Platelets respond to U46619 stimulation by undergoing activation, as measured by Ca^{2+} release (Figure 6.7B), and aggregation (Figure 6.7C and D). The aggregation, but not the activation, of platelets was reduced in PRP from ASA-treated mice, as expected from TXA_2 signalling pathway (Figure 6.1). These data confirm the previous knowledge that platelets are the target of TXA_2 signalling, both autocrine and paracrine, and they respond by undergoing activation and aggregation. Aspirin treatment interferes with platelet aggregation by reducing the *de novo* synthesis of platelet-derived TXA_2 and the stimulation of platelets by TXA_2, through a COX-1 dependent mechanism.

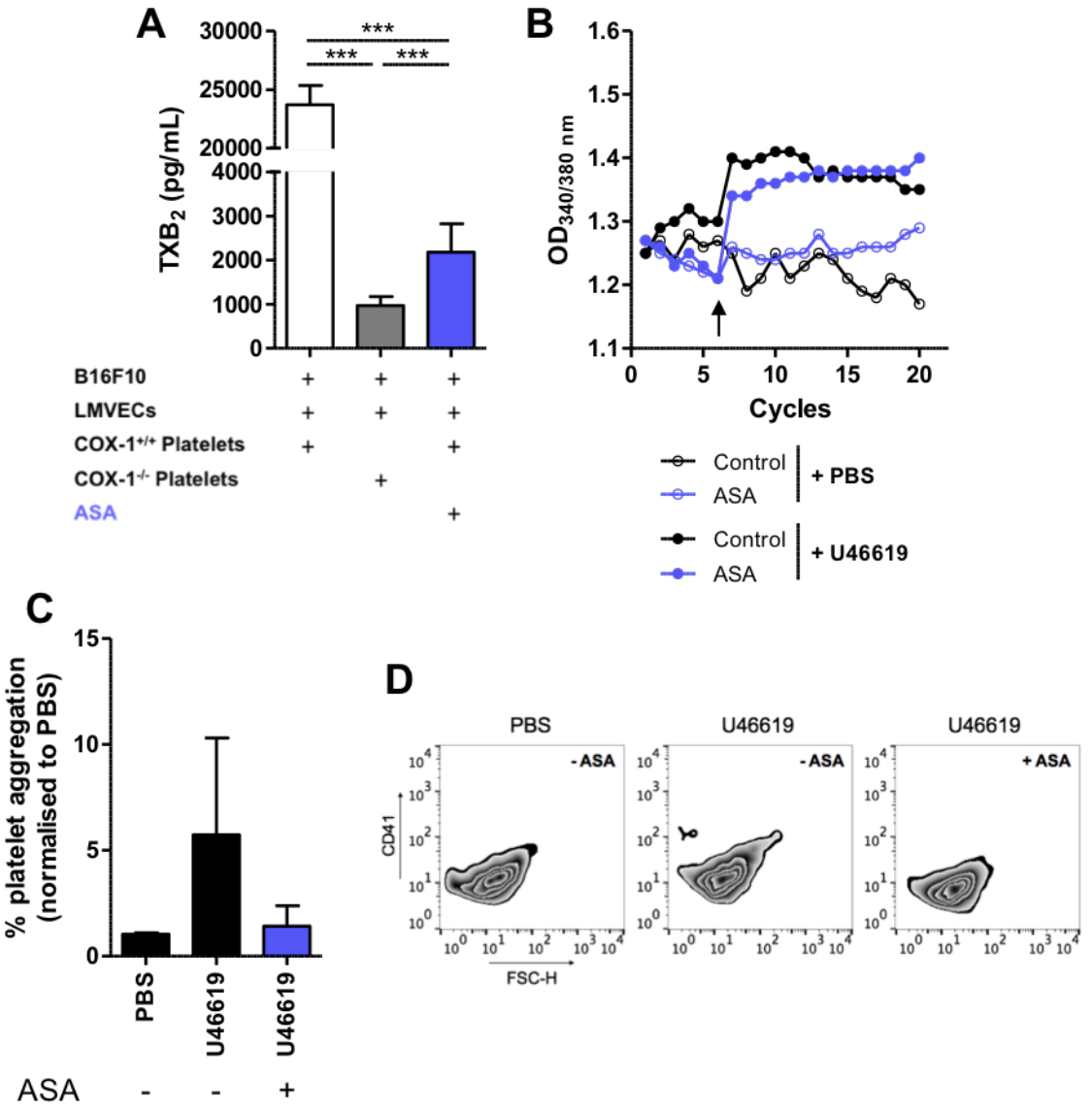

Figure 6.7 – Aspirin impairs U44619-induced platelet aggregation but not the initial activation.

(A) Concentration of TXB_2 in conditioned medium of co-culture of B16F10, LMVECs and platelets, in the presence of vehicle (Control) or ASA. Platelets were isolated from wild type (COX-$1^{+/+}$) or COX-$1^{-/-}$ mice (n=3 independent experiments; mean + SD, 1-way ANOVA with Tukey's Multiple Comparison test).

(B) Measurement of intracellular Ca^{2+} release through fluorescent dye Fura-2-AM, assessed in PRP from C57BL/6 mice treated with ASA or vehicle for 48h. PRP was stimulated with vehicle (PBS) or U46619 at the time point indicated with the arrow (n=1 experiment).

(C-D) Quantification (C) and representative dot plots (D) of agonist-induced platelet aggregation, measured through FACS analysis of CD41-stained platelets derived from vehicle (Control) or ASA treated mice (n=4 mice per group; mean + SD, 1-way ANOVA with Tukey's Multiple Comparison test). PBS and U46619 (0.3 μM) were used as agonists.

6.3.3.3 Platelet-derived TXA_2 seems to contribute to metastasis

Plasmatic levels of TXB_2 represent systemic synthesis of TXA_2 *in vivo* in the absence of platelet activation, while serum levels represent *ex vivo* generation of TXA_2 by stimulated platelets. We have observed that the concentration of TXB_2 in serum (Figure 6.8A), but not in plasma (Figure 6.8B), positively correlated with the number of metastatic lung nodules in ASA-treated mice. Thus, TXA_2 produced by non-activated platelets and extra-platelets targets, such as monocytes and endothelial cells, did not correlate with metastasis. On the contrary, platelet-derived TXA_2 seems to be involved in the development of metastasis.

All together, these data suggest that aspirin affects metastasis through the inhibition of COX-1 in platelets, which induces the abrogation of TXA_2 synthesis and signalling to platelets and extra-platelets targets.

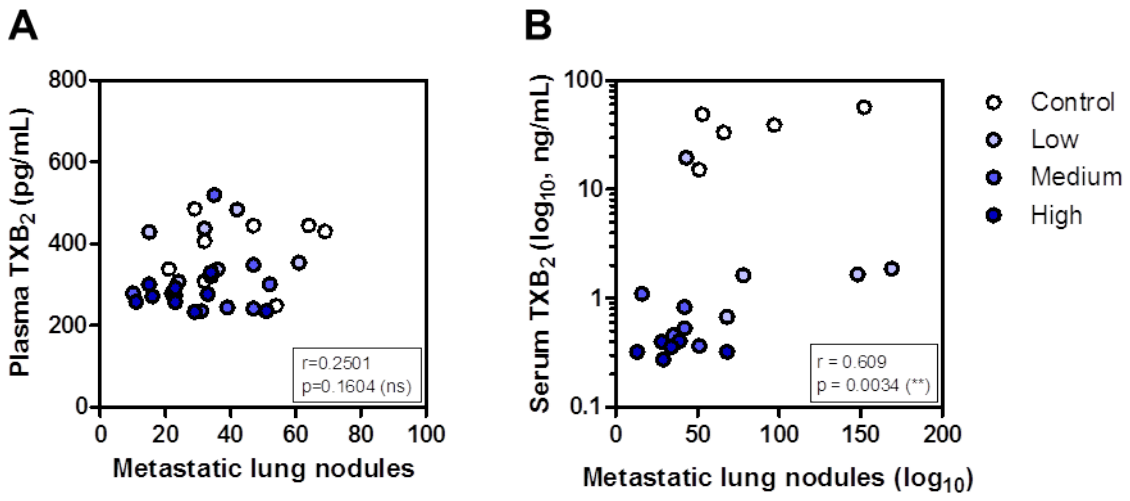

Figure 6.8 – Platelet-derived TXA_2 correlates with metastatic lung nodules.

(A) Correlation plot of the plasma concentration of TXB_2 versus the number of metastatic lung nodules, measured in C57BL/6 treated with vehicle (Control, n=8 mice) or ASA (Low, Medium and High, n=7, 9 and 9 mice, respectively; Spearman rank correlation).

(B) Correlation plot of the serum concentration of TXB_2 versus the number of metastatic lung nodules, measured in C57BL/6 treated with vehicle (n=5 mice) or ASA (Low, Medium and High, n=5, 5 and 6 mice, respectively; Pearson r correlation).

6.4 DISCUSSION

6.4.1 The inhibition of TXA_2 signalling reduces early steps of metastasis

In the previous Chapter we have shown that COX-1 activity contributes to a series of sequential steps of the early metastatic cascade. Here we have attempted to understand the contribution of TXA_2 to the development of metastasis by employing selective inhibitors of TXA_2 signalling. We have chosen two TXA_2 inhibitors, Ozagrel (OZA), a selective inhibitor of TXAS, and Picotamide (PICO), a dual-action inhibitor of TXAS and antagonist of TP. PICO was found to reduce metastatic lung nodules to a similar extent to ASA and SC-560 (Figure 6.3). This observation suggested that TXA_2 might be the effector of COX-1 responsible for the anti-metastatic effect of aspirin. To our knowledge, very few publications can be found that report the effect of TXA_2 inhibition on experimental[624,625] and spontaneous[598,624] metastasis, suggesting that the contribution of TXA_2 to metastasis development has been widely disregarded.

Similarly to aspirin, inhibition of TXA_2 signalling was particularly effective during the first day after tumour cell challenge. Both OZA and PICO reduced the number of tumour cells in lungs at one day after injection (Figure 6.4), suggesting an effect on the early survival and/or adhesion of disseminating tumour cells. However, the effect of PICO was more pronounced than the one of OZA. This result could be due to the higher efficiency of PICO to reduce TXB_2, which corresponds to an almost complete abrogation of platelet aggregation (Figure 6.2). Instead, at the minimum effective dose of 400 mg/L, OZA can reduce TXB_2 by 75%, which is above the limit of platelet aggregation inhibition. Additionally, under OZA treatment the residual TXA_2 levels might still signal to TP receptor expressed by adjacent cells. Finally, TXAS inhibitors are associated with the increase of alternative agonists of platelets TP (i.e. PGG_2 and PGH_2)[629,630]. Together, this evidence is

in agreement with previous studies suggesting the relative inefficacy of TXAS inhibitors as anti-platelet drugs and prompted us to use PICO for the following *in vivo* studies.

Another similarity between TXA_2 and COX-1 inhibition is the kinetics of their inhibition of metastasis. We have found that PICO reduces metastasis only when administered during the intravascular phase (Figure 6.4C), suggesting that TXA_2 synthesis and signalling are required for the haematogenous transit of tumour cells.

In our model no anti-metastatic effect was seen under PICO treatment when treatment was carried out after tumour cell extravasation, suggesting that TXA_2 signalling has little effect during the later phases of metastasis. Additionally, we did not detect any obvious difference in the size of lung nodules between vehicle- and PICO-treated animals, suggesting that metastasis progression was not affected. This finding is in contrast with a previous report, where the administration of TXAS inhibitor from 3 days post-injection reduced the number of metastatic lung nodules and the pro-angiogenic effect of TXA_2 was considered responsible[3]. This controversy could be addressed if we consider that in our model tumour cells are not able to synthesise TXA_2, although they can employ the binding of COX-1-expressing platelets to release TXA_2 locally during the intravascular phase. Thus, the levels of TXA_2 after tumour cells extravasation might not be sufficient to induce angiogenesis.

We have also provided more conclusive evidence that TXA_2 could be the main COX-1 product responsible for the anti-metastatic effect of aspirin. In fact, the administration of ASA supplemented with U46619 restores control levels of plasmatic TXA_2 and is sufficient to abrogate the anti-metastatic effect of ASA alone (Figure 6.5). Even more strikingly, the administration of ASA with U46619 during the first day post-injection, followed by treatment with ASA alone for the next 20 days, does not affect the number of metastatic nodules in comparison to control. To our knowledge, this is the first evidence to directly

link aspirin and COX-1-derived TXA_2 to a reduction of metastasis and to isolate the intravascular phase as the target of its anti-metastatic effect.

These findings shed a new light on the role of anti-coagulant therapies on metastasis. *Per se*, the inhibition of platelet aggregation on tumour cells has an anti-metastatic effect. Yet, it is inevitably associated with the impairment of *de novo* TXA_2 synthesis irrespectively of the inhibition mechanism, an effect that has been generally overlooked. Aspirin couples the inhibition of TXA_2 signalling on platelets, responsible for its anti-thrombotic effect, and on other cell types, possibly affecting metastasis to a further extent.

Additionally, our results suggest that drugs targeting more selective products along the COX pathway could be better candidates to achieve an anti-metastatic effect. In particular, dual-action inhibitors of TXAS and TP couple the inhibition of TXA_2 generation to the antagonism of signalling from residual TXA_2, which cannot be achieved through COX-1 inhibition. Moreover, aspirin intake is associated with side effects like bleeding complications and gastronintestinal perforations, the latter due to the inhibition of COX-1-derived PGI_2. These complications, together with the heterogeneity of doses and duration regimes, have contributed to a general uncertainty in the evaluation of the risk/benefit balance of aspirin as anti-cancer and anti-metastatic agent. In contrast, dual-action TXA_2 inhibitors do not interfere with other COX-1 derived prostanoid, thus they might be a safer choice for the prevention of metastases.

6.4.2 Sources and targets of TXA_2 signalling

Several lines of evidence presented here suggest the contribution of TXA_2 to the haematogenous transit of tumour cells. TXA_2 is the most abundant product of COX-1 activity in the circulatory system, where it oversees physiological and pathological functions. The synthesis of TXA_2 fluctuates in response to pro-thrombotic and pro-

inflammatory stimuli. Moreover, cancer is often associated with deregulated levels of TXA_2.

In order to understand the molecular and cellular mechanisms underlying TXA_2 contribution to metastasis, we have started to investigate the source and targets of TXA_2 during early phases of metastasis. *In vitro* and *ex vivo* detection of COX-1, TP and TXAS has revealed that in our model only platelets are equipped to both synthesise and respond to TXA_2 (Figure 6.6 and Supplementary figure S7). In agreement with this finding, TXA_2 was mainly generated by platelets in single culture or in co-cultures with tumour and endothelial cells (Figure 6.6C). The initiation of platelet activation and TXA_2 release *in vitro* in the absence of agonists could be due to the incubation in static conditions[650] or to the presence of growth factors in the culture medium. Moreover, the stimulation of platelets with U46619 induced their activation (measured as release of intracellular Ca^{2+}) and aggregation (Figure 6.7). Thus, in our system, platelets are the main source and target of TXA_2, where its signalling induces their activation and aggregation in an autocrine manner.

In contrast, lung microvascular endothelial cells expressed COX-1 and TP, suggesting that under static conditions they can be target, but not source, of TXA_2, as suggested by the measurement of TXA_2 in their single culture (Figure 6.6). The expression of COX-1 by endothelial cells has been previously reported and it is thought to control the synthesis of anti-thrombotic PGI_2[651]. The levels of TXA_2 are dramatically increased in the co-culture of endothelial cells and platelets (Figure 6.6), to a higher extent than the incubation of tumour cells with platelets. This effect could be attributed to the dynamic interplay between platelets and endothelial cells for the regulation of TXA_2 levels during vascular injury. In fact, TXA_2 released by activated platelets stimulates the overexpression of TF and PAF by endothelial cells, which in turn increases the activation of platelets. Thus, the generation of TXA_2 by activated platelets is exponentially increased upon contact with the endothelium. Theoretically, endothelial cells can partially contribute to the levels of TXA_2

in the conditioned medium. In fact, degranulated platelets release factors such as VEGF and TNF-α, which are known to induce the production of TXA_2 by endothelial cells[594,598]. However, TXA_2 release is completely abrogated by COX-1 depletion in platelets, even if the initial degranulation of platelets might still take place, suggesting that the platelets are responsible for the synthesis of TXA_2. Hence, endothelial cells and platelets take part into a bilateral interplay that results in the potent release of TXA_2 by platelets.

Dissimilarly to other tumour cell lines[565,566,569,570], B16F10 cells do not release TXA_2 in tissue culture, likely because they lack the expression of proteins involved in its biosynthesis (Figure 6.6B). Nevertheless, they induce an increase of TXA_2 release in co-culture with platelets (Figure 6.6C). This effect is likely due to the additional activation of platelets through a TF-mediated mechanism, but not to the generation of TXA_2 by tumour cells. In this sense, tumour cells function as a catalytic surface for the activation of platelets. The lack of synthesis or response of B16F10 cells in our model further supports the idea that the anti-metastatic effect by aspirin is achieved through an inhibition of COX-1-TXA_2 in the microenvironment, rather than on tumour cells. MC-38 cells express high levels of COX-1 protein (data not shown), but the effect of aspirin on MC-38-derived metastases is not greater than on B16F10-derived ones, suggesting that the contribution of tumour cell-derived TXA_2 is minimal. However, the contribution of TXA_2 signalling on TP-expressing tumour cells needs to be further evaluated.

The analysis of expression patterns of proteins involved in the synthesis and signalling of TXA_2 can also provide information on the targets of COX-1 and TXA_2 inhibitors. On the one hand, ASA and SC-560 would target platelets, endothelial cells, monocytes/macrophages and alveolar macrophages. On the other hand, OZA would affect platelets (TXAS) and PICO would affect platelets (TXAS and TP), endothelial cells (TP) and vascular smooth muscle cells (TP). It follows that platelets can be targeted by all treatments here employed, although at different stages of TXA_2 synthesis and signalling. Indeed, we have shown that the inhibition of upstream COX-1 in platelets, either by

genetic knock-out or aspirin treatment, is sufficient to abrogate the synthesis of TXA_2, even in the presence of functional TXAS. These results confirm previous evidence on the efficacy of aspirin in reducing circulating TXA_2. Moreover, tumour cells are excluded from on-target effects of all treatment and can only be affected by out-of target effects.

All together, these data suggest that platelets represent a hub for TXA_2 signalling pathway. On the one hand they synthesise TXA_2 in response to interaction with tumour cells and endothelial cells, and potentially other cell types *in vivo*, such as monocytes/macrophages. On the other hand, they respond to TXA_2 autocrine signalling by undergoing activation, aggregation and a second wave of TXA_2 generation, which further amplify their response.

6.4.3 Proposed model of TXA_2 signalling in the metastatic cascade

In the previous Chapters we have confined the anti-metastatic effect of COX-1 inhibition to the intravascular phase of metastasis, where the successful execution of consecutive steps of the metastatic cascade necessitates COX-1 activity. In this Chapter we have recognised the contribution of TXA_2 for the establishment of metastasis. As expected, COX-1 and TXA_2 are required for the execution of temporarily overlapping events.

Although TXA_2 is a downstream effector of COX-1 activity, it is not a direct product of COX-1, because its synthesis is also mediated by TXAS. Additionally, COX-1 inhibition cannot interfere with TXA_2 signalling to its cognate receptor TP. Thus, the relationship between COX-1 and TXA_2 inhibition is not necessary linear. In this Chapter we have confirmed that, by targeting COX-1, aspirin affects TXA_2 synthesis to a similar extent to COX-1 deficiency. Moreover, platelets seem to be the main target of aspirin. Although further studies will be needed to address this hypothesis, we have built a model describing the involvement of microenvironment-derived TXA_2 in metastasis on the basis of the obtained results (Figure 6.9).

Tumour cells represent a catalytic surface for the activation and aggregation of platelets, which locally release large amounts of TXA_2. Thus, tumour cell-platelets aggregated work as circulating reservoirs of TXA_2, even when tumour cells are not able to generate this prostanoid. This is the case of B16F10 (Figure 6.6) and possibly other tumour types with low expression of COX-1 (Supplementary figure S3). The autocrine TXA_2 signalling on platelets supports thrombus expansion and further TXA_2 generation. Within the lung vasculature, the release of TXA_2 induces the constriction of vascular smooth muscle cells, promoting the passive arrest of tumour cell-platelets aggregates. Concomitantly, TXA_2 signals to TP receptor on endothelial cells and induces the expression of VCAM-1, as previously indicated[591,592]. Other cytokines released by intracellular granules of activated platelets can also induce endothelial cells activation[141]. B16F10 cells adhere to VCAM-1 directly, through the expression of VLA-4, or via bound platelets. On the other hand, TXA_2 can induce monocytes chemoattractant protein 1 (CCL2/MCP-1) generation by endothelial cells[595], which recruits monocytes/macrophages in proximity of the tumour cells. This recruitment is facilitated by the arrest of monocytes on endothelial cells through VLA-4-VCAM-1 interaction[141]. Finally, TXA_2[599] and other platelet-derived factors[18,135,652] induce microvascular permeabilisation and facilitate tumour cells extravasation. Platelets, endothelial cells and monocytes also take part into a positive feedback loop that further increases platelet aggregation and TXA_2 generation. In fact, platelet-derived TXA_2 induces expression of TF by endothelial cells[594] and monocytes[608], which increases the size of clots in the tumour cell-platelet-monocyte clusters.

The contribution of platelet-derived TXA_2 has been addressed in the past in the context of haemostasis, however its role in the onset of metastasis is yet not understood. According to this model, TXA_2 promotes metastasis not only through its autocrine signalling on platelets, but also through the paracrine signalling to adjacent cell types in the early metastatic niche. This signalling network can be inhibited by aspirin, leading to a reduced seeding efficiency and metastasis.

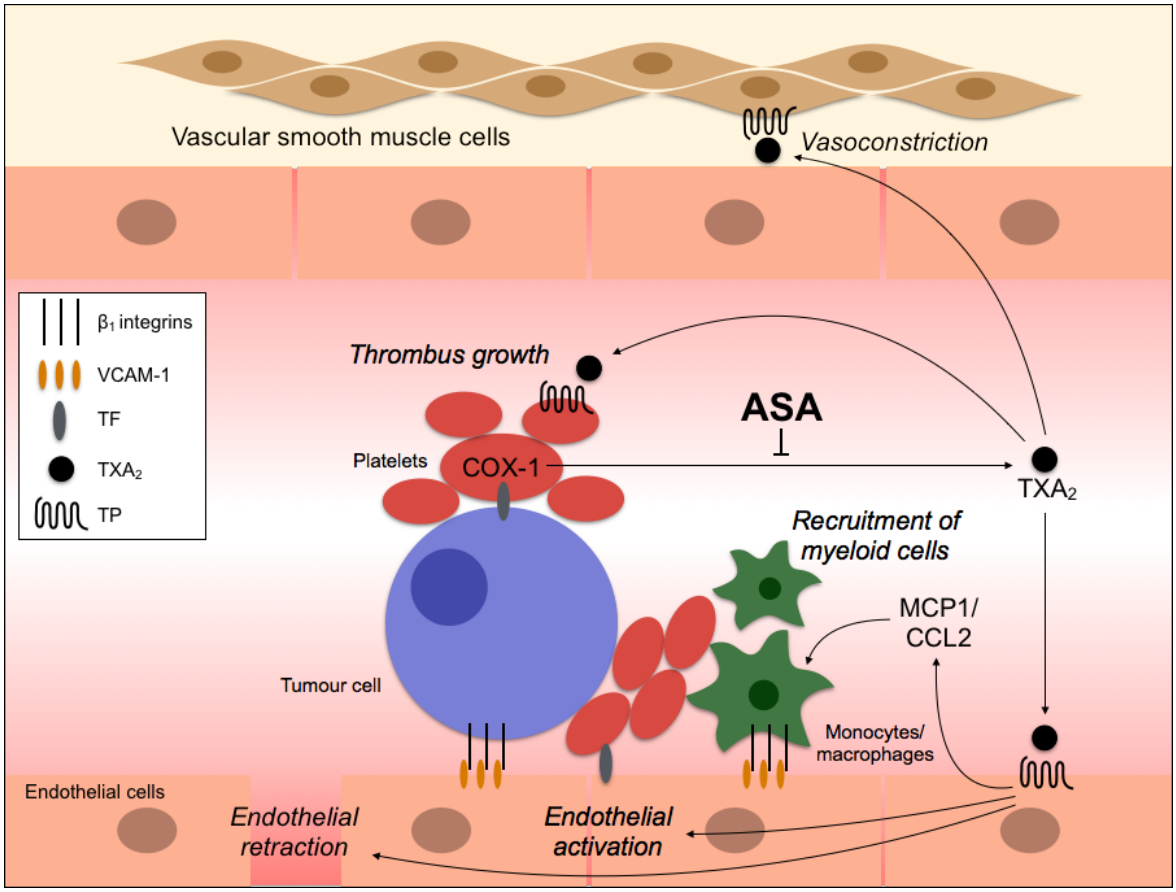

Figure 6.9 – TXA_2 signalling promotes metastasis.

Diagram depicting the proposed model by which TXA_2 promotes metastasis. The aggregation of platelets on tumour cells stimulates the *de novo* synthesis of TXA_2. TXA_2 signals to platelets in autocrine and paracrine manner and increases thrombosis on tumour cells, thus amplifying TXA_2 release. Concomitantly, TXA_2 induces the contraction of vascular smooth muscle cells, inducing vasoconstriction. TXA_2-TP signalling on endothelial cells induces the expression of VCAM-1, which mediates tumour cell and monocytes/macrophages adhesion. The recruitment of monocytes might be facilitated by CCL2/MCP-1 release by endothelial cells in response to TXA_2. Finally, TXA_2 and other platelet-derived cytokines induce endothelial cell retraction and might facilitate tumour cell extravasation.

TF= tissue factor; TXA_2= Thromboxane A_2; TP= TXA_2 receptor; VCAM-1= vascular cell adhesion molecule-1.

6.4.4 Conclusions and future perspectives

Together, in this Chapter we have shown the contribution of TXA_2 signalling to the development of metastasis and identified the source and targets of TXA_2 signalling in the vascular system, which is the metastatic niche of our model. Moreover, we have tried to explain the anti-metastatic effect of COX-1 inhibition under the light of the known effects of TXA_2 in the vascular system. Our data are compatible with a model where TXA_2 derived from COX-1 activity in platelets signals to other non-tumour cells in the metastatic niche, reinforcing the idea that the anti-metastatic effect of COX-1-TXA_2 inhibition is mostly microenvironment-centred. However, it would be inappropriate to draw final conclusions from our current data on the effect of TXA_2 signalling in the metastatic cascade. In future work, the employment of PICO and COX-$1^{-/-}$ or aspirinated platelets in our *in vivo* model will help to define the relative of platelet-derived TXA_2 signalling in the metastatic niche.

CHAPTER 7

Concluding remarks

The aim of this research project was to identify the mechanisms underlying the anti-metastatic effect of aspirin. Throughout this thesis we have provided evidence that the main target of aspirin for the reduction of metastasis is COX-1. Indeed, the inhibition of COX-1 alone by therapeutic or genetic means was sufficient to achieve a reduction of metastatic lung nodules by more than 50% in a range of metastasis models. This finding is novel and directly implies a role of COX-1 in the metastatic process.

We have shown that COX-1 activity is required during the intravascular transit of tumour cells, while it is not necessary for the persistent growth of the metastatic lung nodules. Looking more closely into the underlying mechanisms, the inhibition of COX-1 impairs multiple consecutive steps of the haematogenous transit of tumour cells, leading to the early inhibition of tumour cells persistence in the lung vasculature. Thus, COX-1 activity contributes to the generation of a permissive early metastatic niche. The central hub of this niche is platelets. We have found that the inhibition of COX-1 affects tumour cells interaction with platelets, which *per se* is sufficient to decrease metastasis in a number of models[18,103,113,243-249,269]. Additionally, the decrease of platelet association with tumour cells is associated with the impairment of multiple subsequent steps of the metastatic cascade, such as endothelial cell activation, adhesion of tumour cells to the endothelium, interaction with monocytes/macrophages and transendothelial migration.

The central role of platelets in generating a favourable environment within the circulation might depend on their synthesis of TXA_2, the main COX-1 product in the blood stream during pro-thrombotic states. Indeed, the inhibition of TXA_2 synthesis and signalling by selective drugs is sufficient to reduce metastasis by targeting the intravascular phase. According to our proposed model, TXA_2 derived from platelet aggregates on the surface

of tumour cells signals to other platelets, vascular smooth muscle cells, endothelial cells and monocytes macrophages to generate a favourable early metastatic niche that promotes tumour cell seeding and metastasis (Figure 6.8).

The importance of TXA_2 signalling during the establishment of metastasis is further supported by the observation that the anti-metastatic effect of aspirin is associated with the inhibition of TXA_2 synthesis by platelets through a COX-1-dependent mechanism. Importantly, we have shown that the restoration of basal levels of TXA_2 during aspirin treatment, even just during the intravascular phase of metastasis, completely abolished the anti-metastatic effect of aspirin. To our knowledge, this is the first evidence supporting the notion that TXA_2 is the main COX-1 product responsible for the preventive effect of aspirin on metastasis.

Overall, these results shed a new light on COX-1-TXA_2 pathway in the context of metastasis, well beyond its role in thrombosis. According to our findings, we suggest that TXA_2 contributes to the generation of a favourable metastatic niche in the circulation that promotes tumour cell seeding and metastasis.

7.1 Potential clinical relevance

Although it would be inappropriate to make direct comparisons between our data and the clinical practice, we have made efforts to employ clinically relevant doses and similar delivery route of aspirin in our *in vivo* model in comparison to the clinic. This approach has a higher potential to identify targets for drug development. The work presented here identifies COX-1 and more specifically TXA_2 as a potentially druggable targets in the metastatic cascade. In particular, we have shown that the inhibition of COX-1-TXA_2 by low-medium dose of aspirin is effective exclusively during the intravascular phase of metastasis, even when treatment was interrupted after tumour cells extravasation. Accordingly, the inhibition of COX-1-TXA_2 after tumour cells extravasation does not

decrease metastatic burden. These observations suggest the potential use of aspirin as adjuvant therapy, particularly effective in patients diagnosed with cancer but with no overt metastasis. The recently started Phase III ADD-ASPIRIN trial (http://www.addaspirintrial.org) will help to address the efficacy of aspirin in the prevention of tumour relapse and metastasis appearance.

Aspirin is a low-cost agent widely available in most countries and has the potential to be employed to prevent cancer and metastasis in the general population. However, even if aspirin will prove effective in high-risk groups, it significantly increases the risk of developing severe gastrointestinal symptoms and complications. The risk would increase with long-term treatment of 10 years of more. Since currently no biomarkers are available to predict the appearance of side effects, it is unlikely that aspirin will be introduced as prophylactic agent in the general population. Our data suggest that the use of more selective TXA_2 inhibitors might represent an alternative choice to selectively target TXA_2, but not other beneficial COX-1 products responsible for the side effects of aspirin. TXA_2 selective inhibitors present a better anti-thrombotic profile and can be administered at lower doses, thus they might represent a safer choice as prophylactic therapies for cancer patients and the general population.

7.2 Limitations of our research and future perspectives

During this research project we have employed an experimental model of pulmonary metastasis. This model is particularly advantageous to investigate the early steps of the metastatic cascade, but it fails to recapitulate all phases of the metastatic cascade, in particular intravasation and establishment of the pre-metastatic niche. Additionally, the seeding process of experimental metastasis is very different in comparison to clinical settings, where tumour cells with invasive traits are positively selected and continuously shed from the primary tumour. These differences might change the behaviour of tumour

cells in regards of metastasis establishment[529]. The employment of spontaneous model of metastasis could help address these points.

Additionally, some of the presented experiments were performed *in vitro* in simplified models of the blood circulation, where the contribution of other cell types, such as monocytes/macrophages, was not accounted for. The effect of aspirin on these steps of the metastatic cascade will be addressed in more details *in vivo* settings.

Finally, although we reported a clear contribution of TXA_2 to the anti-metastatic effect of aspirin, the suggested model of TXA_2 signalling during the intravascular phase is mostly speculative. In future plans we will address the contribution of TXA_2 signalling on endothelial activation, monocytes/macrophages recruitment and tumour TEM by employing selective inhibitor of TXA_2. Additionally, the contribution of platelet-derived TXA_2 will be investigated through an adaptive transfer of platelets with impaired COX-1 activity and TXA_2 synthesis, achieved through pharmacological or genetic means. Together these data will contribute to further understand the interplay between tumour cells and non-tumour microenvironment in the early metastatic niche and will provide new insights for the development of therapies for metastasis prevention.

REFERENCES

1 Talmadge, J. E. & Fidler, I. J. AACR centennial series: the biology of cancer metastasis: historical perspective. *Cancer Res* **70**, 5649-5669, doi:10.1158/0008-5472.can-10-1040 (2010).
2 Fidler, I. J. Metastasis: guantitative analysis of distribution and fate of tumor embolilabeled with 125 I-5-iodo-2'-deoxyuridine. *Journal of the National Cancer Institute* **45**, 773-782 (1970).
3 Butler, T. P. & Gullino, P. M. Quantitation of cell shedding into efferent blood of mammary adenocarcinoma. *Cancer research* **35**, 512-516 (1975).
4 Tarin, D. *et al.* Mechanisms of human tumor metastasis studied in patients with peritoneovenous shunts. *Cancer research* **44**, 3584-3592 (1984).
5 Karnezis, T., Shayan, R., Fox, S., Achen, M. G. & Stacker, S. A. The connection between lymphangiogenic signalling and prostaglandin biology: a missing link in the metastatic pathway. *Oncotarget* **3**, 893-906 (2012).
6 Gupta, G. P. & Massagué, J. Cancer Metastasis: Building a Framework. *Cell* **127**, 679-695, doi:10.1016/j.cell.2006.11.001 (2006).
7 Nowell, P. C. The clonal evolution of tumor cell populations. *Science* **194**, 23-28 (1976).
8 Nowell, P. C. Chromosomal and molecular clues to tumor progression. *Seminars in oncology* **16**, 116-127 (1989).
9 Virchow, R. Cellular pathology. As based upon physiological and pathological histology. Lecture XVI--Atheromatous affection of arteries. 1858. *Nutrition reviews* **47**, 23-25 (1989).
10 Ewing, J. *Neoplastic diseases; a treatise on tumors*. 3d ed rev. and enl., with 546 illustrations. edn, (W.B. Saunders, 1928).
11 Paget, S. The distribution of secondary growths in cancer of the breast. 1889. *Cancer Metastasis Rev* **8**, 98-101 (1989).
12 Sugarbaker, E. D. The organ selectivity of experimentally induced metastases in rats. *Cancer* **5**, 606-612 (1952).
13 Kinsey, D. L. An experimental study of preferential metastasis. *Cancer* **13**, 674-676 (1960).
14 Hart, I. R. & Fidler, I. J. Role of organ selectivity in the determination of metastatic patterns of B16 melanoma. *Cancer research* **40**, 2281-2287 (1980).
15 Chiang, A. C. & Massague, J. Molecular basis of metastasis. *N Engl J Med* **359**, 2814-2823, doi:10.1056/NEJMra0805239 (2008).
16 Hiratsuka, S. *et al.* MMP9 induction by vascular endothelial growth factor receptor-1 is involved in lung-specific metastasis. *Cancer Cell* **2**, 289-300 (2002).
17 Padua, D. *et al.* TGFbeta primes breast tumors for lung metastasis seeding through angiopoietin-like 4. *Cell* **133**, 66-77, doi:10.1016/j.cell.2008.01.046 (2008).
18 Labelle, M., Begum, S. & Hynes, R. O. Direct signaling between platelets and cancer cells induces an epithelial-mesenchymal-like transition and promotes metastasis. *Cancer Cell* **20**, 576-590, doi:10.1016/j.ccr.2011.09.009 (2011).
19 Nguyen, D. X. & Massague, J. Genetic determinants of cancer metastasis. *Nature reviews. Genetics* **8**, 341-352, doi:10.1038/nrg2101 (2007).
20 Kaplan, R. N. *et al.* VEGFR1-positive haematopoietic bone marrow progenitors initiate the pre-metastatic niche. *Nature* **438**, 820-827, doi:10.1038/nature04186 (2005).
21 Hiratsuka, S., Watanabe, A., Aburatani, H. & Maru, Y. Tumour-mediated upregulation of chemoattractants and recruitment of myeloid cells predetermines lung metastasis. *Nature cell biology* **8**, 1369-1375, doi:10.1038/ncb1507 (2006).
22 Hiratsuka, S. *et al.* The S100A8-serum amyloid A3-TLR4 paracrine cascade establishes a pre-metastatic phase. *Nat Cell Biol* **10**, 1349-1355, doi:10.1038/ncb1794 (2008).
23 Costa-Silva, B. *et al.* Pancreatic cancer exosomes initiate pre-metastatic niche formation in the liver. *Nat Cell Biol* **17**, 816-826, doi:10.1038/ncb3169 (2015).
24 Peinado, H. *et al.* Melanoma exosomes educate bone marrow progenitor cells toward a pro-metastatic phenotype through MET. *Nat Med* **18**, 883-891, doi:10.1038/nm.2753 (2012).
25 Psaila, B. & Lyden, D. The metastatic niche: adapting the foreign soil. *Nat Rev Cancer* **9**, 285-293, doi:10.1038/nrc2621 (2009).
26 Gil-Bernabe, A. M. *et al.* Recruitment of monocytes/macrophages by tissue factor-mediated coagulation is essential for metastatic cell survival and premetastatic niche establishment in mice. *Blood* **119**, 3164-3175, doi:10.1182/blood-2011-08-376426 (2012).

27 Erler, J. T. *et al.* Hypoxia-induced lysyl oxidase is a critical mediator of bone marrow cell recruitment to form the premetastatic niche. *Cancer Cell* **15**, 35-44, doi:10.1016/j.ccr.2008.11.012 (2009).

28 Olaso, E. *et al.* Proangiogenic role of tumor-activated hepatic stellate cells in experimental melanoma metastasis. *Hepatology* **37**, 674-685, doi:10.1053/jhep.2003.50068 (2003).

29 Qian, B. *et al.* A distinct macrophage population mediates metastatic breast cancer cell extravasation, establishment and growth. *PLoS One* **4**, e6562, doi:10.1371/journal.pone.0006562 (2009).

30 Steeg, P. S. Targeting metastasis. *Nat Rev Cancer* **16**, 201-218, doi:10.1038/nrc.2016.25 (2016).

31 Cifone, M. A. & Fidler, I. J. Increasing metastatic potential is associated with increasing genetic instability of clones isolated from murine neoplasms. *Proceedings of the National Academy of Sciences of the United States of America* **78**, 6949-6952 (1981).

32 Hill, R. P., Chambers, A. F., Ling, V. & Harris, J. F. Dynamic heterogeneity: rapid generation of metastatic variants in mouse B16 melanoma cells. *Science* **224**, 998-1001 (1984).

33 Masramon, L. *et al.* Genetic instability and divergence of clonal populations in colon cancer cells in vitro. *Journal of cell science* **119**, 1477-1482, doi:10.1242/jcs.02871 (2006).

34 Jones, T. D. *et al.* Clonal origin of lymph node metastases in bladder carcinoma. *Cancer* **104**, 1901-1910, doi:10.1002/cncr.21466 (2005).

35 Kuwai, T. *et al.* Intratumoral heterogeneity for expression of tyrosine kinase growth factor receptors in human colon cancer surgical specimens and orthotopic tumors. *American Journal of Pathology* **172**, 358-366, doi:10.2353/ajpath.2008.070625 (2008).

36 Nakamura, T. *et al.* Zonal heterogeneity for gene expression in human pancreatic carcinoma. *Cancer Research* **67**, 7597-7604, doi:10.1158/0008-5472.Can-07-0874 (2007).

37 Steeg, P. S., Camphausen, K. A. & Smith, Q. R. Brain metastases as preventive and therapeutic targets. *Nature reviews. Cancer* **11**, 352-363, doi:10.1038/nrc3053 (2011).

38 Steeg, P. S. Perspective: The right trials. *Nature* **485**, S58-59, doi:10.1038/485S58a (2012).

39 Weber, G. F. Why does cancer therapy lack effective anti-metastasis drugs? *Cancer letters* **328**, 207-211, doi:10.1016/j.canlet.2012.09.025 (2013).

40 Francia, G., Cruz-Munoz, W., Man, S., Xu, P. & Kerbel, R. S. Mouse models of advanced spontaneous metastasis for experimental therapeutics. *Nat Rev Cancer* **11**, 135-141, doi:10.1038/nrc3001 (2011).

41 Thiery, J. P., Acloque, H., Huang, R. Y. J. & Nieto, M. A. Epithelial-Mesenchymal Transitions in Development and Disease. *Cell* **139**, 871-890, doi:10.1016/j.cell.2009.11.007 (2009).

42 Chaffer, C. L. & Weinberg, R. A. A perspective on cancer cell metastasis. *Science* **331**, 1559-1564, doi:10.1126/science.1203543 (2011).

43 Gupta, G. P. & Massague, J. Cancer metastasis: building a framework. *Cell* **127**, 679-695, doi:10.1016/j.cell.2006.11.001 (2006).

44 Lamouille, S., Xu, J. & Derynck, R. Molecular mechanisms of epithelial-mesenchymal transition. *Nat Rev Mol Cell Biol* **15**, 178-196, doi:10.1038/nrm3758 (2014).

45 Cavallaro, U. & Christofori, G. Cell adhesion and signalling by cadherins and Ig-CAMs in cancer. *Nature Reviews Cancer* **4**, 118-132, doi:10.1038/nrc1276 (2004).

46 van Zijl, F., Krupitza, G. & Mikulits, W. Initial steps of metastasis: Cell invasion and endothelial transmigration. *Mutat Res-Rev Mutat* **728**, 23-34, doi:10.1016/j.mrrev.2011.05.002 (2011).

47 Chiang, S. P., Cabrera, R. M. & Segall, J. E. Tumor cell intravasation. *Am J Physiol Cell Physiol* **311**, C1-C14, doi:10.1152/ajpcell.00238.2015 (2016).

48 Yang, X. *et al.* VEGF-B promotes cancer metastasis through a VEGF-A-independent mechanism and serves as a marker of poor prognosis for cancer patients. *Proc Natl Acad Sci U S A* **112**, E2900-2909, doi:10.1073/pnas.1503500112 (2015).

49 Harney, A. S. *et al.* Real-Time Imaging Reveals Local, Transient Vascular Permeability, and Tumor Cell Intravasation Stimulated by TIE2hi Macrophage-Derived VEGFA. *Cancer Discov* **5**, 932-943, doi:10.1158/2159-8290.cd-15-0012 (2015).

50 Tien, Y. W. *et al.* Tumor angiogenesis and its possible role in intravasation of colorectal epithelial cells. *Clin Cancer Res* **7**, 1627-1632 (2001).

51 Sohail, A. *et al.* Characterization of the dimerization interface of membrane type 4 (MT4)-matrix metalloproteinase. *J Biol Chem* **286**, 33178-33189, doi:10.1074/jbc.M111.253369 (2011).

52 Chabottaux, V. *et al.* Membrane-type 4 matrix metalloproteinase (MT4-MMP) induces lung metastasis by alteration of primary breast tumour vascular architecture. *J Cell Mol Med* **13**, 4002-4013, doi:10.1111/j.1582-4934.2009.00764.x (2009).

53 Yu, M. *et al.* Circulating breast tumor cells exhibit dynamic changes in epithelial and mesenchymal composition. *Science* **339**, 580-584, doi:10.1126/science.1228522 (2013).

54 Aceto, N. *et al.* Circulating tumor cell clusters are oligoclonal precursors of breast cancer metastasis. *Cell* **158**, 1110-1122, doi:10.1016/j.cell.2014.07.013 (2014).

55 Hodgkinson, C. L. *et al.* Tumorigenicity and genetic profiling of circulating tumor cells in small-cell lung cancer. *Nat Med* **20**, 897-903, doi:10.1038/nm.3600 (2014).

56 Krebs, M. G. *et al.* Evaluation and prognostic significance of circulating tumor cells in patients with non-small-cell lung cancer. *J Clin Oncol* **29**, 1556-1563, doi:10.1200/JCO.2010.28.7045 (2011).

57 de Bono, J. S. *et al.* Circulating tumor cells predict survival benefit from treatment in metastatic castration-resistant prostate cancer. *Clin Cancer Res* **14**, 6302-6309, doi:10.1158/1078-0432.CCR-08-0872 (2008).

58 Cristofanilli, M. *et al.* Circulating tumor cells, disease progression, and survival in metastatic breast cancer. *N Engl J Med* **351**, 781-791, doi:10.1056/NEJMoa040766 (2004).

59 Cohen, S. J. *et al.* Prognostic significance of circulating tumor cells in patients with metastatic colorectal cancer. *Annals of oncology : official journal of the European Society for Medical Oncology / ESMO* **20**, 1223-1229, doi:10.1093/annonc/mdn786 (2009).

60 Pantel, K. & Speicher, M. R. The biology of circulating tumor cells. *Oncogene* **35**, 1216-1224, doi:10.1038/onc.2015.192 (2016).

61 Stott, S. L. *et al.* Isolation of circulating tumor cells using a microvortex-generating herringbone-chip. *Proc Natl Acad Sci U S A* **107**, 18392-18397, doi:10.1073/pnas.1012539107 (2010).

62 Friedl, P. & Gilmour, D. Collective cell migration in morphogenesis, regeneration and cancer. *Nat Rev Mol Cell Biol* **10**, 445-457, doi:10.1038/nrm2720 (2009).

63 LeBleu, V. S. *et al.* PGC-1alpha mediates mitochondrial biogenesis and oxidative phosphorylation in cancer cells to promote metastasis. *Nat Cell Biol* **16**, 992-1003, 1001-1015, doi:10.1038/ncb3039 (2014).

64 Meng, S. *et al.* Circulating tumor cells in patients with breast cancer dormancy. *Clin Cancer Res* **10**, 8152-8162, doi:10.1158/1078-0432.CCR-04-1110 (2004).

65 Fidler, I. J. Metastasis: quantitative analysis of distribution and fate of tumor emboli labeled with 125 I-5-iodo-2'-deoxyuridine. *J Natl Cancer Inst* **45**, 773-782 (1970).

66 Barnes, J. M., Nauseef, J. T. & Henry, M. D. Resistance to fluid shear stress is a conserved biophysical property of malignant cells. *PLoS One* **7**, e50973, doi:10.1371/journal.pone.0050973 (2012).

67 Villegas, F. R. *et al.* Prognostic significance of tumor infiltrating natural killer cells subset CD57 in patients with squamous cell lung cancer. *Lung Cancer* **35**, 23-28 (2002).

68 Ishigami, S. *et al.* Prognostic value of intratumoral natural killer cells in gastric carcinoma. *Cancer* **88**, 577-583 (2000).

69 Coca, S. *et al.* The prognostic significance of intratumoral natural killer cells in patients with colorectal carcinoma. *Cancer* **79**, 2320-2328 (1997).

70 Nieswandt, B., Hafner, M., Echtenacher, B. & Mannel, D. N. Lysis of tumor cells by natural killer cells in mice is impeded by platelets. *Cancer Res* **59**, 1295-1300 (1999).

71 Cheng, M., Chen, Y., Xiao, W., Sun, R. & Tian, Z. NK cell-based immunotherapy for malignant diseases. *Cell Mol Immunol* **10**, 230-252, doi:10.1038/cmi.2013.10 (2013).

72 Trapani, J. A., Davis, J., Sutton, V. R. & Smyth, M. J. Proapoptotic functions of cytotoxic lymphocyte granule constituents in vitro and in vivo. *Curr Opin Immunol* **12**, 323-329, doi:Doi 10.1016/S0952-7915(00)00094-7 (2000).

73 Kagi, D. *et al.* Cytotoxicity Mediated by T-Cells and Natural-Killer-Cells Is Greatly Impaired in Perforin Deficient Mice. *Nature* **369**, 31-37, doi:DOI 10.1038/369031a0 (1994).

74 Fernandez, L. *et al.* Activated and expanded natural killer cells target osteosarcoma tumor initiating cells in an NKG2D-NKG2DL dependent manner. *Cancer Lett* **368**, 54-63, doi:10.1016/j.canlet.2015.07.042 (2015).

75 Hong, Z. F. *et al.* Natural killer cells inhibit pulmonary metastasis of hepatocellular carcinoma in nude mice. *Oncology letters* **11**, 2019-2026, doi:10.3892/ol.2016.4170 (2016).

76 Guma, S. R., Lee, D. A., Ling, Y., Gordon, N. & Kleinerman, E. S. Aerosol interleukin-2 induces natural killer cell proliferation in the lung and combination therapy improves the survival of mice with osteosarcoma lung metastasis. *Pediatr Blood Cancer* **61**, 1362-1368, doi:10.1002/pbc.25019 (2014).

77 Kopp, H. G., Placke, T. & Salih, H. R. Platelet-derived transforming growth factor-beta down-regulates NKG2D thereby inhibiting natural killer cell antitumor reactivity. *Cancer Res* **69**, 7775-7783, doi:10.1158/0008-5472.can-09-2123 (2009).

78 Smyth, M. J. *et al.* Sequential production of interferon-gamma by NK1.1(+) T cells and natural killer cells is essential for the antimetastatic effect of alpha-galactosylceramide. *Blood* **99**, 1259-1266, doi:DOI 10.1182/blood.V99.4.1259 (2002).

79 Street, S. E. A., Cretney, E. & Smyth, M. J. Perforin and interferon-gamma activities independently control tumor initiation, growth, and metastasis. *Blood* **97**, 192-197, doi:DOI 10.1182/blood.V97.1.192 (2001).

80 Khwaja, A., Rodriguez-Viciana, P., Wennstrom, S., Warne, P. H. & Downward, J. Matrix adhesion and Ras transformation both activate a phosphoinositide 3-OH kinase and protein kinase B/Akt cellular survival pathway. *Embo j* **16**, 2783-2793, doi:10.1093/emboj/16.10.2783 (1997).

81 Collins, N. L. *et al.* G1/S cell cycle arrest provides anoikis resistance through Erk-mediated Bim suppression. *Mol Cell Biol* **25**, 5282-5291, doi:10.1128/mcb.25.12.5282-5291.2005 (2005).

82 Frisch, S. M., Vuori, K., Ruoslahti, E. & Chan-Hui, P. Y. Control of adhesion-dependent cell survival by focal adhesion kinase. *J Cell Biol* **134**, 793-799 (1996).

83 Paoli, P., Giannoni, E. & Chiarugi, P. Anoikis molecular pathways and its role in cancer progression. *Biochim Biophys Acta* **1833**, 3481-3498, doi:10.1016/j.bbamcr.2013.06.026 (2013).

84 Yang, J. *et al.* Twist, a master regulator of morphogenesis, plays an essential role in tumor metastasis. *Cell* **117**, 927-939, doi:10.1016/j.cell.2004.06.006 (2004).

85 Takeyama, Y. *et al.* Knockdown of ZEB1, a master epithelial-to-mesenchymal transition (EMT) gene, suppresses anchorage-independent cell growth of lung cancer cells. *Cancer Lett* **296**, 216-224, doi:10.1016/j.canlet.2010.04.008 (2010).

86 Kwok, W. K. *et al.* Up-regulation of TWIST in prostate cancer and its implication as a therapeutic target. *Cancer Res* **65**, 5153-5162, doi:10.1158/0008-5472.can-04-3785 (2005).

87 Egan, K., Cooke, N. & Kenny, D. Living in shear: platelets protect cancer cells from shear induced damage. *Clin Exp Metastasis* **31**, 697-704, doi:10.1007/s10585-014-9660-7 (2014).

88 Mitchell, M. J. & King, M. R. Fluid Shear Stress Sensitizes Cancer Cells to Receptor-Mediated Apoptosis via Trimeric Death Receptors. *New journal of physics* **15**, 015008, doi:10.1088/1367-2630/15/1/015008 (2013).

89 Chang, S. F. *et al.* Tumor cell cycle arrest induced by shear stress: Roles of integrins and Smad. *Proc Natl Acad Sci U S A* **105**, 3927-3932, doi:10.1073/pnas.0712353105 (2008).

90 Zhang, L. *et al.* The identification and characterization of breast cancer CTCs competent for brain metastasis. *Sci Transl Med* **5**, 180ra148, doi:10.1126/scitranslmed.3005109 (2013).

91 Morozevich, G. E., Kozlova, N. I., Chubukina, A. N. & Berman, A. E. Role of integrin alphavbeta3 in substrate-dependent apoptosis of human intestinal carcinoma cells. *Biochemistry (Mosc)* **68**, 416-423 (2003).

92 Zheng, D. Q., Woodard, A. S., Fornaro, M., Tallini, G. & Languino, L. R. Prostatic carcinoma cell migration via alpha(v)beta3 integrin is modulated by a focal adhesion kinase pathway. *Cancer Res* **59**, 1655-1664 (1999).

93 Janes, S. M. & Watt, F. M. Switch from alphavbeta5 to alphavbeta6 integrin expression protects squamous cell carcinomas from anoikis. *J Cell Biol* **166**, 419-431, doi:10.1083/jcb.200312074 (2004).

94 Bon, G. *et al.* Loss of beta4 integrin subunit reduces the tumorigenicity of MCF7 mammary cells and causes apoptosis upon hormone deprivation. *Clin Cancer Res* **12**, 3280-3287, doi:10.1158/1078-0432.CCR-05-2223 (2006).

95 Jirouskova, M., Shet, A. S. & Johnson, G. J. A guide to murine platelet structure, function, assays, and genetic alterations. *J Thromb Haemost* **5**, 661-669, doi:10.1111/j.1538-7836.2007.02407.x (2007).

96 Kaushansky, K. Lineage-specific hematopoietic growth factors. *N Engl J Med* **354**, 2034-2045, doi:10.1056/NEJMra052706 (2006).

97 Diacovo, T. G., Roth, S. J., Buccola, J. M., Bainton, D. F. & Springer, T. A. Neutrophil rolling, arrest, and transmigration across activated, surface-adherent platelets via sequential action of P-selectin and the beta 2-integrin CD11b/CD18. *Blood* **88**, 146-157 (1996).

98 Folkman, J., Browder, T. & Palmblad, J. Angiogenesis research: guidelines for translation to clinical application. *Thromb Haemost* **86**, 23-33 (2001).

99 Thon, J. N. & Italiano, J. E. Platelets: production, morphology and ultrastructure. *Handb Exp Pharmacol*, 3-22, doi:10.1007/978-3-642-29423-5_1 (2012).

100 Bauer, M. *et al.* Dichotomous regulation of myosin phosphorylation and shape change by Rho-kinase and calcium in intact human platelets. *Blood* **94**, 1665-1672 (1999).

101 George, J. N. Platelets. *Lancet* **355**, 1531-1539, doi:10.1016/s0140-6736(00)02175-9 (2000).

102 Schenone, M., Furie, B. C. & Furie, B. The blood coagulation cascade. *Current Opinion in Hematology* **11**, 272-277, doi:DOI 10.1097/01.moh.0000130308.37353.d4 (2004).

103 Labelle, M., Begum, S. & Hynes, R. O. Platelets guide the formation of early metastatic niches. *Proc Natl Acad Sci U S A* **111**, E3053-3061, doi:10.1073/pnas.1411082111 (2014).

104 Mackman, N. Role of tissue factor in hemostasis, thrombosis, and vascular development. *Arteriosclerosis, thrombosis, and vascular biology* **24**, 1015-1022, doi:10.1161/01.atv.0000130465.23430.74 (2004).

105 Eilertsen, K. E. & Osterud, B. Tissue factor: (patho)physiology and cellular biology. *Blood Coagul Fibrin* **15**, 521-538, doi:Doi 10.1097/00001721-200410000-00001 (2004).

106 Furie, B. & Furie, B. C. Mechanisms of thrombus formation. *N Engl J Med* **359**, 938-949, doi:10.1056/NEJMra0801082 (2008).

107 Semeraro, N. *et al.* Direct induction of tissue factor synthesis by endotoxin in human macrophages from diverse anatomical sites. *Immunology* **50**, 529-535 (1983).

108 Bevilacqua, M. P., Pober, J. S., Majeau, G. R., Cotran, R. S. & Gimbrone, M. A., Jr. Interleukin 1 (IL-1) induces biosynthesis and cell surface expression of procoagulant activity in human vascular endothelial cells. *J Exp Med* **160**, 618-623 (1984).

109 Callander, N. S., Varki, N. & Rao, L. V. Immunohistochemical identification of tissue factor in solid tumors. *Cancer* **70**, 1194-1201 (1992).

110 Contrino, J., Hair, G., Kreutzer, D. L. & Rickles, F. R. In situ detection of tissue factor in vascular endothelial cells: correlation with the malignant phenotype of human breast disease. *Nat Med* **2**, 209-215 (1996).

111 Vrana, J. A., Stang, M. T., Grande, J. P. & Getz, M. J. Expression of tissue factor in tumor stroma correlates with progression to invasive human breast cancer: paracrine regulation by carcinoma cell-derived members of the transforming growth factor beta family. *Cancer Res* **56**, 5063-5070 (1996).

112 Allford, S. L. & Machin, S. J. Haemostasis. *Surgery (Oxford)* **25**, 241-244, doi:http://dx.doi.org/10.1016/j.mpsur.2007.05.002 (2007).

113 Gil-Bernabe, A. M., Lucotti, S. & Muschel, R. J. Coagulation and metastasis: what does the experimental literature tell us? *Br J Haematol* **162**, 433-441, doi:10.1111/bjh.12381 (2013).

114 de Groot, P. G., Urbanus, R. T. & Roest, M. Platelet interaction with the vessel wall. *Handb Exp Pharmacol*, 87-110, doi:10.1007/978-3-642-29423-5_4 (2012).

115 Felding-Habermann, B. *et al.* Integrin activation controls metastasis in human breast cancer. *Proc Natl Acad Sci U S A* **98**, 1853-1858, doi:10.1073/pnas.98.4.1853 (2001).

116 Falanga, A., Panova-Noeva, M. & Russo, L. Procoagulant mechanisms in tumour cells. *Best Pract Res Clin Haematol* **22**, 49-60, doi:10.1016/j.beha.2008.12.009 (2009).

117 Falati, S. *et al.* Accumulation of tissue factor into developing thrombi in vivo is dependent upon microparticle P-selectin glycoprotein ligand 1 and platelet P-selectin. *Journal of Experimental Medicine* **197**, 1585-1598, doi:10.1084/jem.20021868 (2003).

118 Furie, B. & Furie, B. C. Thrombus formation in vivo. *Journal of Clinical Investigation* **115**, 3355-3362, doi:10.1172/Jci26987 (2005).

119 Laubli, H., Spanaus, K. S. & Borsig, L. Selectin-mediated activation of endothelial cells induces expression of CCL5 and promotes metastasis through recruitment of monocytes. *Blood* **114**, 4583-4591, doi:10.1182/blood-2008-10-186585 (2009).

120 Furie, B., Furie, B. C. & Flaumenhaft, R. A journey with platelet P-selectin: The molecular basis of granule secretion, signalling and cell adhesion. *Thromb Haemostasis* **86**, 214-221 (2001).

121 Shao, B. *et al.* Carcinoma mucins trigger reciprocal activation of platelets and neutrophils in a murine model of Trousseau syndrome. *Blood* **118**, 4015-4023, doi:10.1182/blood-2011-07-368514 (2011).

122 Zwicker, J. I. *et al.* Trousseau's syndrome revisited: Tissue factor-bearing microparticles in pancreatic cancer. *Blood* **106**, 79a-79a (2005).

123 Mesri, M. & Altieri, D. C. Leukocyte microparticles stimulate endothelial cell cytokine release and tissue factor induction in a JNK1 signaling pathway. *Journal of Biological Chemistry* **274**, 23111-23118, doi:DOI 10.1074/jbc.274.33.23111 (1999).

124 Biro, E. *et al.* Human cell-derived microparticles promote thrombus formation in vivo in a tissue factor-dependent manner. *Journal of Thrombosis and Haemostasis* **1**, 2561-2568, doi:DOI 10.1046/j.1538-7836.2003.00456.x (2003).

125 Falati, S. *et al.* Accumulation of tissue factor into developing thrombi in vivo is dependent upon microparticle P-selectin glycoprotein ligand 1 and platelet P-selectin. *J Exp Med* **197**, 1585-1598, doi:10.1084/jem.20021868 (2003).

126 Kirchhofer, D., Tschopp, T. B., Hadvary, P. & Baumgartner, H. R. Endothelial-Cells Stimulated with Tumor-Necrosis-Factor-Alpha Express Varying Amounts of Tissue Factor Resulting in Inhomogenous Fibrin Deposition in a Native Blood-Flow System - Effects of Thrombin Inhibitors. *Journal of Clinical Investigation* **93**, 2073-2083, doi:Doi 10.1172/Jci117202 (1994).

127 Wagner, J. G. & Roth, R. A. Neutrophil migration mechanisms, with an emphasis on the pulmonary vasculature. *Pharmacol Rev* **52**, 349-374 (2000).

128 Chambers, A. F., Groom, A. C. & MacDonald, I. C. Dissemination and growth of cancer cells in metastatic sites. *Nat Rev Cancer* **2**, 563-572, doi:10.1038/nrc865 (2002).

129 Hiratsuka, S. *et al.* Endothelial focal adhesion kinase mediates cancer cell homing to discrete regions of the lungs via E-selectin up-regulation. *Proc Natl Acad Sci U S A* **108**, 3725-3730, doi:10.1073/pnas.1100446108 (2011).

130 Zarbock, A., Ley, K., McEver, R. P. & Hidalgo, A. Leukocyte ligands for endothelial selectins: specialized glycoconjugates that mediate rolling and signaling under flow. *Blood* **118**, 6743-6751, doi:10.1182/blood-2011-07-343566 (2011).

131 Bevilacqua, M. P. & Nelson, R. M. Selectins. *J Clin Invest* **91**, 379-387, doi:10.1172/jci116210 (1993).

132 Cheung, L. S., Raman, P. S., Balzer, E. M., Wirtz, D. & Konstantopoulos, K. Biophysics of selectin-ligand interactions in inflammation and cancer. *Phys Biol* **8**, 015013, doi:10.1088/1478-3975/8/1/015013 (2011).

133 Ludwig, R. J. *et al.* Endothelial P-selectin as a target of heparin action in experimental melanoma lung metastasis. *Cancer Res* **64**, 2743-2750 (2004).

134 Napier, S. L., Healy, Z. R., Schnaar, R. L. & Konstantopoulos, K. Selectin ligand expression regulates the initial vascular interactions of colon carcinoma cells: the roles of CD44v and alternative sialofucosylated selectin ligands. *J Biol Chem* **282**, 3433-3441, doi:10.1074/jbc.M607219200 (2007).

135 Gay, L. J. & Felding-Habermann, B. Contribution of platelets to tumour metastasis. *Nat Rev Cancer* **11**, 123-134, doi:10.1038/nrc3004 (2011).

136 Morigi, M. *et al.* Fluid shear stress modulates surface expression of adhesion molecules by endothelial cells. *Blood* **85**, 1696-1703 (1995).

137 Kansas, G. S. Selectins and their ligands: current concepts and controversies. *Blood* **88**, 3259-3287 (1996).

138 St Hill, C. A. Interactions between endothelial selectins and cancer cells regulate metastasis. *Frontiers in bioscience (Landmark edition)* **16**, 3233-3251 (2011).

139 Eichbaum, C. *et al.* Breast cancer cell-derived cytokines, macrophages and cell adhesion: implications for metastasis. *Anticancer Res* **31**, 3219-3227 (2011).

140 Auguste, P. *et al.* The host inflammatory response promotes liver metastasis by increasing tumor cell arrest and extravasation. *Am J Pathol* **170**, 1781-1792, doi:10.2353/ajpath.2007.060886 (2007).

141 Schlesinger, M. & Bendas, G. Vascular cell adhesion molecule-1 (VCAM-1)--an increasing insight into its role in tumorigenicity and metastasis. *Int J Cancer* **136**, 2504-2514, doi:10.1002/ijc.28927 (2015).

142 Pober, J. S. Endothelial activation: intracellular signaling pathways. *Arthritis Res* **4 Suppl 3**, S109-116, doi:10.1186/ar576 (2002).

143 Shirure, V. S., Reynolds, N. M. & Burdick, M. M. Mac-2 binding protein is a novel E-selectin ligand expressed by breast cancer cells. *PLoS One* **7**, e44529, doi:10.1371/journal.pone.0044529 (2012).

144 Strell, C. & Entschladen, F. Extravasation of leukocytes in comparison to tumor cells. *Cell Commun Signal* **6**, 10, doi:10.1186/1478-811X-6-10 (2008).

145 Miles, F. L., Pruitt, F. L., van Golen, K. L. & Cooper, C. R. Stepping out of the flow: capillary extravasation in cancer metastasis. *Clin Exp Metastasis* **25**, 305-324, doi:10.1007/s10585-007-9098-2 (2008).

146 Ferjancic, S. *et al.* VCAM-1 and VAP-1 recruit myeloid cells that promote pulmonary metastasis in mice. *Blood* **121**, 3289-3297, doi:10.1182/blood-2012-08-449819 (2013).

147 Wawryk, S. O. *et al.* The role of the LFA-1/ICAM-1 interaction in human leukocyte homing and adhesion. *Immunol Rev* **108**, 135-161 (1989).

148 Wu, Q. D., Wang, J. H., Condron, C., Bouchier-Hayes, D. & Redmond, H. P. Human neutrophils facilitate tumor cell transendothelial migration. *Am J Physiol Cell Physiol* **280**, C814-822 (2001).

149 Okahara, H., Yagita, H., Miyake, K. & Okumura, K. Involvement of very late activation antigen 4 (VLA-4) and vascular cell adhesion molecule 1 (VCAM-1) in tumor necrosis factor alpha enhancement of experimental metastasis. *Cancer Res* **54**, 3233-3236 (1994).

150 Garofalo, A. *et al.* Involvement of the very late antigen 4 integrin on melanoma in interleukin 1-augmented experimental metastases. *Cancer Res* **55**, 414-419 (1995).

151 Reymond, N., d'Agua, B. B. & Ridley, A. J. Crossing the endothelial barrier during metastasis. *Nat Rev Cancer* **13**, 858-870, doi:10.1038/nrc3628 (2013).

152 Barthel, S. R. *et al.* Definition of molecular determinants of prostate cancer cell bone extravasation. *Cancer Res* **73**, 942-952, doi:10.1158/0008-5472.CAN-12-3264 (2013).

153 Kawakami-Kimura, N. *et al.* Involvement of hepatocyte growth factor in increased integrin expression on HepG2 cells triggered by adhesion to endothelial cells. *Br J Cancer* **75**, 47-53 (1997).

154 Laferriere, J., Houle, F. & Huot, J. Adhesion of HT-29 colon carcinoma cells to endothelial cells requires sequential events involving E-selectin and integrin beta4. *Clin Exp Metastasis* **21**, 257-264 (2004).

155 Wang, X., Scott, E., Sawyers, C. L. & Friedman, A. D. C/EBPalpha bypasses granulocyte colony-stimulating factor signals to rapidly induce PU.1 gene expression, stimulate granulocytic differentiation, and limit proliferation in 32D cl3 myeloblasts. *Blood* **94**, 560-571 (1999).

156 Wiktor-Jedrzejczak, W. & Gordon, S. Cytokine regulation of the macrophage (M phi) system studied using the colony stimulating factor-1-deficient op/op mouse. *Physiological reviews* **76**, 927-947 (1996).

157 Stanley, E. R., Guilbert, L. J., Tushinski, R. J. & Bartelmez, S. H. CSF-1--a mononuclear phagocyte lineage-specific hemopoietic growth factor. *J Cell Biochem* **21**, 151-159, doi:10.1002/jcb.240210206 (1983).

158 Borregaard, N. Neutrophils, from marrow to microbes. *Immunity* **33**, 657-670, doi:10.1016/j.immuni.2010.11.011 (2010).

159 Mantovani, A., Cassatella, M. A., Costantini, C. & Jaillon, S. Neutrophils in the activation and regulation of innate and adaptive immunity. *Nat Rev Immunol* **11**, 519-531, doi:10.1038/nri3024 (2011).

160 Kolaczkowska, E. & Kubes, P. Neutrophil recruitment and function in health and inflammation. *Nat Rev Immunol* **13**, 159-175, doi:10.1038/nri3399 (2013).

161 Arndt, H., Bolanowski, M. A. & Granger, D. N. Role of interleukin 8 on leucocyte-endothelial cell adhesion in intestinal inflammation. *Gut* **38**, 911-915, doi:DOI 10.1136/gut.38.6.911 (1996).

162 Huh, S. J., Liang, S., Sharma, A., Dong, C. & Robertson, G. P. Transiently entrapped circulating tumor cells interact with neutrophils to facilitate lung metastasis development. *Cancer Res* **70**, 6071-6082, doi:10.1158/0008-5472.can-09-4442 (2010).

163 Diamond, M. S. & Springer, T. A. The dynamic regulation of integrin adhesiveness. *Curr Biol* **4**, 506-517 (1994).

164 Detmers, P. A. *et al.* Neutrophil-activating protein 1/interleukin 8 stimulates the binding activity of the leukocyte adhesion receptor CD11b/CD18 on human neutrophils. *J Exp Med* **171**, 1155-1162 (1990).

165 Bainton, D. F., Miller, L. J., Kishimoto, T. K. & Springer, T. A. Leukocyte adhesion receptors are stored in peroxidase-negative granules of human neutrophils. *J Exp Med* **166**, 1641-1653 (1987).

166 Slattery, M. J. & Dong, C. Neutrophils influence melanoma adhesion and migration under flow conditions. *Int J Cancer* **106**, 713-722, doi:10.1002/ijc.11297 (2003).

167 Randolph, G. J., Beaulieu, S., Lebecque, S., Steinman, R. M. & Muller, W. A. Differentiation of monocytes into dendritic cells in a model of transendothelial trafficking. *Science* **282**, 480-483 (1998).

168 Gordon, S. & Taylor, P. R. Monocyte and macrophage heterogeneity. *Nat Rev Immunol* **5**, 953-964, doi:10.1038/nri1733 (2005).

169 Bousso, P. T-cell activation by dendritic cells in the lymph node: lessons from the movies. *Nature Reviews Immunology* **8**, 675-684, doi:10.1038/nri2379 (2008).

170 Passlick, B., Flieger, D. & Ziegler-Heitbrock, H. W. Identification and characterization of a novel monocyte subpopulation in human peripheral blood. *Blood* **74**, 2527-2534 (1989).

171 Geissmann, F., Jung, S. & Littman, D. R. Blood monocytes consist of two principal subsets with distinct migratory properties. *Immunity* **19**, 71-82 (2003).

172 Gordon, S. Alternative activation of macrophages. *Nat Rev Immunol* **3**, 23-35, doi:10.1038/nri978 (2003).

173 Engblom, C., Pfirschke, C. & Pittet, M. J. The role of myeloid cells in cancer therapies. *Nat Rev Cancer* **16**, 447-462, doi:10.1038/nrc.2016.54 (2016).

174 Palframan, R. T. *et al.* Inflammatory chemokine transport and presentation in HEV: a remote control mechanism for monocyte recruitment to lymph nodes in inflamed tissues. *J Exp Med* **194**, 1361-1373 (2001).

175 Sunderkotter, C. *et al.* Subpopulations of mouse blood monocytes differ in maturation stage and inflammatory response. *J Immunol* **172**, 4410-4417 (2004).

176 Qian, B. Z. *et al.* CCL2 recruits inflammatory monocytes to facilitate breast-tumour metastasis. *Nature* **475**, 222-225, doi:10.1038/nature10138 (2011).

177 Ushach, I. & Zlotnik, A. Biological role of granulocyte macrophage colony-stimulating factor (GM-CSF) and macrophage colony-stimulating factor (M-CSF) on cells of the myeloid lineage. *J Leukoc Biol*, doi:10.1189/jlb.3RU0316-144R (2016).

178 Smith, H. O. *et al.* The role of colony-stimulating factor 1 and its receptor in the etiopathogenesis of endometrial adenocarcinoma. *Clin Cancer Res* **1**, 313-325 (1995).

179 Kacinski, B. M. CSF-1 and its receptor in ovarian, endometrial and breast cancer. *Annals of medicine* **27**, 79-85 (1995).

180 Lin, E. Y., Nguyen, A. V., Russell, R. G. & Pollard, J. W. Colony-stimulating factor 1 promotes progression of mammary tumors to malignancy. *J Exp Med* **193**, 727-740 (2001).

181 Chen, Q., Zhang, X. H. & Massague, J. Macrophage binding to receptor VCAM-1 transmits survival signals in breast cancer cells that invade the lungs. *Cancer Cell* **20**, 538-549, doi:10.1016/j.ccr.2011.08.025 (2011).

182 Ding, Y. B. *et al.* Association of VCAM-1 overexpression with oncogenesis, tumor angiogenesis and metastasis of gastric carcinoma. *World J Gastroenterol* **9**, 1409-1414 (2003).

183 Ruco, L. P. *et al.* Expression of ICAM-1 and VCAM-1 in human malignant mesothelioma. *J Pathol* **179**, 266-271, doi:10.1002/(SICI)1096-9896(199607)179:3<266::AID-PATH592>3.0.CO;2-Y (1996).

184 Shin, J., Kim, J., Ryu, B., Chi, S. G. & Park, H. Caveolin-1 is associated with VCAM-1 dependent adhesion of gastric cancer cells to endothelial cells. *Cellular physiology and biochemistry : international journal of experimental cellular physiology, biochemistry, and pharmacology* **17**, 211-220, doi:10.1159/000094126 (2006).

185 Minn, A. J. *et al.* Lung metastasis genes couple breast tumor size and metastatic spread. *Proc Natl Acad Sci U S A* **104**, 6740-6745, doi:10.1073/pnas.0701138104 (2007).

186 Massberg, S. *et al.* Platelets secrete stromal cell-derived factor 1alpha and recruit bone marrow-derived progenitor cells to arterial thrombi in vivo. *J Exp Med* **203**, 1221-1233, doi:10.1084/jem.20051772 (2006).

187 Labelle, M. & Hynes, R. O. The initial hours of metastasis: the importance of cooperative host-tumor cell interactions during hematogenous dissemination. *Cancer Discov* **2**, 1091-1099, doi:10.1158/2159-8290.CD-12-0329 (2012).
188 Dole, V. S., Bergmeier, W., Mitchell, H. A., Eichenberger, S. C. & Wagner, D. D. Activated platelets induce Weibel-Palade-body secretion and leukocyte rolling in vivo: role of P-selectin. *Blood* **106**, 2334-2339, doi:10.1182/blood-2005-04-1530 (2005).
189 Ludwig, R. J. *et al.* Activated, not resting, platelets increase leukocyte rolling in murine skin utilizing a distinct set of adhesion molecules. *J Invest Dermatol* **122**, 830-836, doi:10.1111/j.0022-202X.2004.22318.x (2004).
190 Huo, Y. *et al.* Circulating activated platelets exacerbate atherosclerosis in mice deficient in apolipoprotein E. *Nat Med* **9**, 61-67, doi:10.1038/nm810 (2003).
191 Muller, W. A. The regulation of transendothelial migration: new knowledge and new questions. *Cardiovasc Res* **107**, 310-320, doi:10.1093/cvr/cvv145 (2015).
192 Carman, C. V. & Springer, T. A. Trans-cellular migration: cell-cell contacts get intimate. *Curr Opin Cell Biol* **20**, 533-540, doi:10.1016/j.ceb.2008.05.007 (2008).
193 Tremblay, P. L., Huot, J. & Auger, F. A. Mechanisms by which E-selectin regulates diapedesis of colon cancer cells under flow conditions. *Cancer Res* **68**, 5167-5176, doi:10.1158/0008-5472.CAN-08-1229 (2008).
194 Khuon, S. *et al.* Myosin light chain kinase mediates transcellular intravasation of breast cancer cells through the underlying endothelial cells: a three-dimensional FRET study. *J Cell Sci* **123**, 431-440, doi:10.1242/jcs.053793 (2010).
195 Egawa, G. *et al.* Intravital analysis of vascular permeability in mice using two-photon microscopy. *Scientific reports* **3**, doi:ARTN 1932
10.1038/srep01932 (2013).
196 Dejana, E. & Orsenigo, F. Endothelial adherens junctions at a glance. *J Cell Sci* **126**, 2545-2549, doi:10.1242/jcs.124529 (2013).
197 Garcia-Roman, J. & Zentella-Dehesa, A. Vascular permeability changes involved in tumor metastasis. *Cancer Lett* **335**, 259-269, doi:10.1016/j.canlet.2013.03.005 (2013).
198 Bazzoni, G. & Dejana, E. Endothelial cell-to-cell junctions: molecular organization and role in vascular homeostasis. *Physiological reviews* **84**, 869-901, doi:10.1152/physrev.00035.2003 (2004).
199 Nitta, T. *et al.* Size-selective loosening of the blood-brain barrier in claudin-5-deficient mice. *J Cell Biol* **161**, 653-660, doi:10.1083/jcb.200302070 (2003).
200 Lee, T. H., Avraham, H. K., Jiang, S. & Avraham, S. Vascular endothelial growth factor modulates the transendothelial migration of MDA-MB-231 breast cancer cells through regulation of brain microvascular endothelial cell permeability. *J Biol Chem* **278**, 5277-5284, doi:10.1074/jbc.M210063200 (2003).
201 Honn, K. V. *et al.* Enhanced endothelial cell retraction mediated by 12(S)-HETE: a proposed mechanism for the role of platelets in tumor cell metastasis. *Exp Cell Res* **210**, 1-9, doi:10.1006/excr.1994.1001 (1994).
202 Honn, K. V., Grossi, I. M., Diglio, C. A., Wojtukiewicz, M. & Taylor, J. D. Enhanced tumor cell adhesion to the subendothelial matrix resulting from 12(S)-HETE-induced endothelial cell retraction. *FASEB J* **3**, 2285-2293 (1989).
203 Honn, K. V. *et al.* Tumor cell-derived 12(S)-hydroxyeicosatetraenoic acid induces microvascular endothelial cell retraction. *Cancer Res* **54**, 565-574 (1994).
204 el-Sabban, M. E. & Pauli, B. U. Cytoplasmic dye transfer between metastatic tumor cells and vascular endothelium. *J Cell Biol* **115**, 1375-1382 (1991).
205 Wolf, M. J. *et al.* Endothelial CCR2 signaling induced by colon carcinoma cells enables extravasation via the JAK2-Stat5 and p38MAPK pathway. *Cancer Cell* **22**, 91-105, doi:10.1016/j.ccr.2012.05.023 (2012).
206 Tang, D. G., Diglio, C. A. & Honn, K. V. 12(S)-HETE-induced microvascular endothelial cell retraction results from PKC-dependent rearrangement of cytoskeletal elements and alpha V beta 3 integrins. *Prostaglandins* **45**, 249-267 (1993).
207 Li, B. *et al.* Involvement of Rho/ROCK signalling in small cell lung cancer migration through human brain microvascular endothelial cells. *FEBS Lett* **580**, 4252-4260, doi:10.1016/j.febslet.2006.06.056 (2006).
208 Tremblay, P. L., Auger, F. A. & Huot, J. Regulation of transendothelial migration of colon cancer cells by E-selectin-mediated activation of p38 and ERK MAP kinases. *Oncogene* **25**, 6563-6573, doi:10.1038/sj.onc.1209664 (2006).

209 Simoneau, B., Houle, F. & Huot, J. Regulation of endothelial permeability and transendothelial migration of cancer cells by tropomyosin-1 phosphorylation. *Vasc Cell* **4**, 18, doi:10.1186/2045-824X-4-18 (2012).

210 Kebers, F. *et al.* Induction of endothelial cell apoptosis by solid tumor cells. *Exp Cell Res* **240**, 197-205, doi:10.1006/excr.1998.3935 (1998).

211 Strilic, B. *et al.* Tumour-cell-induced endothelial cell necroptosis via death receptor 6 promotes metastasis. *Nature* **536**, 215-218, doi:10.1038/nature19076 (2016).

212 Ridley, A. J. Life at the Leading Edge. *Cell* **145**, 1012-1022, doi:10.1016/j.cell.2011.06.010 (2011).

213 Ridley, A. J. Life at the leading edge. *Cell* **145**, 1012-1022, doi:10.1016/j.cell.2011.06.010 (2011).

214 Poincloux, R., Lizarraga, F. & Chavrier, P. Matrix invasion by tumour cells: a focus on MT1-MMP trafficking to invadopodia. *J Cell Sci* **122**, 3015-3024, doi:10.1242/jcs.034561 (2009).

215 Reymond, N. *et al.* Cdc42 promotes transendothelial migration of cancer cells through beta1 integrin. *J Cell Biol* **199**, 653-668, doi:10.1083/jcb.201205169 (2012).

216 Sequeira, L., Dubyk, C. W., Riesenberger, T. A., Cooper, C. R. & van Golen, K. L. Rho GTPases in PC-3 prostate cancer cell morphology, invasion and tumor cell diapedesis. *Clin Exp Metastasis* **25**, 569-579, doi:10.1007/s10585-008-9173-3 (2008).

217 Huang, Y. *et al.* Pulmonary vascular destabilization in the premetastatic phase facilitates lung metastasis. *Cancer Res* **69**, 7529-7537, doi:10.1158/0008-5472.can-08-4382 (2009).

218 Malanchi, I. *et al.* Interactions between cancer stem cells and their niche govern metastatic colonization. *Nature* **481**, 85-89, doi:10.1038/nature10694 (2012).

219 Oskarsson, T. *et al.* Breast cancer cells produce tenascin C as a metastatic niche component to colonize the lungs. *Nat Med* **17**, 867-874, doi:10.1038/nm.2379 (2011).

220 Levental, K. R. *et al.* Matrix crosslinking forces tumor progression by enhancing integrin signaling. *Cell* **139**, 891-906, doi:10.1016/j.cell.2009.10.027 (2009).

221 Cox, T. R. *et al.* LOX-mediated collagen crosslinking is responsible for fibrosis-enhanced metastasis. *Cancer Res* **73**, 1721-1732, doi:10.1158/0008-5472.can-12-2233 (2013).

222 Chao, Y. L., Shepard, C. R. & Wells, A. Breast carcinoma cells re-express E-cadherin during mesenchymal to epithelial reverting transition. *Mol Cancer* **9**, 179, doi:10.1186/1476-4598-9-179 (2010).

223 Brabletz, T. *et al.* Variable beta-catenin expression in colorectal cancers indicates tumor progression driven by the tumor environment. *Proc Natl Acad Sci U S A* **98**, 10356-10361, doi:10.1073/pnas.171610498 (2001).

224 Korpal, M. *et al.* Direct targeting of Sec23a by miR-200s influences cancer cell secretome and promotes metastatic colonization. *Nat Med* **17**, 1101-1108, doi:10.1038/nm.2401 (2011).

225 Pattabiraman, D. R. *et al.* Activation of PKA leads to mesenchymal-to-epithelial transition and loss of tumor-initiating ability. *Science* **351**, aad3680, doi:10.1126/science.aad3680 (2016).

226 Stankic, M. *et al.* TGF-beta-Id1 signaling opposes Twist1 and promotes metastatic colonization via a mesenchymal-to-epithelial transition. *Cell Rep* **5**, 1228-1242, doi:10.1016/j.celrep.2013.11.014 (2013).

227 Pantel, K. *et al.* Frequency and prognostic significance of isolated tumour cells in bone marrow of patients with non-small-cell lung cancer without overt metastases. *Lancet* **347**, 649-653 (1996).

228 Ghajar, C. M. Metastasis prevention by targeting the dormant niche. *Nat Rev Cancer* **15**, 238-247, doi:10.1038/nrc3910 (2015).

229 Ghajar, C. M. *et al.* The perivascular niche regulates breast tumour dormancy. *Nat Cell Biol* **15**, 807-817, doi:10.1038/ncb2767 (2013).

230 Naumov, G. N. *et al.* Ineffectiveness of doxorubicin treatment on solitary dormant mammary carcinoma cells or late-developing metastases. *Breast Cancer Res Treat* **82**, 199-206, doi:10.1023/B:BREA.0000004377.12288.3c (2003).

231 Janni, W. *et al.* Persistence of disseminated tumor cells in the bone marrow of breast cancer patients predicts increased risk for relapse--a European pooled analysis. *Clin Cancer Res* **17**, 2967-2976, doi:10.1158/1078-0432.CCR-10-2515 (2011).

232 Krawczyk, N. *et al.* HER2 status on persistent disseminated tumor cells after adjuvant therapy may differ from initial HER2 status on primary tumor. *Anticancer Res* **29**, 4019-4024 (2009).

233 Braun, S. *et al.* Lack of effect of adjuvant chemotherapy on the elimination of single dormant tumor cells in bone marrow of high-risk breast cancer patients. *J Clin Oncol* **18**, 80-86 (2000).

234 Khorana, A. A. & Connolly, G. C. Assessing Risk of Venous Thromboembolism in the Patient With Cancer. *Journal of Clinical Oncology* **27**, 4839-4847, doi:10.1200/Jco.2009.22.3271 (2009).

235 Palumbo, J. S. Mechanisms linking tumor cell-associated procoagulant function to tumor dissemination. *Seminars in Thrombosis and Hemostasis* **34**, 154-160, doi:10.1055/s-2008-1079255 (2008).

236 Heit, J. A. Cancer and venous thromboembolism: scope of the problem. *Cancer control : journal of the Moffitt Cancer Center* **12 Suppl 1**, 5-10 (2005).

237 Mueller, B. M. & Ruf, W. Requirement for binding of catalytically active factor VIIa in tissue factor-dependent experimental metastasis. *J Clin Invest* **101**, 1372-1378, doi:10.1172/JCI930 (1998).

238 Mueller, B. M., Reisfeld, R. A., Edgington, T. S. & Ruf, W. Expression of tissue factor by melanoma cells promotes efficient hematogenous metastasis. *Proc Natl Acad Sci U S A* **89**, 11832-11836 (1992).

239 Hembrough, T. A. *et al.* Tissue factor/factor VIIa inhibitors block angiogenesis and tumor growth through a nonhemostatic mechanism. *Cancer Res* **63**, 2997-3000 (2003).

240 Bromberg, M. E., Sundaram, R., Homer, R. J., Garen, A. & Konigsberg, W. H. Role of tissue factor in metastasis: functions of the cytoplasmic and extracellular domains of the molecule. *Thromb Haemost* **82**, 88-92 (1999).

241 Bromberg, M. E., Konigsberg, W. H., Madison, J. F., Pawashe, A. & Garen, A. Tissue factor promotes melanoma metastasis by a pathway independent of blood coagulation. *Proc Natl Acad Sci U S A* **92**, 8205-8209 (1995).

242 Bromberg, M. E., Bailly, M. A. & Konigsberg, W. H. Role of protease-activated receptor 1 in tumor metastasis promoted by tissue factor. *Thromb Haemost* **86**, 1210-1214 (2001).

243 Gasic, G. J., Gasic, T. B., Galanti, N., Johnson, T. & Murphy, S. Platelet-tumor-cell interactions in mice. The role of platelets in the spread of malignant disease. *International journal of cancer. Journal international du cancer* **11**, 704-718 (1973).

244 Gasic, G. J., Gasic, T. B. & Stewart, C. C. Antimetastatic effects associated with platelet reduction. *Proc Natl Acad Sci U S A* **61**, 46-52 (1968).

245 Palumbo, J. S. *et al.* Platelets and fibrin(ogen) increase metastatic potential by impeding natural killer cell-mediated elimination of tumor cells. *Blood* **105**, 178-185, doi:10.1182/blood-2004-06-2272 (2005).

246 Pearlstein, E., Ambrogio, C. & Karpatkin, S. Effect of antiplatelet antibody on the development of pulmonary metastases following injection of CT26 colon adenocarcinoma, Lewis lung carcinoma, and B16 amelanotic melanoma tumor cells into mice. *Cancer Res* **44**, 3884-3887 (1984).

247 Karpatkin, S., Pearlstein, E., Ambrogio, C. & Coller, B. S. Role of adhesive proteins in platelet tumor interaction in vitro and metastasis formation in vivo. *J Clin Invest* **81**, 1012-1019, doi:10.1172/JCI113411 (1988).

248 Nierodzik, M. L., Plotkin, A., Kajumo, F. & Karpatkin, S. Thrombin stimulates tumor-platelet adhesion in vitro and metastasis in vivo. *J Clin Invest* **87**, 229-236, doi:10.1172/jci114976 (1991).

249 Camerer, E. *et al.* Platelets, protease-activated receptors, and fibrinogen in hematogenous metastasis. *Blood* **104**, 397-401, doi:10.1182/blood-2004-02-0434 (2004).

250 Offermanns, S., Toombs, C. F., Hu, Y. H. & Simon, M. I. Defective platelet activation in G alpha(q)-deficient mice. *Nature* **389**, 183-186, doi:10.1038/38284 (1997).

251 Jain, S. *et al.* Platelet glycoprotein Ib alpha supports experimental lung metastasis. *Proc Natl Acad Sci U S A* **104**, 9024-9028, doi:10.1073/pnas.0700625104 (2007).

252 Connolly, A. J., Ishihara, H., Kahn, M. L., Farese, R. V., Jr. & Coughlin, S. R. Role of the thrombin receptor in development and evidence for a second receptor. *Nature* **381**, 516-519, doi:10.1038/381516a0 (1996).

253 Shivdasani, R. A. *et al.* Transcription factor NF-E2 is required for platelet formation independent of the actions of thrombopoietin/MGDF in megakaryocyte development. *Cell* **81**, 695-704 (1995).

254 Stenberg, P. E., Levin, J., Baker, G., Mok, Y. & Corash, L. Neuraminidase-induced thrombocytopenia in mice: effects on thrombopoiesis. *J Cell Physiol* **147**, 7-16, doi:10.1002/jcp.1041470103 (1991).

255 Choi, S. I., Simone, J. V. & Jorney, L. J. Neuraminidase-induced thrombocytopenia in rats. *Br J Haematol* **22**, 93-101 (1972).

256 Erpenbeck, L., Nieswandt, B., Schon, M., Pozgajova, M. & Schon, M. P. Inhibition of platelet GPIb alpha and promotion of melanoma metastasis. *J Invest Dermatol* **130**, 576-586, doi:10.1038/jid.2009.278 (2010).

257 Palumbo, J. S. *et al.* Tumor cell-associated tissue factor and circulating hemostatic factors cooperate to increase metastatic potential through natural killer cell-dependent and-independent mechanisms. *Blood* **110**, 133-141, doi:10.1182/blood-2007-01-065995 (2007).

258 Amirkhosravi, A. *et al.* Tissue factor pathway inhibitor reduces experimental lung metastasis of B16 melanoma. *Thromb Haemost* **87**, 930-936 (2002).

259 Milsom, C., Anderson, G. M., Weitz, J. I. & Rak, J. Elevated tissue factor procoagulant activity in CD133-positive cancer cells. *J Thromb Haemost* **5**, 2550-2552, doi:10.1111/j.1538-7836.2007.02766.x (2007).

260 Ngo, C. V. *et al.* CNTO 859, a humanized anti-tissue factor monoclonal antibody, is a potent inhibitor of breast cancer metastasis and tumor growth in xenograft models. *Int J Cancer* **120**, 1261-1267, doi:10.1002/ijc.22426 (2007).

261 Plow, E. F. *et al.* Related binding mechanisms for fibrinogen, fibronectin, von Willebrand factor, and thrombospondin on thrombin-stimulated human platelets. *Blood* **66**, 724-727 (1985).

262 Plow, E. F., Srouji, A. H., Meyer, D., Marguerie, G. & Ginsberg, M. H. Evidence that three adhesive proteins interact with a common recognition site on activated platelets. *J Biol Chem* **259**, 5388-5391 (1984).

263 Nierodzik, M. L., Klepfish, A. & Karpatkin, S. Role of platelets, thrombin, integrin IIb-IIIa, fibronectin and von Willebrand factor on tumor adhesion in vitro and metastasis in vivo. *Thromb Haemost* **74**, 282-290 (1995).

264 Borsig, L. *et al.* Heparin and cancer revisited: mechanistic connections involving platelets, P-selectin, carcinoma mucins, and tumor metastasis. *Proc Natl Acad Sci U S A* **98**, 3352-3357, doi:10.1073/pnas.061615598 (2001).

265 Kim, Y. J., Borsig, L., Varki, N. M. & Varki, A. P-selectin deficiency attenuates tumor growth and metastasis. *Proc Natl Acad Sci U S A* **95**, 9325-9330 (1998).

266 Bobek, V. *et al.* Anticoagulant drugs increase natural killer cell activity in lung cancer. *Lung Cancer* **47**, 215-223, doi:10.1016/j.lungcan.2004.06.012 (2005).

267 Im, J. H. *et al.* Coagulation facilitates tumor cell spreading in the pulmonary vasculature during early metastatic colony formation. *Cancer Res* **64**, 8613-8619, doi:10.1158/0008-5472.CAN-04-2078 (2004).

268 Hu, L., Lee, M., Campbell, W., Perez-Soler, R. & Karpatkin, S. Role of endogenous thrombin in tumor implantation, seeding, and spontaneous metastasis. *Blood* **104**, 2746-2751, doi:10.1182/blood-2004-03-1047 (2004).

269 Esumi, N., Fan, D. & Fidler, I. J. Inhibition of murine melanoma experimental metastasis by recombinant desulfatohirudin, a highly specific thrombin inhibitor. *Cancer Res* **51**, 4549-4556 (1991).

270 Coupland, L. A., Chong, B. H. & Parish, C. R. Platelets and P-selectin control tumor cell metastasis in an organ-specific manner and independently of NK cells. *Cancer Res* **72**, 4662-4671, doi:10.1158/0008-5472.can-11-4010 (2012).

271 Placke, T. *et al.* Platelet-derived MHC class I confers a pseudonormal phenotype to cancer cells that subverts the antitumor reactivity of natural killer immune cells. *Cancer Res* **72**, 440-448, doi:10.1158/0008-5472.can-11-1872 (2012).

272 Gersuk, G. M., Chang, W. C. & Pattengale, P. K. Inhibition of human natural killer cell activity by platelet-derived growth factor. II. Membrane binding studies, effects of recombinant IFN-alpha and IL-2, and lack of effect on T cell and antibody-dependent cellular cytotoxicity. *J Immunol* **141**, 4031-4038 (1988).

273 Gersuk, G. M., Holloway, J. M., Chang, W. C. & Pattengale, P. K. Inhibition of human natural killer cell activity by platelet-derived growth factor. *Natural immunity and cell growth regulation* **5**, 283-293 (1986).

274 Gersuk, G. M. *et al.* Inhibition of human natural killer cell activity by platelet-derived growth factor (PDGF). III. Membrane binding studies and differential biological effect of recombinant PDGF isoforms. *Scandinavian journal of immunology* **33**, 521-532 (1991).
275 Lee, J. C., Lee, K. M., Kim, D. W. & Heo, D. S. Elevated TGF-beta1 secretion and down-modulation of NKG2D underlies impaired NK cytotoxicity in cancer patients. *J Immunol* **172**, 7335-7340 (2004).
276 Rook, A. H. *et al.* Effects of transforming growth factor beta on the functions of natural killer cells: depressed cytolytic activity and blunting of interferon responsiveness. *J Immunol* **136**, 3916-3920 (1986).
277 Bombeli, T., Schwartz, B. R. & Harlan, J. M. Adhesion of activated platelets to endothelial cells: evidence for a GPIIbIIIa-dependent bridging mechanism and novel roles for endothelial intercellular adhesion molecule 1 (ICAM-1), alphavbeta3 integrin, and GPIbalpha. *J Exp Med* **187**, 329-339 (1998).
278 Weis, S., Cui, J., Barnes, L. & Cheresh, D. Endothelial barrier disruption by VEGF-mediated Src activity potentiates tumor cell extravasation and metastasis. *J Cell Biol* **167**, 223-229, doi:10.1083/jcb.200408130 (2004).
279 Coppinger, J. A. *et al.* Characterization of the proteins released from activated platelets leads to localization of novel platelet proteins in human atherosclerotic lesions. *Blood* **103**, 2096-2104, doi:10.1182/blood-2003-08-2804 (2004).
280 Valiente, M. *et al.* Serpins promote cancer cell survival and vascular co-option in brain metastasis. *Cell* **156**, 1002-1016, doi:10.1016/j.cell.2014.01.040 (2014).
281 Blazejczyk, A., Papiernik, D., Porshneva, K., Sadowska, J. & Wietrzyk, J. Endothelium and cancer metastasis: Perspectives for antimetastatic therapy. *Pharmacol Rep* **67**, 711-718, doi:10.1016/j.pharep.2015.05.014 (2015).
282 Luther, T. *et al.* Functional implications of tissue factor localization to cell-cell contacts in myocardium. *J Pathol* **192**, 121-130, doi:10.1002/1096-9896(2000)9999:9999<::AID-PATH667>3.0.CO;2-I (2000).
283 Ott, I., Fischer, E. G., Miyagi, Y., Mueller, B. M. & Ruf, W. A role for tissue factor in cell adhesion and migration mediated by interaction with actin-binding protein 280. *J Cell Biol* **140**, 1241-1253 (1998).
284 Jiang, X., Guo, Y. L. & Bromberg, M. E. Formation of tissue factor-factor VIIa-factor Xa complex prevents apoptosis in human breast cancer cells. *Thromb Haemost* **96**, 196-201 (2006).
285 Dorfleutner, A., Hintermann, E., Tarui, T., Takada, Y. & Ruf, W. Cross-talk of integrin alpha3beta1 and tissue factor in cell migration. *Mol Biol Cell* **15**, 4416-4425, doi:10.1091/mbc.E03-09-0640 (2004).
286 Ott, I. *et al.* Tissue factor cytoplasmic domain stimulates migration by activation of the GTPase Rac1 and the mitogen-activated protein kinase p38. *Circulation* **111**, 349-355, doi:10.1161/01.CIR.0000153333.52294.42 (2005).
287 Abe, K. *et al.* Regulation of vascular endothelial growth factor production and angiogenesis by the cytoplasmic tail of tissue factor. *Proc Natl Acad Sci U S A* **96**, 8663-8668 (1999).
288 Camerer, E., Huang, W. & Coughlin, S. R. Tissue factor- and factor X-dependent activation of protease-activated receptor 2 by factor VIIa. *Proc Natl Acad Sci U S A* **97**, 5255-5260 (2000).
289 Palumbo, J. S. & Degen, J. L. Mechanisms linking tumor cell-associated procoagulant function to tumor metastasis. *Thrombosis research* **120 Suppl 2**, S22-28, doi:10.1016/S0049-3848(07)70127-5 (2007).
290 Orian-Rousseau, V. CD44, a therapeutic target for metastasising tumours. *Eur J Cancer* **46**, 1271-1277, doi:10.1016/j.ejca.2010.02.024 (2010).
291 Seiter, S. *et al.* Prevention of tumor metastasis formation by anti-variant CD44. *J Exp Med* **177**, 443-455 (1993).
292 Klemke, M., Weschenfelder, T., Konstandin, M. H. & Samstag, Y. High affinity interaction of integrin alpha4beta1 (VLA-4) and vascular cell adhesion molecule 1 (VCAM-1) enhances migration of human melanoma cells across activated endothelial cell layers. *J Cell Physiol* **212**, 368-374, doi:10.1002/jcp.21029 (2007).
293 Stroeken, P. J., van Rijthoven, E. A., van der Valk, M. A. & Roos, E. Targeted disruption of the beta1 integrin gene in a lymphoma cell line greatly reduces metastatic capacity. *Cancer Res* **58**, 1569-1577 (1998).

294 Gotte, M. & Yip, G. W. Heparanase, hyaluronan, and CD44 in cancers: a breast carcinoma perspective. *Cancer Res* **66**, 10233-10237, doi:10.1158/0008-5472.CAN-06-1464 (2006).

295 Kainz, C. *et al.* Prognostic value of CD44 splice variants in human stage III cervical cancer. *Eur J Cancer* **31A**, 1706-1709 (1995).

296 Wielenga, V. J., van der Neut, R., Offerhaus, G. J. & Pals, S. T. CD44 glycoproteins in colorectal cancer: expression, function, and prognostic value. *Adv Cancer Res* **77**, 169-187 (2000).

297 Khatib, A. M., Fallavollita, L., Wancewicz, E. V., Monia, B. P. & Brodt, P. Inhibition of hepatic endothelial E-selectin expression by C-raf antisense oligonucleotides blocks colorectal carcinoma liver metastasis. *Cancer Res* **62**, 5393-5398 (2002).

298 Brodt, P. *et al.* Liver endothelial E-selectin mediates carcinoma cell adhesion and promotes liver metastasis. *Int J Cancer* **71**, 612-619 (1997).

299 Bendas, G. & Borsig, L. Cancer cell adhesion and metastasis: selectins, integrins, and the inhibitory potential of heparins. *Int J Cell Biol* **2012**, 676731, doi:10.1155/2012/676731 (2012).

300 Zen, K. *et al.* CD44v4 is a major E-selectin ligand that mediates breast cancer cell transendothelial migration. *PLoS One* **3**, e1826, doi:10.1371/journal.pone.0001826 (2008).

301 Draffin, J. E., McFarlane, S., Hill, A., Johnston, P. G. & Waugh, D. J. CD44 potentiates the adherence of metastatic prostate and breast cancer cells to bone marrow endothelial cells. *Cancer Res* **64**, 5702-5711, doi:10.1158/0008-5472.CAN-04-0389 (2004).

302 Yu, L. G. *et al.* Galectin-3 interaction with Thomsen-Friedenreich disaccharide on cancer-associated MUC1 causes increased cancer cell endothelial adhesion. *J Biol Chem* **282**, 773-781, doi:10.1074/jbc.M606862200 (2007).

303 Rahn, J. J. *et al.* MUC1 mediates transendothelial migration in vitro by ligating endothelial cell ICAM-1. *Clin Exp Metastasis* **22**, 475-483, doi:10.1007/s10585-005-3098-x (2005).

304 Dardik, R., Savion, N., Kaufmann, Y. & Varon, D. Thrombin promotes platelet-mediated melanoma cell adhesion to endothelial cells under flow conditions: role of platelet glycoproteins P-selectin and GPIIb-IIIA. *Br J Cancer* **77**, 2069-2075 (1998).

305 Felding-Habermann, B., Habermann, R., Saldivar, E. & Ruggeri, Z. M. Role of beta3 integrins in melanoma cell adhesion to activated platelets under flow. *J Biol Chem* **271**, 5892-5900 (1996).

306 Jin, H. *et al.* A homing mechanism for bone marrow-derived progenitor cell recruitment to the neovasculature. *J Clin Invest* **116**, 652-662, doi:10.1172/JCI24751 (2006).

307 Thornhill, M. H. *et al.* Tumor necrosis factor combines with IL-4 or IFN-gamma to selectively enhance endothelial cell adhesiveness for T cells. The contribution of vascular cell adhesion molecule-1-dependent and -independent binding mechanisms. *J Immunol* **146**, 592-598 (1991).

308 Fidler, I. J. & Schroit, A. J. Recognition and destruction of neoplastic cells by activated macrophages: discrimination of altered self. *Biochim Biophys Acta* **948**, 151-173 (1988).

309 Laubli, H., Stevenson, J. L., Varki, A., Varki, N. M. & Borsig, L. L-selectin facilitation of metastasis involves temporal induction of Fut7-dependent ligands at sites of tumor cell arrest. *Cancer Res* **66**, 1536-1542, doi:10.1158/0008-5472.CAN-05-3121 (2006).

310 Borsig, L., Wong, R., Hynes, R. O., Varki, N. M. & Varki, A. Synergistic effects of L- and P-selectin in facilitating tumor metastasis can involve non-mucin ligands and implicate leukocytes as enhancers of metastasis. *Proc Natl Acad Sci U S A* **99**, 2193-2198, doi:10.1073/pnas.261704098 (2002).

311 Qian, B. Z. *et al.* FLT1 signaling in metastasis-associated macrophages activates an inflammatory signature that promotes breast cancer metastasis. *Journal of Experimental Medicine* **212**, 1433-1448, doi:10.1084/jem.20141555 (2015).

312 Leek, R. D. *et al.* Association of macrophage infiltration with angiogenesis and prognosis in invasive breast carcinoma. *Cancer Res* **56**, 4625-4629 (1996).

313 Oberg, A., Samii, S., Stenling, R. & Lindmark, G. Different occurrence of CD8+, CD45R0+, and CD68+ immune cells in regional lymph node metastases from colorectal cancer as potential prognostic predictors. *Int J Colorectal Dis* **17**, 25-29 (2002).

314 Wyckoff, J. *et al.* A paracrine loop between tumor cells and macrophages is required for tumor cell migration in mammary tumors. *Cancer Res* **64**, 7022-7029, doi:10.1158/0008-5472.can-04-1449 (2004).

315 Hernandez, L. *et al.* The EGF/CSF-1 paracrine invasion loop can be triggered by heregulin beta1 and CXCL12. *Cancer Res* **69**, 3221-3227, doi:10.1158/0008-5472.can-08-2871 (2009).
316 Wyckoff, J. B. *et al.* Direct visualization of macrophage-assisted tumor cell intravasation in mammary tumors. *Cancer Res* **67**, 2649-2656, doi:10.1158/0008-5472.can-06-1823 (2007).
317 Ingman, W. V., Wyckoff, J., Gouon-Evans, V., Condeelis, J. & Pollard, J. W. Macrophages promote collagen fibrillogenesis around terminal end buds of the developing mammary gland. *Dev Dyn* **235**, 3222-3229, doi:10.1002/dvdy.20972 (2006).
318 Kessenbrock, K., Plaks, V. & Werb, Z. Matrix metalloproteinases: regulators of the tumor microenvironment. *Cell* **141**, 52-67, doi:10.1016/j.cell.2010.03.015 (2010).
319 Gao, D. *et al.* Myeloid progenitor cells in the premetastatic lung promote metastases by inducing mesenchymal to epithelial transition. *Cancer Res* **72**, 1384-1394, doi:10.1158/0008-5472.can-11-2905 (2012).
320 Noy, R. & Pollard, J. W. Tumor-associated macrophages: from mechanisms to therapy. *Immunity* **41**, 49-61, doi:10.1016/j.immuni.2014.06.010 (2014).
321 Vane, J. R. & Botting, R. M. The mechanism of action of aspirin. *Thrombosis research* **110**, 255-258 (2003).
322 Beaver, W. T. Mild analgesics. A review of their clinical pharmacology. *Am J Med Sci* **250**, 577-604 contd (1965).
323 Engineer, D. M., Morris, H. R., Piper, P. J. & Sirois, P. The release of prostaglandins and thromboxanes from guinea-pig lung by slow reacting substance of anaphylaxis, and its inhibition. *Br J Pharmacol* **64**, 211-218 (1978).
324 Vane, J. R. Inhibition of prostaglandin synthesis as a mechanism of action for aspirin-like drugs. *Nature: New biology* **231**, 232-235 (1971).
325 Collier, J. G. & Flower, R. J. Effect of aspirin on human seminal prostaglandins. *Lancet* **2**, 852-853 (1971).
326 Ferreira, S. H., Moncada, S. & Vane, J. R. Indomethacin and aspirin abolish prostaglandin release from the spleen. *Nature: New biology* **231**, 237-239 (1971).
327 Smith, J. B. & Willis, A. L. Aspirin selectively inhibits prostaglandin production in human platelets. *Nature: New biology* **231**, 235-237 (1971).
328 Vane, J. R. & Botting, R. M. Mechanism of action of aspirin-like drugs. *Seminars in arthritis and rheumatism* **26**, 2-10 (1997).
329 Vane, J. R. & Botting, R. M. Mechanism of action of anti-inflammatory drugs. *Scandinavian journal of rheumatology. Supplement* **102**, 9-21 (1996).
330 Iniguez, M. A., Rodriguez, A., Volpert, O. V., Fresno, M. & Redondo, J. M. Cyclooxygenase-2: a therapeutic target in angiogenesis. *Trends in molecular medicine* **9**, 73-78 (2003).
331 Botting, R. M. Vane's discovery of the mechanism of action of aspirin changed our understanding of its clinical pharmacology. *Pharmacol Rep* **62**, 518-525 (2010).
332 Smith, W. L., DeWitt, D. L. & Garavito, R. M. Cyclooxygenases: structural, cellular, and molecular biology. *Annu Rev Biochem* **69**, 145-182, doi:10.1146/annurev.biochem.69.1.145 (2000).
333 Xu, X. M., Tang, J. L., Chen, X., Wang, L. H. & Wu, K. K. Involvement of two Sp1 elements in basal endothelial prostaglandin H synthase-1 promoter activity. *J Biol Chem* **272**, 6943-6950 (1997).
334 Kraemer, S. A., Meade, E. A. & DeWitt, D. L. Prostaglandin endoperoxide synthase gene structure: identification of the transcriptional start site and 5'-flanking regulatory sequences. *Archives of biochemistry and biophysics* **293**, 391-400 (1992).
335 Rao, P. & Knaus, E. E. Evolution of nonsteroidal anti-inflammatory drugs (NSAIDs): cyclooxygenase (COX) inhibition and beyond. *J Pharm Pharm Sci* **11**, 81s-110s (2008).
336 Patrono, C., Garcia Rodriguez, L. A., Landolfi, R. & Baigent, C. Low-dose aspirin for the prevention of atherothrombosis. *N Engl J Med* **353**, 2373-2383, doi:10.1056/NEJMra052717 (2005).
337 Thun, M. J., Jacobs, E. J. & Patrono, C. The role of aspirin in cancer prevention. *Nat Rev Clin Oncol* **9**, 259-267, doi:10.1038/nrclinonc.2011.199 (2012).
338 Smith, W. L. & DeWitt, D. L. Biochemistry of prostaglandin endoperoxide H synthase-1 and synthase-2 and their differential susceptibility to nonsteroidal anti-inflammatory drugs. *Seminars in nephrology* **15**, 179-194 (1995).

339 Lucido, M. J., Orlando, B. J., Vecchio, A. J. & Malkowski, M. G. Crystal Structure of Aspirin-Acetylated Human Cyclooxygenase-2: Insight into the Formation of Products with Reversed Stereochemistry. *Biochemistry* **55**, 1226-1238, doi:10.1021/acs.biochem.5b01378 (2016).
340 Gierse, J. K. *et al.* A single amino acid difference between cyclooxygenase-1 (COX-1) and -2 (COX-2) reverses the selectivity of COX-2 specific inhibitors. *Journal of Biological Chemistry* **271**, 15810-15814 (1996).
341 Lei, J. P., Zhou, Y. Z., Xie, D. Q. & Zhang, Y. K. Mechanistic Insights into a Classic Wonder Drug-Aspirin. *J Am Chem Soc* **137**, 70-73, doi:10.1021/ja5112964 (2015).
342 Kihara, Y. *et al.* Modeling of eicosanoid fluxes reveals functional coupling between cyclooxygenases and terminal synthases. *Biophys J* **106**, 966-975, doi:10.1016/j.bpj.2014.01.015 (2014).
343 Smyth, E. M., Grosser, T., Wang, M., Yu, Y. & FitzGerald, G. A. Prostanoids in health and disease. *J Lipid Res* **50 Suppl**, S423-428, doi:10.1194/jlr.R800094-JLR200 (2009).
344 Botting, R. M. Vane's discovery of the mechanism of action of aspirin changed our understanding of its clinical pharmacology. *Pharmacological Reports* **62**, 518-525 (2010).
345 Smith, W. L., DeWitt, D. L. & Garavito, R. M. Cyclooxygenases: Structural, cellular, and molecular biology. *Annual Review of Biochemistry* **69**, 145-182, doi:DOI 10.1146/annurev.biochem.69.1.145 (2000).
346 Konieczkowski, M. & Skrinska, V. A. Increased synthesis of thromboxane A(2) and expression of procoagulant activity by monocytes in response to arachidonic acid in diabetes mellitus. *Prostaglandins Leukot Essent Fatty Acids* **65**, 133-138, doi:10.1054/plef.2001.0301 (2001).
347 Pawlowski, N. A., Kaplan, G., Hamill, A. L., Cohn, Z. A. & Scott, W. A. Arachidonic acid metabolism by human monocytes. Studies with platelet-depleted cultures. *J Exp Med* **158**, 393-412 (1983).
348 McAdam, B. F. *et al.* Systemic biosynthesis of prostacyclin by cyclooxygenase (COX)-2: the human pharmacology of a selective inhibitor of COX-2. *Proc Natl Acad Sci U S A* **96**, 272-277 (1999).
349 Catella-Lawson, F. *et al.* Effects of specific inhibition of cyclooxygenase-2 on sodium balance, hemodynamics, and vasoactive eicosanoids. *Journal of Pharmacology and Experimental Therapeutics* **289**, 735-741 (1999).
350 Kirkby, N. S. *et al.* Cyclooxygenase-1, not cyclooxygenase-2, is responsible for physiological production of prostacyclin in the cardiovascular system. *P Natl Acad Sci USA* **109**, 17597-17602, doi:10.1073/pnas.1209192109 (2012).
351 Smolenski, A. Novel roles of cAMP/cGMP-dependent signaling in platelets. *J Thromb Haemost* **10**, 167-176, doi:10.1111/j.1538-7836.2011.04576.x (2012).
352 Kawabe, J., Ushikubi, F. & Hasebe, N. Prostacyclin in vascular diseases. - Recent insights and future perspectives. *Circ J* **74**, 836-843 (2010).
353 Cheng, Y. *et al.* Role of prostacyclin in the cardiovascular response to thromboxane A2. *Science* **296**, 539-541, doi:10.1126/science.1068711 (2002).
354 Harada, N., Okajima, K., Murakami, K., Isobe, H. & Liu, W. Gastric prostacyclin (PGI2) prevents stress-induced gastric mucosal injury in rats primarily by inhibiting leukocyte activation. *Prostaglandins & other lipid mediators* **57**, 291-303 (1999).
355 Gaskill, H. V., 3rd, Sirinek, K. R. & Levine, B. A. Prostacyclin-mediated gastric cytoprotection is dependent on mucosal blood flow. *Surgery* **92**, 220-225 (1982).
356 Takeuchi, K., Kato, S., Ogawa, Y., Kanatsu, K. & Umeda, M. Role of endogenous prostacyclin in gastric ulcerogenic and healing responses--a study using IP-receptor knockout mice. *Journal of physiology, Paris* **95**, 75-80 (2001).
357 Satoh, T. *et al.* CNS-specific prostacyclin ligands as neuronal survival-promoting factors in the brain. *Eur J Neurosci* **11**, 3115-3124, doi:DOI 10.1046/j.1460-9568.1999.00791.x (1999).
358 Stitham, J., Midgett, C., Martin, K. A. & Hwa, J. Prostacyclin: an inflammatory paradox. *Frontiers in pharmacology* **2**, doi:UNSP 24 10.3389/fphar.2011.00024 (2011).
359 Momin, A. & McNaughton, P. A. Regulation of firing frequency in nociceptive neurons by pro-inflammatory mediators. *Experimental brain research* **196**, 45-52, doi:10.1007/s00221-009-1744-2 (2009).

360 Hara, S. *et al.* Prostaglandin E synthases: Understanding their pathophysiological roles through mouse genetic models. *Biochimie* **92**, 651-659, doi:10.1016/j.biochi.2010.02.007 (2010).

361 Harris, S. G., Padilla, J., Koumas, L., Ray, D. & Phipps, R. P. Prostaglandins as modulators of immunity. *Trends in immunology* **23**, 144-150 (2002).

362 Napolitani, G., Acosta-Rodriguez, E. V., Lanzavecchia, A. & Sallusto, F. Prostaglandin E2 enhances Th17 responses via modulation of IL-17 and IFN-gamma production by memory CD4+ T cells. *Eur J Immunol* **39**, 1301-1312, doi:10.1002/eji.200838969 (2009).

363 Chizzolini, C. *et al.* Prostaglandin E2 synergistically with interleukin-23 favors human Th17 expansion. *Blood* **112**, 3696-3703, doi:10.1182/blood-2008-05-155408 (2008).

364 Boniface, K. *et al.* Prostaglandin E2 regulates Th17 cell differentiation and function through cyclic AMP and EP2/EP4 receptor signaling. *J Exp Med* **206**, 535-548, doi:10.1084/jem.20082293 (2009).

365 Harizi, H. & Gualde, N. Pivotal role of PGE2 and IL-10 in the cross-regulation of dendritic cell-derived inflammatory mediators. *Cell Mol Immunol* **3**, 271-277 (2006).

366 Levy, G. Pharmacokinetics of salicylate elimination in man. *J Pharm Sci* **54**, 959-967 (1965).

367 Zaugg, S., Zhang, X., Sweedler, J. & Thormann, W. Determination of salicylate, gentisic acid and salicyluric acid in human urine by capillary electrophoresis with laser-induced fluorescence detection. *Journal of chromatography. B, Biomedical sciences and applications* **752**, 17-31 (2001).

368 Mahmoud, N. N. *et al.* Aspirin prevents tumors in a murine model of familial adenomatous polyposis. *Surgery* **124**, 225-231 (1998).

369 La Maestra, S. *et al.* Modulation by aspirin and naproxen of nucleotide alterations and tumors in the lung of mice exposed to environmental cigarette smoke since birth. *Carcinogenesis* **36**, 1531-1538, doi:10.1093/carcin/bgv149 (2015).

370 Li, L. *et al.* Aspirin inhibits growth of ovarian cancer by upregulating caspase-3 and downregulating bcl-2. *Oncology letters* **12**, 93-96, doi:10.3892/ol.2016.4607 (2016).

371 Piazuelo, E. *et al.* Acetylsalicylic Acid Exhibits Antitumor Effects in Esophageal Adenocarcinoma Cells In Vitro and In Vivo. *Digestive diseases and sciences*, doi:10.1007/s10620-016-4225-z (2016).

372 Mattheolabakis, G. *et al.* Phospho-Aspirin (MDC-22) Prevents Pancreatic Carcinogenesis in Mice. *Cancer Prev Res (Phila)* **9**, 624-634, doi:10.1158/1940-6207.capr-15-0344 (2016).

373 Mikami, J. *et al.* Antitumor effect of antiplatelet agents in gastric cancer cells: an in vivo and in vitro study. *Gastric cancer : official journal of the International Gastric Cancer Association and the Japanese Gastric Cancer Association* **19**, 817-826, doi:10.1007/s10120-015-0556-2 (2016).

374 Liao, D. *et al.* Aspirin Suppresses the Growth and Metastasis of Osteosarcoma through the NF-kappaB Pathway. *Clin Cancer Res* **21**, 5349-5359, doi:10.1158/1078-0432.ccr-15-0198 (2015).

375 Zhang, Y. *et al.* Aspirin counteracts cancer stem cell features, desmoplasia and gemcitabine resistance in pancreatic cancer. *Oncotarget* **6**, 9999-10015, doi:10.18632/oncotarget.3171 (2015).

376 Owens, A. P., 3rd *et al.* Platelet Inhibitors Reduce Rupture in a Mouse Model of Established Abdominal Aortic Aneurysm. *Arteriosclerosis, thrombosis, and vascular biology* **35**, 2032-2041, doi:10.1161/ATVBAHA.115.305537 (2015).

377 Passacquale, G. *et al.* Aspirin-induced histone acetylation in endothelial cells enhances synthesis of the secreted isoform of netrin-1 thus inhibiting monocyte vascular infiltration. *Br J Pharmacol* **172**, 3548-3564, doi:10.1111/bph.13144 (2015).

378 Wang, Y. *et al.* Treatment of colonic transplantation tumor-bearing mice with a high-dose aspirin in a short period of time. *Int J Colorectal Dis* **31**, 1099-1100, doi:10.1007/s00384-015-2427-z (2016).

379 Kolenich, J. J., Mansour, E. G. & Flynn, A. Haematological effects of aspirin. *Lancet* **2**, 714 (1972).

380 Tsai, C. S. *et al.* Acetylsalicylic acid regulates MMP-2 activity and inhibits colorectal invasion of murine B16F0 melanoma cells in C57BL/6J mice: effects of prostaglandin F(2)alpha. *Biomedicine & pharmacotherapy = Biomedecine & pharmacotherapie* **63**, 522-527, doi:10.1016/j.biopha.2008.07.094 (2009).

381 Carmel, R. J. & Brown, J. M. The effect of cyclophosphamide and other drugs on the incidence of pulmonary metastases in mice. *Cancer Res* **37**, 145-151 (1977).

382 Kort, W. J. *et al.* Reductive effect of aspirin treatment on primary tumor growth and metastasis of implanted fibrosarcoma in rats. *J Natl Cancer Inst* **76**, 711-720 (1986).

383 Amano, H. *et al.* Roles of a prostaglandin E-type receptor, EP3, in upregulation of matrix metalloproteinase-9 and vascular endothelial growth factor during enhancement of tumor metastasis. *Cancer science* **100**, 2318-2324, doi:10.1111/j.1349-7006.2009.01322.x (2009).

384 Futakuchi, M. *et al.* Suppression of lung metastasis by aspirin but not indomethacin in an in vivo model of chemically induced hepatocellular carcinoma. *Japanese journal of cancer research : Gann* **93**, 1175-1181 (2002).

385 Yu, L. X. *et al.* Platelets promote tumour metastasis via interaction between TLR4 and tumour cell-released high-mobility group box1 protein. *Nat Commun* **5**, 5256, doi:10.1038/ncomms6256 (2014).

386 Grignani, G. *et al.* Interactions between neoplastic cells with different metastasizing capacity and platelet function. *European journal of cancer & clinical oncology* **19**, 519-525 (1983).

387 Lu, L. *et al.* Aspirin minimized the pro-metastasis effect of sorafenib and improved survival by up-regulating HTATIP2 in hepatocellular carcinoma. *PLoS One* **8**, e65023, doi:10.1371/journal.pone.0065023 (2013).

388 Guillem-Llobat, P. *et al.* Aspirin prevents colorectal cancer metastasis in mice by splitting the crosstalk between platelets and tumor cells. *Oncotarget* **7**, 32462-32477, doi:10.18632/oncotarget.8655 (2016).

389 Glaves, D. & Weiss, L. Initial tumor cell arrest in animals of defined coagulative status. *Int J Cancer* **21**, 741-746 (1978).

390 Brown, D. C., Purushotham, A. D. & George, W. D. Inhibition of pulmonary tumor seeding by antiplatelet and fibrinolytic therapy in an animal experimental model. *Journal of surgical oncology* **55**, 154-159 (1994).

391 Futakuchi, M., Ogawa, K., Tamano, S., Takahashi, S. & Shirai, T. Suppression of metastasis by nuclear factor kappaB inhibitors in an in vivo lung metastasis model of chemically induced hepatocellular carcinoma. *Cancer science* **95**, 18-24 (2004).

392 Bosetti, C., Rosato, V., Gallus, S., Cuzick, J. & La Vecchia, C. Aspirin and cancer risk: a quantitative review to 2011. *Annals of oncology : official journal of the European Society for Medical Oncology / ESMO* **23**, 1403-1415, doi:10.1093/annonc/mds113 (2012).

393 Rosenberg, L. *et al.* A hypothesis: nonsteroidal anti-inflammatory drugs reduce the incidence of large-bowel cancer. *J Natl Cancer Inst* **83**, 355-358 (1991).

394 Garcia-Rodriguez, L. A. & Huerta-Alvarez, C. Reduced risk of colorectal cancer among long-term users of aspirin and nonaspirin nonsteroidal antiinflammatory drugs. *Epidemiology (Cambridge, Mass.)* **12**, 88-93 (2001).

395 Greenberg, E. R., Baron, J. A., Freeman, D. H., Jr., Mandel, J. S. & Haile, R. Reduced risk of large-bowel adenomas among aspirin users. The Polyp Prevention Study Group. *J Natl Cancer Inst* **85**, 912-916 (1993).

396 Thun, M. J., Namboodiri, M. M. & Heath, C. W., Jr. Aspirin use and reduced risk of fatal colon cancer. *N Engl J Med* **325**, 1593-1596, doi:10.1056/nejm199112053252301 (1991).

397 Kune, G. A., Kune, S. & Watson, L. F. Colorectal cancer risk, chronic illnesses, operations, and medications: case control results from the Melbourne Colorectal Cancer Study. *Cancer Res* **48**, 4399-4404 (1988).

398 Schreinemachers, D. M. & Everson, R. B. Aspirin use and lung, colon, and breast cancer incidence in a prospective study. *Epidemiology (Cambridge, Mass.)* **5**, 138-146 (1994).

399 Giovannucci, E. *et al.* Aspirin use and the risk for colorectal cancer and adenoma in male health professionals. *Annals of internal medicine* **121**, 241-246 (1994).

400 Harris, R. E. *et al.* Breast cancer and nonsteroidal anti-inflammatory drugs: prospective results from the Women's Health Initiative. *Cancer Res* **63**, 6096-6101 (2003).

401 Collet, J. P. *et al.* Colorectal cancer prevention by non-steroidal anti-inflammatory drugs: effects of dosage and timing. *Br J Cancer* **81**, 62-68, doi:10.1038/sj.bjc.6690651 (1999).

402 Chan, A. T. *et al.* Long-term aspirin use and mortality in women. *Archives of internal medicine* **167**, 562-572, doi:10.1001/archinte.167.6.562 (2007).

403 Zaorsky, N. G., Buyyounouski, M. K., Li, T. & Horwitz, E. M. Aspirin and statin nonuse associated with early biochemical failure after prostate radiation therapy. *International*

journal of radiation oncology, biology, physics **84**, e13-17, doi:10.1016/j.ijrobp.2012.02.050 (2012).
404 Leitzmann, M. F. *et al.* Aspirin use in relation to risk of prostate cancer. *Cancer epidemiology, biomarkers & prevention : a publication of the American Association for Cancer Research, cosponsored by the American Society of Preventive Oncology* **11**, 1108-1111 (2002).
405 Symeonidis, D. *et al.* Impact of antiplatelet treatment on colorectal cancer staging characteristics. *World journal of gastrointestinal endoscopy* **4**, 409-413, doi:10.4253/wjge.v4.i9.409 (2012).
406 Jonsson, F. *et al.* Low-dose aspirin use and cancer characteristics: a population-based cohort study. *Br J Cancer*, doi:10.1038/bjc.2013.411 (2013).
407 Holmes, M. D. *et al.* Aspirin intake and survival after breast cancer. *J Clin Oncol* **28**, 1467-1472, doi:10.1200/JCO.2009.22.7918 (2010).
408 Flossmann, E., Rothwell, P. M., British Doctors Aspirin, T. & the, U. K. T. I. A. A. T. Effect of aspirin on long-term risk of colorectal cancer: consistent evidence from randomised and observational studies. *Lancet* **369**, 1603-1613, doi:10.1016/S0140-6736(07)60747-8 (2007).
409 Choe, K. S., Correa, D., Jani, A. B. & Liauw, S. L. The use of anticoagulants improves biochemical control of localized prostate cancer treated with radiotherapy. *Cancer* **116**, 1820-1826, doi:10.1002/cncr.24890 (2010).
410 Algra, A. M. & Rothwell, P. M. Effects of regular aspirin on long-term cancer incidence and metastasis: a systematic comparison of evidence from observational studies versus randomised trials. *Lancet Oncol* **13**, 518-527, doi:10.1016/s1470-2045(12)70112-2 (2012).
411 Asgari, M. M., Maruti, S. S. & White, E. A large cohort study of nonsteroidal anti-inflammatory drug use and melanoma incidence. *J Natl Cancer Inst* **100**, 967-971, doi:10.1093/jnci/djn154 (2008).
412 Cook, N. R. *et al.* Low-dose aspirin in the primary prevention of cancer: the Women's Health Study: a randomized controlled trial. *Jama* **294**, 47-55, doi:10.1001/jama.294.1.47 (2005).
413 Peto, R. *et al.* Randomised trial of prophylactic daily aspirin in British male doctors. *British medical journal (Clinical research ed.)* **296**, 313-316 (1988).
414 Gann, P. H., Manson, J. E., Glynn, R. J., Buring, J. E. & Hennekens, C. H. Low-dose aspirin and incidence of colorectal tumors in a randomized trial. *J Natl Cancer Inst* **85**, 1220-1224 (1993).
415 Logan, R. F., Grainge, M. J., Shepherd, V. C., Armitage, N. C. & Muir, K. R. Aspirin and folic acid for the prevention of recurrent colorectal adenomas. *Gastroenterology* **134**, 29-38, doi:10.1053/j.gastro.2007.10.014 (2008).
416 Benamouzig, R. *et al.* Daily soluble aspirin and prevention of colorectal adenoma recurrence: one-year results of the APACC trial. *Gastroenterology* **125**, 328-336 (2003).
417 Sandler, R. S. *et al.* A randomized trial of aspirin to prevent colorectal adenomas in patients with previous colorectal cancer. *N Engl J Med* **348**, 883-890, doi:10.1056/NEJMoa021633 (2003).
418 Baron, J. A. *et al.* A randomized trial of aspirin to prevent colorectal adenomas. *N Engl J Med* **348**, 891-899, doi:10.1056/NEJMoa021735 (2003).
419 Farrell, B., Godwin, J., Richards, S. & Warlow, C. The United Kingdom transient ischaemic attack (UK-TIA) aspirin trial: final results. *Journal of neurology, neurosurgery, and psychiatry* **54**, 1044-1054 (1991).
420 Burn, J. *et al.* Long-term effect of aspirin on cancer risk in carriers of hereditary colorectal cancer: an analysis from the CAPP2 randomised controlled trial. *Lancet* **378**, 2081-2087, doi:10.1016/S0140-6736(11)61049-0 (2011).
421 Rothwell, P. M. *et al.* Effect of daily aspirin on long-term risk of death due to cancer: analysis of individual patient data from randomised trials. *Lancet* **377**, 31-41, doi:10.1016/s0140-6736(10)62110-1 (2011).
422 Sturmer, T. *et al.* Aspirin use and colorectal cancer: post-trial follow-up data from the Physicians' Health Study. *Annals of internal medicine* **128**, 713-720 (1998).
423 Cook, N. R., Lee, I. M., Zhang, S. M., Moorthy, M. V. & Buring, J. E. Alternate-day, low-dose aspirin and cancer risk: long-term observational follow-up of a randomized trial. *Annals of internal medicine* **159**, 77-85, doi:10.7326/0003-4819-159-2-201307160-00002 (2013).

424 Asano, T. K. & McLeod, R. S. Nonsteroidal anti-inflammatory drugs and aspirin for the prevention of colorectal adenomas and cancer: a systematic review. *Diseases of the colon and rectum* **47**, 665-673, doi:10.1007/s10350-003-0111-9 (2004).

425 Cole, B. F. *et al.* Aspirin for the chemoprevention of colorectal adenomas: meta-analysis of the randomized trials. *J Natl Cancer Inst* **101**, 256-266, doi:10.1093/jnci/djn485 (2009).

426 Rothwell, P. M. *et al.* Short-term effects of daily aspirin on cancer incidence, mortality, and non-vascular death: analysis of the time course of risks and benefits in 51 randomised controlled trials. *Lancet* **379**, 1602-1612, doi:10.1016/S0140-6736(11)61720-0 (2012).

427 Rothwell, P. M. *et al.* Long-term effect of aspirin on colorectal cancer incidence and mortality: 20-year follow-up of five randomised trials. *Lancet* **376**, 1741-1750, doi:10.1016/s0140-6736(10)61543-7 (2010).

428 Rothwell, P. M. *et al.* Effect of daily aspirin on risk of cancer metastasis: a study of incident cancers during randomised controlled trials. *Lancet* **379**, 1591-1601, doi:10.1016/S0140-6736(12)60209-8 (2012).

429 Burn, J. & Sheth, H. The role of aspirin in preventing colorectal cancer. *Br Med Bull* **119**, 17-24, doi:10.1093/bmb/ldw028 (2016).

430 Cuzick, J. *et al.* Estimates of benefits and harms of prophylactic use of aspirin in the general population. *Annals of oncology : official journal of the European Society for Medical Oncology / ESMO* **26**, 47-57, doi:10.1093/annonc/mdu225 (2015).

431 Baigent, C. *et al.* Aspirin in the primary and secondary prevention of vascular disease: collaborative meta-analysis of individual participant data from randomised trials. *Lancet* **373**, 1849-1860, doi:10.1016/s0140-6736(09)60503-1 (2009).

432 Thorat, M. A. & Cuzick, J. Prophylactic use of aspirin: systematic review of harms and approaches to mitigation in the general population. *European journal of epidemiology* **30**, 5-18, doi:10.1007/s10654-014-9971-7 (2015).

433 Sutcliffe, P. *et al.* Aspirin for prophylactic use in the primary prevention of cardiovascular disease and cancer: a systematic review and overview of reviews. *Health Technol Asses* **17**, 1-+ (2013).

434 Coyle, C., Cafferty, F. H. & Langley, R. E. Aspirin and Colorectal Cancer Prevention and Treatment: Is It for Everyone? *Current colorectal cancer reports* **12**, 27-34, doi:10.1007/s11888-016-0306-9 (2016).

435 Reagan-Shaw, S., Nihal, M. & Ahmad, N. Dose translation from animal to human studies revisited. *FASEB J* **22**, 659-661, doi:10.1096/fj.07-9574LSF (2008).

436 Cyrus, T. *et al.* Effect of low-dose aspirin on vascular inflammation, plaque stability, and atherogenesis in low-density lipoprotein receptor-deficient mice. *Circulation* **106**, 1282-1287 (2002).

437 Paul, A. *et al.* The continuous administration of aspirin attenuates atherosclerosis in apolipoprotein E-deficient mice. *Life Sci* **68**, 457-465 (2000).

438 Pena Silva, R. A. *et al.* Paradoxical Increase in Mortality and Rupture of Intracranial Aneurysms in Microsomal Prostaglandin E2 Synthase Type 1-Deficient Mice: Attenuation by Aspirin. *Neurosurgery* **77**, 613-620, doi:10.1227/neu.0000000000000883 (2015).

439 Satoh, H. & Urushidani, T. Soluble Dietary Fiber Can Protect the Gastrointestinal Mucosa Against Nonsteroidal Anti-Inflammatory Drugs in Mice. *Digestive diseases and sciences* **61**, 1903-1914, doi:10.1007/s10620-016-4086-5 (2016).

440 Goyal, S., Lyzogubov, V. V., Ali, O., Bora, N. S. & Uwaydat, S. H. Effect of Aspirin on models of RPE pathology. *Clinical & experimental ophthalmology*, doi:10.1111/ceo.12721 (2016).

441 Tarantino, E. *et al.* Role of thromboxane-dependent platelet activation in venous thrombosis: Aspirin effects in mouse model. *Pharmacological research* **107**, 415-425, doi:10.1016/j.phrs.2016.04.001 (2016).

442 Zhang, D., Luo, G., Ding, X. & Lu, C. Preclinical experimental models of drug metabolism and disposition in drug discovery and development. *Acta Pharmaceutica Sinica B* **2**, 549-561, doi:http://dx.doi.org/10.1016/j.apsb.2012.10.004 (2012).

443 Yin, M. J., Yamamoto, Y. & Gaynor, R. B. The anti-inflammatory agents aspirin and salicylate inhibit the activity of I(kappa)B kinase-beta. *Nature* **396**, 77-80, doi:10.1038/23948 (1998).

444 Kopp, E. & Ghosh, S. Inhibition of NF-kappa B by sodium salicylate and aspirin. *Science* **265**, 956-959 (1994).

445 Grilli, M., Pizzi, M., Memo, M. & Spano, P. Neuroprotection by aspirin and sodium salicylate through blockade of NF-kappaB activation. *Science* **274**, 1383-1385 (1996).
446 Zimmermann, K. C., Waterhouse, N. J., Goldstein, J. C., Schuler, M. & Green, D. R. Aspirin induces apoptosis through release of cytochrome c from mitochondria. *Neoplasia* **2**, 505-513, doi:DOI 10.1038/sj.neo.7900120 (2000).
447 Mahdi, J. G., Alkarrawi, M. A., Mahdi, A. J., Bowen, I. D. & Humam, D. Calcium salicylate-mediated apoptosis in human HT-1080 fibrosarcoma cells. *Cell Proliferat* **39**, 249-260, doi:DOI 10.1111/j.1365-2184.2006.00390.x (2006).
448 Zhang, L., Yu, J., Park, B. H., Kinzler, K. W. & Vogelstein, B. Role of BAX in the apoptotic response to anticancer agents. *Science* **290**, 989-+, doi:DOI 10.1126/science.290.5493.989 (2000).
449 Zhang, Z. H. & DuBois, R. N. Par-4, a proapoptotic gene, is regulated by NSAIDs in human colon carcinoma cells. *Gastroenterology* **118**, 1012-1017, doi:Doi 10.1016/S0016-5085(00)70352-0 (2000).
450 Shureiqi, I. *et al.* Nonsteroidal anti-inflammatory drugs induce apoptosis in esophageal cancer cells by restoring 15-lipoxygenase-1 expression. *Cancer Research* **61**, 4879-4884 (2001).
451 Pan, M. R., Chang, H. C. & Hung, W. C. Non-steroidal anti-inflammatory drugs suppress the ERK signaling pathway via block of Ras/c-Raf interaction and activation of MAP kinase phosphatases. *Cell Signal* **20**, 1134-1141, doi:10.1016/j.cellsig.2008.02.004 (2008).
452 Jiang, M. C., Liao, C. F. & Lee, P. H. Aspirin inhibits matrix metalloproteinase-2 activity, increases E-cadherin production, and inhibits in vitro invasion of tumor cells. *Biochem Biophys Res Commun* **282**, 671-677, doi:10.1006/bbrc.2001.4637 (2001).
453 Koontongkaew, S., Monthanapisut, P. & Saensuk, T. Inhibition of arachidonic acid metabolism decreases tumor cell invasion and matrix metalloproteinase expression. *Prostaglandins & other lipid mediators* **93**, 100-108, doi:10.1016/j.prostaglandins.2010.07.002 (2010).
454 Abiru, S. *et al.* Aspirin and NS-398 inhibit hepatocyte growth factor-induced invasiveness of human hepatoma cells. *Hepatology* **35**, 1117-1124, doi:10.1053/jhep.2002.32676 (2002).
455 Yoshida, S. *et al.* COX-2/VEGF-dependent facilitation of tumor-associated angiogenesis and tumor growth in vivo. *Lab Invest* **83**, 1385-1394 (2003).
456 Colleselli, D., Bijuklic, K., Mosheimer, B. A. & Kahler, C. M. Inhibition of cyclooxygenase (COX)-2 affects endothelial progenitor cell proliferation. *Exp Cell Res* **312**, 2933-2941, doi:10.1016/j.yexcr.2006.05.021 (2006).
457 Dahlen, B., Boreus, L. O., Anderson, P., Andersson, R. & Zetterstrom, O. Plasma acetylsalicylic acid and salicylic acid levels during aspirin provocation in aspirin-sensitive subjects. *Allergy* **49**, 43-49 (1994).
458 Patrignani, P. *et al.* Reappraisal of the clinical pharmacology of low-dose aspirin by comparing novel direct and traditional indirect biomarkers of drug action. *J Thromb Haemost* **12**, 1320-1330, doi:10.1111/jth.12637 (2014).
459 Bellosillo, B. *et al.* Aspirin and salicylate induce apoptosis and activation of caspases in B-cell chronic lymphocytic leukemia cells. *Blood* **92**, 1406-1414 (1998).
460 Wu, K. *et al.* Roles of the cyclooxygenase 2 matrix metalloproteinase 1 pathway in brain metastasis of breast cancer. *J Biol Chem* **290**, 9842-9854, doi:10.1074/jbc.M114.602185 (2015).
461 Sano, H. *et al.* Expression of cyclooxygenase-1 and -2 in human colorectal cancer. *Cancer Res* **55**, 3785-3789 (1995).
462 Kargman, S. L. *et al.* Expression of prostaglandin G/H synthase-1 and -2 protein in human colon cancer. *Cancer Res* **55**, 2556-2559 (1995).
463 Sheehan, K. M. *et al.* The relationship between cyclooxygenase-2 expression and colorectal cancer. *Jama* **282**, 1254-1257 (1999).
464 Elder, D. J., Baker, J. A., Banu, N. A., Moorghen, M. & Paraskeva, C. Human colorectal adenomas demonstrate a size-dependent increase in epithelial cyclooxygenase-2 expression. *J Pathol* **198**, 428-434, doi:10.1002/path.1232 (2002).
465 Eberhart, C. E. *et al.* Up-regulation of cyclooxygenase 2 gene expression in human colorectal adenomas and adenocarcinomas. *Gastroenterology* **107**, 1183-1188 (1994).
466 Liu, C. H. *et al.* Overexpression of cyclooxygenase-2 is sufficient to induce tumorigenesis in transgenic mice. *J Biol Chem* **276**, 18563-18569, doi:10.1074/jbc.M010787200 (2001).

467 Ristimaki, A. *et al.* Prognostic significance of elevated cyclooxygenase-2 expression in breast cancer. *Cancer Res* **62**, 632-635 (2002).

468 Chen, W. S. *et al.* Tumor invasiveness and liver metastasis of colon cancer cells correlated with cyclooxygenase-2 (COX-2) expression and inhibited by a COX-2-selective inhibitor, etodolac. *Int J Cancer* **91**, 894-899 (2001).

469 Singh, B. *et al.* COX-2 involvement in breast cancer metastasis to bone. *Oncogene* **26**, 3789-3796, doi:10.1038/sj.onc.1210154 (2007).

470 Xu, L. *et al.* COX-2 inhibition potentiates antiangiogenic cancer therapy and prevents metastasis in preclinical models. *Sci Transl Med* **6**, 242ra284, doi:10.1126/scitranslmed.3008455 (2014).

471 Yoshinaka, R., Shibata, M. A., Morimoto, J., Tanigawa, N. & Otsuki, Y. COX-2 inhibitor celecoxib suppresses tumor growth and lung metastasis of a murine mammary cancer. *Anticancer Res* **26**, 4245-4254 (2006).

472 Leone, V. *et al.* PGE2 inhibits apoptosis in human adenocarcinoma Caco-2 cell line through Ras-PI3K association and cAMP-dependent kinase A activation. *American journal of physiology. Gastrointestinal and liver physiology* **293**, G673-681, doi:10.1152/ajpgi.00584.2006 (2007).

473 Pozzi, A. *et al.* Colon carcinoma cell growth is associated with prostaglandin E2/EP4 receptor-evoked ERK activation. *J Biol Chem* **279**, 29797-29804, doi:10.1074/jbc.M313989200 (2004).

474 Pai, R. *et al.* Prostaglandin E2 transactivates EGF receptor: a novel mechanism for promoting colon cancer growth and gastrointestinal hypertrophy. *Nat Med* **8**, 289-293, doi:10.1038/nm0302-289 (2002).

475 Sheng, H., Shao, J., Washington, M. K. & DuBois, R. N. Prostaglandin E2 increases growth and motility of colorectal carcinoma cells. *J Biol Chem* **276**, 18075-18081, doi:10.1074/jbc.M009689200 (2001).

476 Tessner, T. G., Muhale, F., Riehl, T. E., Anant, S. & Stenson, W. F. Prostaglandin E2 reduces radiation-induced epithelial apoptosis through a mechanism involving AKT activation and bax translocation. *J Clin Invest* **114**, 1676-1685, doi:10.1172/jci22218 (2004).

477 Wang, D., Buchanan, F. G., Wang, H., Dey, S. K. & DuBois, R. N. Prostaglandin E2 enhances intestinal adenoma growth via activation of the Ras-mitogen-activated protein kinase cascade. *Cancer Res* **65**, 1822-1829, doi:10.1158/0008-5472.can-04-3671 (2005).

478 Jones, M. K. *et al.* Inhibition of angiogenesis by nonsteroidal anti-inflammatory drugs: insight into mechanisms and implications for cancer growth and ulcer healing. *Nat Med* **5**, 1418-1423, doi:10.1038/70995 (1999).

479 Williams, C. S., Tsujii, M., Reese, J., Dey, S. K. & DuBois, R. N. Host cyclooxygenase-2 modulates carcinoma growth. *J Clin Invest* **105**, 1589-1594, doi:10.1172/jci9621 (2000).

480 Sonoshita, M. *et al.* Acceleration of intestinal polyposis through prostaglandin receptor EP2 in Apc(Delta 716) knockout mice. *Nat Med* **7**, 1048-1051, doi:10.1038/nm0901-1048 (2001).

481 Ahmadi, M., Emery, D. C. & Morgan, D. J. Prevention of both direct and cross-priming of antitumor CD8+ T-cell responses following overproduction of prostaglandin E2 by tumor cells in vivo. *Cancer Res* **68**, 7520-7529, doi:10.1158/0008-5472.can-08-1060 (2008).

482 Harizi, H. & Gualde, N. The impact of eicosanoids on the crosstalk between innate and adaptive immunity: the key roles of dendritic cells. *Tissue antigens* **65**, 507-514, doi:10.1111/j.1399-0039.2005.00394.x (2005).

483 Buchanan, F. G., Wang, D., Bargiacchi, F. & DuBois, R. N. Prostaglandin E2 regulates cell migration via the intracellular activation of the epidermal growth factor receptor. *J Biol Chem* **278**, 35451-35457, doi:10.1074/jbc.M302474200 (2003).

484 Tsujii, M., Kawano, S. & DuBois, R. N. Cyclooxygenase-2 expression in human colon cancer cells increases metastatic potential. *Proc Natl Acad Sci U S A* **94**, 3336-3340 (1997).

485 Hanahan, D. & Weinberg, R. A. Hallmarks of cancer: the next generation. *Cell* **144**, 646-674, doi:10.1016/j.cell.2011.02.013 (2011).

486 Grivennikov, S. I., Greten, F. R. & Karin, M. Immunity, inflammation, and cancer. *Cell* **140**, 883-899, doi:10.1016/j.cell.2010.01.025 (2010).

487 Grignani, G., Pacchiarini, L., Almasio, P., Pagliarino, M. & Gamba, G. Activation of platelet prostaglandin biosynthesis pathway during neoplastic cell-induced platelet aggregation. *Thrombosis research* **34**, 147-157 (1984).

488 Lian, L. *et al.* Inhibition of MCF-7 breast cancer cell-induced platelet aggregation using a combination of antiplatelet drugs. *Oncology letters* **5**, 675-680, doi:10.3892/ol.2012.1074 (2013).

489 Marelli-Berg, F. M., Peek, E., Lidington, E. A., Stauss, H. J. & Lechler, R. I. Isolation of endothelial cells from murine tissue. *Journal of immunological methods* **244**, 205-215 (2000).

490 Armstrong, P. C. *et al.* Novel whole blood assay for phenotyping platelet reactivity in mice identifies ICAM-1 as a mediator of platelet-monocyte interaction. *Blood* **126**, e11-18, doi:10.1182/blood-2015-01-621656 (2015).

491 Tucker, K. L. *et al.* A dual role for integrin-linked kinase in platelets: regulating integrin function and alpha-granule secretion. *Blood* **112**, 4523-4531, doi:10.1182/blood-2008-03-148502 (2008).

492 Mairey, E. *et al.* Cerebral microcirculation shear stress levels determine Neisseria meningitidis attachment sites along the blood-brain barrier. *Journal of Experimental Medicine* **203**, 1939-1950, doi:10.1084/jem.20060482 (2006).

493 Jung, S. *et al.* Analysis of fractalkine receptor CX(3)CR1 function by targeted deletion and green fluorescent protein reporter gene insertion. *Mol Cell Biol* **20**, 4106-4114 (2000).

494 Reymond, N. *et al.* RhoC and ROCKs regulate cancer cell interactions with endothelial cells. *Mol Oncol* **9**, 1043-1055, doi:10.1016/j.molonc.2015.01.004 (2015).

495 Cathcart, M. C., Reynolds, J. V., O'Byrne, K. J. & Pidgeon, G. P. The role of prostacyclin synthase and thromboxane synthase signaling in the development and progression of cancer. *Biochim Biophys Acta* **1805**, 153-166, doi:10.1016/j.bbcan.2010.01.006 (2010).

496 Granstrom, E., Hamberg, M., Hansson, G. & Kindahl, H. Chemical instability of 15-keto-13,14-dihydro-PGE2: the reason for low assay reliability. *Prostaglandins* **19**, 933-957 (1980).

497 Patrignani, P. *et al.* Biochemical and pharmacological characterization of the cyclooxygenase activity of human blood prostaglandin endoperoxide synthases. *J Pharmacol Exp Ther* **271**, 1705-1712 (1994).

498 Reilly, I. A. & FitzGerald, G. A. Inhibition of thromboxane formation in vivo and ex vivo: implications for therapy with platelet inhibitory drugs. *Blood* **69**, 180-186 (1987).

499 Solheim, S., Arnesen, H., Eikvar, L., Hurlen, M. & Seljeflot, I. Influence of aspirin on inflammatory markers in patients after acute myocardial infarction. *Am J Cardiol* **92**, 843-845 (2003).

500 Lang Kuhs, K. A. *et al.* Association between Regular Aspirin Use and Circulating Markers of Inflammation: A Study within the Prostate, Lung, Colorectal, and Ovarian Cancer Screening Trial. *Cancer epidemiology, biomarkers & prevention : a publication of the American Association for Cancer Research, cosponsored by the American Society of Preventive Oncology* **24**, 825-832, doi:10.1158/1055-9965.epi-14-1363 (2015).

501 Hawkey, C. J. COX-1 and COX-2 inhibitors. *Best practice & research. Clinical gastroenterology* **15**, 801-820, doi:10.1053/bega.2001.0236 (2001).

502 Gierse, J. K. *et al.* A single amino acid difference between cyclooxygenase-1 (COX-1) and -2 (COX-2) reverses the selectivity of COX-2 specific inhibitors. *J Biol Chem* **271**, 15810-15814 (1996).

503 Vitale, P., Panella, A., Scilimati, A. & Perrone, M. G. COX-1 Inhibitors: Beyond Structure Toward Therapy. *Med Res Rev* **36**, 641-671, doi:10.1002/med.21389 (2016).

504 Smith, C. J. *et al.* Pharmacological analysis of cyclooxygenase-1 in inflammation. *Proc Natl Acad Sci U S A* **95**, 13313-13318 (1998).

505 Huff, R. *et al.* A structural feature of N-[2-(cyclohexyloxy)-4-nitrophenyl] methanesulfonamide (NS-398) that governs its selectivity and affinity for cyclooxygenase 2 (COX2). *Inflamm Res* **44 Suppl 2**, S145-146 (1995).

506 Kothekar, V., Sahi, S., Srinivasan, M., Mohan, A. & Mishra, J. Recognition of cyclooxygenase-2 (COX-2) active site by NSAIDs: a computer modelling study. *Indian J Biochem Biophys* **38**, 56-63 (2001).

507 Vecchio, A. J. & Malkowski, M. G. The structure of NS-398 bound to cyclooxygenase-2. *J Struct Biol* **176**, 254-258, doi:10.1016/j.jsb.2011.07.019 (2011).

508 Di Minno, G., Silver, M. J. & Murphy, S. Monitoring the entry of new platelets into the circulation after ingestion of aspirin. *Blood* **61**, 1081-1085 (1983).

509 Li, W., Xu, X. L., Zhang, J., Cai, J. H. & Tang, Y. X. Effects of cyclooxygenase inhibitors on survival time in ovarian cancer xenograft-bearing mice. *Oncology letters* **4**, 1269-1273, doi:10.3892/ol.2012.929 (2012).

510 Li, W. *et al.* Effect of the combination of a cyclooxygenase-1 selective inhibitor and taxol on proliferation, apoptosis and angiogenesis of ovarian cancer in vivo. *Oncology letters* **4**, 168-174, doi:10.3892/ol.2012.688 (2012).

511 LaPointe, M. C., Mendez, M., Leung, A., Tao, Z. & Yang, X. P. Inhibition of cyclooxygenase-2 improves cardiac function after myocardial infarction in the mouse. *American journal of physiology. Heart and circulatory physiology* **286**, H1416-1424, doi:10.1152/ajpheart.00136.2003 (2004).

512 West, J. D. *et al.* Antagonism of the thromboxane-prostanoid receptor is cardioprotective against right ventricular pressure overload. *Pulmonary circulation* **6**, 211-223, doi:10.1086/686140 (2016).

513 Hwang, S. L. *et al.* Effect of aspirin and indomethacin on prostaglandin E2 synthesis in C6 glioma cells. *Kaohsiung J Med Sci* **20**, 1-5, doi:10.1016/S1607-551X(09)70076-2 (2004).

514 Lanza-Jacoby, S. *et al.* The cyclooxygenase-2 inhibitor, celecoxib, prevents the development of mammary tumors in Her-2/neu mice. *Cancer epidemiology, biomarkers & prevention : a publication of the American Association for Cancer Research, cosponsored by the American Society of Preventive Oncology* **12**, 1486-1491 (2003).

515 Roberts, E. G. *et al.* COX-2 inhibition and cancer: experimental findings and clinical correlates. *The West Virginia medical journal* **100**, 96-101 (2004).

516 Gamradt, S. C. *et al.* The effect of cyclooxygenase-2 (COX-2) inhibition on human prostate cancer induced osteoblastic and osteolytic lesions in bone. *Anticancer Res* **25**, 107-115 (2005).

517 Chan, A. T., Ogino, S. & Fuchs, C. S. Aspirin and the risk of colorectal cancer in relation to the expression of COX-2. *New Engl J Med* **356**, 2131-2142, doi:DOI 10.1056/NEJMoa067208 (2007).

518 Wagner, M. *et al.* Resistance of prostate cancer cell lines to COX-2 inhibitor treatment. *Biochem Biophys Res Commun* **332**, 800-807, doi:10.1016/j.bbrc.2005.05.025 (2005).

519 Orr, F. W., Adamson, I. Y. & Young, L. Promotion of pulmonary metastasis in mice by bleomycin-induced endothelial injury. *Cancer Res* **46**, 891-897 (1986).

520 Liotta, L. A., Vembu, D., Saini, R. K. & Boone, C. In vivo monitoring of the death rate of artificial murine pulmonary micrometastases. *Cancer Res* **38**, 1231-1236 (1978).

521 Varani, J., Lovett, E. J., Elgebaly, S., Lundy, J. & Ward, P. A. In vitro and in vivo adherence of tumor cell variants correlated with tumor formation. *Am J Pathol* **101**, 345-352 (1980).

522 Aslakson, C. J., Rak, J. W., Miller, B. E. & Miller, F. R. Differential influence of organ site on three subpopulations of a single mouse mammary tumor at two distinct steps in metastasis. *Int J Cancer* **47**, 466-472 (1991).

523 Al-Mehdi, A. B. *et al.* Intravascular origin of metastasis from the proliferation of endothelium-attached tumor cells: a new model for metastasis. *Nat Med* **6**, 100-102, doi:10.1038/71429 (2000).

524 Wong, C. W. *et al.* Apoptosis: an early event in metastatic inefficiency. *Cancer Res* **61**, 333-338 (2001).

525 Alix-Panabieres, C. & Pantel, K. Challenges in circulating tumour cell research. *Nat Rev Cancer* **14**, 623-631, doi:10.1038/nrc3820 (2014).

526 Gundem, G. *et al.* The evolutionary history of lethal metastatic prostate cancer. *Nature* **520**, 353-357, doi:10.1038/nature14347 (2015).

527 Hoover, H. C., Jr. & Ketcham, A. S. Metastasis of metastases. *Am J Surg* **130**, 405-411 (1975).

528 Kim, M. Y. *et al.* Tumor self-seeding by circulating cancer cells. *Cell* **139**, 1315-1326, doi:10.1016/j.cell.2009.11.025 (2009).

529 Khanna, C. & Hunter, K. Modeling metastasis in vivo. *Carcinogenesis* **26**, 513-523, doi:10.1093/carcin/bgh261 (2005).

530 Saxena, M. & Christofori, G. Rebuilding cancer metastasis in the mouse. *Mol Oncol* **7**, 283-296, doi:10.1016/j.molonc.2013.02.009 (2013).

531 Fidler, I. J. & Nicolson, G. L. Organ selectivity for implantation survival and growth of B16 melanoma variant tumor lines. *J Natl Cancer Inst* **57**, 1199-1202 (1976).

532 Bogenmann, E. A metastatic neuroblastoma model in SCID mice. *Int J Cancer* **67**, 379-385, doi:10.1002/(SICI)1097-0215(19960729)67:3<379::AID-IJC12>3.0.CO;2-3 (1996).

533 Nanni, P. *et al.* Human rhabdomyosarcoma cells in nude mice as a model for metastasis and differentiation. *Invasion Metastasis* **9**, 231-241 (1989).

534 Iwakawa, M., Ando, K., Ohkawa, H., Koike, S. & Chen, Y. J. A murine model for bone marrow metastasis established by an i.v. injection of C-1300 neuroblastoma in A/J mice. *Clin Exp Metastasis* **12**, 231-237 (1994).

535 Minn, A. J. *et al.* Genes that mediate breast cancer metastasis to lung. *Nature* **436**, 518-524, doi:10.1038/nature03799 (2005).

536 Becker, M. *et al.* Sensitive PCR method for the detection and real-time quantification of human cells in xenotransplantation systems. *Br J Cancer* **87**, 1328-1335, doi:10.1038/sj.bjc.6600573 (2002).

537 Cameron, M. D. *et al.* Temporal progression of metastasis in lung: cell survival, dormancy, and location dependence of metastatic inefficiency. *Cancer Res* **60**, 2541-2546 (2000).

538 Kim, J., Yu, W., Kovalski, K. & Ossowski, L. Requirement for specific proteases in cancer cell intravasation as revealed by a novel semiquantitative PCR-based assay. *Cell* **94**, 353-362 (1998).

539 Malek, A., Catapano, C. V., Czubayko, F. & Aigner, A. A sensitive polymerase chain reaction-based method for detection and quantification of metastasis in human xenograft mouse models. *Clin Exp Metastasis* **27**, 261-271, doi:10.1007/s10585-010-9324-1 (2010).

540 Schneider, T., Osl, F., Friess, T., Stockinger, H. & Scheuer, W. V. Quantification of human Alu sequences by real-time PCR--an improved method to measure therapeutic efficacy of anti-metastatic drugs in human xenotransplants. *Clin Exp Metastasis* **19**, 571-582 (2002).

541 Fisher, A. B., Dodia, C. & Linask, J. Perfusate composition and edema formation in isolated rat lungs. *Exp Lung Res* **1**, 13-21 (1980).

542 Al-Mehdi, A. B., Shuman, H. & Fisher, A. B. Intracellular generation of reactive oxygen species during nonhypoxic lung ischemia. *Am J Physiol* **272**, L294-300 (1997).

543 Al-Mehdi, A. B. *et al.* Endothelial NADPH oxidase as the source of oxidants in lungs exposed to ischemia or high K+. *Circ Res* **83**, 730-737 (1998).

544 Wang, H. *et al.* Tumor cell alpha3beta1 integrin and vascular laminin-5 mediate pulmonary arrest and metastasis. *J Cell Biol* **164**, 935-941, doi:10.1083/jcb.200309112 (2004).

545 Ellenbroek, S. I. & van Rheenen, J. Imaging hallmarks of cancer in living mice. *Nat Rev Cancer* **14**, 406-418, doi:10.1038/nrc3742 (2014).

546 Entenberg, D. *et al.* In vivo subcellular resolution optical imaging in the lung reveals early metastatic proliferation and motility. *Intravital* **4**, doi:10.1080/21659087.2015.1086613 (2015).

547 Konstantopoulos, K. & McIntire, L. V. Effects of fluid dynamic forces on vascular cell adhesion. *J Clin Invest* **98**, 2661-2665, doi:10.1172/JCI119088 (1996).

548 Bernards, R. & Weinberg, R. A. Metastasis genes: A progression puzzle. *Nature* **418**, 823-823, doi:10.1038/418823a (2002).

549 Husemann, Y. *et al.* Systemic spread is an early step in breast cancer. *Cancer Cell* **13**, 58-68, doi:10.1016/j.ccr.2007.12.003 (2008).

550 Stegner, D. & Nieswandt, B. Platelet receptor signaling in thrombus formation. *J Mol Med (Berl)* **89**, 109-121, doi:10.1007/s00109-010-0691-5 (2011).

551 Norris, L. A. Blood coagulation. *Best Pract Res Clin Obstet Gynaecol* **17**, 369-383 (2003).

552 Green, D. Coagulation cascade. *Hemodial Int* **10 Suppl 2**, S2-4, doi:10.1111/j.1542-4758.2006.00119.x (2006).

553 Whiteheart, S. W. Platelet granules: surprise packages. *Blood* **118**, 1190-1191, doi:10.1182/blood-2011-06-359836 (2011).

554 Bye, A. P., Unsworth, A. J. & Gibbins, J. M. Platelet signaling: a complex interplay between inhibitory and activatory networks. *J Thromb Haemost* **14**, 918-930, doi:10.1111/jth.13302 (2016).

555 Uehara, Y. *et al.* Regulatory effects of eicosanoids on thymidine uptake by vascular smooth muscle cells of rats. *Prostaglandins* **36**, 847-857 (1988).

556 Vasquez, S. X. *et al.* Optimization of microCT imaging and blood vessel diameter quantitation of preclinical specimen vasculature with radiopaque polymer injection medium. *PLoS One* **6**, e19099, doi:10.1371/journal.pone.0019099 (2011).

557 Taichman, D. B. *et al.* Tumor cell surface alpha 4 beta 1 integrin mediates adhesion to vascular endothelium: demonstration of an interaction with the N-terminal domains of INCAM-110/VCAM-1. *Cell Regul* **2**, 347-355 (1991).

558 Huang, A. J. *et al.* Endothelial cell cytosolic free calcium regulates neutrophil migration across monolayers of endothelial cells. *J Cell Biol* **120**, 1371-1380 (1993).

559 Deem, T. L. & Cook-Mills, J. M. Vascular cell adhesion molecule 1 (VCAM-1) activation of endothelial cell matrix metalloproteinases: role of reactive oxygen species. *Blood* **104**, 2385-2393, doi:10.1182/blood-2004-02-0665 (2004).

560 Gately, S. & Li, W. W. Multiple roles of COX-2 in tumor angiogenesis: a target for antiangiogenic therapy. *Semin Oncol* **31**, 2-11 (2004).

561 Shen, S. *et al.* Vascular endothelial growth factor enhances cancer cell adhesion to microvascular endothelium in vivo. *Exp Physiol* **95**, 369-379, doi:10.1113/expphysiol.2009.050260 (2010).

562 Che, S. P., DeLeonardis, C., Shuler, M. L. & Stokol, T. Tissue factor-expressing tumor cells can bind to immobilized recombinant tissue factor pathway inhibitor under static and shear conditions in vitro. *PLoS One* **10**, e0123717, doi:10.1371/journal.pone.0123717 (2015).

563 Rolin, S., Masereel, B. & Dogne, J. M. Prostanoids as pharmacological targets in COPD and asthma. *Eur J Pharmacol* **533**, 89-100, doi:10.1016/j.ejphar.2005.12.058 (2006).

564 Michelson, A. D. *Platelets*. Third edition. edn, (Elsevier/Academic Press, 2013).

565 Sakai, H. *et al.* Upregulation of thromboxane synthase in human colorectal carcinoma and the cancer cell proliferation by thromboxane A2. *FEBS Lett* **580**, 3368-3374, doi:10.1016/j.febslet.2006.05.007 (2006).

566 Moussa, O. *et al.* Prognostic and functional significance of thromboxane synthase gene overexpression in invasive bladder cancer. *Cancer Res* **65**, 11581-11587, doi:10.1158/0008-5472.CAN-05-1622 (2005).

567 Kreutzer, M. *et al.* Specific components of prostanoid-signaling pathways are present in non-small cell lung cancer cells. *Oncol Rep* **18**, 497-501 (2007).

568 Huang, R. Y. *et al.* 4-Methylnitrosamino-1-3-pyridyl-1-butanone (NNK) promotes lung cancer cell survival by stimulating thromboxane A2 and its receptor. *Oncogene* **30**, 106-116, doi:10.1038/onc.2010.390 (2011).

569 Kajita, S., Ruebel, K. H., Casey, M. B., Nakamura, N. & Lloyd, R. V. Role of COX-2, thromboxane A2 synthase, and prostaglandin I2 synthase in papillary thyroid carcinoma growth. *Mod Pathol* **18**, 221-227, doi:10.1038/modpathol.3800285 (2005).

570 Nie, D. *et al.* Differential expression of thromboxane synthase in prostate carcinoma: role in tumor cell motility. *Am J Pathol* **164**, 429-439, doi:10.1016/S0002-9440(10)63133-1 (2004).

571 Dassesse, T. *et al.* Activation of the thromboxane A2 pathway in human prostate cancer correlates with tumor Gleason score and pathologic stage. *Eur Urol* **50**, 1021-1031; discussion 1031, doi:10.1016/j.eururo.2006.01.036 (2006).

572 Cathcart, M. C. *et al.* Examination of thromboxane synthase as a prognostic factor and therapeutic target in non-small cell lung cancer. *Mol Cancer* **10**, 25, doi:10.1186/1476-4598-10-25 (2011).

573 Pinto, S. *et al.* Increased thromboxane A2 production at primary tumor site in metastasizing squamous cell carcinoma of the larynx. *Prostaglandins Leukot Essent Fatty Acids* **49**, 527-530 (1993).

574 Bryant, J. Correlation between metastatic patterns in renal cell carcinoma and tissue distribution of thromboxane synthetase. *Acta Oncol* **33**, 708-709 (1994).

575 Giese, A. *et al.* Thromboxane synthase regulates the migratory phenotype of human glioma cells. *Neuro Oncol* **1**, 3-13 (1999).

576 Yoshimoto, A., Kasahara, K., Kawashima, A., Fujimura, M. & Nakao, S. Characterization of the prostaglandin biosynthetic pathway in non-small cell lung cancer: a comparison with small cell lung cancer and correlation with angiogenesis, angiogenic factors and metastases. *Oncol Rep* **13**, 1049-1057 (2005).

577 Brass, L. F., Shaller, C. C. & Belmonte, E. J. Inositol 1,4,5-triphosphate-induced granule secretion in platelets. Evidence that the activation of phospholipase C mediated by platelet thromboxane receptors involves a guanine nucleotide binding protein-dependent mechanism distinct from that of thrombin. *J Clin Invest* **79**, 1269-1275, doi:10.1172/JCI112947 (1987).

578 Rittenhouse, S. E. Phosphoinositide 3-kinase activation and platelet function. *Blood* **88**, 4401-4414 (1996).

579 Shock, D. D., He, K., Wencel-Drake, J. D. & Parise, L. V. Ras activation in platelets after stimulation of the thrombin receptor, thromboxane A2 receptor or protein kinase C. *Biochem J* **321 (Pt 2)**, 525-530 (1997).
580 Dovizio, M., Alberti, S., Guillem-Llobat, P. & Patrignani, P. Role of platelets in inflammation and cancer: novel therapeutic strategies. *Basic Clin Pharmacol Toxicol* **114**, 118-127, doi:10.1111/bcpt.12156 (2014).
581 Gratacap, M. P., Payrastre, B., Nieswandt, B. & Offermanns, S. Differential regulation of Rho and Rac through heterotrimeric G-proteins and cyclic nucleotides. *J Biol Chem* **276**, 47906-47913, doi:10.1074/jbc.M104442200 (2001).
582 Li, Z., Delaney, M. K., O'Brien, K. A. & Du, X. Signaling during platelet adhesion and activation. *Arteriosclerosis, thrombosis, and vascular biology* **30**, 2341-2349, doi:10.1161/atvbaha.110.207522 (2010).
583 Wettschureck, N. & Offermanns, S. Mammalian G proteins and their cell type specific functions. *Physiological reviews* **85**, 1159-1204, doi:10.1152/physrev.00003.2005 (2005).
584 Ohkubo, S., Nakahata, N. & Ohizumi, Y. Thromboxane A2-mediated shape change: independent of Gq-phospholipase C--Ca2+ pathway in rabbit platelets. *Br J Pharmacol* **117**, 1095-1104 (1996).
585 Klages, B., Brandt, U., Simon, M. I., Schultz, G. & Offermanns, S. Activation of G12/G13 results in shape change and Rho/Rho-kinase-mediated myosin light chain phosphorylation in mouse platelets. *J Cell Biol* **144**, 745-754 (1999).
586 Dorsam, R. T., Kim, S., Jin, J. & Kunapuli, S. P. Coordinated signaling through both G12/13 and G(i) pathways is sufficient to activate GPIIb/IIIa in human platelets. *J Biol Chem* **277**, 47588-47595, doi:10.1074/jbc.M208778200 (2002).
587 Simpson, A. W., Hallam, T. J. & Rink, T. J. Low concentrations of the stable prostaglandin endoperoxide U44069 stimulate shape change in quin2-loaded platelets without a measurable increase in [Ca2+]i. *FEBS Lett* **201**, 301-305 (1986).
588 Nieswandt, B., Schulte, V., Zywietz, A., Gratacap, M. P. & Offermanns, S. Costimulation of Gi- and G12/G13-mediated signaling pathways induces integrin alpha IIbbeta 3 activation in platelets. *J Biol Chem* **277**, 39493-39498, doi:10.1074/jbc.M207256200 (2002).
589 Ishizuka, T. *et al.* Thromboxane A2 receptor blockade suppresses intercellular adhesion molecule-1 expression by stimulated vascular endothelial cells. *Eur J Pharmacol* **312**, 367-377 (1996).
590 Ishizuka, T. *et al.* Stimulation with thromboxane A2 (TXA2) receptor agonist enhances ICAM-1, VCAM-1 or ELAM-1 expression by human vascular endothelial cells. *Clin Exp Immunol* **112**, 464-470 (1998).
591 Ashton, A. W., Ware, G. M., Kaul, D. K. & Ware, J. A. Inhibition of tumor necrosis factor alpha-mediated NFkappaB activation and leukocyte adhesion, with enhanced endothelial apoptosis, by G protein-linked receptor (TP) ligands. *J Biol Chem* **278**, 11858-11866, doi:10.1074/jbc.M210766200 (2003).
592 He, J. *et al.* Liver kinase B1 is required for thromboxane receptor-dependent nuclear factor-kappaB activation and inflammatory responses. *Arteriosclerosis, thrombosis, and vascular biology* **33**, 1297-1305, doi:10.1161/ATVBAHA.113.301296 (2013).
593 Cayatte, A. J. *et al.* The thromboxane receptor antagonist S18886 but not aspirin inhibits atherogenesis in apo E-deficient mice: evidence that eicosanoids other than thromboxane contribute to atherosclerosis. *Arteriosclerosis, thrombosis, and vascular biology* **20**, 1724-1728 (2000).
594 Del Turco, S. *et al.* Involvement of the TP receptor in TNF-alpha-induced endothelial tissue factor expression. *Vascul Pharmacol* **62**, 49-56, doi:10.1016/j.vph.2014.03.007 (2014).
595 Ishizuka, T., Sawada, S., Sugama, K. & Kurita, A. Thromboxane A2 (TXA2) receptor blockade suppresses monocyte chemoattractant protein-1 (MCP-1) expression by stimulated vascular endothelial cells. *Clin Exp Immunol* **120**, 71-78 (2000).
596 Li, X. & Tai, H. H. Activation of thromboxane A2 receptor (TP) increases the expression of monocyte chemoattractant protein -1 (MCP-1)/chemokine (C-C motif) ligand 2 (CCL2) and recruits macrophages to promote invasion of lung cancer cells. *PLoS One* **8**, e54073, doi:10.1371/journal.pone.0054073 (2013).
597 Daniel, T. O., Liu, H., Morrow, J. D., Crews, B. C. & Marnett, L. J. Thromboxane A2 is a mediator of cyclooxygenase-2-dependent endothelial migration and angiogenesis. *Cancer Res* **59**, 4574-4577 (1999).

598 Nie, D. *et al.* Thromboxane A(2) regulation of endothelial cell migration, angiogenesis, and tumor metastasis. *Biochem Biophys Res Commun* **267**, 245-251, doi:10.1006/bbrc.1999.1840 (2000).
599 Bertolino, F., Valentin, J. P., Maffre, M., Bessac, A. M. & John, G. W. TxA2 receptor activation elicits organ-specific increases in microvascular permeability in the rat. *Am J Physiol* **268**, R366-374 (1995).
600 Michel, F. *et al.* Thromboxane A2/prostaglandin H2 receptor activation mediates angiotensin II-induced postischemic neovascularization. *Arteriosclerosis, thrombosis, and vascular biology* **26**, 488-493, doi:10.1161/01.ATV.0000201969.93348.74 (2006).
601 Caughey, G. E., Cleland, L. G., Gamble, J. R. & James, M. J. Up-regulation of endothelial cyclooxygenase-2 and prostanoid synthesis by platelets. Role of thromboxane A2. *J Biol Chem* **276**, 37839-37845, doi:10.1074/jbc.M010606200 (2001).
602 Hunt, J. A., Merritt, J. E., MacDermot, J. & Keen, M. Characterization of the thromboxane receptor mediating prostacyclin release from cultured endothelial cells. *Biochem Pharmacol* **43**, 1747-1752 (1992).
603 Barry, O. P., Pratico, D., Lawson, J. A. & FitzGerald, G. A. Transcellular activation of platelets and endothelial cells by bioactive lipids in platelet microparticles. *J Clin Invest* **99**, 2118-2127, doi:10.1172/JCI119385 (1997).
604 Dorn, G. W., 2nd & Becker, M. W. Thromboxane A2 stimulated signal transduction in vascular smooth muscle. *J Pharmacol Exp Ther* **265**, 447-456 (1993).
605 Tripp, C. S., Unanue, E. R. & Needleman, P. Monocyte migration explains the changes in macrophage arachidonate metabolism during the immune response. *Proc Natl Acad Sci U S A* **83**, 9655-9659 (1986).
606 Eligini, S., Barbieri, S. S., Arenaz, I., Tremoli, E. & Colli, S. Paracrine up-regulation of monocyte cyclooxygenase-2 by platelets: role of transforming growth factor-beta1. *Cardiovasc Res* **74**, 270-278, doi:10.1016/j.cardiores.2006.12.013 (2007).
607 Wang, J. W. *et al.* Multitargeting of selected prostanoid receptors provides agents with enhanced anti-inflammatory activity in macrophages. *FASEB J* **30**, 394-404, doi:10.1096/fj.15-275610 (2016).
608 Eligini, S. *et al.* Indobufen inhibits tissue factor in human monocytes through a thromboxane-mediated mechanism. *Cardiovasc Res* **69**, 218-226, doi:10.1016/j.cardiores.2005.07.013 (2006).
609 Allan, C. J. & Halushka, P. V. Characterization of human peripheral blood monocyte thromboxane A2 receptors. *J Pharmacol Exp Ther* **270**, 446-452 (1994).
610 Watkins, G., Douglas-Jones, A., Mansel, R. E. & Jiang, W. G. Expression of thromboxane synthase, TBXAS1 and the thromboxane A2 receptor, TBXA2R, in human breast cancer. *Int Semin Surg Oncol* **2**, 23, doi:10.1186/1477-7800-2-23 (2005).
611 Gustafsson, A. *et al.* Prostanoid receptor expression in colorectal cancer related to tumor stage, differentiation and progression. *Acta Oncol* **46**, 1107-1112, doi:10.1080/02841860701403061 (2007).
612 Wei, J., Yan, W., Li, X., Ding, Y. & Tai, H. H. Thromboxane receptor alpha mediates tumor growth and angiogenesis via induction of vascular endothelial growth factor expression in human lung cancer cells. *Lung Cancer* **69**, 26-32, doi:10.1016/j.lungcan.2009.09.009 (2010).
613 Nie, D. *et al.* Thromboxane A2 receptors in prostate carcinoma: expression and its role in regulating cell motility via small GTPase Rho. *Cancer Res* **68**, 115-121, doi:10.1158/0008-5472.CAN-07-1018 (2008).
614 Ekambaram, P., Lambiv, W., Cazzolli, R., Ashton, A. W. & Honn, K. V. The thromboxane synthase and receptor signaling pathway in cancer: an emerging paradigm in cancer progression and metastasis. *Cancer Metastasis Rev* **30**, 397-408, doi:10.1007/s10555-011-9297-9 (2011).
615 Moussa, O. *et al.* Novel role of thromboxane receptors beta isoform in bladder cancer pathogenesis. *Cancer Res* **68**, 4097-4104, doi:10.1158/0008-5472.CAN-07-6560 (2008).
616 McDonough, W., Tran, N., Giese, A., Norman, S. A. & Berens, M. E. Altered gene expression in human astrocytoma cells selected for migration: I. Thromboxane synthase. *J Neuropathol Exp Neurol* **57**, 449-455 (1998).
617 Honn, K. V. & Meyer, J. Thromboxanes and prostacyclin: positive and negative modulators of tumor growth. *Biochem Biophys Res Commun* **102**, 1122-1129 (1981).

618 Li, X. & Tai, H. H. Activation of thromboxane A(2) receptors induces orphan nuclear receptor Nurr1 expression and stimulates cell proliferation in human lung cancer cells. *Carcinogenesis* **30**, 1606-1613, doi:10.1093/carcin/bgp161 (2009).
619 Leung, K. C. *et al.* Inhibition of thromboxane synthase induces lung cancer cell death via increasing the nuclear p27. *Exp Cell Res* **315**, 2974-2981, doi:10.1016/j.yexcr.2009.06.025 (2009).
620 Dovizio, M. *et al.* Pharmacological inhibition of platelet-tumor cell cross-talk prevents platelet-induced overexpression of cyclooxygenase-2 in HT29 human colon carcinoma cells. *Mol Pharmacol* **84**, 25-40, doi:10.1124/mol.113.084988 (2013).
621 Turner, E. C. *et al.* Identification of an interaction between the TPalpha and TPbeta isoforms of the human thromboxane A2 receptor with protein kinase C-related kinase (PRK) 1: implications for prostate cancer. *J Biol Chem* **286**, 15440-15457, doi:10.1074/jbc.M110.181180 (2011).
622 Kelly, P. *et al.* A role for the G12 family of heterotrimeric G proteins in prostate cancer invasion. *J Biol Chem* **281**, 26483-26490, doi:10.1074/jbc.M604376200 (2006).
623 Pradono, P. *et al.* Gene transfer of thromboxane A(2) synthase and prostaglandin I(2) synthase antithetically altered tumor angiogenesis and tumor growth. *Cancer Res* **62**, 63-66 (2002).
624 Honn, K. V. Inhibition of tumor cell metastasis by modulation of the vascular prostacyclin/thromboxane A2 system. *Clin Exp Metastasis* **1**, 103-114 (1983).
625 Matsui, Y. *et al.* Thromboxane A(2) receptor signaling facilitates tumor colonization through P-selectin-mediated interaction of tumor cells with platelets and endothelial cells. *Cancer science* **103**, 700-707, doi:10.1111/j.1349-7006.2012.02200.x (2012).
626 Patrignani, P., Filabozzi, P. & Patrono, C. Selective cumulative inhibition of platelet thromboxane production by low-dose aspirin in healthy subjects. *J Clin Invest* **69**, 1366-1372 (1982).
627 Marcus, A. J., Weksler, B. B., Jaffe, E. A. & Broekman, M. J. Synthesis of prostacyclin from platelet-derived endoperoxides by cultured human endothelial cells. *J Clin Invest* **66**, 979-986, doi:10.1172/jci109967 (1980).
628 FitzGerald, G. A., Reilly, I. A. & Pedersen, A. K. The biochemical pharmacology of thromboxane synthase inhibition in man. *Circulation* **72**, 1194-1201 (1985).
629 Nakahata, N. Thromboxane A2: physiology/pathophysiology, cellular signal transduction and pharmacology. *Pharmacol Ther* **118**, 18-35, doi:10.1016/j.pharmthera.2008.01.001 (2008).
630 Verstraete, M. Introduction: thromboxane in biological systems and the possible impact of its inhibition. *Br J Clin Pharmacol* **15 Suppl 1**, 7S-11S (1983).
631 Nakazawa, M., Iizuka, K., Ujiie, A., Hiraku, S. & Ohki, S. [Research and development of ozagrel, a highly selective inhibitor of TXA2 synthase]. *Yakugaku Zasshi* **114**, 911-933 (1994).
632 Suzuki, S. *et al.* Clinical study of OKY-046, a thromboxane synthetase inhibitor, in prevention of cerebral vasospasms and delayed cerebral ischaemic symptoms after subarachnoid haemorrhage due to aneurysmal rupture: a randomized double-blind study. *Neurol Res* **11**, 79-88 (1989).
633 Shikano, M., Ito, T., Ogawa, K. & Satake, T. Effects of a selective thromboxane synthetase inhibitor (OKY-046) in patients with coronary artery disease during exercise. *Japanese heart journal* **28**, 663-674 (1987).
634 Zhang, J. *et al.* Ozagrel for acute ischemic stroke: a meta-analysis of data from randomized controlled trials. *Neurol Res* **34**, 346-353, doi:10.1179/1743132812Y.0000000022 (2012).
635 Fujimura, M., Nishioka, S., Kumabashiri, I., Matsuda, T. & Mifune, J. Effects of aerosol administration of a thromboxane synthetase inhibitor (OKY-046) on bronchial responsiveness to acetylcholine in asthmatic subjects. *Chest* **98**, 276-279 (1990).
636 Fujimura, M., Sakamoto, S. & Matsuda, T. Attenuating effect of a thromboxane synthetase inhibitor (OKY-046) on bronchial responsiveness to methacholine is specific to bronchial asthma. *Chest* **98**, 656-660 (1990).
637 Fontana, P., Zufferey, A., Daali, Y. & Reny, J. L. Antiplatelet therapy: targeting the TxA2 pathway. *J Cardiovasc Transl Res* **7**, 29-38, doi:10.1007/s12265-013-9529-1 (2014).

638 Bousser, M. G. *et al.* Terutroban versus aspirin in patients with cerebral ischaemic events (PERFORM): a randomised, double-blind, parallel-group trial. *Lancet* **377**, 2013-2022, doi:10.1016/S0140-6736(11)60600-4 (2011).
639 Randomized trial of ridogrel, a combined thromboxane A2 synthase inhibitor and thromboxane A2/prostaglandin endoperoxide receptor antagonist, versus aspirin as adjunct to thrombolysis in patients with acute myocardial infarction. The Ridogrel Versus Aspirin Patency Trial (RAPT). *Circulation* **89**, 588-595 (1994).
640 Patrono, C. Biosynthesis and pharmacological modulation of thromboxane in humans. *Circulation* **81**, I12-15; discussion I22-13 (1990).
641 Modesti, P. A., Colella, A., Abbate, R., Gensini, G. & Neri Serneri, G. Competitive inhibition of platelet thromboxane A2 receptor binding by picotamide. *Eur J Pharmacol* **169**, 85-93 (1989).
642 Modesti, P. A. *et al.* Binding kinetics and antiplatelet activities of picotamide, a thromboxane A2 receptor antagonist. *Br J Pharmacol* **112**, 81-86 (1994).
643 Gresele, P., Deckmyn, H., Arnout, J., Nenci, G. G. & Vermylen, J. Characterization of N,N'-bis(3-picolyl)-4-methoxy-isophtalamide (picotamide) as a dual thromboxane synthase inhibitor/thromboxane A2 receptor antagonist in human platelets. *Thromb Haemost* **61**, 479-484 (1989).
644 Ratti, S., Quarato, P., Casagrande, C., Fumagalli, R. & Corsini, A. Picotamide, an antithromboxane agent, inhibits the migration and proliferation of arterial myocytes. *Eur J Pharmacol* **355**, 77-83 (1998).
645 Balsano, F. & Violi, F. Effect of picotamide on the clinical progression of peripheral vascular disease. A double-blind placebo-controlled study. The ADEP Group. *Circulation* **87**, 1563-1569 (1993).
646 Neri Serneri, G. G., Coccheri, S., Marubini, E., Violi, F. & Drug Evaluation in Atherosclerotic Vascular Disease in Diabetics Study, G. Picotamide, a combined inhibitor of thromboxane A2 synthase and receptor, reduces 2-year mortality in diabetics with peripheral arterial disease: the DAVID study. *Eur Heart J* **25**, 1845-1852, doi:10.1016/j.ehj.2004.07.013 (2004).
647 Milani, M., Longoni, A. & Maderna, M. Effects of picotamide, an antiplatelet agent, on cardiovascular, events in 438 claudicant patients with diabetes: a retrospective analysis of the ADEP study. *Br J Clin Pharmacol* **42**, 782-785 (1996).
648 Davi, G., Santilli, F. & Vazzana, N. Thromboxane receptors antagonists and/or synthase inhibitors. *Handb Exp Pharmacol*, 261-286, doi:10.1007/978-3-642-29423-5_11 (2012).
649 Amraoui, F. *et al.* SFlt-1 elevates blood pressure by augmenting endothelin-1-mediated vasoconstriction in mice. *PLoS One* **9**, e91897, doi:10.1371/journal.pone.0091897 (2014).
650 De Franceschi, M. S. *et al.* Decreased platelet aggregation by shear stress-stimulated endothelial cells in vitro: description of a method and first results in diabetes. *Diab Vasc Dis Res* **12**, 53-61, doi:10.1177/1479164114553784 (2015).
651 Kirkby, N. S. *et al.* Cyclooxygenase-1, not cyclooxygenase-2, is responsible for physiological production of prostacyclin in the cardiovascular system. *Proc Natl Acad Sci U S A* **109**, 17597-17602, doi:10.1073/pnas.1209192109 (2012).
652 Sarker, M. H., Hu, D. E. & Fraser, P. A. Regulation of cerebromicrovascular permeability by lysophosphatidic acid. *Microcirculation* **17**, 39-46, doi:10.1111/j.1549-8719.2010.00001.x (2010).

APPENDIX

Supplementary figures

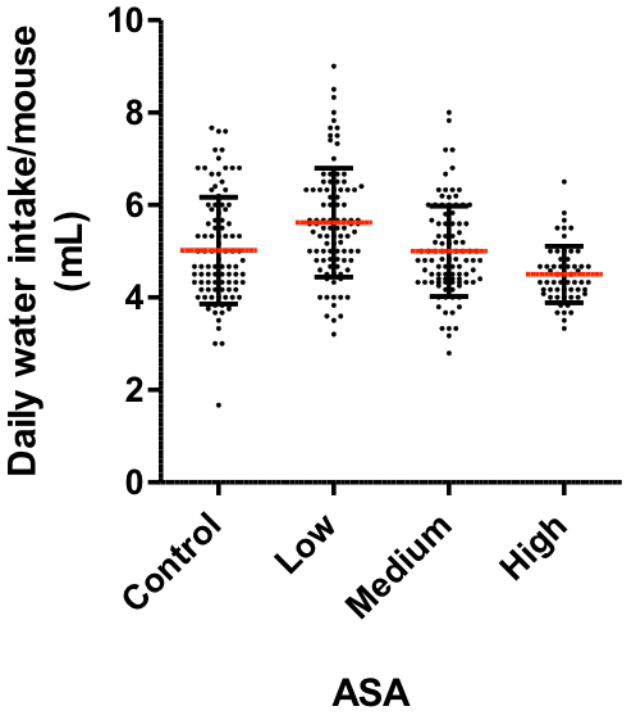

Supplementary figure S1- Daily intake of drinking water per mouse.

Expected average daily intake drinking water per C57BL/6 mouse, extrapolated from the drinking water consumption of the whole cage over a period of 3 weeks. Mice were treated with vehicle (Control, n=97 mice) or ASA (Low, Medium and High doses, n=95, 98 and 56 mice, respectively).

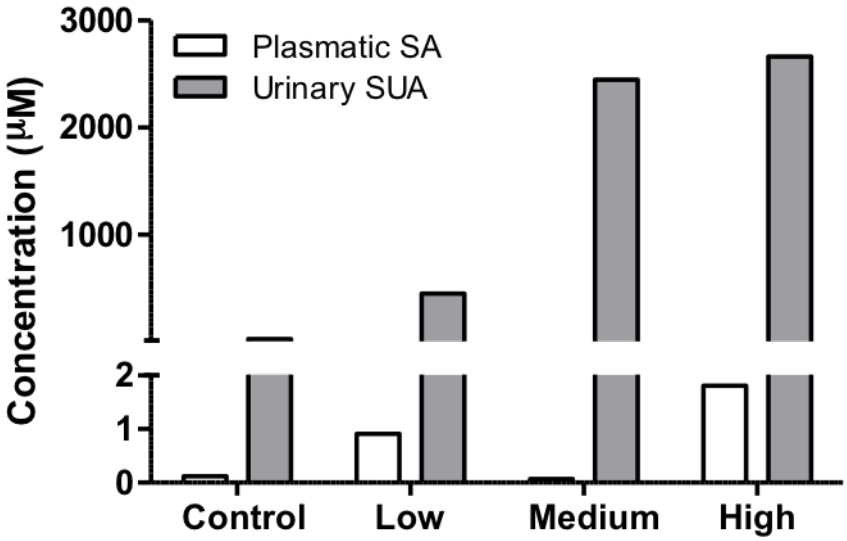

Supplementary figure S2 - Levels of plasmatic SA and SUA in ASA-treated mice.

Concentration of salicylic acid (SA) in plasma and salicyluric acid (SUA) in urine measured in samples collected from the same C57BL/6 mouse treated with ASA for 2 weeks (n=1 mouse). The higher concentration of SUA to SA is due to the accumulation of SUA in urine over time.

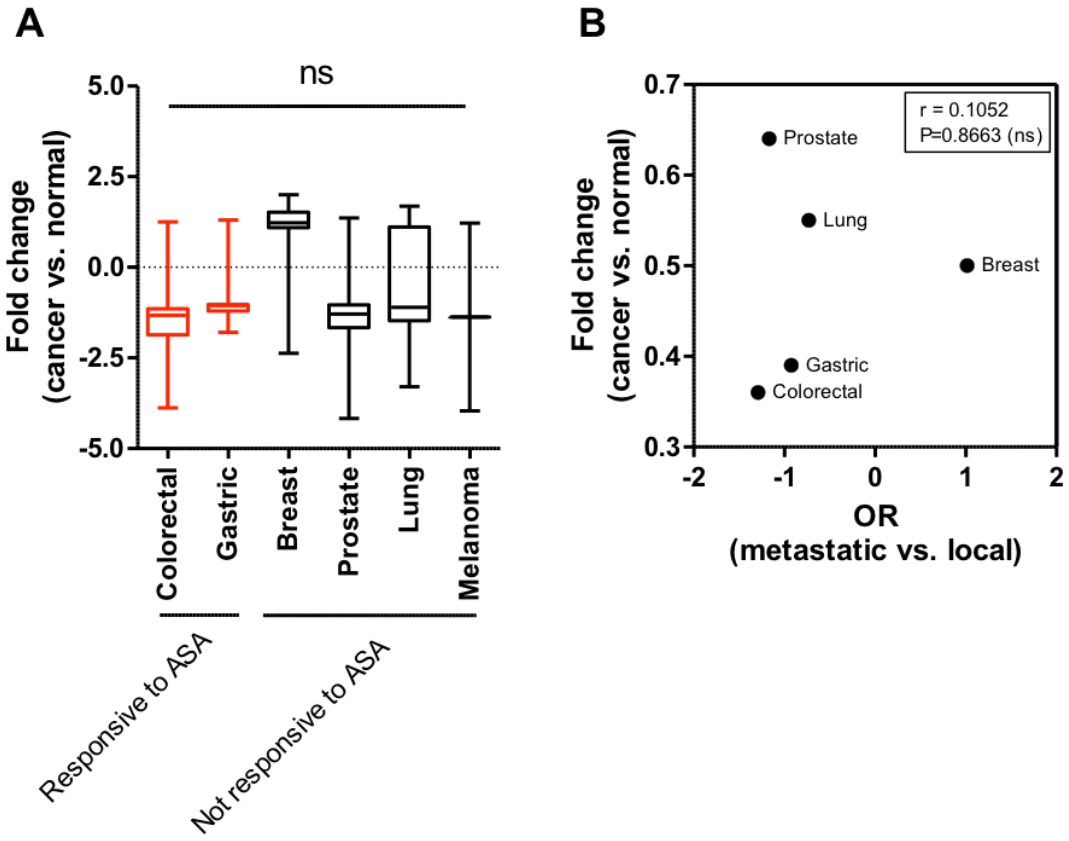

Supplementary figure S3 - COX-1 expression in clinical tumour samples does not correlate with the anti-metastatic effect of aspirin.

(A) Comparative analysis of COX-1 (PTGS1) mRNA expression in human tumour specimen vs. normal tissue cohorts from ONCOMINE (Oncomine™ v4.5). Different adenocarcinomas (colorectal, gastric, breast and prostate cancer) and non-adenocarcinomas (lung and melanoma) were chosen as they represent the most frequent types of cancer reported in the metanalysis by Rothwell et al.[428]. For colorectal and gastric cancer, studies involving samples of (adeno)carcinoma were selected. All cancer types express COX-1 to a similar extent to normal tissues, regardless whether aspirin reduced (colorectal and gastric, responsive to ASA) or did not reduce (breast, prostate, lung and melanoma, not responsive to ASA) the risk to become metastatic.

(B) Correlation analysis between the relative COX-1 expression (cancer vs. normal) and the odds ratio (OR) of metastatic cancer (metastatic vs. local disease) for the most common cancer types included in the metanalysis of Rothwell et al.[428] (mean values, Pearson r correlation).

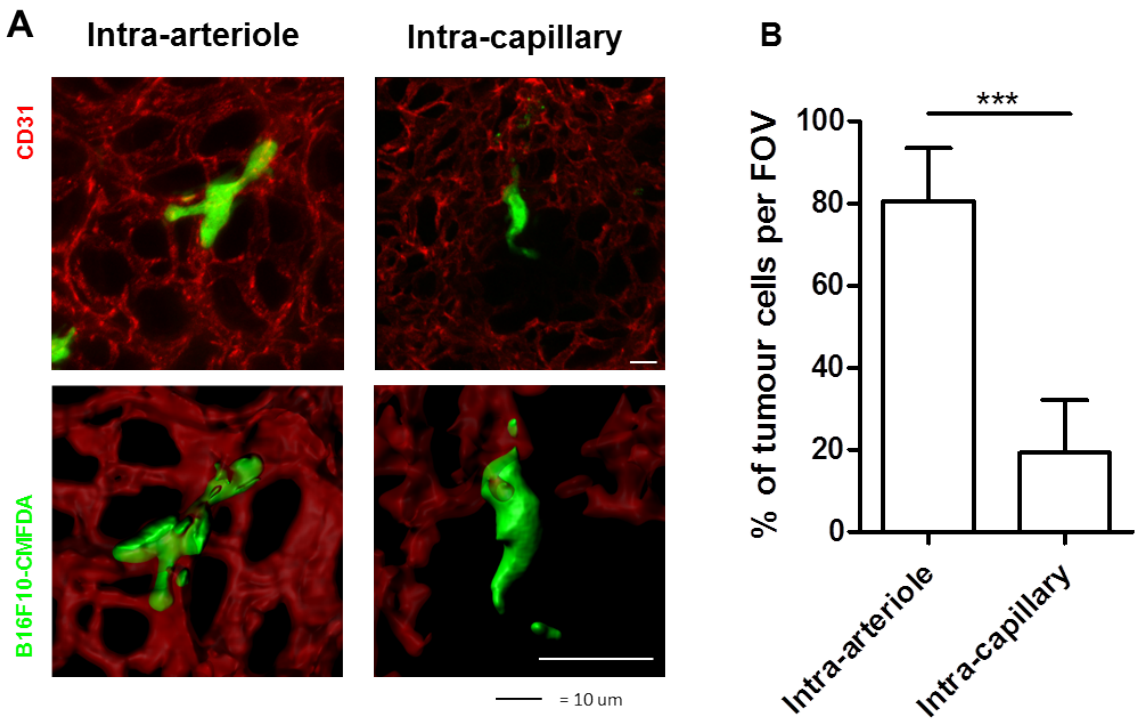

Supplementary figure S4 – Different modes of initial arrest of tumour cells in the pulmonary vasculature.

(A) Representative MIP of 3D confocal stacks and surface reconstruction of confocal images (20x) of whole lungs of C57BL/6 mice intravenously injected with B16F10-CMFDA cells (green) and anti-CD31-APC antibody (red), to label the vasculature. Lungs were harvested immediately after injection. On the basis of CD31 antibody exclusion from the downstream vessels, tumour cells were classified as localised in a arteriole (left) or in a capillary (right).

(B) Quantification of the percentage of intra-arteriole or intra-capillary tumour cells from confocal images (n=3 mice per group, ≥10 FOVs per repetition were analysed; mean + SD, unpaired t test).

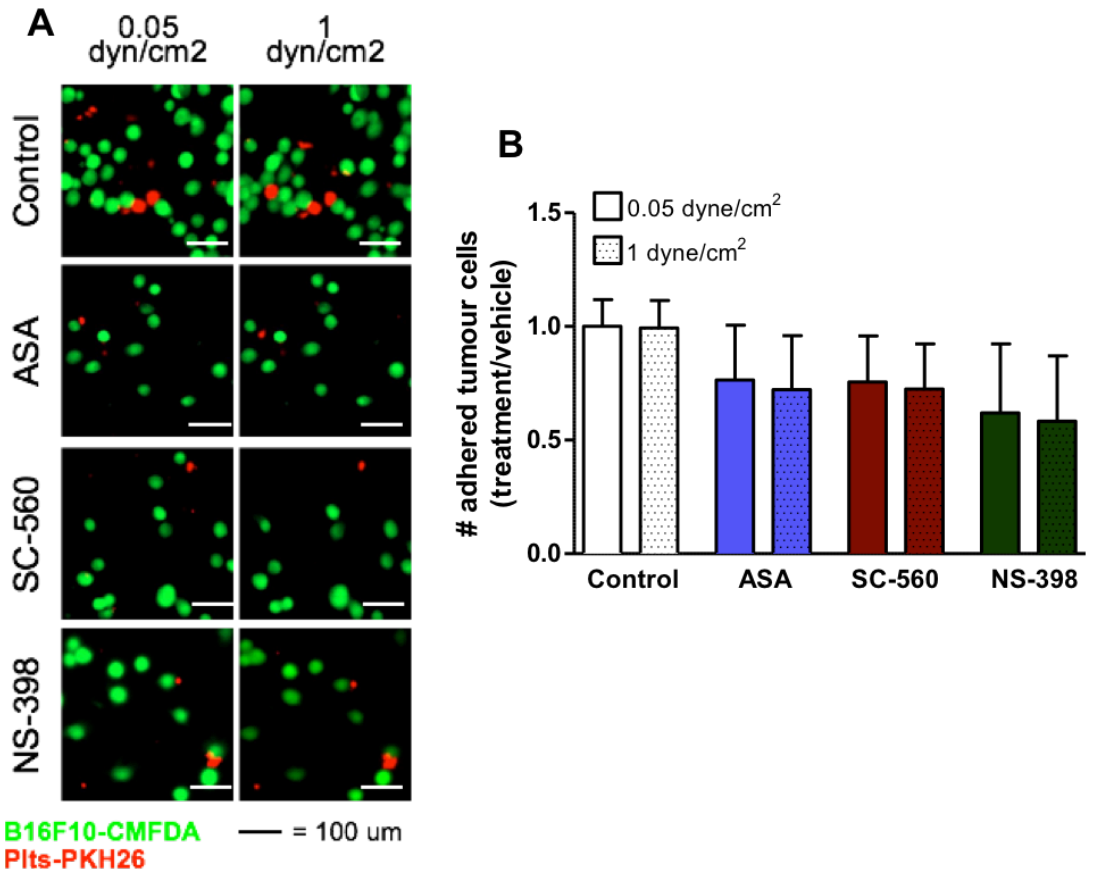

Supplementary figure S5 - Tumour cell adhesion to the endothelium is not affected by high shear stress.

(A) Representative epifluorescence images (10x) of tumour cells (B16F10-CMFDA, green), platelets (Plts-PKH26, red) and endothelial cells (LMVECs, DIC), after 10 minutes of 0.05 dyn/cm^2 (left panels) or subsequent 2 minutes at 1 dyn/cm^2 (right panels) shear stress. Tumour cells, platelets and endothelial cells were pre-treated separately with vehicle (Control), ASA, SC-560 or NS-398.

(B) Relative number of tumour cells, normalised to vehicle, adhered to endothelial cells in the presence of platelets after shear stress of 0.05 dyn/cm^2 or 1 dyn/cm^2, upon vehicle, ASA, SC-560 or NS-398 pre-treatment (n=4 independent experiments, 10 FOVs per repetition were analysed; mean + SD, 1-way ANOVA with Tukey's Multiple Comparison test).

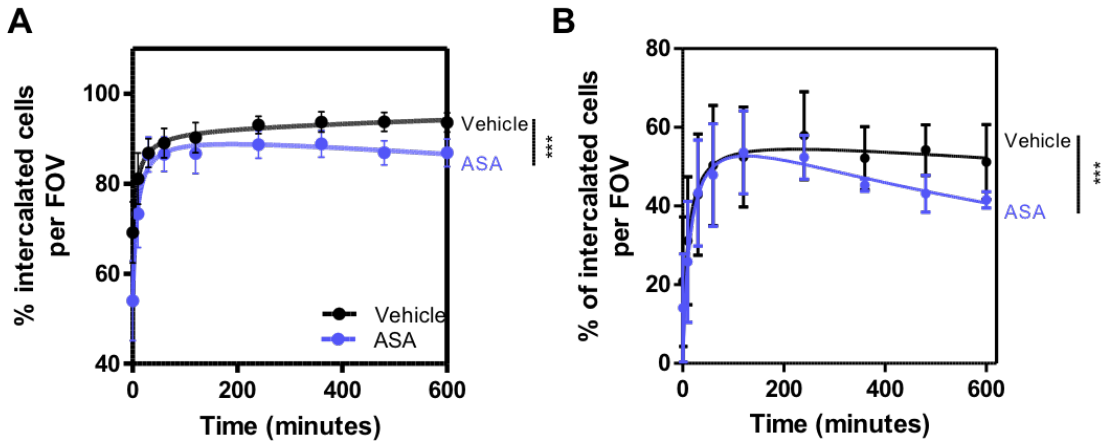

Supplementary figure S6 – Comparison of different methods for the quantification of tumour cell intercalation.

(A) Percentage of tumour cells (B16F10-CMFDA) intercalated within a monolayer of endothelial cells (LMVECs), monitored for 10 hours and counted manually. To do so, tumour cells were visually scored as not intercalated, intercalating and intercalated in epifluorescence images (see Figure 5.7A) (n=1 experiment, 9 FOVs per repetition were analysed; mean ± SD, Nonlinear fit with extra sum-of-square F test).

(B) Percentage of intercalated tumour cells, monitored for 10 hours and automatically scored. Briefly, tumour cells surface was reconstructed and their ellipticity was measured through Imaris software. Tumour cells were scored as not intercalated, intercalating or intercalated by setting ellipticity thresholds (see Figure 5.7A) (n=3 independent experiments, 9 FOVs per repetition were analysed; mean ± SD, Nonlinear fit with extra sum-of-square F test).

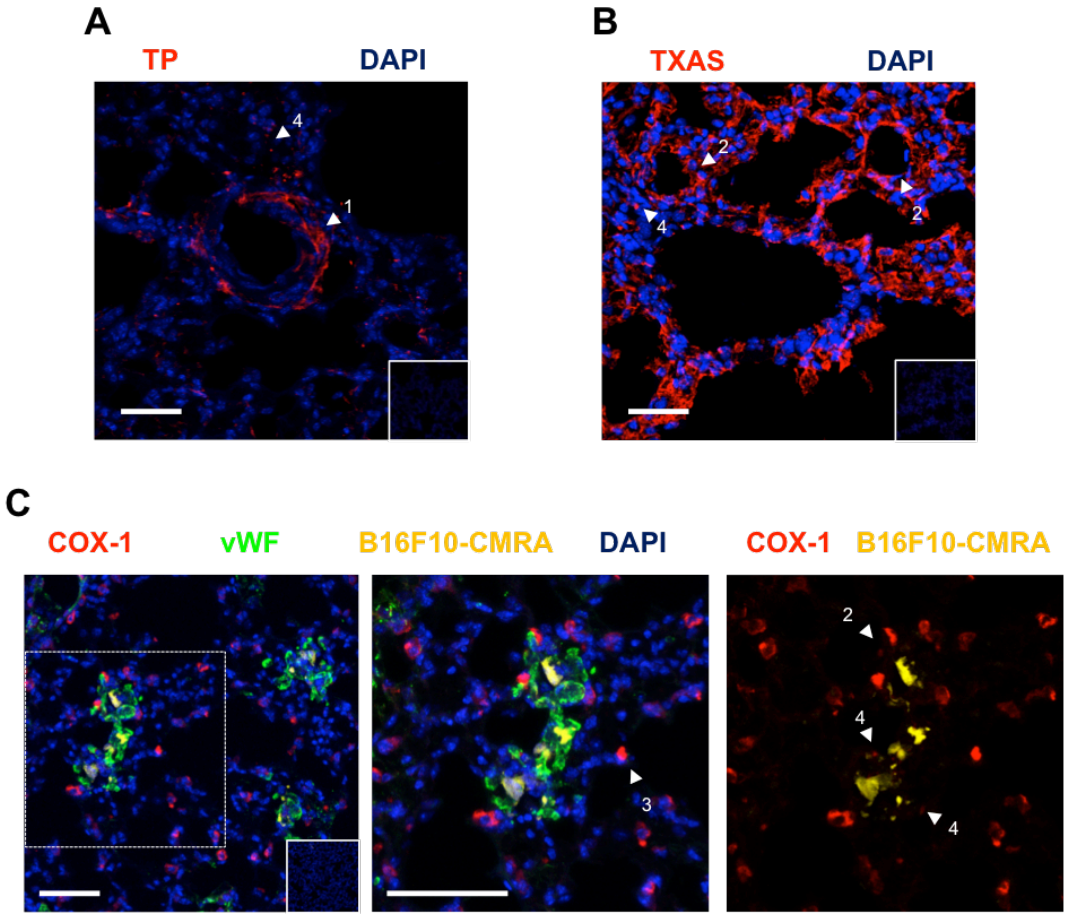

Supplementary figure S7 – Immunofluorescence detection of proteins involved in TXA_2 signalling in lung sections.

(A-C) Representative MIP of 3D confocal stacks of lung sections from C57BL/6 or *Cx$_3$cr1$^{gfp/+}$* mice. Expression of TP (A), TXAS (B), COX-1 (C) was detected in lungs harvested from naïve C57BL/6 mice (A-B) or mice intravenously injected with tumour cells (B16F10-GFP). Lung vessels were labelled with vWF (green) in (C). Based on the tissue morphology, 1 indicates vascular smooth muscle cells, 2 indicates endothelial cells, 3 indicates alveolar macrophages and 4 indicates platelets (n≥3 lungs). Isotype controls are represented in bottom-right inserts. Scale bars represent 100 µm.